From perturbative to non-perturbative renormalization in Tensorial Group Field Theories

Vincent Lahoche

NNT : 2016SACLS392

Thèse de doctorat de l'Université Paris-Saclay préparée à l'Université Paris-Sud

Ecole doctorale n°564
Physique en île de France
Spécialité de doctorat : Physique

par

M. Vincent Lahoche

De la renormalisation perturbative à la renormalisation non-perturbative dans les théories de champ sur groupe à interactions tensorielles

Thèse présentée et soutenue au Laboratoire de physique théorique d'Orsay, le 10 Octobre 2016.

Composition du Jury :

M.	Renaud Parentani	Professeur LPT, Orsay, France	Président du jury
M.	Etera Livine	Professeur Ecole Normale Supérieure, Lyon, France	Rapporteur
M.	Raimar Wulkenhaar	Professeur Westfälischen Wilhelms-Universität, Münster, Germany	Rapporteur
Mme	Bianca Dittrich	Professeur Perimeter Institut, Waterloo, Canada	Examinatrice
M.	Vincent Rivasseau	Professeur LPT, Orsay, France	Directeur de thèse
M.	Daniele Oriti	Professeur Albert Einstein Institut, Golm, Germany	Co-directeur

Acknowledgments

First of all, my thanks go to my two supervisors, Vincent Rivasseau and Daniele Oriti. Their contributions and their advices were very complementary during these three years. Vincent offered me the opportunity to realize this thesis, presenting it as a chance, and if at that time I thought I had understood the idea, it is only now, at the very end, that the full value of these words appears. I learned a lot thanks to them, and as enlightened supervisors, they offered me the most perfect balance between freedom and supervision. They allowed me to enter the world of research, to enter into several collaborations, and without them this thesis would not have been the same. For this I am very grateful.

Write these lines, I realize how difficult it is to list all the events and people which have contributed, directly or not, to the achievement of this thesis. So I apologize to everyone I will forget.

I also thank the jury members for their presence, and especially my two referees, Etera Livine and Raimar Wulkenhaar, for their precious comments after their careful reading of this manuscript.

I would like to thank all the persons I collaborated with, or discussed thoroughly, and who have contributed to make these three years very pleasant: Dario Benedetti, Dine Ousmane Samary, Sylvain Carrozza, Thibault Delepouve, Luca Lionni, Stephane Dartois, Harold Erbin ... I thank also the team of the Paris area: Adrian Tanasa, Razvan Gurau, Valentin Bonzom ...

My friends and my family have been a constant support, during these three years by also throughout all the time of my academic studies, for which this thesis is the final outcome. I especially think about my father, my mother and my brother of course, but also my grand-mother, Eva, who left us and to who this PhD was so important. I like to think that she would be proud of the result of these studious years.

Finally, research is a very special kind of work. It has no schedule, nor holydays and no real separation from private life. This work owes a lot to the support, the patience and the love of the one who shares my life, my wife Julie Lahoche, who gave me during these past two years the energy to carry out this thesis.

De la renormalisation perturbative à la renormalisation non-perturbative dans les théories de champ sur groupe à interactions tensorielles

Résumé en Français

La gravité quantique, à savoir la compréhension des phénomènes gravitationnels dans le formalisme de la physique quantique demeure un problème ouvert pour la physique contemporaine. La théorie des cordes reste l'approche la plus courante pour aborder cette problématique. Mais il existe une autre stratégie, fondée sur l'approche de la *géométrie aléatoire* et dite "indépendante de fond". Les théories de champs sur groupe à interactions tensorielles (Tensorial Group Field Theories (TGFTs) en Anglais) sont des candidates sérieuses et prometteuses dans cette voie. Elles sont à la fois le point de convergence et une source d'inter-fécondité entre deux approches essentiellement indépendantes : Les Théories de champs sur groupe d'une part (Group Field Theories (GFTs) en Anglais), et les modèles de tenseurs aléatoires (Random Tensor Models (RTMs) en Anglais) d'autre part. Les GFTs sont une classe particulière de théories des champs définies sur des variétés munies d'une structure de groupe et caractérisées par une forme spécifique de non-localité au niveau de leurs interactions, donnant aux diagrammes de Feynman de la théorie des perturbations la structure combinatoire de *complexes cellulaires* au lieu de celle de simples graphes. Les diagrammes de Feynman des GFTs ont ainsi la structure des *mousses de spins* (Spin Foams (SFs) en Anglais) des formulations covariantes de la *gravité quantique à boucle* (Loop Quantum Gravity (LQG) en Anglais), dont les GFTs correspondent à une seconde quantification. Les GFTs offrent ainsi un cadre théorique unifié pour les mousses de spins et la LQG. Les modèles de tenseurs aléatoires quant à eux sont une extension, en dimension supérieure à deux, des modèles de matrices utilisés pour la quantification de la gravité à deux dimensions, et forme le bagage mathématique et combinatoire de fond des GFTs. Les premiers modèles de tenseurs sont apparus dans les années 1990. Mais la grande révolution dans cette approche date de 2009, avec les travaux de Gurau et ses collaborateurs. Ils ont introduit les modèles de tenseurs colorés (Colored Tensor Models (CTM) en Anglais), caractérisés par une invariance spécifique de leurs interactions sous l'action du groupe unitaire $U(N)^d$, N étant la taille des tenseurs et d leur rang (A noter que d est également la dimension des complexes d-dimensionnels générés par le développement perturbatif "à la Feynman"). Pour ces modèles, il a été montré que l'on peut définir rigoureusement un développement en $1/N$, comme pour les modèles

de matrices, et que ce développement est contrôlé par un indice, "Le degré de Gurau", qui n'est pas un invariant topologique en dimension $d > 2$, mais se réduit essentiellement au *genre* en dimension 2.

Le secteur dominant de la théorie, occupé par les graphes planaires pour les matrices aléatoires a également été identifié pour les tenseurs colorés de rang arbitraire. Il s'agit du secteur dit "melonique", dont les graphes correspondent à des complexes sphériques. Le comportement critique des modèles dans ce secteur a également été étudié, et des transitions de phases ont été mises en évidence vers des phases de *polymères branchés*.

L'incorporation du critère de tensorialité hérité des tenseurs dans les GFTs, au niveau des interactions est le chemin classique menant aux TGFTs, qui ne sont rien d'autre que des GFTs dont les interactions présentent la même structure et les mêmes propriétés d'invariance que les interactions des modèles de tenseurs colorés. Ainsi, les TGFTs possèdent à la fois les ingrédients "pré-géométriques" suggérés par la LQG et les modèles de mousses de spins et le solide fond mathématique des modèles de tenseurs aléatoires. Cette inter-fécondité des deux approches permet non seulement d'établir solidement le comptage de puissance des théories, mais fournit également un principe de localité appelé *tracialité*, permettant de définir un groupe de renormalisation dans un cadre théorique où les interactions sont *à priori* non-locales. A noté que tous les modèles considérés dans cette thèse ont en commun l'incorporation d'une forme spécifique d'invariance de Jauge, dite *contrainte de fermeture*, traduisant une forme de platitude locale de la métrique de la variété triangulée. Cette condition, de plus, donne aux amplitudes de Feynman l'apparence d'une théorie de Jauge discrétisée sur un réseau aléatoire, dont la structure est générée par le développement perturbatif.

L'importance de la renormalisation pour les TGFTs est double. En premier lieu, la renormalisation est un ingrédient essentiel pour donner une définition rigoureuse d'une théorie des champs dès que des divergences apparaissent, ce qui est le cas dans la plupart des TGFTs. En second lieu, le groupe de renormalisation permet de déduire le comportement effectif d'une théorie dont les détails fins sont progressivement intégrés, et reste un outil essentiel en théorie des champs pour l'étude et la compréhension des transitions de phases. Or, de telles transitions de phase sont fortement suspectées comme étant le mécanisme par lequel les degrés de liberté de la théorie fondamentale, les "atomes d'espace-temps" s'organisent, se *condensent* pour former une structure pré-géométrique s'approchant de notre espace-temps classique, décrite dans un cadre effectif impliquant un grand nombre de

degrés de libertés quantiques. Ce scénario d'émergence d'un espace-temps continu depuis la description fondamentale de degrés de libertés discrets, appelé *géométrogénèse* reste un problème ouvert pour les approches indépendantes de fond de la théorie quantique de la gravitation. Toutefois, le scénario de condensation est appuyé par plusieurs travaux récents en cosmologie quantique et en physique des horizons isolés. La mise en œuvre d'un programme de renormalisation, et le développement d'outils a même de construire le groupe de renormalisation de la classe des TGFTs est donc un problème majeure dans cette direction de recherche. Beaucoup de travaux ont été effectués dans ce domaine, dont une partie au cours de cette thèse, et la construction du *groupe de renormalisation fonctionnel* a récemment permis de mettre en évidence de nombreux effets non perturbatifs, comme l'existence de points fixes non-triviaux, suggérant des transitions de phase.

Cette thèse a pour objet l'étude du groupe de renormalisation dans les TGFTs, prenant la suite des travaux déjà effectués dans ce domaine. En partant du cadre perturbatif, on se propose d'explorer le régime non-perturbatif, en suivant essentiellement deux approches : *Le groupe de renormalisation fonctionnel*, basé sur le formalisme de *Wetterich-Morris*, et la théorie constructive des champs, en suivant la technique de la LVE (*loop-vertex expansion* en Anglais).

Les trois premiers Chapitres dressent un panorama de l'état de l'art du domaine, et présentent les notions de bases utiles à la compréhension des Chapitres ultérieurs. Le premier chapitre est une introduction générale à la problématique de la gravité quantique, et une ouverture vers le formalisme des GFTs. Le second Chapitre introduit les GFTs pour elles mêmes, et met en exergue les relations entre différentes approches de la gravité quantique, la LQG, les mousses de spins, et la géométrie aléatoire à deux dimensions dans le cadre des modèles de matrices. Le troisième Chapitre enfin introduit les GFTs colorés, et justifie le choix des couleurs dans la définition des modèles. Deux arguments sont essentiellement avancés. Le premier concerne la suppression des triangulations singulières, qui non seulement sont présentent dans les modèles non colorés type Boulatov, mais dominent les sommes perturbatives. Le second concerne la possibilité de définir sans ambiguïté un groupe des difféomorphismes déformé discret, au moins en dimension 3. A la suite de ses arguments, les définitions et concepts de base sont ensuite présentés et illustrés. Le *degré de Gurau* est introduit, et la famille des graphes meloniques, jouant le rôle des graphes planaires des modèles de matrices est définie. Enfin, les comportements critiques du secteur dominant et du secteurs juste sous-dominant sont présentés, ouvrant la voie vers l'étude de la limite continue de la théorie. A cette occasion, la nature de *polymères branchés* des graphes meloniques est soulignée par la valeur prise par l'exposant critique dans ce secteur, justifiant ainsi la nécessité d'explorer les secteurs sous-dominants.

Le chapitre 4 présente les bases de la renormalisation dans le cadre spécifique des TGFTs. Là encore, les concepts sont introduits progressivement, bien que ce chapitre marque une rupture avec les précédents, puisqu'il présente également, et notamment dans sa seconde partie des résultats originaux obtenues durant la thèse. Sont ainsi présentés dans un premiers temps les notions clefs de *tracialité*, d'*analyse multi-échelle*, de *graphes hauts et bas*, de *forêts de Zimmermann*, d'*amplitude renormalisée* et de *série effective*. Parmi ces notions, la plupart sont standard, seule la notion de tracialité, jouant le rôle essentielle de "principe de localité" est une nouveauté spécifique aux TGFTs. La seconde partie du Chapitre se focalise sur un modèle particulier, Abélien, juste-renormalisable en dimension 6, pour lequel on montre que les amplitudes renormalisées sont finies à tout ordre. Enfin, dans le secteur divergent de la théorie, on montre qu'un système d'équations fermées existe, pour lequel les résultats précédent assurent qu'il existe bien une solution sur le domaine d'analycité de la série perturbative restreinte au secteur melonique.

Les chapitres 5 et 6 quittent le cadre perturbatif pour une approche non-perturbative du groupe de renormalisation, basée sur le formalisme du groupe de renormalisation fonctionnel et de l'équation de Wetterich-Morris. Le chapitre 4 présente le formalisme, et ses adaptations au cadre spécifique de la TGFT étudiée, concernant notamment la structure non-locale des interactions considérées, la présence d'une invariance de jauge particulière, et le choix d'une notion appropriée de dimension canonique pour les observables. Une fois dérivée l'équation de Wetterich-Morris, le choix d'une troncation particulière dans l'espace des couplages pour le modèle de rang 6 considéré dans le Chapitre 4 permet d'écrire un système d'équations fermé rendu autonome par l'utilisation des variables adimensionnées vis à vis de la dimension canonique. Ce système est ensuite étudié, d'abord au voisinage du point fixe Gaussien, montrant la *liberté asymptotique* du modèle considéré, puis numériquement et sans approximation, montrant l'existence d'un point fixe non-Gaussien dont les caractéristiques évoquent le point fixe de Wilson et Fisher et une transition de phase. Le Chapitre 5 lui s'intéresse à un modèle de rang 3, version Abélienne sur un tore de dimension trois d'un modèle basé sur le groupe $SU(2)$ et étudier dans la littérature pour ses connexions possibles avec la gravité quantique à trois dimensions. Plus précisément, on considère l'interpolation analytique entre deux famille de modèles, basés respectivement sur un groupe de dimension 3 et 4. Ses modèles ont été montrés juste-renormalisables pour des interactions meloniques de valence 6 et 4 respectivement, et un développement en epsilon au voisinage de la dimension 4 du groupe a mis en évidence un point fixe non-Gaussien. Le formalisme de la FRG permet de suivre la trajectoire de ce point fixe pour des troncations quartiques et des valeurs arbitraires de $0 \geq \epsilon \leq 1$, dont la présence est également confirmée pour une troncation de rang six. Finalement, cette troncation, en dimension 3 du

groupe, révèle l'existence d'un point fixe non-Gaussien attractif dans l'ultraviolet, suggérant un scénario de "sureté asymptotique" pour ce modèle.

Le chapitre 7 finalement, clôt la thèse par l'application dans le cadre des TGFTs des méthodes constructives connues sous le nom de *développement boucle-vertex* (loop-vertex expansion, LVE en Anglais) et *développement boucle-vertex multi-échelles* (multi-scale loop-vertex expansion, MLVE en Anglais). Les méthodes constructives visent en générales a étudier les propriétés analytiques des séries perturbatives, et a en définir un domaine d'analyticité. La LVE est une de ses techniques, associant une *transformation de Hubbard-Stratonovich* à la *formule de forêt BKAR*. La transformation de Hubbard-Stratonovich remplace la théorie tensorielle initiale par une théorie multi-matricielle, dont les interactions sont en nombre infinie. La *contrainte de fermeture*, réduit les degrés de libertés matriciels à des degrés vectoriels correspondant aux parties diagonales des dites matrices. La méthode de la LVE permet de remplacer la série perturbative originelle indexée par des graphes de Feynman, par une série indexée par des arbres. L'avantage repose sur le fait que les arbres prolifèrent bien moins vite que les graphes de Feynman avec le nombre de vertex, dont la croissance rapide est une source de divergence de la série. La technique a été appliquée directement et avec succès au cas d'un modèle sans divergence ultraviolette, et dans sa version raffinée, incluant un développement multi-échelle, à un modèle de TGFT super-renormalisable. La suite, visant a réalisé le même travail dans le cas d'un modèle juste-renormalisable reste toutefois un problème plus compliqué, laissé à une publication ultérieure.

Contents

Chapter 1

Motivations

"From a fundamental point of view
it is totally wrong to aim at basing
a theory only on observable quantities.
For in reality it is just the other way around.
Only the theory decides about what can be observed"
(Einstein according to Heisenberg, 1979)

1.1 Gravitation and Quantum Theory

The XXth century have seen two major achievements in fundamental physics: quantum theory and general relativity. Both drastically modified our understanding and our representations of Nature. General relativity interprets the gravitational phenomena as pure geometric effects, the trajectories of the test particles being geodesic on a curved space-time with Lorentzian signature, the metric tensor of this space-time being nothing but the gravitational field [6]. The most important conceptual modification in the general relativity framework is the dynamic nature of space-time. Indeed, the space-time in general relativity is no longer the fixed arena of the Newtonian physics, and becomes itself a physical system, whose geometry, the values of the tensor metric, depends on its interaction with all material system that it contains, via the *Einstein equation* (without cosmological constant):

$$R_{\mu\nu} - \frac{1}{2} R g_{\mu\nu} = \frac{8\pi G}{c^4} T_{\mu\nu} \,. \tag{1.1}$$

As to the quantum theory, which concerns essentially the microscopic physics, it revealed the limits of the classical Newtonian conceptual pictures, and the notions of trajectories, forces, picturability, as well as the idea of classical determinism disappeared in the quantum picture. Moreover, the quantum revolution is not only conceptual, but also technical. Indeed, it requires a new mathematical framework, far away from the familiar physical mathematics which have been used since Newton. In the "standard" representation of the theory, the classical phase space is replaced by an Hilbert-space, whose elements are *state-vectors*, encoding the physical state of the considered system. Moreover, the observables, whose spectra can be experimentally measured, become Hermitian operators acting on the state-vectors. Out of these operators, the Hamiltonien $\hat{H}$ can be considered as the most important. It controls the state evolution through Schrödinger's equation

$$i\hbar \frac{d}{dt} |\Psi(t)\rangle = \hat{H} |\Psi(t)\rangle \,. \tag{1.2}$$

Finally, in the probabilistic interpretation of the theory, the square of the absolute value of the components of a normalized vector-state in a complete basis corresponds to the probability to find the system alongside the corresponding basis vector. General relativity and quantum physics are said to be irreconcilable, but we can argue that such a split is not a problem of language. For instance, quantum mechanics can be expressed in a geometric framework [8], in which the Hilbert-space state is replaced by a Kähler manifold, playing the role of a quantum phase-space (with metric data added to the symplectic structure), and the probability corresponds to the geodesic distance between two points on this space. The incompatibility between the two theories comes from their requirement for space-time. In quantum mechanics for instance, the time parameter, as well as space, remains the absolute Newtonian one. The principles of quantum physics can be translated into the space-time of special relativity, and this achievement is known as quantum field theory. Therefore quantum physics does not require absolute time and absolute space. But it seems to require an absolute arena, that is the space and time of the Newtonian physics or the space-time of the special relativity. Even if we can build a quantum field theory on a curved classical space-time, if there is a global Killing vector of time type (as is the case for a Schwarzschild black-hole), the quantization procedure considers the field as a "test-field", and ignores its influence on the background, determined by a classical distribution of mass-energy. The reason is not only technical, but conceptual. For instance, an hybrid dynamic for space-time, described by a semi-classical Einstein equation as:

$$R_{\mu\nu} - \frac{1}{2} R g_{\mu\nu} = \frac{8\pi G}{c^4} \langle \Psi | \hat{T}_{\mu\nu} | \Psi \rangle \,, \tag{1.3}$$

for some quantum state Ψ and the corresponding energy-momentum tensor operator $\hat{T}_{\mu\nu}$, is inconsistent with the superposition principle, and in particular with "Schrödinger cats". This is a standard argument due to Unruh [9], which considered a physical system inside a box, formed by two masses connected by a spring and a radioactive source. Until a radioactive decay happens, the two masses remain rigidly connected. But one radioactive decay is enough to break this rigid connection, giving a swing move to the masses. As a result, denoting by $|0\rangle$ and $|1\rangle$ the two states of the system, the physical state at time t describing the situation is a superposition state:

$$|\Psi(t)\rangle = a_0 |0\rangle + a_1 |1\rangle \,, \tag{1.4}$$

where the amplitudes a_0 and a_1 are approximately given by $|a_0|^2 = e^{-\lambda t}$, $|a_1|^2 \approx 1 - e^{-\lambda t}$, where λ denotes the radioactive constant decay. In a semi-Newtonian approximation, only the mean value of the Hamiltonian operator $\hat{H}$ is relevant for $\langle \hat{T}_{\mu\nu} \rangle$, which is, assuming that the two vector states $|0\rangle$ and $|1\rangle$ are (at least approximately) eigenstates of $\hat{H}$:

$$\langle \Phi | \hat{H} | \Psi \rangle \approx e^{-\lambda t} \langle 0 | \hat{H} | 0 \rangle + (1 - e^{-\lambda t}) \langle 1 | \hat{H} | 1 \rangle \,. \tag{1.5}$$

Such a term for the right-hand-side of the equation 1.3 implies slow variations for the gravitational field, which could be measured by a Cavendish balance, and have never been observed [10]. Other Unruh arguments end up to the same conclusion: it is impossible to maintain a complete conceptual separation between the description of the gravitational field and of the quantized microscopic system. From this point of view, the reconciliation between quantum physics and general relativity goes much beyond aesthetic considerations based on the reductionist motivation of *unification*.

Of course, historically, the search for unification has been very fruitful, and has made at least part of the success of the standard model of particle physics. Nevertheless note that, even if the standard model has received many experimental confirmations, our understanding of it

beyond the perturbative level remains very incomplete. In this point of view general relativity is in a much better situation. However gravitation is certainly not included yet in the standard model, and is not a Yang-Mills theory, as the other three interactions, namely electromagnetism, weak and strong forces. Moreover, it is a long range interaction which is always attractive, in contrast with the others. These considerations may be related to the difficulty of unifying gravity with the other forces. Nevertheless the standard model forces and general relativity are also not completely estranged to each other. They come in contact in several phenomena, even if they are rare. A good example is given by cosmology and black-holes physics. Indeed, the singularity theorems of Penrose and Hawking [11] ensure the break-down of general relativity. For black-holes, the horizon entropy is another point of contact between gravity, quantum mechanics (and thermodynamic), which is explicit in the formula of Bekenstein and Hawking:

$$S_{BH} = \frac{k_B c^3}{4\hbar G} A \,, \tag{1.6}$$

where A is the area of the horizon, and k_B is the Boltzmann constant. The beauty of this formula comes from the association of all the fundamental constants: the speed of light c, the Planck constant $\hbar$, and the gravitational constant G. Therefore it is not solely an extrapolation of the domain of validity of one of the current fundamental theories, but a real point of contact between quantum, statistical and gravitational physics. The fact that black-hole horizon has an entropy suggests that it has a microscopic canonical description. This is why the computation of the horizon remains a challenge and a test for any candidate theory of quantum gravity.

1.2 The difficulty to quantize the gravitational field

One first attempt to quantize the gravitational field is to treat it exactly as the other interactions, for instance as the electromagnetic field. We can consider the metric $g_{\mu\nu}$ as the sum of a background (Minkowski or other) metric $\eta_{\mu\nu}$ plus a perturbation $\gamma_{\mu\nu}$. At the classical level, and at first order in $\gamma_{\mu\nu}$, this leads to the classical theory of gravitational waves, which can be quantized canonically as electromagnetic waves, leading to the concept of *graviton*, a particle with zero mass and spin 2. More formally, the resulting theory, taking into account all non-linear effects, can be obtained by considering the partition function of a path integral *à la Feynman*:

$$Z = \int \mathcal{D}\gamma_{\mu\nu} e^{-\mathcal{S}_{EH}(\eta_{\mu\nu}+\gamma_{\mu\nu})} \,, \tag{1.7}$$

where $\mathcal{D}\gamma_{\mu\nu}$ is a formal Lebesgue measure and $\mathcal{S}_{EH}$ the Einstein-Hilbert action. This approach to the problem is very conservative, as the other fields still live in a fixed background arena with a fixed metric. The first complication of this traditional approach appears immediately, since the resulting theory is not renormalizable. The situation can be improved by introducing super-symmetry, with cancellation of one and two loop counter-terms. Extending this kind of cancellation to all orders seems to require the full complications of *superstring theory* [5]. In this more complicated formalism all point-like particles are replaced by vibration modes of extended one dimensional objets, the strings. This ambitious "theory of everything" passes several important tests, such as providing a unified theory of matter and radiation including gravity and all standard model interactions and a microcanonical derivation of black-hole entropy and the Bekenstein-Hawking formula. Nevertheless it is fair to add that it passes these tests at the price of introducing many new unobserved degrees of freedom (new particles, extra dimensions)

and that even then, ultraviolet finiteness is not rigorously established at all orders. Given the enormous amount of efforts devoted to study superstrings during the last thirty years, it seems unlikely to be fully proved in a near future.

The second complication is more conceptual, but not independent from the first. As argued in [6], the introduction of a background space is in contradiction with general relativity[1], for which the gravitational field corresponds to the full metric. Moreover, the use of the background metric seems the source of the ultra-violet divergencies. This last point is one of the main motivations for the *background independent* approaches, in which the gravitational field is not treated separately from space-time, and which it is the point of view adopted all along this thesis.

To summarize, we can already distinguish at least two strategies to approach the problem. The first one, which is often the point of view preferred by particle physicists, and best embodied in string theory, still at least starts with a fixed space-time arena with its background metric, in which objects move, whether they are particles, gravitons or strings. In particular the gravitational degrees of freedom are embodied in a perturbation $\gamma_{\mu\nu}$. The price to pay seems to be that it leads to many new unobserved additional degrees of freedom, such as super-symmetric particles and extra-dimensions. In this point of view, unification is the main goal, and quantization of gravity is a mere byproduct. Note that history does not necessarily contradict this approach. A favorite example is the Fermi theory, which is non-renormalizable, but appears as a low-energy limit of a renormalizable theory, through the introduction of new degrees of freedom at high energy, namely the Bosons $W_\pm$ and Z_0. However this undeniable success remains insufficient to make this strategy totally convincing as a general rule. Remark in particular that in this respect gravity is quite different from weak interactions, because for a satisfying well-defined theory of quantum gravity, renormalizability is not the sole key requirement (see footnote 1).

The second strategy, often preferred by physicists with a background in general relativity, focuses on quantizing gravity alone and postpones the unification question. It can in particular follow the path opened up by Wheeler and DeWitt in 1967 [12]. Using the ADM decomposition, providing a slicing of space-time according to a time, they wrote down a "Schrödinger" equation for gravity:

$$\left((\hbar G)^2(q_{ab}q_{cd} - \frac{1}{2}q_{ac}q_{bd})\frac{\delta}{\delta q_{ac}}\frac{\delta}{\delta q_{bd}} - \det q R[q]\right)\Psi(q) = 0 \tag{1.8}$$

where q denotes the 3-metric on the slices, and Ψ is the famous "wave function of the universe". It is the first background independent quantum equation for gravity, which treats space-time itself as the gravitational field. This is the beginning of an history which is nowadays incarnated in the canonical approach of *loop quantum gravity* (LQG) and its covariant formulations as *spin foams models*. Loop quantum gravity, that we shall briefly discuss in the second chapter, allows to quantize gravity, but only at the kinematical level. Implementation of the dynamics through the so-called scalar constraint, and a complete implementation of four dimensional diffeomorphism invariance remains an open challenge for the theory. Despite these difficulties, two interesting lessons can be learnt from canonical loop quantum gravity. The first one is that the success of the quantization procedure is closely related to the choice of the variables encoding the classical degrees of freedom. The second is the prediction of the discreteness of the area and volume operators at the kinematical level. This last point, the discreteness of space-time at the Planck scale, is of great importance. Understanding the path between this discrete setting and the continuum space-time of general relativity is a main goal of quantum gravity. From the LQG point of view,

[1]Note that the contradiction is not only ideological. As explained for instance in [7], there is no canonical way to decompose the full metric in a sum "background+fluctuations".

this transition is difficult to study, because the formalism does not allow to treat a large number of degrees of freedom. It remains a challenge for the theory. The situation seems to improve in the covariant point of view of spin foam models. It allows to introduce some proper dynamic, and so, to define a scalar constraint for the kinetic states. But as we shall explain in Chapter 2, up to now, the best, most complete way to encode both the discreteness of the geometry and the dynamic in such a covariant approach is the *group field theory* formalism [2] .

Although we focused until now our discussion on string theory as a mainstream approach to quantum gravity and on loop quantum gravity because of its connection to the subject of this thesis, we should mention at this point that there are many other approaches to quantum gravity, neither of the string theory nor of the LQG type, which are currently also the subject of active research. We can cite the asymptotic safety scenario, dynamical and causal triangulations, non-commutative geometry, Horava-Lifschitz gravity, causal sets...

The relationship we have briefly sketched between loop quantum gravity, spin foams and group field theories can be thought as a kind of logical trajectory in the history of ideas. But it is not the only one, and one can arrive roughly at the group field theory formalism through a functional rather than Hamiltonian quantization in which one simply tries to discretize and randomize geometry within a field theory framework. Indeed group field theory performs a kind of synthesis between a main message of general relativity, summarized as *gravitation* $\sim$ *geometry*, and a main message of quantum mechanics, summarized as *quantizing* $\sim$ *discretizing and randomizing*[2].

Quantizing Gravity $\sim$ Discretizing and Randomizing Geometry

is therefore in our opinion a good mantra and guiding thread towards a theory of quantum gravity. Following this thread leads in particular to the very successful background-independent approach to two dimensional quantum gravity through *random matrix models*. In this approach, a rather detailed understanding of the transition from discrete to continuum random spaces can be now achieved. Moreover during the last decade, non-commutative field theories generalizing matrix models have been introduced which are both renormalizable and asymptotically safe [13].

Group field theories can be seen as an extension of such matrix models and non-commutative field theories to higher dimensions. During the last years, an improved class of group field theories, called tensor group field theories, has been introduced. Such theories have modified propagators and interactions with an additional tensorial symmetry. When I started this thesis, perturbative renormalization had been just established for a rather large class of such models, including some models of direct interest to quantum gravity, especially in three dimensions. Moreover many such models had been proved *asymptotically free*, like QCD, the theory of strong interactions. These two properties are very promising. However, the non-perturbative aspects of these models remained to be studied. In this context, my PhD work can be mainly described as applying non-perturbative techniques of quantum field theory to deepen our understanding of these tensor group field theories.

1.3 Organization of this thesis

The organization of the thesis is the following. After this introduction, the second chapter gives a general presentation of group field theory and its recent results. The third chapter introduces

[2]Of course quantum randomness is different from ordinary statistical randomness, but the two notions are reconciled in the *Euclidean* (imaginary time) setting.

colored and tensor group field theory. The addition of *colors* by Gurau in 2009 led quickly to the solution of an old open problem, namely the correct generalization of the large N expansion of matrix models to tensor models. It also led to the introduction of a new class of group field theories, called tensor group field theories. They have a kind of substitute for the usual notion of locality, called *traciality*, together with a rigorous notion of *power counting* which stems directly from the large N tensorial expansion. They have also modified propagators allowing for a multiscale analysis. Combining power counting with traciality and the multiscale analysis allows for their successful perturbative renormalization at all orders.

This perturbative renormalization is the subject of the fourth chapter. We introduce on a specific model all the concepts of perturbative renormalization. At the same time we summarize and discuss the results contained in our first publication, with Daniele Oriti and Vincent Rivasseau [1]. In particular we emphasize the interest of the *intermediate field* decomposition and of the closed equations for the *melonic sector* which leads the theory in terms of power counting. A main interest of this chapter is also to put forward all the concepts that we shall use in the following three chapters.

Chapters 5 and 6 indeed introduce a non-perturbative framework for the renormalization group flow discussed at the end of Chapter 4. We introduce there the *Wetterich equation* for tensor group field theories with closure constraint, and explain in detail how we can extract non-perturbative physical information from it. We focus essentially on three perturbative just-renormalizable theories. In the case studied in Chapter 5, we show the existence of a non-trivial Wilson-Fisher-like fixed point and of a critical line in the phase space of the theory, which seem to indicate a phase transition to a condensed phase, both in the ultra-violet and infrared regimes. Chapter 6 is devoted to the application of this method to just-renormalizable models with melonic interactions of valence six, in dimensions three. We concentrate on the the ultra-violet sector show the existence of some isolated fixed points, and argue in favor of asymptotic safety the the theory. The pertinence of each fixed point is discussed, in regard to the choice of the truncation, and the analysis is supported by an analytic continuation from a ϕ^4 quartic melonic model defined on the group $SU(2) \times U(1)$ to the ϕ^6 model on the group $SU(2)$ These two chapters are based on a published paper in collaboration with Dario Benedetti [3], and on two soon to be published papers, with Sylvain Carrozza and Dine Samary Ousmane.

The seventh and last chapter is based on two papers [4], in which we apply for the first time constructive field theory techniques to tensorial group field theories with closure constraints. We focus on the two simplest models of this type, with quartic interactions, which are respectively UV-divergences free and super-renormalizable, and for which we establish Borel-summability in the coupling constant. The first model can be treated with the constructive technique of the *loop vertex expansion*, whereas the second model requires the enhanced technque called *multi-scale loop vertex expansion.*

Finally in our conclusion we discuss a program, already partly under way, of possible extensions of this work. In particular we want to study the perturbative renormalization of group field theories including simplicial constraints, a possible $1/d$ expansion for the model discussed in Chapter 4, and the application of the Wetterich method to an "enhanced" field theoretic model mixing planar and branched polymers phases.

Bibliography

[1] V. Lahoche and D. Oriti, "Renormalization of a tensorial field theory on the homogeneous space SU(2)/U(1)," arXiv:1506.08393 [hep-th];

[2] D. Oriti, "The microscopic dynamics of quantum space as a group field theory," in *Foundations of space and time*, G. Ellis, et al. (eds.) (Cambridge University Press, Cambridge UK, 2012), arXiv:1110.5606 [hep-th];

[3] D. Benedetti and V. Lahoche "Functional Renormalization Group Approach for Tensorial Group Field Theory: a Rank-6 Model with Closure Constraint", arXiv:1508.06384 [hep-th];

[4] V Lahoche, "Constructive Tensorial Group Field Theory II: The $U(1) - T_4^4$ Model," arXiv: 1510.05051 [hep-th];

V Lahoche, "Constructive Tensorial Group Field Theory I: The $U(1) - T_3^4$ Model," arXiv: 1510.05050 [hep-th];

[5] Kaku, Michio, "Introduction to Superstring and M-Theory" (2nd ed.). New York, USA: Springer-Verlag 1999.

[6] Carlo Rovelli, "Quantum gravity," Cambridge University Press, 2004;

Carlo Rovelli and Francesca Vidotto, "Covariant Loop Quantum Gravity," Cambridge University Press, 2015;

Thomas Thiemann, "Modern canonical quantum general relativity," Cambridge University Press, 2007;

John Baez, Javier P. Muniain, "Gauge field, knots and gravity," World Scientific, 1994;

Claus Kiefer, "Quantum gravity," Oxford University Press, 2007;

[7] A Perez, "The Spin Foam Approach to Quantum Gravity," Living Rev. Rel., 16:3, 2013, 1205.2019.

[8] T. A. Schilling, "Geometry of Quantum Mechanics", PhD Thesis. Pennsylvania State University, 1996;

A. Ashtekar and T. Schilling, "Geometrical Formulation f Quantum Mechanics" arXiv: gr-qc/9706069, 1997;

[9] WG Unruh. "Steps towards a quantum theory of gravity". Quantum Theory of Gravity, 1:234, 1984;

[10] D. N. Page and C. D. . Geilker. "Indirect evidence for quantum gravity". Phys. Rev. Lett., **47**, 979-982, 1981;

[11] S.W Hawking and G;F.R Ellis. “The large scale structure of space-time", Cambridge University Press, 1973.

[12] B. S. DeWitt, "Quantum Theory of Gravity. I. The Canonical Theory". Phys. Rev. **160**, 1113-1148, 1967.

[13] H. Grosse and R. Wulkenhaar, “Renormalisation of phi**4 theory on noncommutative R**4 in the matrix base,” Commun. Math. Phys. **256**, 305, 2005; arXiv:hep-th/0401128;

M. Disertori, R. Gurau, J. Magnen and V. Rivasseau, “Vanishing of Beta Function of Non Commutative Phi**4(4) Theory to all orders,” Phys. Lett. B **649**, 95, 2007); hep-th/0612251.

Chapter 2

Group field theories for quantum gravity

This chapter is a presentation of group field theories (GFTs), which are the basic tool of this thesis. The first occurrence of GFTs in the literature came as a development of tensor models, which are themselves an extension of matrix models for dimension space higher than 2 [2]. In this context, the domain of tensors indices are formally replaced by a group manifold. Moreover, some *pregeometric constraints* are added, and the most popular is the *closure constraint*, which takes the form of a gauge invariance, and gives to the Feynman perturbative expansion the structure of a random lattice with discrete gauge connection. For quantum gravity models, the choice of the group manifold depends on the space-time dimension and signature, and the current choices are $SU(2)$ or $SL(2,\mathbb{R})$ in dimension 3, and $SO(4)$, $SL(2,\mathbb{C})$ in dimension 4. The motivation of the authors was to make contact with other formulations of quantum gravity, especially the Ponzano-Regge and the Turaev-Viro models in dimension 3 [2], as well as with *simplicial quantum gravity*, Regge calculus and topological BF theory in dimension higher than 3. Then, in a historical perspective, group field theories emerged as improved tensor models "over" a group manifold, enriched with algebraic data and gauge invariance.

As an interesting result, it has been shown that the GFT formulation of state sum models for purely topological field theories is related to loop quantum gravity, whose *spin networks* states match with the boundary states of the corresponding GFTs, and conversely describe the Hilbert space of the GFTs. Then, GFTs can be understood as quantum field theories for spin networks, providing them with a covariant and coherent dynamic, in the sense that they allow to reproduce any spin foam model, arising as Feynman amplitude in the perturbative expansion, with a summation rule given by the perturbative expansion itself. That this sum makes sense beyond the formal level is however not generally guaranteed, and is one of the motivations for this thesis, renormalization being the best tool in a field theory framework to answer this question.

The plan of this chapter is the following. After a brief and formal presentation of GFTs in Section 2.1.1, we give a brief presentation of canonical quantum gravity and of spin foams, and explore their relations with GFTs in Section 2.2. In Section 2.3 we shall explore the relations with matrix models and random geometry approach, and finally, in Section 2.4, we shall list some achievements of the GFT approach.

2.1 Formal definition and basic example

2.1.1 A field theory over a group manifold

At the classical level, a rank-d GFT is a theory for a complex field ϕ defined on d-copies of a group manifold $\mathbf{G}$:

$$\begin{aligned} \phi &: \mathbf{G}^d \to \mathbb{C} \\ \mathbf{g} &:= (g_1, ..., g_d) \to \phi(\mathbf{g}), \end{aligned} \tag{2.1}$$

whose action has the generic form:

$$\begin{aligned} \mathcal{S}(\phi, \bar{\phi}) = &\int d\mathbf{g} d\bar{\mathbf{g}} \bar{\phi}(\bar{\mathbf{g}}) \mathcal{K}(\bar{\mathbf{g}}, \mathbf{g}) \phi(\mathbf{g}) \\ &+ \sum_b \frac{\lambda_b}{\mathrm{Sym}(b)} \int \prod_{i=1}^{n_b} d\mathbf{g}_i d\bar{\mathbf{g}}_i \bar{\phi}(\bar{\mathbf{g}}_i) \phi(\mathbf{g}_i) \mathcal{V}_b(\mathbf{g}_1, \bar{\mathbf{g}}_1; ...; \mathbf{g}_{n_b}, \bar{\mathbf{g}}_{n_b}). \end{aligned} \tag{2.2}$$

This expression is the occasion to introduce the notation that we shall use in the rest of this thesis. $d\mathbf{g} := \prod_{i=1}^d dg_i$ is the product of the Haar measure over the group manifold. The index b labels all the monomial interaction terms, weighted by coupling constant λ_b. n_b corresponds to the number of fields of type ϕ or $\bar{\phi}$ involved in the interaction labeled by b. The factor $1/\mathrm{Sym}(b)$ in front of the interaction, which is the inverse of the dimension of the symmetry group of b, ensures that the symmetry factors of the perturbative expansion of the corresponding quantum theory match exactly with the dimension of the automorphism group of the Feynman diagrams. The kernels $\mathcal{V}_b$ are products of delta functions, identifying some group variables between different fields, and a source of *non-locality*, which is a characteristic of GFTs in contrast with standard *local field theories* over space-time. Then, the definition 2.2 points out that a specific GFT corresponds to a choice of a group manifold $\mathbf{G}$, of a rank d, as well as of a kinetic kernel $\mathcal{K}$ and interactions $\mathcal{V}_b$.

The quantum theory is formally defined by the partition function :

$$Z(\{\lambda_b\}) := \int \mathcal{D}\phi \mathcal{D}\bar{\phi} e^{-\mathcal{S}(\phi, \bar{\phi})} = \sum_{\mathcal{G}} \frac{1}{\mathrm{Sym}(\mathcal{G})} \prod_{b \in \mathcal{G}} \big(- \lambda_b \big) \mathcal{A}_{\mathcal{G}} \ , \tag{2.3}$$

where $\mathcal{D}\phi$ (resp. $\mathcal{D}\bar{\phi}$) denotes the formal Lebesgue measure over $L^2(\mathbf{G}^d)$, $\mathcal{A}_{\mathcal{G}}$ is the Feynman amplitude associated to the Feynman diagram $\mathcal{G}$, with automorphism group dimension $\mathrm{Sym}(\mathcal{G})$. The amplitudes are obtained from the Feynman rules, and are expressed as products of propagators i.e. in term of the inverse of the kinetic kernel $\mathcal{K}$. However, if the explicit expression depends on the specific GFT, the non-locality of the interactions gives the Feynman diagrams the structure of cellular complexes rather than graphs, i.e. sets of vertices, lines and faces.

With this definition, the amplitudes of the GFT do not differ from the amplitudes of the tensor models. But as explained in the abstract of this chapter, GFTs are usually enriched by some group-theoretic data. One of these enrichments, the *closure constraint*, takes the form of a gauge invariance under diagonal right action of $\mathbf{G}$ on the field variables:

$$\phi(g_1, ..., g_d) = \phi(g_1 h, ..., g_d h) \qquad \forall h \in \mathbf{G}. \tag{2.4}$$

The role played by this gauge invariance and its relationship with LQG can be well understood at the kinematic level, by considering the Hilbert space of the free theory and the related obervables. Then, we shall close this short section with some results about the kinematic Hilbert

space, useful for the discussions of Section 2.2.2.

In an operational framework, the quantum theory can be defined by imposing commutation relations, as well as in standard quantum mechanics. We shall see that in order to make contact with LQG, the relevant definition for commutation relations between operators $\hat{\phi}$ and $\hat{\phi}^\dagger$ have to be the following:

$$[\hat{\phi}(\mathbf{g}), \hat{\phi}^\dagger(\bar{\mathbf{g}})] = \hat{P}(\mathbf{g}, \bar{\mathbf{g}}) \ , [\hat{\phi}(\mathbf{g}), \hat{\phi}(\mathbf{g}')] = [\hat{\phi}^\dagger(\bar{\mathbf{g}}), \hat{\phi}^\dagger(\bar{\mathbf{g}}')] = 0 \ , \tag{2.5}$$

where $\hat{P}$ is the projector into the gauge invariant fields, whose components $\hat{P}(\mathbf{g}, \bar{\mathbf{g}})$ are defined by:

$$\hat{P}(\mathbf{g}, \bar{\mathbf{g}}) := \int_{\mathbf{G}} dh \prod_{i=1}^{d} \delta(g_i h \bar{g}_i^{-1}). \tag{2.6}$$

As in standard quantum field theory, we construct the *Fock space* as an infinite sum of tensorial product of Hilbert spaces $\mathcal{H}_v := L^2(\mathbf{G}^d)$ for a single quantum of space. The Fock space is then obtained as a superposition of such individual particule states:

$$\mathcal{F} := \bigoplus_{V=0}^{\infty} \mathrm{Sym}\big(\mathcal{H}_v^{(1)} \otimes \mathcal{H}_v^{(2)} \otimes \cdots \otimes \mathcal{H}_v^{(V)}\big) \tag{2.7}$$

where Sym in this context means the symmetrisation of the tensorial products with respect to the labels $1, 2, ..., V$. The choice of this symmetrisation is in accordance with the commutation relations 2.5, corresponding to a *Bosonic statistic*. For each summand in 2.7, the inner product descends from the one on $L^2(\mathbf{G}^{d\times V}/\mathbf{G}^V)$.

As in standard quantum field theory, observables are functionals of the field operators $\hat{\phi}$ and $\hat{\phi}^\dagger$ acting on the Fock space $\mathcal{F}$. However, in contrast with ordinary quantum field theory, for the GFTs, the relevant operators may be *non-local*, as well as for the generic interaction structure of the classical action 2.2.

Finally, note that the definition of GFT given in this section only concerns a single field, and does not include gravitational degrees of freedom i.e. describes topological and not geometric configurations. This point will be discussed in the next section. A large part of this thesis is in fact only dedicated to the material described in this section. The issue of the geometric models requires an *extended GFT formalism*, and is for instance discussed in [2].

2.1.2 The Boulatov model and Ponzano-Regge amplitudes

The Boulatov model is a good example of a GFT for 3-d quantum gravity, whose perturbation theory generates Ponzano-Regge amplitudes [2], that we shall discuss in Section 2.2.2. Assuming that the field ϕ has support on $SU(2)^3$, which is a natural assumption in dimension 3, and is square integrable with respect to the Haar measure over the group manifold, we impose the gauge invariance 2.4 at the classical level, and the classical action for this model has only two terms, which are:

$$\begin{aligned} \mathcal{S}(\phi) \ &= \ \int \prod_{i=1}^{3} dg_i \phi^2(g_1, g_2, g_3) \\ &\quad + \lambda \int \prod_{i=1}^{6} dg_i \phi(g_1, g_2, g_3)\phi(g_3, g_5, g_4)\phi(g_5, g_2, g_6)\phi(g_4, g_6, g_1). \end{aligned} \tag{2.8}$$

Note that in this case we have a single field ϕ rather than ϕ and $\bar{\phi}$. Each field variable is associated to each of the three boundary lines of a triangle, and the interaction term in 2.8 sticks four triangles together, according to their common boundary lines, to form a tetrahedron (a 3-simplex). The kinetic term, corresponding to the simplest choice for $\mathcal{K}$, dictates the gluing rules for these tetrahedra along triangles (see Figure 2.1).

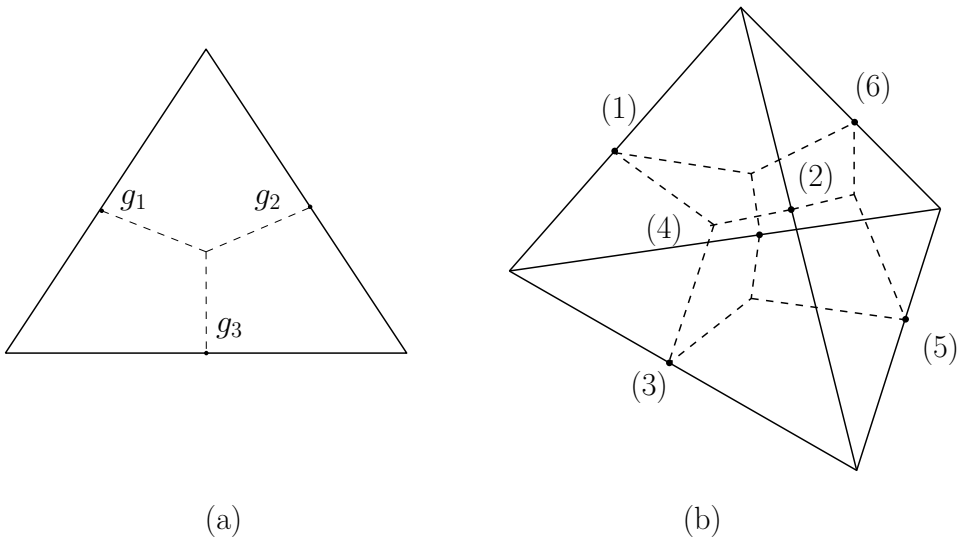

(a) (b)

Figure 2.1: Graphical definition of the field variables (a) and interaction vertex (b).

At the quantum level, the field theory is defined by the partition function, and the closure constraint has to be implemented at the graph level in the perturbative expansion by convolution of the fields variables with the projector $\hat{P}$. Due to the fact that, by definition, $\hat{P}^2 = \hat{P}$, the projection can be imposed only in the kinetic term, or in other words, in the definition of the propagator:

$$\int \mathcal{D}\phi e^{-\mathcal{S}_{kin}(\phi)} \phi(g_1, g_2, g_3)\phi(g_1', g_2', g_3') =: C(g_1, g_2, g_3; g_1', g_2', g_3') \ , \tag{2.9}$$

where $\mathcal{S}_{kin}$ denotes the kinetic part of the action. The standard strategy consists in averaging over the group manifold, imposing the identification

$$C(g_1 h, g_2 h, g_3 h; g_1', g_2', g_3') = C(g_1, g_2, g_3; g_1', g_2', g_3') \, \forall h \in SU(2). \tag{2.10}$$

With the definition of the kinetic action in 2.8, it is not difficult to convince oneself that the good choice is:

$$C(g_1 h, g_2 h, g_3 h; g_1', g_2', g_3') = \int_{SU(2)} dh \prod_{i=1}^{3} \delta(g_i h {g_i'}^{-1}) \equiv \hat{P}(g_1 h, g_2 h, g_3 h; g_1', g_2', g_3'). \tag{2.11}$$

With these definitions, the generic expressions for the amplitudes $\mathcal{A}_\mathcal{G}$ in the perturbative expansion 2.3 can be obtained from the Feynman rules, and we find:

$$\mathcal{A}_\mathcal{G} = \int \prod_{e \in \mathcal{G}} dh_e \prod_{f \in \mathcal{G}} \delta(H_f) \ , \tag{2.12}$$

where H_f, the *holonomy around face* f is defined as the oriented product of holonomies,

$$H_f := \vec{\prod}_{e \in \partial f} h_e \ , \tag{2.13}$$

where $\partial f \subset \mathcal{G}$ denotes the boundary of the face f. Then, the formal perturbative expansion of the quantum partition function writes as:

$$Z(\lambda) = \sum_{\mathcal{G}} \frac{(-\lambda)^{V(\mathcal{G})}}{\mathrm{Sym}(\mathcal{G})} \mathcal{A}_{\mathcal{G}} \ , \tag{2.14}$$

where the last sum over $\mathcal{G}$ runs over all the vacuum (i.e. without boundaries) 2-complexes, and $V(\mathcal{G})$ denotes the number of vertices in $\mathcal{G}$. The amplitude 2.12 matches exactly with the well known Ponzano-Regge amplitudes for spin foams in dimension 3, that we shall shortly discuss in the next section. For the moment, note that, interestingly, the amplitude 2.12 takes the form of a discretized gauge theory, with discrete connections along the lines of a random lattice generated by the perturbation theory itself. The identification with a gauge theory becomes complete by noting that the amplitude 2.12 remains unchanged under the discrete gauge transformation:

$$h_e \to g_{s(e)} h_e g_{t(e)}^{-1} \ , \tag{2.15}$$

where the labels s and t mean "source" and "target" vertices of the line e. A complementary point of view on the physical picture given by the Boulatov model can be obtained in the *Lie algebra representation* as a *non-commutative Fourier transform* [8]. In our case, this improved Fourier transform is a mapping from $L^2(SO(3)^3)$ to $L^2_\star(\mathfrak{so}(3)^3)$, where the label $\star$ refers to a non-commutative $\star$-product. Formally, the Fourier transform of a field $\phi \in L^2(SO(3)^3)$, say $\hat{\phi}$, is defined as:

$$\hat{\phi}(x_1, x_2, x_3) := \int d\mathbf{g} \phi(g_1, g_2, g_3) \prod_{i=1}^{3} e_{g_i}(x_i) \ , \tag{2.16}$$

where $x_i \in \mathfrak{so}(3)\, i = 1, 2, 3$, $e_g : \mathfrak{so}(3) \to U(1)$ are "non-commutative plane waves", and the technical subtleties that functions over $SO(3)^3$ are now understood as functions over $SU(2)$, invariant under the transformation $g \to -g$ of their group variables[1]. The choice of a complete family of plane waves is not unique. Here, we adopt the definition:

$$e_g(x) := e^{i\mathrm{Tr}(x|g|)} \qquad \forall g \in SU(2) \, , \tag{2.17}$$

where $|g| := \frac{\mathrm{Tr}(g)}{|\mathrm{Tr}(g)|} g$, and Tr means the trace in the fundamental representation of $SU(2)$. The non-commutative $\star$-product, dual to the convolution product for functions on the group, can be defined between planes waves:

$$(e_g \star e_{g'})(x) := e_{gg'}(x) \ . \tag{2.18}$$

The Lie group variables have the advantage to provide a direct metric interpretation, as 3-vectors associated to the edges of dual triangles, as explained in [8]. Moreover, it is especially interesting in regard to the geometric constraints. More precisely, due to the basic properties of the Fourier transform, the projector $\hat{P}$ over the gauge invariant field defined in 2.6 turns to be a Dirac distribution $\delta_0(x_1 + x_2 + x_3)$, where δ_x is defined as

$$\delta_x(y) := \int dg e_{g^{-1}}(x) e_g(y) \, , \tag{2.19}$$

and verifies:

$$\int dy (\delta_x \star f)(y) = \int dy (f \star \delta_x)(y) = f(x) \ . \tag{2.20}$$

[1]Which is nothing but the translation of the group identification:$SO(3) = SU(2)/\mathbb{Z}_2$.

As a result, on shell, the edge vectors x_1, x_2, x_3 of a dual triangle are such that:

$$x_1 + x_2 + x_3 \equiv 0 \ , \tag{2.21}$$

which is exactly the constraint verified by the edge vectors of a flat triangle ! Then, the gauge invariance can be nicely understood as a local flatness condition for elementary quantum triangles. The GFT, in this point of view, is a quantum theory describing interactions of such flat triangles. More details can be found in [8].

2.2 Relation with loop quantum gravity and spin foams

2.2.1 Canonical quantization of general relativity

The most popular approach to canonical quantization of general relativity is loop quantum gravity. Conceptually, it is closely related to the old idea first proposed by Wheeler and DeWitt, know as Wheeler-DeWitt (WdW) equation. The WdW equation was a first step in building a background independent quantum theory of gravity, but it has suffered dramatically of the choice of the variables used by the authors to formulate their theory. These authors were accustomed to a metric-description of the classical field prior to quantization, and the resulting quantum equation inherited some untractables technical difficulties (in particular, there was no well defined associated Hilbert space). Then, even if it represents a conceptual progress towards a quantum theory, the WdW approach remains highly formal, and far from any true achievement. Loop quantum gravity started with new variables proposed by Ashtekar [6] in the early 1980s to describe general relativity. In this description, the constraints over the classical phase space in the ADM formulation are drastically simplified, allowing to circumvent the intractable problem of operator ordering occuring in the WdW formulation, and to start the first steps of a rigorous canonical program, at least up to the construction of a *kinematical Hilbert space* [6].

The starting point of LQG is the *vierbein* formalism. Let $\mathcal{M}$ be the space-time manifold, assumed to be hyperbolic for canonical formulation. One introduces the frame field $e : \mathcal{M} \times \mathbb{R}^{3,1} \to T\mathcal{M}$, providing a trivialization of $T\mathcal{M}$, and sending, for each $x \in T\mathcal{M}$, the standard basis of $\mathbb{R}^{3,1}$ to a basis of tangent vectors at x. More concretely, we introduce the vierbein field-form:

$$e^I(x) = e^I_\mu(x) dx^\mu \quad x \in \mathcal{M} \, , \tag{2.22}$$

where the Greek indices $\mu = 0, ..., 3$ refer to the spacetime and the Latin indices $I = 0, ..., 3$ refer to the canonical basis of the internal Minkowski space. In this formalism, what we usually call metric looses its fundamental status, and is deduced from the knowledge of the fields $\{e^I_\mu\}$:

$$g_{\mu\nu}(x) := e^I_\mu(x) e^J_\nu(x) \eta_{IJ} \tag{2.23}$$

where we use the Einstein convention for summation over repeated indices. Interestingly, this definition makes clearly apparent an internal symmetry, coming from the invariance under any local Lorentz transformation. In this formalism, the Einstein's equations (without matter fields) can be derived from a first order variational principle, called the Holst action:

$$\mathcal{S}_H(e, \omega) = \frac{1}{\kappa} \int_{\mathcal{M}} \mathrm{Tr} \left[\left(\star \, e \wedge e + \frac{1}{\gamma} e \wedge e \right) \wedge F(\omega) \right] \, , \tag{2.24}$$

where κ is the gravity constant, which can be expressed in terms of Newton's constant and of c, the celerity of light. ω is the (Lie algebra valued) 1-form spin-connection, whose curvature

is $F(\omega) := d\omega + \omega \wedge \omega$, $\star$ is the standard Hodge star, and $\gamma \in \mathbb{C}$ is the Barbero-Immirizi parameter[2], which is undetermined at the classical level. Slicing the manifold $\mathcal{M} = (\Sigma, \mathbb{R})$ in a $3+1$ decomposition framework, and using the density of vierbein $E^a_i := \det(e) e^a_i$, $a = 1, 2, 3$ rather than the metric as a coordinate in phase space, the conjugate variable, the *Ashtekar connection*, writes as:

$$A^i_a := \frac{1}{2}\epsilon^i_{jk}\omega^{jk}_a + \gamma\omega^{0i}_a, \tag{2.25}$$

with canonical Poisson bracket:

$$\{E^a_i(x), A^j_b(y)\} = \kappa\gamma\delta^a_b\delta^j_i\delta(x-y). \tag{2.26}$$

In this formalism, E^a_i plays the role of an "electric field", and A^i_a is an $SU(2)$ connection encoding parallel transport over the $3d$ foliation Σ. As spoiled in the introduction of this section, the most interesting part of this formulation appears in the expression of the three first-class constraints on the classical phase space:

$$G_i = \mathcal{D}_a E^a_i\,, \quad \mathcal{C}_a = E^b_i F^i_{ba}\,, \quad \mathcal{C} = \epsilon^{ijk}E^a_i E^b_j F_{abk} + 2\left(1 - \frac{1}{\gamma^2}\right)E^a_{[i}E^b_{j]}(A^i_a - \omega^i_a)(A^j_b - \omega^j_b)\,. \tag{2.27}$$

Each of these constraints restricts the phase space to a physical sub-manifold, and in addition generates gauge transformations. The first one, called *Gauss constraint* generates $SU(2)$ local transformations over the foliation, the second one, called *vector constraint* generates spatial diffeomorphism (over the foliation), and finally the third and last constraint, called *scalar constraint* is related to the invariance under a change of time.

In this formulation, the description of the quantum theory is encoded in a complex-valued wave function $\Psi : \mathcal{A} \to \mathbb{C}$ over the space $\mathcal{A}$ of the $3d$ $SU(2)$ connections. The quantization of the classical theory follows Dirac's program [24]. The first step requires a representation of classical phase space variable as (self-adjoint) operators acting on a suitable subspace of (square integrable) functionals over $\mathcal{A}$ with Hilbert-space structure, whose eigenvalues describe the quantized physical quantities. Then we have to take into account the quantized version of classical constraints. The subset of states in $\mathcal{H}_{kin}$ annihilated by the quantum constraints inherits a Hilbert space structure, and we call $\mathcal{H}_{phy}$ this physical Hilbert space. The LQG formalism allows to start the first steps of the quantization program. It provides a well defined kinematical Hilbert space $\mathcal{H}_{kin}$, on which the two first constraints can be solved. Moreover, the resulting Hilbert space has been proved to be unique, up to some assumptions [6]. However, some difficulties remain for the scalar constraint, encoding the dynamic of the LQG states.

The kinematical Hilbert space $\mathcal{H}_{kin}$ is defined as the space spanned by *cylindrical functionals*:

$$\Psi_{\Gamma,f}[A] = f\big(h_{\gamma_1}(A), ..., h_{\gamma_n}(A)\big) \qquad A \in \mathcal{A}\,, \tag{2.28}$$

where $\Gamma = \{\gamma_1, ..., \gamma_n\}$ is a set of n smooth oriented paths on Σ, which form a closed oriented graph, $f : SU(2)^n \to \mathbb{C}$ is a smooth function defined on n copies of $SU(2)$, and

$$h_\gamma(A) := \mathcal{P}\exp\left(\int_\gamma A\right)\,, \tag{2.29}$$

[2]Note that, even if the classical theory is defined for all $\gamma \in \mathbb{C}$, the quantification procedure fails for purely imaginary Immirizi parameters.

where $\mathcal{P}$ is the path ordering, denoting the holonomy along the path γ. For these states 2.28, we have the natural scalar product:

$$(\Psi_{\Gamma,g}|\Psi_{\Gamma,f}) := \int_{SU(2)^n} \prod_{i=1}^{n} dh_i \overline{g(h_1,...,h_n)} f(h_1,...,h_n) \tag{2.30}$$

where dh_i denotes the Haar measure over $SU(2)$. Note that this scalar product can be extended to the case where the closed oriented graphs are different for the two functions, considering a bigger graph containing the two considered graphs as subgraphs. Roughly speaking, $\mathcal{H}_{kin}$ is the completion with respect to the scalar product 2.30 of the vector space spanned by cylindrical functionals, which is isomorphic to the Hilbert space $L^2(\bar{\mathcal{A}}, d\mu_{AL})$, the space of square-integrable functionals over the generalized connection space $\bar{\mathcal{A}}$ with respect to the *Ashtekar-Lewandowski measure* $d\mu_{AL}$ [see [6]].

The Gauss constraint can be solved straightforwardly in this Hilbert space, since its action on cylindrical functionals can be inferred from its action on holonomies,

$$h_\gamma(A) \to g_{s(\gamma)} h_\gamma(A) g^{-1}_{t(\gamma)}. \tag{2.31}$$

Then, we call *gauge invariant Hilbert space*, and denote by $\mathcal{H}_G$ the subspace of $\mathcal{H}_{kin}$ spanned by gauge invariant cylindrical functionals. Using a standard Peter-Weyl decomposition, an explicit orthonormal basis can be obtained for these functionals, as tensor invariants under tensorial products of irreductible representation of the $SU(2)$ group, that we call *spin-network functionals*. A spin-network functional $\Psi_{\Gamma,\{j_\gamma\},\{\imath_v\}}$ - whose a basic example is pictured in Figure 2.2 - is a set of representation matrices of $SU(2)$, labeled by j_γ and associated to each link $\gamma \in \Gamma$, contracted with a set of intertwiners $\imath_v$ between the representations carried by the links hooked to the node $v \in \Gamma$:

$$\Psi_{\Gamma,\{j_\gamma\},\{\imath_n\}}(A) = \prod_{v\in\Gamma} \imath_v \cdot \prod_{\gamma\in\Gamma} D^{j_\gamma}(h_\gamma(A)), \tag{2.32}$$

where $D^{j_\gamma}(h_\gamma(A))$ denotes the matrix of the irreductible representation of $SU(2)$ labeled by j_γ and associated to the group element $h_\gamma(A)$. The $\cdot$ means contraction between indices.

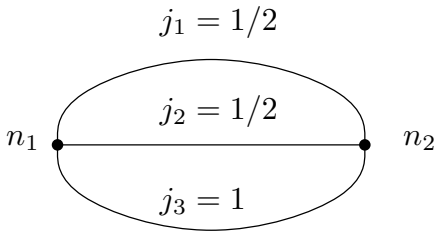

Figure 2.2: A basic example of a spin network state, namely a closed graph with two trivalent nodes, and lines labeled by spin representations

In the same way, we can show that solving the vector constraint requires states which are invariant under the *extended diffeomorphisms* $Diff^*$, and then define the Hilbert space $\mathcal{H}_{Diff}$ as the completion with respect to the scalar product 2.30 of the equivalent class of spin-network states under extended diffeomorphisms, called *s-knot states*. The strategy can be summarized by the following sequence of Hilbert spaces:

$$\mathcal{H}_{kin} \supset \mathcal{H}_G \supset \mathcal{H}_{Diff} \supset \mathcal{H}_{phy}. \tag{2.33}$$

The last step, the implementation of scalar constraint remains an open problem for LQG. Formally, it can be achieved by applying the projector onto the physical states, $\hat{P}_{phy}$,

$$\hat{P}_{phy} := \int_{\mathbb{R}} dt e^{it\hat{\mathcal{C}}} \ , \tag{2.34}$$

such that, for any physical state $|s\rangle \in \mathcal{H}_{phy}$, $\hat{P}_{phy}|s\rangle = |s\rangle$. Obviously, this strategy is highly formal at this stage, because the quantum operator corresponding to the scalar constraint is undefined at the quantum level, but it is an argument in favour of spin foams, which is the subject of Section 2.2.2. Note that, in spite of these difficulties, the physical outcome of LQG is not empty ! It provides an interesting notion of quantum geometry, by transposing classical expressions for area and volumes into operators acting on spin-networks states. More concretely, we can show that *quanta of area* are carried by the links of spin-networks states, with value $\pm 8\pi\gamma\ell_p^2\sqrt{j(j+1)}$ for the representation j, the sign depending on the orientation of the surface. In the same way, we can show that the volume operator is quantized, with values associated to each node of the spin-networks. Note that loop quantum gravity, that we shall discuss in the next section, can be fruitfully described in a *non-commutative flux representation*, using the group Fourier transform defined in Section 2.1.2, see [5].

We can make contact with group field theories as follows. Alternatively to the geometrical picture given by Figure 2.1, a single field can be interpreted as an elementary d-valent spin network vertex. As an illustration of the link between GFT kinematic Hilbert space described in Section 2.1.1 and LQG, we choose $\mathbf{G} = SU(2)$. Using the Peter-Weyl decomposition theorem, the single particule state $|\phi(\mathbf{g})\rangle := \hat{\phi}(\mathbf{g})|0\rangle$

$$\phi(\mathbf{g}) = \sum_{j_\ell, m_\ell, m'_\ell} c_{\{j_\ell, m_\ell, m'_\ell\}} \prod_{\ell=1}^{d} D^{j_\ell}_{m_\ell, m'_\ell}(g_\ell) =: \sum_{j_\ell, m_\ell, m'_\ell} \varphi_{\{j_\ell, m_\ell, m'_\ell\}}(\mathbf{g}) \ , \tag{2.35}$$

and the gauge constraint 2.4 allows group averaging, leading to:

$$\phi(\mathbf{g}) = \sum_{j_\ell, m_\ell, m'_\ell} \varphi_{\{j_\ell, m_\ell, m'_\ell\}}(\mathbf{g})\, \imath_{\{j_\ell, m_\ell, m'_\ell\}} \ , \tag{2.36}$$

with : $\imath_{\{j_\ell, m_\ell, m'_\ell\}} := \int dh \prod_{\ell=1}^{d} D^{j_\ell}_{m_\ell, m'_\ell}(g_\ell h) \in {}_{\cdot 1}\big(SU(2)^{\otimes d}\big)$. A general V-particule state writes as:

$$\phi(\{\mathbf{g}_I\}) = \sum_{\{j_{\ell_I}, m_{\ell_I}, m'_{\ell_I}\}} \varphi_{\{j_{\ell_I}, m_{\ell_I}, m'_{\ell_I}\}}(\{\mathbf{g}_I\}) \prod_{i=1}^{V} \imath^{(i)}_{j_{\ell_I}, m_{\ell_I}, m'_{\ell_I}} \ , \tag{2.37}$$

which can be interpreted as a wave function for V particules in a first quantisation language. Then, considering a closed d-valent graph Γ with V vertices, we can build a wave function for Γ by group-averaging such a wave-function, pairwise along open links:

$$\Psi_\Gamma(\{(g_i^a)^{-1} g_j^b\}) = \prod_{e \in E(\Gamma)} \int_{SU(2)} d\alpha_{ij}^{ab} \phi(\{\alpha_{ij}^{ab} g_i^a\}) = \tag{2.38}$$

$$\sum_{\{j_{\ell_I}, m_{\ell_I}, m'_{\ell_I}\}} \Big[\prod_{e \in E(\Gamma)} \int_{SU(2)} d\alpha_{ij}^{ab} \varphi_{\{j_{\ell_I}, m_{\ell_I}, m'_{\ell_I}\}}(\{\alpha_{ij}^{ab} g_i^a\}) \Big] \prod_{i=1}^{V} \imath^{(i)}_{j_{\ell_I}, m_{\ell_I}, m'_{\ell_I}},$$

where $E(\Gamma)$ denotes the set of edges $e = [(ia),(jb)]$, linking the vertices i and j from the edge a hooked to i to the edge b hooked to j, and where $\alpha_{ij}^{ab} = \alpha_{ji}^{ab}$. 2.38 is nothing but an example of a LQG gauge invariant cylindrical function, and provides a faithful embedding of elements of the LQG kinematical Hilbert space $L^2(SU(2)^E/SU(2)^V, d\mu = \prod_{e\in E} dh_e)$ into $L^2((SU(2)^d/SU(2))^V, d\mu)$. There are some fundamental differences between the kinematical Hilbert spaces for LQG and GFTs, pointed out in [7]. For instance, if the GFT kinematic state encodes combinatorial and algebraic structure of LQG states, there is no natural embedding of GFTs kinematic states into a continuous manifold, meaning that there is no action of a well-defined diffeomorphism group. In the current GFT point of view, these differences are accepted, and understood as a consequence of the effective nature of general relativity. Then, in this point of view GFTs provide a fundamental framework, from which we expect to construct a pattern from discreteness to continuum in a proper "thermodynamic limit", a physical picture motivated by the choice of Bose statistics, as well as by the absence of a consistent continuum intuition.

In the second quantization formalism of GFTs, the operator $\hat{P}_{phy}$ which projects onto solutions of the Hamiltonian constraint can be written as an operator acting on the Fock space, and can be decomposed as a sum of $n+m$-body operators, involving n operators $\hat{\varphi}$ and m operators $\hat{\varphi}^\dagger$ [21]:

$$\hat{P}_{phy} = \sum_{n,m} \lambda_{n,m} \int [d\mathbf{g}]^n [d\mathbf{g}']^m P_{n+m}(\{\mathbf{g}_I\}_{I=1,\dots,n}, \{\mathbf{g}'_J\}_{J=1,\dots,m}) \prod_{I=1}^{n} \hat{\varphi}(\mathbf{g}_I) \prod_{J=1}^{m} \hat{\varphi}^\dagger(\mathbf{g}_J) \tag{2.39}$$

such that, for any physical states $|S\rangle$,

$$\hat{F}|S\rangle = \left[\hat{P}_{phy} - \int d\mathbf{g} \hat{\varphi}^\dagger(\mathbf{g})\hat{\varphi}(\mathbf{g})\right]|S\rangle = 0. \tag{2.40}$$

Heuristically, the path from this second quantized framework to the GFT classical action can be understood, up to some assumptions, as follows [see [7]]. Let us consider the grand-canonical ensemble with partition function:

$$Z_g = \sum_S \langle S|e^{-(\hat{F}-\mu\hat{N})}|S\rangle \ , \tag{2.41}$$

where $\hat{N} := \int d\mathbf{g}\hat{\varphi}^\dagger(\mathbf{g})\hat{\varphi}(\mathbf{g})$ and, as currently, the sign of the chemical potential μ determines whether states with many or few "atoms of space" are favoured. This definition, rewritten in the (over-complete) basis of coherent states $|\phi\rangle := e^{\int d\mathbf{g}\phi(\mathbf{g})\hat{\varphi}^\dagger(\mathbf{g})}|0\rangle$, leads to:

$$Z_g = \int \mathcal{D}\phi\mathcal{D}\bar{\phi} e^{-|\phi|^2} \langle\phi|e^{-(\hat{F}-\mu\hat{N})}|\phi\rangle =: \int \mathcal{D}\phi\mathcal{D}\bar{\phi} e^{-\mathcal{S}_{eff}(\phi,\bar{\phi})} \ , \tag{2.42}$$

where $\mathcal{D}\phi$ denotes the formal Lebesgue path-integral measure, and the *effective action* corresponds to the classical action of the GFT, plus quantum corrections [7, 21]:

$$\mathcal{S}_{eff}(\phi,\bar{\phi}) = \mathcal{S}(\phi,\bar{\phi}) + Q.C = \frac{\langle\phi|\hat{F}|\phi\rangle}{\langle\phi|\phi\rangle} + Q.C, \tag{2.43}$$

where $\mathcal{S}$ may be identifyed with the classical GFT action 2.2, providing in particular the relation $m^2 = 1-\mu$. The quantum corrections generate new interactions, or modify the coupling constant

values. We insist on the fact that this construction is highly heuristic, and the partition function, as well as the integration measure, have to be properly defined. At this end, the GFT formulation allows to use the tools of standard quantum field theories, *renormalization*, *constructive techniques*,.... These techniques allow to define the theory perturbatively, i.e. for physical processes involving a few degrees of freedom, as well as in the complementary regime involving a lot of degrees of freedom. In quantum gravity, we are especially interested in the second regime. The main challenge for background independent quantum gravity approaches is to recover the classical general relativity in the *classical continuum limit*, and many results have been already obtained [17, 21]. It has for instance been established that, even in the classical limit, a state involving a few geometrical degrees of freedom allows to recover some partial information on classical physics, and for special regimes only [7]. The so-called "classical approximation" is then not necessarily related to the continuum one, and such an effective continuum limit requires in principle a lot of microscopic degrees of freedom, which can then be understood as a "thermodynamic limit", very far from the perturbative regime.

2.2.2 Covariant loop quantum gravity and spin foam models

By covariant loop quantum gravity, we refer in fact to the so-called *spin-foam models*. Historically, spin foam models were introduced to circumvent the difficulties encountered in the canonical approach with the scalar constraint [6]. Basically, the spin foam approach is an attempt to define properly the Feynman amplitudes:

$$\langle S_1|S_2\rangle = \int \mathcal{D}g e^{i\mathcal{S}_{GR}(g)}, \tag{2.44}$$

where $|S_i\rangle\, i = 1, 2$ are two (physical) 3-dimensional geometry states which are boundaries of the space-time g, $\mathcal{D}g$ is a probability measure on the space-time interpolating the two 3-geometries, and $\mathcal{S}_{GR}$ is the classical action for general relativity. Such an amplitude, written in this form, is highly formal, and the right and the left hand sides are both undefined mathematically. This warning does not only concern the path-integral, but the left hand side as well, because *a priori* we have no "background independent labels" for boundary states. Moreover, the object of the sum itself remains unclear, because no prescription coming from the classical theory indicates if we have to sum over metric degrees of freedom in a fixed topology, and on the topologies as well.

Heuristically, spin foams can be approached by reproducing the Feynman derivation of the path-integral applied to the projector 2.34, i.e. cutting the integral over t and inserting the closure relation in the spin-networks basis, leading to the *spin foam general Ansatz* [5, 6]:

$$\langle S_1|S_2\rangle = \sum_{\mathcal{F}|S_1\cup S_2=\partial\mathcal{F}} \mathcal{A}_{\mathcal{F}}\ , \tag{2.45}$$

where $S_i = (\Gamma_i, \{j_{e_i}\}, \{\imath_{v_i}\})\, i = 1, 2$ are spin-network states, and the spin foam $\mathcal{F}$ interpolates between them, in the following sense. $\mathcal{F} = (\mathcal{G}, \{j_f\}, \{\imath_e\})$ is a decorated 2-complex $\mathcal{G}$ whose boundary is the union of the two spin-network graphs $\partial\mathcal{G} = \Gamma_1 \cup \Gamma_2$, $\{j_f\}$ denotes the set of $SU(2)$ representations associated to the faces $\{f\}$, and $\{\imath_e\}$ is the set of intertwiners shared by the edges $\{e\}$, such that any face touching a boundary edge has the same spin representation, and that any edge e touching a boundary vertex shares exactly the same intertwiner. Conceptually, the decomposition 2.45 is exactly the same as 2.44. The superiority of the second with respect to the first is clear : not only the left hand side is now well defined, but the combinatorial sum "over

histories" on the right hand side make sense as well. However, the heuristic argument given above for the derivation of the spin foam Ansatz does not precise how the amplitude $\mathcal{A}_\mathcal{F}$ is computed. There are in fact essentially three paths to spin foams. The one that we have described above is historically the first, and as explained just above, it has to be completed, because the dynamics of LQG is itself not well defined. In this approach, the general strategy consists in reversing the construction, and infers the physical Hilbert space from the definition of a suitable spin-foam model, giving a prescription for the computation of the amplitudes. The references [6] detail the construction of spin foam models following this strategy. It is important for our purpose to mention that in spin foam approaches, the 2-complexes that we have denoted by $\mathcal{F}$ are physically interpreted to be dual to simplicial decompositions of a topological 4-dimensional manifold.

The second strategy mentioned above can be seen as a continuation of the Ponzano-Regge model for 3-dimensional Euclidean quantum gravity. The corresponding classical theory is described by the topological action

$$\mathcal{S}_{3d}(e,\omega) = \int_\mathcal{M} \mathrm{Tr}(e \wedge F(\omega)) \ , \tag{2.46}$$

where the $\mathfrak{su}(2)$-valued 1-form e is the triad form, and $F(\omega)$ is the curvature of the $\mathfrak{su}(2)$-connection ω. Varying with respect to the triad provides the classical 3-dimensional version of the Einstein equation, namely $F(\omega) = 0$, meaning that space-time is flat, and that relevant degrees of freedom are topological. A formal argument suggests that this remains the case at the quantum level. Indeed, integrating over e in the partition function leads to:

$$\mathcal{Z}_{3d} = \int \mathcal{D}\omega \int \mathcal{D}e e^{i\mathcal{S}_{3d}(e,\omega)} \sim \int \mathcal{D}\omega \delta(F(\omega)) \ . \tag{2.47}$$

Then, this argument seems to indicate that the partition function for $3d$ quantum gravity is nothing but the volume of the set of flat connections over $\mathcal{M}$. The argument can be made rigorous in a discrete setting, by introducing a *cellular decomposition* Δ, as well as its dual decomposition Δ^* for the manifold $\mathcal{M}$. The dual 2-complex Δ^* is assumed to be a set of vertices, say v, dual to 3-cells in Δ, edges e, dual to 2-cells , and faces f, dual to 1-cells in Δ. Elementary 3-cells are tetrahedra, glued one to the other along their boundary triangles. As for lattice gauge field theory, we replace the connection variables by its holonomies $\{h_e \in SO(3)\}$ along the lines $e \in \Delta^*$, and the triad by vectors X^i_ℓ of $\mathbb{R}^3$ along each edge of Δ, which can be understood as integration of the $\mathfrak{su}(2)$ 1-form e^i $(i = 1, 2, 3)$ along this edge, and correspond to the Lie group elements $X_\ell = X^i_\ell \tau_i$ (where the τ_i are the Pauli matrices with suitable normalization). Noting that an edge of the triangulation corresponds to a face of the dual 2-complex, these variables can be denoted as X_f in Δ^*. Then, we can write the discretized classical action as [6]:

$$S_\Delta(X,h) = \frac{1}{8\pi G} \sum_{f\in\Delta^*} \mathrm{Tr}(X_f H_f) \ , \tag{2.48}$$

where

$$H_f = \prod_{e\in\partial f}^{\rightarrow} h_e \ , \tag{2.49}$$

is the oriented product of the holonomies around the boundary of the face f. The quantum theory can then be defined by the partition function:

$$\mathcal{Z}^{PR}_{3d}(\Delta) = \int [dX_f] \int [dh_e] e^{iS_\Delta(X,h)} \sim \int [dh_e] \prod_{f\in\Delta^*} \delta(H_f) \ , \tag{2.50}$$

where $\delta(H_f)$ is the delta-function over $SO(3)$ and where in this case, not only the measures with respect to which we sum, but also the final integration are clearer. Finally let us use the Peter-Weyl theorem for δ-functions

$$\delta(g) = \sum_{j\in\mathbb{N}/2} (2j+1)\chi_j(g) \qquad \forall g \in SU(2) \ , \tag{2.51}$$

where χ_j are the characters of the j^{th} representation of $SU(2)$. Decomposing each character in 2.50 in products of Wigner matrices associated to a single holonomy h_e, and noting that a given h_e appears only three times (one for each edge of the dual triangle), we can integrate over each of them. Each integration gives one $3j$ symbol per edge, which are contracted following the pattern given by the tetrahedral decomposition, leading to the well-known formulation of the Ponzano-Regge partition function

$$\mathcal{Z}_{3d}^{PR}(\Delta) = \sum_{\{j_f\}} \prod_{f\in\Delta^*} (-1)^{2j_f}(2j_f+1) \prod_{v\in\Delta^*} \{6j\}_v \ , \tag{2.52}$$

where $\{6j\}_v$ denotes the $6j$ symbol associated to the spin attribution in Δ^* of the faces running through v. This spin-foam model for quantum gravity in dimension 3 is the first ever proposed. It has been extended in higher dimension, especially in dimension four, with Euclidean or Lorentzian signatures, in the class of constrained topological BF theories classically described by the Holst-Plebanski action:

$$\mathcal{S}[B,\omega,\lambda] = \frac{1}{\kappa}\int_{\mathcal{M}} \left[\left(\star B^{IJ} + \frac{1}{\gamma} B^{IJ} \right) \wedge F_{IJ}(\omega) + \lambda_{IJKL} B^{IJ} \wedge B^{KL} \right] \ , \tag{2.53}$$

where λ_{IJKL} is a Lagrange multiplier, chosen such that the $\mathfrak{so}(1,3)$-valued 2-form B verifies the "on shell" condition:

$$B = \pm e \wedge e \ , \tag{2.54}$$

ensuring that the Holst-Plebanski action turns to the Holst action when the Plebanski constraint is satisfied. The major interest of this approach is that BF theories can be rigorously quantized in this way, as the Ponzano-Regge model. We start by defining a discretization of the space on some cell-complex, as well as a discretized version of the field B and of the connection. Then, we quantize the resulting discretized theory with the path integral method. In dimension higher than 3, and especially in dimension 4, the strategy is to start from the quantization of the topological BF-theory, and to introduce a discrete version of the Plebanski constraint in order to recover the geometric degrees of freedom at the quantum level. This road to the quantum theory is in fact ill-defined, in the sense that it introduces a large variety of models, and some ambiguities in the discretization procedure, which are discussed in the references.

Interestingly for our purpose, the expression 2.50 matches exactly with 2.12, making the relation with GFT more concrete. Whereas we have illustrated the correspondence between spin foams and GFTs [1] in this simple example, the correspondence is in fact widely discussed in the literature. The superiority of the GFT formalism with respect to the spin foam approach and LQG itself is evident. Firstly, the QFT formalism allows to fix the weights for the sums over spin foams (which are not fixed in the spin foam approach). Moreover, these weights can be justified, in the sense that, up to a suitable normalization of couplings, they correspond to the dimension of automorphism group, which can be understood as a discrete version of the diffeomorphism group. Secondly, the field theory framework allows to use standard methods in

quantum field theory, especially renormalization, in order to circumvent the divergences of the amplitudes. Finally, in the GFT framework, the topology of space-time itself is generated by the perturbative expansion as well as the amplitudes. These advantages of the GFT approach are discussed extensively in the references.

2.3 Relationship with random discrete geometry

2.3.1 Discrete random geometry in dimension 2: Matrix models

By definition, matrix models are statistical field theory for matrices. For instance, by denoting M an $N \times N$ Hermitian matrix, we can construct an action for M by requiring invariance under conjugation - providing an exotic locality principle - exactly is the same way as symmetries or gauge invariance in standard QFTs. Note that this principle is nothing but the reflection of the fact that, for such a theory, the point-wise product of standard field theories is replaced by the non-commutative matrix product. With this assumption, and assuming that only connected interactions are relevant, we can show that the action $\mathcal{S}(M)$ for M is a sum of terms of the form $\mathrm{Tr}(M)^k$, $k \in \mathbb{N}^*$. As an example:

$$\mathcal{S}(M) = \frac{1}{2}\mathrm{Tr}M^2 - \lambda \mathrm{Tr}M^3 \ , \tag{2.55}$$

for some coupling constant λ, is the simplest matrix model, with partition function:

$$\mathcal{Z} = \int dM e^{-\mathcal{S}(M)} \ , \tag{2.56}$$

where dM is the invariant measure on the $N \times N$ Hermitian matrices. Expanding the right hand side perturbatively in λ with the propagator

$$C_{ij,kl} = \delta_{jk}\delta_{il} \ , \tag{2.57}$$

we generate Feynman amplitudes labeled by connected ribbon graphs $\mathcal{G}$ rather than graphs. The interaction vertex has three external points, identifying the six strands pairwise. Propagator and vertex are pictured in Figure 2.3, and an example of ribbon graph is given in Figure 2.4.

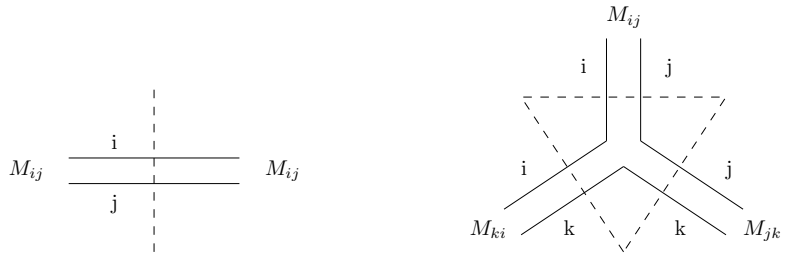

Figure 2.3: Propagator and vertex interaction of the matrix model. The dashed lines correspond to the dual representation: it corresponds to an edge for a propagator, and to a triangle for a vertex.

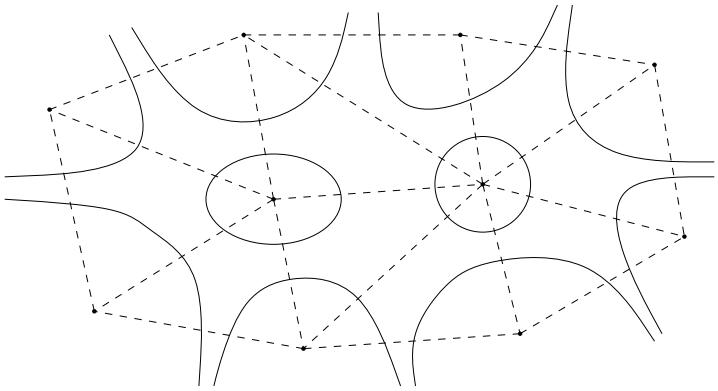

Figure 2.4: An example of a ribbon graph with its dual triangulation.

Using Feynman rules, it is not hard to see that:

$$\mathcal{Z} = \sum_{\mathcal{G}} \frac{1}{s(\mathcal{G})} \lambda^{V(\mathcal{G})} \mathcal{A}_{\mathcal{G}} \ , \tag{2.58}$$

with:

$$\mathcal{A}_{\mathcal{G}} = N^{F(\mathcal{G}) - \frac{1}{2} v(\mathcal{G})} \ , \tag{2.59}$$

and where $F(\mathcal{G})$ and $v(\mathcal{G})$ are respectively the number of faces and vertices of $\mathcal{G}$. Note that we have performed a rescaling of the coupling constant in order to obtain 2.59, in such a way that there are infintely many leading configurations as $N \to \infty$. The interest of this rescaling is explicit in the dual representation. Denoting by $V(\Delta_{\mathcal{G}})$, $E(\Delta_{\mathcal{G}})$, $T(\Delta_{\mathcal{G}})$ respectively the numbers of vertices, edges and triangles in the dual representation $\Delta_{\mathcal{G}}$ of $\mathcal{G}$, and using the topological constraint $2E(\Delta_{\mathcal{G}}) = 3T(\Delta_{\mathcal{G}})$, leads to:

$$F(\mathcal{G}) - \frac{1}{2} v(\mathcal{G}) = V(\Delta_{\mathcal{G}}) - E(\Delta_{\mathcal{G}}) + T(\Delta_{\mathcal{G}}) = 2 - 2g(\Delta_{\mathcal{G}}) \ , \tag{2.60}$$

where we have used the fact that vertices of the dual representation correspond to faces of the original one. We have recognized, in the intermediate expression, the Euler characteristic of $\Delta_{\mathcal{G}}$, and used its standard expression in term of the genus $g(\Delta_{\mathcal{G}})$. The dual representation of the Feynman ribbon graphs then allows to associate a triangulated surface to each of them. Therefore matrix models can be interpreted as statistical models for discretized surfaces, and the type of discretization depends on the form of the interaction that we choose. For instance, an interaction of order four gives quadrangulations rather than triangulations. The fact that the degree of divergence only depends on the genus is also a consequence of the choice of the theory. Indeed, a closed 2-dimensional topological manifold is fully characterized by genus (or equivalently by Euler characteristic) and orientability. Note that we only generate orientable surfaces because of the restriction to Hermitian matrices. Otherwise, non-orientable triangulations would be included.

The fact that, for the orientable case, the genus fully determines the topology of the triangulation allows to capture non-perturbative effects. Indeed, the perturbative expansion 2.58 can be rewritten as a topological expansion :

$$\mathcal{Z} = \sum_{g \in \mathbb{N}^*} N^{2-2g} \mathcal{Z}_g(\lambda) \ , \tag{2.61}$$

where we have defined the sum over all triangulations with genus g as $\mathcal{Z}_g(\lambda)$. Then, the leading order contribution in the $N \to \infty$ limit comes from the triangulations with zero genus, corresponding to spherical topologies. Interestingly, one can show that the partition function for zero genus surfaces, $\mathcal{Z}_0(\lambda)$ has the following critical behavior [3]:

$$\mathcal{Z}_0(\lambda) \sim |\lambda - \lambda_c|^{2-\gamma} \ , \tag{2.62}$$

where $\gamma = -1/2$ in this case. As a result, the free energy of the spherical sector diverges around the critical point $\lambda = \lambda_c$. This is an important conclusion, in accordance with the idea that a continuum phase of the theory occurs when $\lambda \to \lambda_c$. This conclusion is supported by the fact that in the vicinity of the critical value, $\mathcal{Z}_0$ is dominated by arbitrary large triangulations. To make this more concrete, we can assume that each triangle has a fixed area, say a, and compute the mean area :

$$\langle A \rangle = a \langle T(\Delta_\mathcal{G}) \rangle = a \frac{d}{d\lambda} \ln(\mathcal{Z}_0(\lambda)) \sim \frac{a}{|\lambda - \lambda_c|} \ . \tag{2.63}$$

Then, sending $a \to 0$ when $\lambda \to \lambda_c$, such that $\langle A \rangle$ remains unchanged, we find an infinitely refined spherical triangulation for a fixed area, in accordance with the intuitive idea of a continuum limit. Going beyond the spherical sector requires a *double scaling limit*, consisting in taking the two limits $N \to \infty$ and $\lambda \to \lambda_c$ in a correlated manner [3]. More precisely, we can show that $\mathcal{Z}_g$ has the same critical point than $\mathcal{Z}_0$ for any g:

$$\mathcal{Z}_g(\lambda) \sim |\lambda - \lambda_c|^{\frac{(2-\gamma)(2-2g)}{2}} \tag{2.64}$$

which suggests to take both the limits $N \to \infty$ and $\lambda \to \lambda_c$ in such a way that the ratio

$$N|\lambda - \lambda_c|^{(2-\gamma)/2} \tag{2.65}$$

remains fixed. As a result, all the topologies contribute to the free energy when we are close to the critical point:

$$\mathcal{Z} \sim \sum_g f_g \left[N|\lambda - \lambda_c|^{(2-\gamma)/2} \right]^{2-2g}. \tag{2.66}$$

These results suggest a way to understand the continuum limit, but a proper understanding requires a detailed analysis. For instance, using Schwinger-Dyson equations, we can show that *loop observables* turn to be the Witt algebra, which can be related to Wheeler-DeWitt equation in dimension two. The reader interested by technical details may consult standard references [3] on this subject.

We close this section with some physical remarks. We have seen that matrix models are statistical models for triangulated surfaces, but we have not made contact yet with quantum gravity in dimension two ! This correspondence can be understood as follows. Including cosmological constant, classical gravity in dimension two is described by the action:

$$\mathcal{S}_{2d} = \frac{1}{G} \int_\mathcal{M} d^2x \sqrt{-g}(-R(g) + \Lambda) = -\frac{4\pi}{G} \chi(\mathcal{M}) + \frac{\Lambda}{G} A_\mathcal{M} \ , \tag{2.67}$$

where we used the Gauss-Bonnet theorem to compute the integral in term of the Euler characteristic $\chi(\mathcal{M})$, and where we have denoted by $A_\mathcal{M}$ the area of the surface $\mathcal{M}$. Then, the theory only depends on two parameters, and we generally assume that only these two parameters are relevant to define the discretization. As a basic example, introducing an equilateral triangulation $\Delta_\mathcal{M}$ of $\mathcal{M}$, such that each triangle has a fixed area a, the action 2.67 can be discretized as

$$\mathcal{S}_{2d}(\Delta_\mathcal{M}) := -\frac{4\pi}{G} \chi(\Delta_\mathcal{M}) + \frac{\Lambda a}{G} T(\Delta_\mathcal{M}) \ , \tag{2.68}$$

and the quantum theory described by the partition function:

$$\mathcal{Z}_{2d} = \sum_{\Delta} e^{\frac{4\pi}{G}\chi(\Delta_{\mathcal{M}}) - \frac{\Lambda a}{G}T(\Delta_{\mathcal{M}})} \tag{2.69}$$

matches the partition function 2.58, up to the identification:

$$\lambda \leftrightarrow e^{-\Lambda a/G} \ , \qquad N \leftrightarrow e^{4\pi/G} \ . \tag{2.70}$$

As a conclusion, it seems that the large N limit of matrix models (involving a lot of "microscopic" degrees of freedom) matches the weak coupling regime of two dimensional gravity. To summarize, the matrix models are statistical models for random surfaces, which make contact with quantum gravity. In the large N limit, they seem to reach a continuum phase, dominated by spherical topologies. We can extend to all manifolds using a double scaling limit. Relation with GFTs is then obvious. In dimension two, matrix models are therefore the minimalistic backbone of a discrete path integral approach to quantum gravity, in the sense that degrees of freedom are purely combinatorial. This is fine enough because of the purely topological nature of two dimensional quantum gravity. In higher dimensions, however, topological manifold has to be endowed with a differential structure and presumably local Euclidean or Lorentz invariance (the choice depending on the signature of the space that we want to quantize). In GFTs, such a local invariance is assumed at a fundamental level, with the consequence that indices of matrix models become elements of the rotation group, Lorentz group, or a suitable subgroup of them. Moreover, as discussed in the first section, GFTs introduce a discrete connection on the random graphs, with the variables $\{h_e\}$ interpreted as a connection from a reference point inside of a dual triangle associated to a field, to the same point in another triangle sharing an edge with the first one. Some aspects in relation with this point are discussed in [2].

2.3.2 Higher dimensions and tensors

In this section, we briefly discuss the higher dimensional extension to matrix models, say tensor models [14], for which we give only an informal discussion. As matrices with 2 indices in 2 dimensions, it is natural to consider tensor of rank d in dimension d. The recipe used to construct the action for matrices 2.55 can be easily extended for a tensor of rank d. For instance, in dimension 3, a counterpart of 2.55 can be :

$$\mathcal{S}[T] = \frac{1}{2}\sum_{\vec{n}} T_{n_1 n_2 n_3} T_{n_3 n_2 n_1} - \lambda \sum_{\vec{n},\vec{n}'} T_{n_1, n_2 n_3} T_{n_3 n_5 n_4} T_{n_5 n_2 n_6} T_{n_4 n_6 n_1} \ , \tag{2.71}$$

where $\vec{n} \equiv (n_1, n_2, n_3)$, and all indices n_i run from 1 to N. In counterpart of the matrix case, each tensor is interpreted as a $(d-1)$-simplex, and the pattern in which the indices are contracted in the interaction term represents an elementary d-cell. As for matrix models, the challenge is to keep control on the sum over triangulations in the perturbative expansion of the associated statistical model. Unfortunately, unlike the case of matrices, all the generated triangulations are not discretization of topological manifolds. Indeed, singular contributions as pseudo manifolds or more dramatic configurations are generated [see [20] for instance]. The source of these pathological configurations has been clearly identified. They come from the fact that in dimension higher than two, the gluing rules for d-simplices along their $(d-1)$-boundaries do not guarantee elimination of singular structures. Note that such a situation occurs also for the standard GFTs. As a result, no $1/N$ expansion could be formulated for such tensor models, breaking down the

hope to generalize the achievements of matrix models in higher dimensions. Due to this dramatic issue, tensor models were aborted in favor of the *Dynamical triangulations* and *Causal Dynamical Triangulations* programs [19].

However, the failure of the earlier tensors models was not the end of the history, and in 2009, they were reborn with the work of Gurau on a special class of tensor models, called *colored tensor models*. The introduction of colors gave control over the combinatorics and topology, allowing to construct a proper $1/N$ expansion where contributions are labeled by a generalization of genus, the *Gurau degree*, and essentially eliminating the undesired singular structures [20]. Similarly with the matrix case, it has been established that leading order contributions in the large N limit correspond to *melonic diagrams*, which are dual to triangulations of sphere, maximizing the number of faces for a given number of vertices. We shall return to this point in the next chapter (see also [15]).

2.4 Achievements and perspectives

In this section we summarize the current research directions and some achievements of the GFT approach. As explained in this chapter, one of the main challenges of GFTs is to understand how the quantum degrees of freedom organize to make sense as a continuum limit corresponding to a semi-classical space-time. Such a program requires to control the sums over triangulations. However, due to the combinatorial structure of 2-complexes, such a goal is much more complicated than for ordinary Feynman diagrams. As explained at the end of the next section, colored tensor models made possible a huge step forward in that direction. They allow to give control over combinatorics and topology of Feynman graphs, as well as over their sums, providing a power counting and a well defined $1/N$ expansion, whose leading order graphs, the so-called melons, have spherical topology [15]. The same expansion has been achieved for topological GFTs, i.e. GFTs with closure constraint, where the parameter playing the role of N is expressed in term of the cut-off regularizing the theory [12], with the same leading order diagrams as for tensors models and the same suppression of singular topologies. Then, melonic diagrams seem to be universal in any models whose amplitudes scale with the number of faces. This counting is in fact the first step of a proper renormalization program, requiring to control sums over 2-complexes. It highlights the behavior of the theory in the large N limit, involving a lot of degrees of freedom. Because it is in this sector that divergences occur, we call this limit the UV limit, and the opposite one, for small N, the IR limit. Note, however, that this convention is the opposite of the one considered in loop quantum gravity, where large spins correspond to large area and volumes. But such a conflict is essentially semantic, due to the confusion between classical limit of quantum object, and classical limit of the (quantum) continuum limit. Anyway, ignoring physical meaning of these limits, such a conflict does not affect the renormalization procedure. From this point of view, only the localisation of divergent graphs is relevant. That we call this sector UV, IR, or otherwise is clearly secondary. We shall return on this specific point in the next chapter. Note that systematic renormalization requires a *notion of scale* at the graph level, in order to apply standard techniques as *multi-scale analysis*, as well as a good notion of locality. There is one class of models which provides both conditions, namely the so called *tensorial group field theories* (TGFTs), that we shall introduce in the next chapter and shall be concerned with in the rest of this thesis. "Tensorial" in this context refers to a specific pattern of contraction between tensorial indices, coming from colored models, and it is this tensorial invariance that provides a notion of locality, called *traciality*, which enables one to clearly define the contraction notion of "high" (i.e. UV) subgraphs. In addition, this class of models is characterized by the presence of

a Laplace-Beltrami type kinetic operator in the classical action:

$$\mathcal{S}_{kin} = \int d\mathbf{g}\bar{\phi}(\mathbf{g})\Big(-\sum_{i=1}^{d}\Delta_{\mathbf{G}_i} + m^2\Big)\phi(\mathbf{g}) \ . \tag{2.72}$$

$\Delta_{\mathbf{G}}$ denotes the Laplace-Beltrami operator on the group manifold $\mathbf{G}$. This non-trivial kinetic operator, motivated in particular by the computation of radiative corrections in topological GFTs [10], endows the graphs with a notion of scale corresponding to its eigenvalues. Some results have been obtained for this class of models, with or without closure constraint in several dimensions, and some of these topological models have been proved to be renormalizable in dimensions 3 and 4 [10]. Moreover, a classification of some interesting renormalizable models with *melonic interactions* has been obtained. A similar systematic analysis of renormalizability is currently in progress for models implementing the *simplcity constraint*, as an additional geometric condition imposed at the quantum level in order to guarantee that (in dimension four) bivectors associated to boundary triangles of a quantum tetrahedron are built from edges vectors of a geometric quantum tetrahedron [9]. In the future, renormalizability for models of the EPRL or BO types would be an important achievement for a more realistic quantum field theory for space time.

Another important tool, closely related to perturbative renormalization is the *renormalization group*, which determines the flow of effective GFT dynamics across scales. It is an helpful framework to map out the phase structure of the theory and is currently extensively studied. In particular, perturbative beta functions have been obtained for several models - including models with non-Abelian gauge invariance and geometric constraints [10]. All these computations seem to indicate that asymptotic freedom or safety is a generic feature of TGFTs. Then, for such models, no *Laudau poles* are to be feared, and the perturbative expansion can be well-defined all the way in the UV sector. Moreover, as in QCD, one expects that this property could be responsible for phase transitions generated dynamically across the scales (as from quarks to hadrons for QCD). One or several such transitions are expected from "discrete to continuum"' [25]. This scenario is sometimes called *geometrogenesis* in the literature. Understanding such phase transitions requires more advanced techniques. The most popular is the *Functional Renormalization Group* (FRG), allowing in many cases to compute the flow far from the perturbative regime (i.e. the Gaussian fixed point), mapping out phase diagrams and finding non-trivial fixed points. Such a program has been started with matrix models [22], and extended to TGFTs as well, with and without closure constraint [17]. We shall return to this point in Chapter 4. In all cases interesting information has been obtained on the phase structure of the theory, and there are indications of a phase transition from a phase characterized by a vanishing mean field to a non-vanishing one. Such a transition can be likely interpreted as a "condensed phase" of quantum degrees of freedom. In the GFT context, the existence of a phase transition has been proved in the melonic sector for topological BF models in any dimensions [13]. However, tensor models went analytically far beyond that stage, and, as for matrix models, critical points and critical exponents have been computed exactly for the leading order (which is the same as for topological GFTs), and likewise for subdominant orders [16].

In relation with the non-perturbative tools, another important current line of research concerns the constructive aspects of GFTs. Constructive field theory is a set of techniques allowing to make sense non only of the amplitudes but of the sum of the perturbative expansion as well. More precisely it allows to prove that this sum is convergent, usually in a certain extended sense such as Borel-summability [22]. The leading order, namely the melonic approximation, is summable in the ordinary sense, as adressed in Chapter 3 of this thesis. But Borel summability of the full

theory, including all subdominant orders, has been now obtained for many tensor models with quartic interactions [23]. The last chapter of this thesis will present the first such constructive results for TGFTs with Boulatov projectors.

To conclude this first chapter, we mention interesting (at least for the author) results about GFTs concerning cosmology and black-hole (more precisely "isolated horizon") entropy. In both case, we focus our attention on a special class of GFT states, the *GFT condensates* [21]. As in standard condensed matter physics, such states are characterized by an arbitrary number of quanta, the simplest case corresponding to the situation in which all these quanta are in the same quantum state. The interesting fact concerns the quantum dynamics of such states. Indeed, it has been established that, taking into account closure and simplicity constraint, such condensed states admit a nice interpretation as a continuum homogeneous space. More precisely, consider the Gross-Pitaevskii-like condensed state :

$$|\Psi\rangle := \mathcal{N}(\Psi) e^{\int d\mathbf{g} \Psi(\mathbf{g}) \hat{\varphi}^\dagger(\mathbf{g})} |0\rangle \ , \tag{2.73}$$

where the "macroscopic wave function" Ψ satisfies geometrical constraints, and $\mathcal{N}$ is a normalization factor. Inserting this Ansatz into the Schwinger-Dyson equations, one can show that the macroscopic wave function verifies [21]:

$$\int d\mathbf{g}' \mathcal{K}(\mathbf{g}, \mathbf{g}') \Psi(\mathbf{g}') + \lambda \frac{\delta \mathcal{V}[\phi, \hat{\phi}]}{\delta \bar{\phi}(\mathbf{g})} \bigg|_{\phi \to \Psi, \bar{\phi} \to \bar{\Psi}} = 0 \ , \tag{2.74}$$

where $\mathcal{K}$ and $\mathcal{V}$ are respectively the kinetic kernel and the interaction part of the classical action:

$$\mathcal{S} = \int d\mathbf{g} d\mathbf{g}' \bar{\phi}(\mathbf{g}) \mathcal{K}(\mathbf{g}, \mathbf{g}') \phi(\mathbf{g}') + \lambda \mathcal{V}[\phi, \bar{\phi}] \ . \tag{2.75}$$

From the interpretation of Ψ as a macroscopic wave function, describing continuum homogeneous geometry, equation 2.74 can be likely interpreted as a non linear extension of the Wheeler-DeWitt equation for quantum cosmology, which turns to be a semi-classical Friedman equation (up to some approximations), for simple models describing Lorentzian and Riemannian gravity. The beautiful point in this approach is that a quantum equation for cosmology and the semi-classical limit can be derived from a fundamental description of quantum gravity, for a suitable choice of quantum states, accordingly to the intuition of the condensation mechanism. The same trick, using condensed states describes continuum spherical (quantum) geometry of an horizon in fully quantum gravity. The quantum states are then described by a density matrix, whose reduced form, obtained by tracing over the bulk degrees of freedom, allows to recover the standard Bekenstein-Hawking entropy for an isolated horizon. This does not require to fix or fine tune the Immirizi parameter, as in the derivation from loop quantum gravity.

Bibliography

[1] R. De Pietri, L. Freidel, K. Krasnov and C. Rovelli "Barrett-Crane model from a Boulatov-Ooguri field theory over a homogeneous space" arXiv:hep-th/9907154;

[2] D. Oriti, "The microscopic dynamics of quantum space as a group field theory," in *Foundations of space and time*, G. Ellis, et al. (eds.) (Cambridge University Press, Cambridge UK, 2012), arXiv:1110.5606 [hep-th];

D. Oriti, "The Group field theory approach to quantum gravity," in *Approaches to quantum gravity*, D. Oriti (ed.) (Cambridge University Press, Cambridge UK, 2009), [gr-qc/0607032];

L. Freidel, "Group field theory: An Overview," Int. J. Theor. Phys. **44**, 1769 (2005) [hep-th/0505016];

A. Baratin and D. Oriti, "Ten questions on Group Field Theory (and their tentative answers)," J. Phys. Conf. Ser. **360**, 012002 (2012) [arXiv:1112.3270 [gr-qc]].

T. Krajewski, "Group field theories," PoS QGQGS **2011**, 005 (2011) [arXiv:1210.6257 [gr-qc]].

[3] P. Di Francesco, P. H. Ginsparg and J. Zinn-Justin, "2-D Gravity and random matrices," Phys. Rept. **254**, 1 (1995) [arXiv:hep-th/9306153];

F. David, "Planar diagrams, two dimensional lattice gravity and surface models," Nuclear Physics B, 257:45-58, 1985;

G.W. Moore, N. Seiberg and M. Staudacher, "From loops to states in 2-D quantum gravity," Nucl.Phys B, 362:665-709, 1991;

P.H. Ginsparg, "Matrix models of 2-d gravity," 1991, hep-th/9112013;

[4] Carlo Rovelli, "Quantum gravity," Cambridge University Press, 2004;

C. Rovelli and F. Vidotto, "Covariant Loop Quantum Gravity," Cambridge University Press, 2015;

T. Thiemann, "Modern canonical quantum general relativity," Cambridge University Press, 2007;

J. Baez and J. P. Muniain, "Gauge field, knots and gravity," World Scientific, 1994;

C. Kiefer, "Quantum gravity," Oxford University Press, 2007;

[5] B. Dittrich, C. Guedes, D. Oriti, "On the space of generalized fluxes for loop quantum gravity," arXiv:1205.6166 [gr-qc]. 10.1088/0264-9381/30/5/055008. Class.Quant.Grav. 30 (2013) 055008.

[6] S. Alexandrov, M. Geiller and K. Noui, "Spin Foams and Canonical Quantization," SIGMA, 8:055, 2012, 1112.1961;

J.C. Baez, " Spin Foam models," Class. Quant. Grav, 15:1827-1858, 1998, gr/qc/9709052;

L. Freidel and K. Krasnov, "A new Spin Foam Model for 4d Gravity," Class. Quant. Grav., 25:125018, 2008, 0708.1595;

L. Freidel and D. Louapre, "Ponzano-Regge model revisited I: Gauge fixing, observables and interacting spinning particles", arXiv:hep-th/0401076;

[7] D. Oriti, "Group field theory as the 2nd quantization of Loop Quantum Gravity," arXiv:1310.7786 [gr-qc]; D. Oriti, "Group Field Theory and Loop Quantum Gravity," arXiv:1408.7112 [gr-qc];

D. Oriti, J. P. Ryan and J. Thürigen, "Group field theories for all loop quantum gravity," New J.Phys. 17, 023042 (2015) [arXiv:1409.3150 [gr-qc]].

[8] L. Freidel and E. Livine, "3d Quantum Gravity and Effective Non-Commutative Quantum Field Theory", arXiv: hep-th/0512113;

L. Freidel and E. Livine, "Ponzano-Regge model revisited III: Feynman diagrams and Effective field theory" arXiv: hep-th/0502106

L. Freidel and S. Majid, "Noncommutative harmonic analysis, sampling theory and the Duflo map in 2+1 quantum gravity," Class. Quant. Grav., 25:045006, 2008, hep-th/0601004;

E. Joung, J. Mourad and K. Noui, "Three Dimensional Quantum Geometry and Deformed Poincare Symmetry," J.Math.Phys., 50:052503, 2009, 0806.4121;

C. Guedes, D. Oriti and M. Raasakka, "Quantization maps, algebra representation and non-commutative Fourier transform for Lie groups," 2013, Arxiv: 1301.7750;

A. Baratin and D. Oriti, "Group field theory with non-commutative metric variables," Phys. Rev. Lett., 105:221302, 2010, 1002.4723;

[9] J.C. Baez and J.W. Barrett, "The Quantum tetrahedron in three-dimensions and four-dimensions," Adv.Theor.Math.Phys., 3:815-850, 1999, gr-qc/9903060;

A. Baratin and D. Oriti, "Quantum Simplicial geometry in the group field theory formalism: reconsidering the Barrett-Crane model," New J.Phys., 13:125011, 2011, 1108.1178;

A. Baratin and D. Oriti, "Group field theory and Simplicial gravity path integrals: A model for Holst-Plebanski gravity," Phys.Rev., D85:044003, 2012, 1111.5842;

[10] L. Freidel, R. Gurau and D. Oriti, "Group field theory renormalization - the 3d case: Power counting of divergences," Phys. Rev. D **80**, 044007 (2009) [arXiv:0905.3772 [hep-th]].

J. Ben Geloun, J. Magnen and V. Rivasseau, "Bosonic Colored Group Field Theory," Eur. Phys. J. C **70**, 1119 (2010) [arXiv:0911.1719 [hep-th]].

J. Ben Geloun, T. Krajewski, J. Magnen and V. Rivasseau, "Linearized Group Field Theory and Power Counting Theorems," Class. Quant. Grav. **27**, 155012 (2010) [arXiv:1002.3592 [hep-th]];

J. Ben Geloun and V. Bonzom, "Radiative corrections in the Boulatov-Ooguri tensor model: The 2-point function," Int. J. Theor. Phys. **50**, 2819 (2011) [arXiv:1101.4294 [hep-th]];

J. Ben Geloun and V. Rivasseau, "A Renormalizable 4-Dimensional Tensor Field Theory," Commun. Math. Phys. **318**, 69 (2013) [arXiv:1111.4997 [hep-th]].

J. Ben Geloun and V. Rivasseau, "Addendum to 'A Renormalizable 4-Dimensional Tensor Field Theory'," Commun. Math. Phys. **322**, 957 (2013) [arXiv:1209.4606 [hep-th]].

J. Ben Geloun and E. R. Livine, "Some classes of renormalizable tensor models," J. Math. Phys. **54**, 082303 (2013) [arXiv:1207.0416 [hep-th]].

J. Ben Geloun, "Renormalizable Models in Rank $d \geq 2$ Tensorial Group Field Theory," Commun. Math. Phys. **332**, 117–188 (2014) [arXiv:1306.1201 [hep-th]];

J. Ben Geloun and D. O. Samary, "3D Tensor Field Theory: Renormalization and One-loop β-functions," Annales Henri Poincare **14**, 1599 (2013) [arXiv:1201.0176 [hep-th]].

J. Ben Geloun, "Two and four-loop β-functions of rank 4 renormalizable tensor field theories," Class. Quant. Grav. **29**, 235011 (2012) [arXiv:1205.5513 [hep-th]].

D. O. Samary, "Beta functions of $U(1)^d$ gauge invariant just renormalizable tensor models," Phys. Rev. D **88**, 105003 (2013) [arXiv:1303.7256 [hep-th]].

S. Carrozza, D. Oriti and V. Rivasseau, "Renormalization of Tensorial Group Field Theories: Abelian U(1) Models in Four Dimensions," Commun. Math. Phys. **327**, 603 (2014) [arXiv:1207.6734 [hep-th]].

S. Carrozza, D. Oriti and V. Rivasseau, "Renormalization of a SU(2) Tensorial Group Field Theory in Three Dimensions," Commun. Math. Phys. **330**, 581 (2014) [arXiv:1303.6772 [hep-th]].

S. Carrozza, "Tensorial methods and renormalization in Group Field Theories," Springer Theses, 2014 (Springer, NY, 2014), arXiv:1310.3736 [hep-th].

D. O. Samary and F. Vignes-Tourneret, "Just Renormalizable TGFT's on $U(1)^d$ with Gauge Invariance," Commun. Math. Phys. **329**, 545 (2014) [arXiv:1211.2618 [hep-th]].

M. Raasakka and A. Tanasa, "Combinatorial Hopf algebra for the Ben Geloun-Rivasseau tensor field theory," Seminaire Lotharingien de Combinatoire 70 (2014), B70d [arXiv:1306.1022 [gr-qc]].

D. O. Samary, "Closed equations of the two-point functions for tensorial group field theory," Class. Quant. Grav. **31**, 185005 (2014) [arXiv:1401.2096 [hep-th]].

J. Ben Geloun, "On the finite amplitudes for open graphs in Abelian dynamical colored Boulatov-Ooguri models," J. Phys. A **46**, 402002 (2013) [arXiv:1307.8299 [hep-th]].

S. Carrozza, "Discrete Renormalization Group for SU(2) Tensorial Group Field Theory," arXiv:1407.4615 [hep-th].

V. Lahoche and D. Oriti, "Renormalization of a tensorial field theory on the homogeneous space SU(2)/U(1)," arXiv:1506.08393 [hep-th].

V. Lahoche, D. Oriti and V. Rivasseau, "Renormalization of an Abelian Tensor Group Field Theory: Solution at Leading Order," JHEP **1504**, 095 (2015) [arXiv:1501.02086 [hep-th]].

[11] V. Rivasseau, "Why are tensor field theories asymptotically free?", arXiv: 507.04190v1.

S. Carrozza, "Group field theory in dimension $4 - \epsilon$," Phys. Rev. D **91**, 065023 (2015) [arXiv:1411.5385 [hep-th]].

[12] S. Carrozza, "Singular topologies in the Boulatov model," arXiv:1112.2886 [gr-qc]. 10.1088/1742-6596/360/1/012045. J.Phys.Conf.Ser. 360 (2012) 012045;

S. Carrozza and D. Oriti, "Bounding bubbles: the vertex representation of 3d Group Field Theory and the suppression of pseudo-manifolds," arXiv:1104.5158 [hep-th]. 10.1103/PhysRevD.85.044004. Phys.Rev. D85 (2012) 044004;

Sylvain Carrozza, Daniele Oriti, "Bubbles and jackets: new scaling bounds in topological group field theories," arXiv:1203.5082 [hep-th], JHEP 1206 (2012) 092.

[13] A. Baratin, S. Carrozza, D. Oriti, J.P. Ryan and M. Smerlak, "Melonic phase transition in group field theory," 2013, [arXiv: 1307.5026];

[14] J. Ambjorn, B. Durhuus and T. Jonsson, "Three-Dimensional Simplicial Quantum Gravity And Generalized Matrix Models," Mod. Phys. Lett. A **6**, 1133 (1991).

M. Gross, "Tensor models and simplicial quantum gravity in $>$ 2-D," Nucl. Phys. Proc. Suppl. **25A**, 144 (1992).

[15] R. Gurau and J. P. Ryan, "Colored Tensor Models - a review," SIGMA, 8:020, 2012,1109.4812;

R. Gurau, "The 1/N expansion of colored tensor models," Annales Henri Poincare **12**, 829 (2011) [arXiv:1011.2726 [gr-qc]].

R. Gurau and V. Rivasseau, "The 1/N expansion of colored tensor models in arbitrary dimension," Europhys. Lett. **95**, 50004 (2011), [arXiv:1101.4182 [gr-qc]].

R. Gurau, "The complete 1/N expansion of colored tensor models in arbitrary dimension," Annales Henri Poincare **13**, 399 (2012) [arXiv:1102.5759 [gr-qc]].

V. Bonzom, R. Gurau, and V. Rivasseau, "Random tensor models in the large N limit: Uncoloring the colored tensor models," Phys. Rev. **D85**, 084037 (2012), [arXiv:1202.3637 [hep-th]].

R. Gurau and J. P. Ryan, "Melons are branched polymers," Annales Henri Poincare **15** no. 11, (2014) 2085, [arXiv:1302.4386 [math-ph]];

[16] V. Bonzom, R. Gurau, A. Riello and V. Rivasseau, "Critical behavior of colored tensor models in the large N limit," Nucl. Phys. B **853** (2011) 174 [arXiv:1105.3122 [hep-th]].

T. Delepouve and R. Gurau, "Phase Transition in Tensor Models," JHEP **1506**, 178 (2015) [arXiv:1504.05745 [hep-th]].

D. Benedetti and R. Gurau, "Symmetry breaking in tensor models," arXiv:1506.08542 [hep-th].

S. Dartois, R. Gurau, and V. Rivasseau, "Double scaling in tensor models with a quartic interaction," JHEP **1309** (2013) 088 [arXiv:1307.5281 [hep-th]];

[17] D. Benedetti and V. Lahoche "Functional Renormalization Group Approach for Tensorial Group Field Theory: a Rank-6 Model with Closure Constraint", arXiv:1508.06384 [hep-th];

D. Benedetti, J. Ben Geloun and D. Oriti, "Functional Renormalisation Group Approach for Tensorial Group Field Theory: a Rank-3 Model," JHEP **1503**, 084 (2015) [arXiv:1411.3180 [hep-th]].

J. Ben Geloun, R. Martini and D. Oriti, "Functional Renormalisation Group analysis of a Tensorial Group Field Theory on $\mathbb{R}^3$," arXiv:1508.01855 [hep-th].

Joseph Ben Geloun, Tim A. Koslowski. "Nontrivial UV behavior of rank-4 tensor field models for quantum gravity," arXiv:1606.04044 [gr-qc];

[18] A. Eichhorn and T. Koslowski, "Continuum limit in matrix models for quantum gravity from the Functional Renormalization Group," Phys. Rev. D **88**, 084016 (2013) [arXiv:1309.1690 [gr-qc]].

A. Eichhorn and T. Koslowski, "Towards phase transitions between discrete and continuum quantum spacetime from the Renormalization Group," Phys. Rev. D **90**, no. 10, 104039 (2014) [arXiv:1408.4127 [gr-qc]].

[19] J. Ambjorn, A. Goerlich, J. Jurkiewicz and R. Loll, "Nonperturbative Quantum Gravity," Phys. Rept., 519:127-210, 2012, 1203.3591;

[20] R. Gurau, "Lost in Translation: Topological Singularities in Group Field Theory," Class. Quant. Grav., 27:235023, 2010, 1006.0714;

[21] D. Oriti, R. Pereira, L. Sindoni, "Coherent states for quantum gravity: towards collective variables," arXiv:1202.0526 [gr-qc]. Class.Quant.Grav. 29 (2012) 135002.

D. Oriti, L. Sindoni, E. Wilson-Ewing, "Emergent Friedmann dynamics with a quantum bounce from quantum gravity condensates," arXiv:1602.05881 [gr-qc];

D. Oriti, D. Pranzetti, L. Sindoni, "Horizon entropy from quantum gravity condensates," arXiv:1510.06991 [gr-qc], Phys.Rev.Lett. 116 (2016) no.21, 211301;

S. Gielen, D. Oriti, "Quantum cosmology from quantum gravity condensates: cosmological variables and lattice-refined dynamics," arXiv:1407.8167 [gr-qc], New J.Phys. 16 (2014) no.12, 123004;

S. Gielen, D. Oriti, L. Sindoni, "Homogeneous cosmologies as group field theory condensates," arXiv:1311.1238 [gr-qc]. JHEP 1406 (2014) 013;

[22] V. Rivasseau, "From perturbative to constructive renormalization", Princeton University Press (1991);

V. Rivasseau and Z. Wang, "Loop Vertex Expansion for Phi**2K Theory in Zero Dimension," J. Math.Phys.51, 092304 (2010), arXiv:1003.1037 [math-ph];

V. Rivasseau and Z. Wang, "How to Resum Feynman Graphs", Ann. Henri Poincare 15, 2069-2083(2014), arXiv:1304.5913 [math-ph].;

[23] R. Gurau, "The $1/N$ Expansion of Tensor Models Beyond Perturbation Theory", Comm. Math. Phys.330, 973-1019 (2014), arXiv:1304.2666.

T. Delepouve, R. Gurau and V. Rivasseau, "Universality and Borel Summability of Arbitrary Quartic Tensor Models", arXiv:1403.0170 [hep-th].

T. Delepouve and V; Rivasseau, "Constructive Tensor Field Theory: The T^4_3 Model", arXiv:1412.5091 [math-ph].

V. Rivasseau, "Constructive Tensor Field Theory," arXiv:1603.07312 [math-ph].

[24] P.A.M. Dirac, Lectures on quantum mechanics, 1964.

[25] V. Rivasseau, "Quantum Gravity and renormalization : The Tensor Track," AIP Conf Proc., 1444:18-29, 2011, 1112.5104;

V. Rivasseau, "The Tensor Track: an Update," 2012, arXiv:1209.5284.

V. Rivasseau, "The Tensor Track, III," Fortsch. Phys. **62**, 81 (2014), arXiv:1311.1461.

V. Rivasseau, "The Tensor Track, IV," arXiv:1604.07860 [hep-th].

Chapter 3

Colors and Tensoriality

As pointed out in the previous chapter, standard GFTs, like e.g. the Boulatov model, are problematic. Indeed they generate singular topologies which are not even pseudo-manifolds and which generically dominate the power counting. These singular topologies appear at each order in the perturbative expansion [1]. To circumvent this difficulty, Gurau [4] introduced in 2009 *colored group field theories* and showed that, unlike standard GFTs, their Feynman graphs are dual to pseudo-manifolds [1]. Colored GFTs and colored tensor models have then considerably developed. The introduction of colors is a way to take control on topological sums and to suppress too singular topologies. Perhaps even more importantly it allows to define properly and canonically the concept of *faces* of the associated Feynman graphs[1], clearly a key point in order to discretize the Einstein-Hilbert action on the dual triangulations, and it provides a $1/N$ expansion as for matrix models. Moreover, a complementary result obtained in 2011 [2] shows that, for topological Boulatov-like models, to encode the action of discrete diffeomorphisms into a field transformation requires the colored framework. Both results signaled the birth of colored GFTs and colored tensors models as a promising renewed approach to quantum gravity. A second evolution for GFTs and tensors came with the discovery of *tensor invariance*. Indeed, it has been shown that color structure can be implemented in an efficient way as a $U(N)^{\times d}$ invariance [3], where d denotes the rank of the tensors, opening the way to *tensorial group field theories* (TGFTs), a formalism in which at last a renormalization program could be launched and has recently witnessed dramatic progress.

The structure of this chapter is the following. In the first section, we shall give a formal definition of colored GFTs in any dimension. Note that we shall focus on a Boulatov-like model, describing topological BF-theories. After a brief reminder of the essential arguments for colors, we shall move on to the special case of colored tensor models, for which we recall some basic topics like the $1/N$ expansion, the characterization of leading order graphs and their critical behavior. We shall then extend these topics to colored GFTs, introduce the tensorial invariance, and show how all this leads us to TGFTs.

[1]For the impatient reader, here is a spoiler of this canonical definition: the set of faces of a regular edge-colored graph is simply the (disjoint) union over all color pairs of the connected components of the subgraph made of edges of the graph with colors in that pair.

3.1 Colored Group Field Theories

3.1.1 Formal definition and colored graphs

Considering $\mathbf{G}$ a group manifold, the colored version of the Boulatov group field theory in dimension d is a field theory for a collection of $d+1$ complex fields : $\phi_c, \bar{\phi}_c : \mathbf{G}^d \to \mathbb{C}$, $c \in [\![0, d]\!]$. Moreover, each field is assumed to satisfy the closure constraint, that is to say, to be invariant under diagonal action of the group manifold:

$$\phi_c(g_1, ..., g_d) = \phi_c(g_1 h, ..., g_d h) \quad \forall h \in \mathbf{G}, \forall c\,. \tag{3.1}$$

The classical field theory is defined by its action $\mathcal{S}$, which is the sum of two terms:

• The "kinetic term", $\mathcal{S}_{kin}$, whose kernels are generically assumed to be identically distributed:

$$\mathcal{S}_{kin}[\{\phi_c, \bar{\phi}_c\}] := \sum_{c=0}^{d} \int_{\mathbf{G}^d} d\mathbf{g} \bar{\phi}_c(\mathbf{g}) \phi_c(\mathbf{g})\,. \tag{3.2}$$

• The interaction part, $-\mathcal{S}_{int} = \lambda \mathcal{V} + \bar{\lambda}\bar{\mathcal{V}}$, with simplicial pattern for contraction of group variables:

$$-\mathcal{S}_{int}[\{\phi_c, \bar{\phi}_c\}, \lambda, \bar{\lambda}] := \lambda \int \prod_{i<j} dg_{ij} \prod_{c=0}^{d} \phi_c(\mathbf{g}_c) + \bar{\lambda} \int \prod_{i<j} dg_{ij} \prod_{c=0}^{d} \bar{\phi}_c(\mathbf{g}_c)\ , \tag{3.3}$$

where $\lambda, \bar{\lambda}$ are coupling constants, $\mathbf{g}_c := (g_{cc-1}, ..., g_{c0}, g_{cd}, ..., g_{cc+1})$ and $g_{ij} = g_{ji}$. Moreover, we adopt the same conventions as in Chapter 1, and for instance dg_{ij} refers to the Haar measure over the group manifold $\mathbf{G}$. The quantum theory is then defined by the partition function. As discussed in Chapter 1, the closure constraint has to be implemented in the definition of the Gaussian measure $d\mu_P[\{\phi_c, \bar{\phi}_c\}]$, or, equivalently, in the definition of the propagator, which in our case, reduces to the projector $\hat{P}$ into the gauge invariant fields subspace:

$$\int d\mu_P[\{\phi_c, \bar{\phi}_c\}] \bar{\phi}_c(\mathbf{g}) \phi_{c'}(\mathbf{g}') = \delta_{cc'} \int_{\mathbf{G}} dh \prod_{c=1}^{d} \delta(g_c h g'_{c'})\ . \tag{3.4}$$

The following partition function defines the quantum theory:

$$\mathcal{Z}(\lambda, \bar{\lambda}) = \int d\mu_P[\{\phi_c, \bar{\phi}_c\}] e^{-\mathcal{S}_{int}[\{\phi_c, \bar{\phi}_c\}, \lambda, \bar{\lambda}]}\ . \tag{3.5}$$

The two terms of the interaction S_{int} are interpreted as involving $(d+1)$ $(d-1)$-simplices, glued pairwise along $(d-2)$ sub-simplices, along a pattern dictated by the requirement that the interaction corresponds to a d-simplex. The rules for contractions are pictorially described on Figure 3.1 and 3.2 below, for the case $d = 3$. Figure 3.1a gives the strand structure of the generic interaction, and Figure 3.1b gives a colored edge representation for each of the two interactions, with the convention that black (respectively white) vertices correspond to the fields ϕ_c (respectively $\bar{\phi}_c$). Figure 3.2 illustrates the correspondence with the dual tetrahedron, and highlights the contraction scheme.

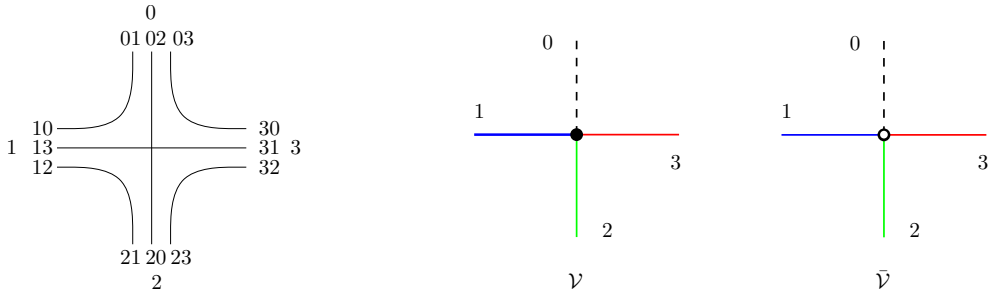

Figure 3.1: Stranded representation of a vertex (a) and colored edges representation of the vertex $\mathcal{V}$ and $\bar{\mathcal{V}}$ (b), both for the special case $d = 3$. We have adopted the standard graphical convention and represented lines of colors 0 by a dashed line.

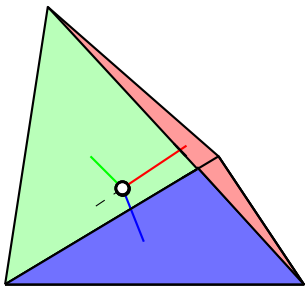

Figure 3.2: Dual tetrahedron associated to the vertex $\mathcal{V}$.

The free energy $\mathcal{W} := \ln(\mathcal{Z})$ can be computed (at least formally) in perturbation theory as a Feynman expansion:

$$\mathcal{W}_{formal} = \sum_{\mathcal{G}} \frac{(\lambda\bar{\lambda})^{V(\mathcal{G})/2}}{\mathrm{Sym}(\mathcal{G})} \mathcal{A}_{\mathcal{G}} \tag{3.6}$$

where each term is labeled by a closed connected $d+1$-*colored bipartite regular graph* $\mathcal{G}$:

Definition 1. *A $d+1$-colored graph $\mathcal{G}$ is a set $\mathcal{G} = (V, E)$, with V and E respectively the sets of vertices and edges, such that:*

• *The set V is bipartite : $V = \mathfrak{V} \cup \bar{\mathfrak{V}}$, such that $\mathfrak{V}$ and $\bar{\mathfrak{V}}$ have the same cardinality, and, for each $e \in E$, $e = (v, \bar{v})$, $v \in \mathfrak{V}$, $\bar{v} \in \bar{\mathfrak{V}}$.*

• *The edge set E is partitioned into $d+1$ subsets : $E = \cup_{c=0}^{d} E^c$, where E^c is the subset of edges of colors c.*

• *Each (black or white) vertex is $d+1$-valent, with all edges incident to a given vertex having distinct colors.*

Figure 3.3 gives an example of such a vacuum graph. At this stage, we have to precise some key points. In a nutshell, we can say that the only difference with conventional GFTs is the obligation for Feynman graphs generated by the perturbative expansion to be *colorable* and *bipartite*. These two conditions are sufficient to generate (infinitely many) random triangulations of any (piecewise linear) pseudo-manifold and only of these. In particular, singularities known as *tadfaces* - i.e. a face running several times around the same line - are automatically suppressed.

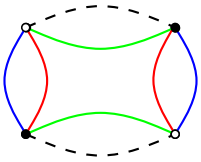

Figure 3.3: An example of vacuum Feynman graph with $d = 3$.

Moreover, due to the color structure, any Feynman graph $\mathcal{G}$ has the structure of a *D-dimensional cellular complex*. This relies on the fact that each d-dimensional tetrahedron is colored, hence carries more information than the basic tetrahedron for standard GFTs. More precisely, given a fixed dimension d, a tetrahedron of a colored triangulation has d type of colored faces, such that the general $(d-k)$-faces are labeled by k-uplet of colors $(1 \leq k \leq d)$. Note that this point, and in particular the unambiguous definition of the concept of face, which is required for discretizing the Einstein-Hilbert action on the triangulated space-time, is perhaps the most important aspect of colored models.

Definition 2. *We call D-bubble with colors $\{i_1, ..., i_D\}$ of a $d+1$-colored graph $\mathcal{G}$ any connected component $\mathcal{B}^{i_1,...,i_D}$ of $\mathcal{G}$ made of edges of colors $\{i_1, ..., i_D\}$ only.*

As an illustration, Figure 3.4 below gives two basic examples of bubbles of the vacuum graph pictured on Figure 3.3.

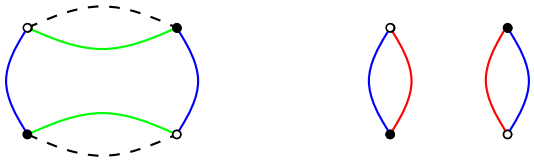

a b

Figure 3.4: Examples of 3-bubbles obtained from the graph of Figure 3.3 by removing the edges of color red (a) and 2-bubbles obtained by removing the green and dashed edges (b).

Definition 3. *Let $\mathcal{G}$ a $d+1$-colored graph. A k-dipole, with $1 \leq k \leq d+1$ is made of two black and white vertices linked by k colored edges.*

Definition 4. *A k-dipole contraction is the deletion of the k colored edges together with the two black and white vertices, such that the remaining edges initially hooked to these vertices are reconnected following their color.*

Figure 3.5 gives an example of k-dipoles and k-dipole contractions. In the same way, we can define the inverse operation, the *k-dipole creation*, which, together with the contraction, forms the *dipole moves*. These moves generate *discrete homeomorphisms*. Interestingly for our purpose is the following proposition [5]:

Proposition 1. *Consider a k-dipole d_k. The two pseudo-manifolds dual to $\mathcal{G}$ and $\mathcal{G}/d_k$ are homeomorphic if at least one of the bubbles separated by d_k is a sphere.*

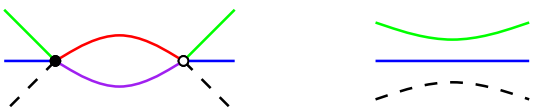

a b

Figure 3.5: An example of 2-dipole with $d = 4$ (a) and the result of its contraction (b).

For completeness, we now introduce the notions of *jacket* and *Gurau degree*:

Definition 5. *Let $\mathcal{G}$ be a $(d+1)$-colored graph. A **jacket** $\mathcal{J}_\sigma$ of $\mathcal{G}$, labeled by a $(d+1)$-cycle σ in the color set (up to orientation), is a ribbon graph made from the same vertices and edges than $\mathcal{G}$, but with the restricted set of faces $\mathcal{F} = \{\sigma^q(0), \sigma^{q+1}(0)\,, q \in \mathbb{Z}_{d+1}\}$.*

Hence a $(d+1)$-colored graph has exactly $d!/2$ jackets, leading to the next definition.

Definition 6. *The **Gurau degree** $\varpi(\mathcal{G})$ of a $d+1$-colored graph $\mathcal{G}$ is the integer given by the sum of the genera of all its $d!/2$ jackets:*

$$\varpi(\mathcal{G}) = \sum_{\mathcal{J}} g_{\mathcal{J}}\,. \tag{3.7}$$

The Gurau degree appears in the large N-expansion for colored tensor models, that we shall discuss in the Section 3.1.3. The notion of jacket is important, not only for the definition of that degree, but for the characterization of the triangulated pseudo-manifold. For instance, in dimension 3, they are dual to quadrangulation of a normal Heegaard surface, bounding two handlebodies [6]. Graphically, from the dual tetrahedron, the choice of a cyclic ordering of the colors corresponds to the choice of a quadrilateral in the tetrahedron, see Figure 3.6. More details about colored graphs can be found in [5].

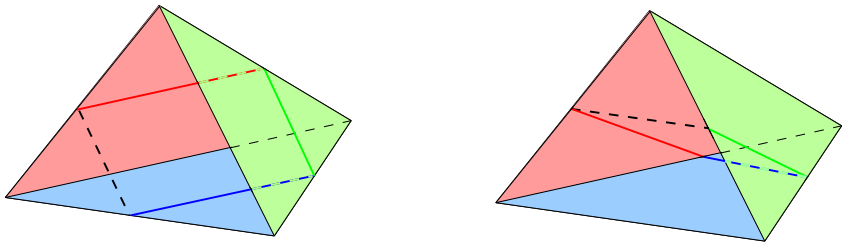

Figure 3.6: Two examples of jacket quads in a tetrahedron, corresponding to two different cycles.

Note that, thanks to the complex nature of the fields ϕ_c, the dual manifold associated to the ribbon graph of any jacket is orientable. Finally, we end this section by the following relation between the degree, the number of faces and the dimension, which will be useful in the next section:

Proposition 2. *Let $\mathcal{G}$ be a $d+1$-colored graph, $V(\mathcal{G})$ and $F(\mathcal{G})$ the cardinality of its sets of black and white vertices and faces. We have:*

$$\frac{2}{(d-1)!}\varpi(\mathcal{G}) = \frac{d(d-1)}{4}V(\mathcal{G}) + d - F(\mathcal{G})\,. \tag{3.8}$$

This proposition follows from combining the Euler relation for each jacket of the graph with the observation that each face, being associated to a pair of colors, always belongs to the *same* number of jackets, namely those in which these two colors are *adjacent* in the cycle defining the jacket.

3.1.2 Comment about diffeomorphisms in dimension three

In this section we recall briefly the relation between colors and diffeomorphisms, which played an important role in the genesis of colored GFTs. The understanding of the discrete counterpart of gravity symmetries in the GFT framework is an important step towards the understanding of the

continuum classical limit and its relation with general relativity. A partial achievement in this direction has been established for $d = 3$ in [2]. The authors have shown that colored Boulatov models have a quantum symmetry, corresponding to the action of the deformed Drinfeld double $\mathcal{D}SO(3) := \mathcal{C}(SO(3)) \rtimes \mathbb{C}SO(3)$, and in particular, uncovered a translation symmetry that they identified as a discrete diffeomorphism invariance. As an additional insight, they showed that diffeomorphism symmetry is unbroken at the quantum level only for the colored models, pointing out the relevance of the color structure for $3d$ gravity and BF theories. We insist however on the fact that, roughly speaking, this argument does not concern realistic four-dimensional quantum gravity models, and as far as the author knows, it has not been successfully extended to dimensions higher than three, except for topological models. In absence of extensions to models implementing simplicity constraints, the argument in favor of colors coming from discrete symmetries remains only partly convincing. Nevertheless it is fair to consider it as another advantage of the colored formalism, at least in the context of toplogical gravity.

3.1.3 The tensors models

In this section we move on to the colored tensor models. These models have the same combinatorial structure as the class of colored GFTs presented above, but with a minimal algebraic structure. It makes the analytic computations of amplitudes easier, and they are an ideal framework to explore only the combinatorial aspects of the colored theories. For general references on this subject, the reader may consult [5, 7].

Definition

Let us start by a definition of colored tensor models in any dimension d (assumed to be higher than 2, where tensors reduce to matrices). A colored tensor model is a statistical description of a set of $d+1$ N^d-indexed complex random variables, denoted as $T^c_{n_1,...,n_d}$, where $c \in [\![0, d]\!]$, and $n_i \in [\![1, N]\!]$, for some positive integer N. The statistical model is defined by the partition function:

$$\mathcal{Z}_{tensors}(\lambda, \bar{\lambda}) = \int \prod_{c, \mathbf{n}_c \in \mathbb{N}^d_N} \frac{1}{2i\pi} dT^c_{n_{c1},...,n_{cd}} d\bar{T}^c_{n_{c1},...,n_{cd}} e^{-\mathcal{S}_{\lambda,\bar{\lambda}}[T,\bar{T}]} \tag{3.9}$$

where $\mathbf{n} := \{n_1, ..., n_d\}$, $dT^c_{n_1,...,n_d} d\bar{T}^c_{n_1,...,n_d}/2i\pi$ is the Lebesgue measure over $\mathbb{C}$, and the action $\mathcal{S}_{\lambda,\bar{\lambda}}$ is the sum of a kinetic and interacting part, both defined as:

$$\mathcal{S}_{kin} = \sum_c \sum_{\mathbf{n}_c} \bar{T}^c_{\mathbf{n}_c} T^c_{\mathbf{n}_c}\,, \tag{3.10}$$

$$-\mathcal{S}_{int}(\lambda, \bar{\lambda}) = \frac{\lambda}{N^{d(d-1)/4}} \sum_{n_{ij}, i<j} \prod_c T^c_{\mathbf{n}_c} + \frac{\bar{\lambda}}{N^{d(d-1)/4}} \sum_{n_{ij}, i<j} \prod_c \bar{T}^c_{\mathbf{n}_c} \tag{3.11}$$

where we have used the short-hand notation

$$T^c_{\mathbf{n}} \equiv T^c_{n_1,...,n_d}, \quad \mathbf{n}_c := \{n_{cc-1}, ..., n_{c1}, n_{cd+1}, ..., n_{cc+1}\} \quad \forall c \in [\![0, d]\!], \tag{3.12}$$

and we assumed that $n_{ij} = n_{ji}$. Note that, because the dual of $U(1)$ is $\mathbb{Z}$, a tensor model may be considered as a colored GFT over the simpler group manifold $U(1)$, written in Fourier representation, and with a sharp cut-off truncation in momentum space.

Large N-expansion

In a perturbative framework, the partition function 3.9 can be expanded in power of λ and $\bar{\lambda}$ as a sum over Feynman $d+1$ colored vacuum graphs:

$$\mathcal{Z}_{tensor}(\lambda,\bar{\lambda}) = \sum_{\mathcal{G}} \frac{(\lambda\bar{\lambda})^{V(\mathcal{G})/2}}{\mathrm{Sym}(\mathcal{G})}\mathcal{A}_{\mathcal{G}}\,. \tag{3.13}$$

Due to the simple algebraic structure of tensors, the amplitude $\mathcal{A}_{\mathcal{G}}$ can be easily computed, and only depends on N. First of all, each (black or white) vertex contributes to the amplitude with a factor $N^{-d(d-1)/4}$. Then, with our choice for the kinetic part of the action, the propagator is simply a product of Kronecker deltas:

$$\int \prod_c dT^c d\bar{T}^c e^{-\mathcal{S}_{kin}} T^{c_1}_{\mathbf{n_1}} \bar{T}^{c_2}_{\mathbf{n_2}} = \delta_{c_1c_2}\prod_c \delta_{n_{1c}n_{2c}}\ , \tag{3.14}$$

implying that each face contributes with a factor N to any amplitude. Taking into account all these contributions, we have then :

$$\mathcal{A}_{\mathcal{G}} = N^{F(\mathcal{G})-\frac{d(d-1)}{4}V(\mathcal{G})}. \tag{3.15}$$

This expression gives the *power counting*, that is to say, the dependence in N of the amplitude. But it is not *a priori* a $1/N$ expansion in the sense of matrix models for instance. In the case of matrix models, the scaling with N depends on a quantity, the genus, which is topological in nature. For the moment (3.15) alone does not prove yet the existence of a $1/N$ expansion. To unlock such an expansion we have to combine (3.15) with Proposition 2. This allows to rewrite the amplitude in terms of the Gurau degree ϖ:

$$\mathcal{A}_{\mathcal{G}} = N^{d-\frac{2}{(d-1)!}\varpi(\mathcal{G})}. \tag{3.16}$$

Contrary to the genus for 2-dimensional manifolds, the Gurau degree ϖ is not a topological invariant[2]. However, it is clear from its definition 6 that it is a positive integer, because the genus is always a positive integer. Hence in any case the amplitude $\mathcal{A}_{\mathcal{G}}$ is bounded by N^d. A leading set of graphs (the ones with $\varpi(\mathcal{G}) = 0$) dominates, and subleading contributions can be organized according to their increasing degree. Reorganizing the perturbative expansion according to the Gurau degree follows the pattern we discussed in Chapter 1 for ribbon graphs according to their genus. The tensorial $1/N$ expansion for colored tensors models follows and generalizes the 'tHooft expansion of matrix models!

Critical behavior: leading and next to leading order

The leading order graphs, with vanishing degree, play the same role as planar graphs for matrix models, and therefore have been actively studied in the first age of colored tensor models. An important step in their understanding was achived in [8], where a proper characterization of these graphs, the so-called *melons-graphs* has been first established.

Definition 7. *A melon is a colored graph $\mathcal{G}$ with zero Gurau degree: $\varpi(\mathcal{G}) = 0$.*

Due to the fact that the genus is a positive number, the vanishing of the degree implies the vanishing of the genus of all the jackets, and then :

[2]The degree combines in fact some topological and some combinatorial information.

Proposition 3. *Topologically, a $d+1$-colored graph with vanishing Gurau degree is dual to the triangulation of a sphere $\mathbb{S}^d$ for $d > 2$.*

Note that this result can be proved by recursion using Proposition 3.1.1. The melons have a simple recursive definition. The simplest of them, the *mother of melons* with only two vertices is pictured in Figure 3.7 below, for which it is easy to check that $\varpi = 0$.

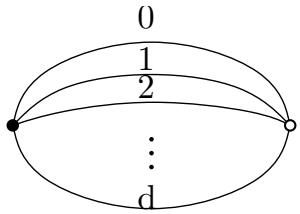

Figure 3.7: The mother of melons: the simplest melon with two black and white vertices.

Let us denote the set of melons with $2p$ vertices as $\mathcal{M}_p$. Obviously, $\mathcal{M}_1$ has only one element. The rule to generate the set $\mathcal{M}_{p+1}$ from $\mathcal{M}_p$ is the following: we replace any colored edge, say of color i of an element $m_p \in \mathcal{M}_p$ by an *elementary melon* as pictured in Figure 3.8, and an example of a generic melon is pictured on Figure 3.9. The proof that the melon family obeys to this recursive definition is a little subtle. Indeed, it is easy to check that such a melonic insertion does not change the degree. And then, the recursive family, as we just described it, is certainly included in the set of melonic graphs. It is however more difficult to prove that melons have necessarily this structure, and this step is the object of [8], where the authors show that a melonic graph has necessarily at least one elementary melon of the type of the right side of Figure 3.8. Because the contraction of such a subgraph does not affect the degree, the proof follows.

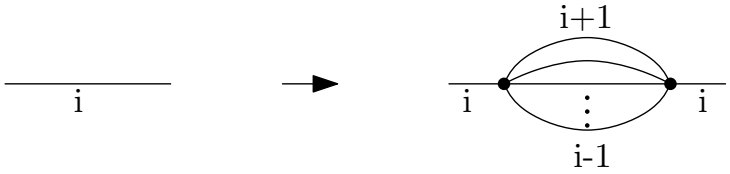

Figure 3.8: A melonic insertion on an edge of color i.

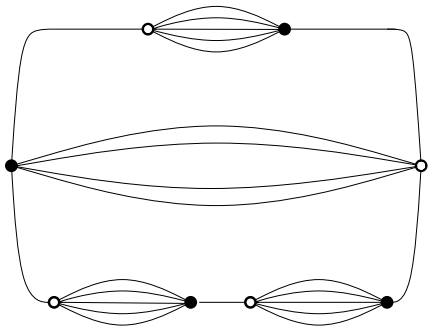

Figure 3.9: Structure of a generic melon graph with $d = 6$.

Interestingly, melonic graphs with a marked edge are in bijection with *d-ary trees*, and therefore can be counted with (generalized) *Catalan numbers* [8].

As for matrix models, the analyticity of the free energy with respect to $g := \lambda\bar{\lambda}$ has been investigated first in the leading sector. Thanks to the recursive structure of melonic graphs, we can easily establish a closed relation with the melonic 2-points function $G_{2,melo}(g)$. Indeed the one particule irreductible (1PI) 2-points function, says Σ_{melo}, is necessarily of the form pictured on the Figure 3.10, where each grey disk is a melonic 2-point function insertion.

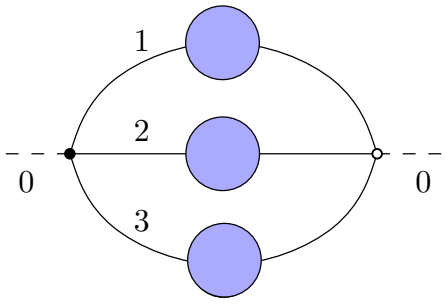

Figure 3.10: Structure of the melonic 1PI 2-point function Σ_{melo}, for external edges of colors 0 and with $d = 3$. Each grey disk represents the 2-point function $G_{2,melo}$ (which is the same for any choice of the colors of the external edges).

Then:

$$\Sigma_{melo} = g G_{2,melo}^{d}. \tag{3.17}$$

Moreover, because the propagator is a product of Kronecker deltas, Σ_{melo} and $G_{2,melo}$ are related by:

$$G_{2,melo} = 1 + \Sigma_{melo} + \Sigma_{melo}^{2} + \cdots = \frac{1}{1 - \Sigma_{melo}}, \tag{3.18}$$

which, together with 3.17, leads to:

$$G_{2,melo}(g) = 1 + g[G_{2,melo}(g)]^{d+1}. \tag{3.19}$$

Solving this equation, we find the following critical behavior in the vicinity of the critical value g_c

$$G_{2,melo}(g) \sim (g - g_c)^{\gamma_{melo}} \ , \tag{3.20}$$

where the critical value g_c depends only on the dimension d : $g_c := d^d/(d+1)^{d+1}$, and the critical (or entropy) exponent $\gamma_{melo} = 1/2$. From this result, and using a *Schwinger-Dyson equation* we deduce also the critical behavior of the free energy:

$$\mathcal{W}_{tensors} \sim \left(\frac{g - g_c}{g_c} \right)^{2 - \gamma_{melo}}. \tag{3.21}$$

The "physical" meaning of this behavior is the same as for matrices. In the vicinity of the critical value g_c, melon graphs of arbitrary order proliferate without control, which, following the authors of [8], can be understood as a phase transition to a continuum phase. Note that, in contrast with the critical value g_c, the critical exponent γ_{melo} does not depend on the dimension d, and then, is a *universal quantity*. The corresponding continuum phase has been studied, and due to the tree structure of melonic graphs, it corresponds to a singular *branched polymers* phase, with Hausdorff dimension 2 and spectral dimension 4/3 (which can be intuitively understood as a consequence of the mapping of d-ary trees to positive random excursions). Due to the branched polymer structure of melons, such a continuum phase does not correspond to the idea of a smooth manifold, with smooth metric. This is why we generally think that many phase transitions are necessary to reach the continuum phase corresponding to our space-time, eventually assisted by the addition of some *pre-geometric data*.

The next to leading order (NLO) sector has also been investigated, see for instance [12]. The authors have established that NLO graphs have degree $\varpi_{NLO} := (d-1)!(d-2)/2$, studied the critical behavior and computed the critical exponent of this sector. Their strategy for characterization of the NLO graphs exploits the fact that not only d-dipole contractions but also 1-dipole

contractions keep the Gurau degree unchanged. Hence, starting with the mother of melons and performing a 2-dipole insertion leads to the graph pictured on Figure 3.11b, which have degree ϖ_{NLO}.

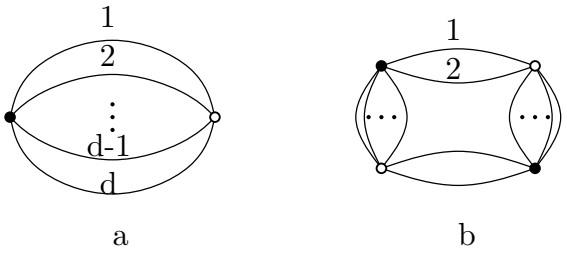

Figure 3.11: 2-dipole insertion between the edges labeled from 3 to d (a) in the mother of melons (b).

The next step consists in the insertion of an elementary melon on one of the edges of the diagram, as in Figure 3.12a which, up to a proper 1-dipole creation, turns to be the diagram of Figure 3.12b. Iterating the procedure gives the family of graph pictured in Figure 3.13, denoted as $\mathcal{G}_{2-dipole,\ell}$ by authors of [12], where ℓ refers to the number of insertions of type 3.12b. From this family, the authors construct a new set of closed graphs by considering all the possible insertions of melonic graphs.

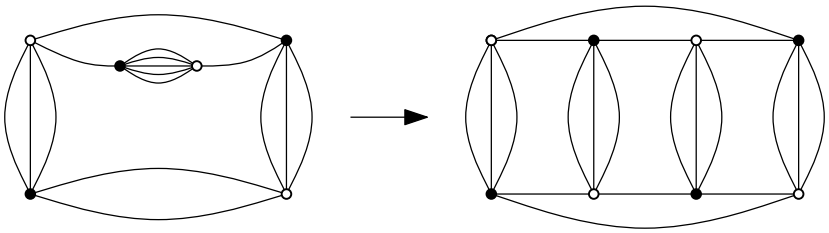

Figure 3.12: Melonic insertion (a) and creation of a 1-dipole (b). $d = 4$.

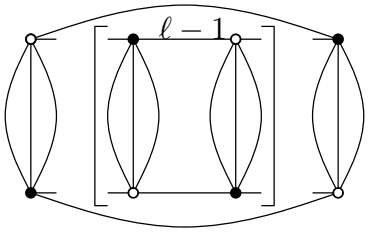

Figure 3.13: General structure of the graph $\mathcal{G}_{2-dipole,\ell}$.

The final step consists in listing all the possibilities for building a 1PI 2-points graph. The first one, the simplest way, consists in replacing one of the internal line of an elementary melon by the NLO 2-point function, says $G_{2,NLO}$, and replacing all the remaining internal lines by $G_{2,melo}$. The second one corresponds to the two schemes for cutting an edge of $\mathcal{G}_{2-dipole,\ell}$ in an optimal way. Then, at the end of the day, we obtain the following expression for the NLO 2-point function $G_{2,NLO}$:

$$G_{2,NLO} = \frac{\frac{d(d+1)}{2} g^2 G_{2,melo}^{2d+2}}{(G_{2,melo} - 2)(1 - dgG_{2,melo})} \quad , \tag{3.22}$$

with critical behavior:

$$G_{2,NLO} \sim \left(1 - \frac{g}{g_c}\right)^{-1/2} \quad , \tag{3.23}$$

which seems to indicate that $\gamma_{NLO} = 3/2$. Note that the critical point for the NLO sector is the same as for the leading sector, which is encouraging for a *double scaling analysis*. Double scaling has been studied in details for colored [10] and for uncolored quartic models [11] (see Section 3.2), and some progress has been made in the understanding of the nature of the corresponding phase transition. In particular, the nature of the symmetry breaking has been studied in [9]. We shall return to these aspects at the beginning of Chapter 4.

3.1.4 Regularization and large N-expansion for GFTs

The definition 3.6 is highly formal, because the delta functions in the propagator introduce some divergences in the computation of a general Feynman graph. In order to circumvent this difficulty, as in standard quantum or statistical field theory, it is critical to adopt a *regularization scheme*. The most popular is the regularization via the *heat kernel* at time α, K_α:

$$\delta(g) = \lim_{\alpha \to 0} K_\alpha(g) \ . \tag{3.24}$$

We recall that the heat kernel satisfies the heat equation [3]:

$$\left(\frac{\partial}{\partial \alpha} - \Delta_g\right) K_\alpha(g) = 0 \ , \tag{3.25}$$

and, assuming that $\mathbf{G}$ is a compact connected Lie group, can be expanded as a sum over irreductible representations ρ of $\mathbf{G}$ as [13]:

$$K_\alpha(g) = \sum_\rho d_\rho e^{-\alpha C_\rho} \mathrm{Tr}_\rho(g) \ , \tag{3.26}$$

where d_ρ is the dimension of the representation ρ, Tr_ρ is the trace in this representation, and C_ρ is the quadratic Casimir operator. Due to the convolution property of heat kernels:

$$\int dh K_\alpha(gh) K_{\alpha'}(h^{-1}g') = K_{\alpha+\alpha'}(gg') \ , \tag{3.27}$$

the amplitude $\mathcal{A}_\mathcal{G}$ can then be expressed as:

$$\mathcal{A}_{\mathcal{G},\alpha} = \int \prod_{e \in E(\mathcal{G})} dh_e \prod_{f \in F(\mathcal{G})} K_{|\partial f|\alpha}\left(\prod_{e \in \partial f}^{\rightarrow} h_e^{\epsilon_{ef}}\right) \ , \tag{3.28}$$

where $E(\mathcal{G})$ and $F(\mathcal{G})$ are respectively the sets of edges and faces of $\mathcal{G}$, ∂f denotes the boundary of the face f, with length $|\partial f|$ (i.e. the number of edges in the boundary of f). Finally, ϵ_{ef} is the *adjacency matrix*, with entries ± 1 if $e \in \partial f$, the sign depending on the relative orientation of the face with respect to the line, and 0 otherwise. Note that this expression only requires 0, 1 and 2-cells (i.e. vertices, edges and faces respectively, reminding that an edge is labeled by a color $c \in [\![0, d]\!]$, and a face is labeled by a pair $(c, c') \in [\![0, d]\!]^2$). Then, we only need to consider the 2-complex associated to $\mathcal{G}$. A large N expansion can be defined as for tensor models, and has been partially investigated in the literature. The strategy is the following. The large parameter N playing the role of the size of the tensor and allowing to organize the perturbative expansion as a proper large N-expansion is no longer necessarily an integer but simply:

$$N = \frac{1}{\sqrt{4\pi\alpha}} \ . \tag{3.29}$$

[3] It can be nicely understood as a consequence of the representation of the heat kernel as a sum of Markovian paths.

Indeed, up to rescaling of the couplings:

$$\lambda \to \lambda / N^{\dim(\mathbf{G})\frac{(d-2)(d-1)}{4}} \ , \tag{3.30}$$

one can show [13] that the amplitude 3.28 scales with N as:

$$\mathcal{A}_{\mathcal{G},\alpha} \lesssim (\lambda\bar{\lambda})^{V(\mathcal{G})/2} \left[N^{\dim(\mathbf{G})}\right]^{(d-1)-\frac{2(d-2)}{d!}\varpi(\mathcal{G})} \ . \tag{3.31}$$

Therefore, as for tensor models, we recover that leading order graphs have degree zero. As for tensors, the critical behavior of the melonic sector has been investigated. More precisely, in the large N limit, defining $\mathcal{W}^{(0)}$ such as : $\mathcal{W} \sim N^{\dim \mathbf{G}(d-1)}\mathcal{W}^{(0)}$, we can prove, using some homology machinery, a higher dimensional generalization of the popular *Kirchhoff tree-matrix theorem* [13], leading to:

$$K \sum_{p\in\mathbb{N}} F_p c^p (\lambda\bar{\lambda})^p \leq \mathcal{W}^{(0)} \leq \sum_{p\in\mathbb{N}} F_p (\lambda\bar{\lambda})^p, \tag{3.32}$$

for some positive constant K and c. The authors of the reference conclude that $\mathcal{W}^{(0)}$ has a finite radius of convergence, hence a critical behavior. However, for the moment, this result concerns only the topological GFTs, and should be extended to more realistic models for $4d$ quantum gravity. Moreover, even if the existence of a critical behavior has been proved, the specific behavior of the free energy (i.e. its critical exponent) remains unknown. Finally, the investigation of the next to leading order behavior is still an open problem.

3.2 Tensor invariance

3.2.1 Uncoloring the colored tensor models

Inspired by the corresponding situation for colored matrix models, a statistical field theory for $d+1$-complex tensors fields can be equivalently understood as an effective statistical field theory for a single rank-d complex tensor field with an infinite number of interactions, called *tensor invariants*. It is characterized by a *unitary symmetry group* $U(N)^{\times d}$, where, as previously, N denotes the size of the tensors. The equivalence between the two constructions can be cheeked explicitly, by integrating the partition function 3.9 over all colors expect the color 0, and has been first considered in [3]. At the perturbative level, in the expansion of the partition function in power of $\lambda\bar{\lambda}$, this procedure can be understood as follows. Instead of summing over $d+1$-colored graphs, we disconnect the 0-lines, and sum separately over their contractions. The remaining graphs are d-colored, which can be disconnected or not, and correspond exactly to the idea of an integration over d-colors. They can be re-summed as an infinite set of interactions, whose couplings depend on the product $\lambda\bar{\lambda}$. Each interaction can be labeled by a d-bubble, and its kernel in simply a product of Kronecker deltas, whose indices are contracted following the pattern dictated by the d-bubble. As an example, the diagram in Figure 3.3 can be understood in this framework as the Wick-contraction of dotted lines between fields represented by black and white vertices, in the interaction vertex:

$$\mathrm{Tr}_{b_1}(T,\bar{T}) = \sum_{\vec{n},\vec{n}\,'} T_{n_1 n_2 n_3} \bar{T}_{n_1 n_2' n_3'} T_{n_1' n_2' n_3'} \bar{T}_{n_1' n_2 n_3} \ , \tag{3.33}$$

where T (resp. $\bar{T}$) are the tensor fields of color 0 in the original colored representation. The label 1 refers to the intermediate colors (see Figure 3.14), and $\vec{n}, \vec{n}\,' \in [\![1, N]\!]^3$.

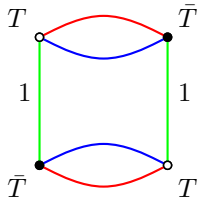

Figure 3.14: Graphical representation of the interaction bubble b_1 given by 3.33. The green edges are associated to the color 1.

The notation Tr_{b_1} has a precise meaning. It takes into account the invariance of the interaction 3.33 under the transformation:

$$T_{n_1 n_2 n_3} \to \sum_{\vec{n}\,'} U^{(1)}_{n_1 n_1'} U^{(2)}_{n_2 n_2'} U^{(3)}_{n_3 n_3'} T_{n_1' n_2' n_3'} \ , \tag{3.34}$$

$$\bar{T}_{n_1 n_2 n_3} \to \sum_{\vec{n}\,'} U^{(1)}_{n_1 n_1'} U^{(2)}_{n_2 n_2'} U^{(3)}_{n_3 n_3'} \bar{T}_{n_1' n_2' n_3'} \ , \tag{3.35}$$

where $U^{(i)}$, $i = 1, 2, 3$ are arbitrary $N \times N$ unitary matrices, whose set is denoted as $\mathcal{U}(N)$.

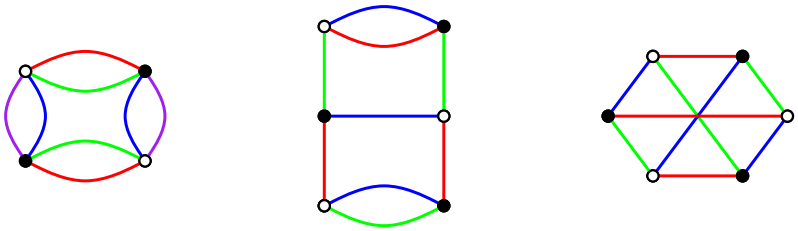

Figure 3.15: Example of interaction bubbles in dimension 4 (a) and 3 (b-c).

Definition 8. *In dimension d, the **interaction bubbles** are d-bubbles, that is to say, connected colored bipartite regular graphs, where the black (resp. white) vertices are associated to the tensors T (rep. $\bar{T}$), and the connectivity structure gives the pattern of contraction for the tensor indices, providing a $\mathcal{U}(N)^{\times d}$ invariance.*

Figure 3.15 gives three examples of interaction bubbles in dimension $d = 3$ and $d = 4$. These interaction bubbles are denoted as an invariant trace $\mathrm{Tr}_b(T, \bar{T})$, labeled by a bubble b, and have the following generic expression:

$$\mathrm{Tr}_b(T, \bar{T}) = \sum_{\{\vec{n}^v, \vec{n}^{\bar{v}}\}} \Big(\prod_{v,\bar{v} \in b} T_{\vec{n}^v} \bar{T}_{\vec{n}^{\bar{v}}} \Big) \Big(\prod_{c=1}^{d} \prod_{l^c_{v\bar{v}} \in b} \delta_{n^v_c n^{\bar{v}}_c} \Big) \ , \tag{3.36}$$

where v (resp. $\bar{v}$) denotes white (resp. black) vertices, and $l_{v\bar{v}}$ denotes the edge of color c joining v and $\bar{v}$. Note that in the expression 3.36, the invariance $\mathcal{U}(N)^{\times d}$ is obvious. As a conclusion, with a little of algebra, we can show that the initial colored model in dimension d defined by 3.9 can be rewritten as an effective statistical field theory for a single complex rank-d tensor T:

$$\mathcal{Z}_{tensors} = \int dT d\bar{T} e^{-\mathcal{S}_{uncolored}[T,\bar{T}]} \ , \tag{3.37}$$

where $dTd\bar{T} := \prod_{\vec{n}} dT_{\vec{n}} d\bar{T}_{\vec{n}}$, and:

$$\mathcal{S}_{uncolored}[T, \bar{T}] := \sum_{\vec{n} \in [\![1,N]\!]^d} \bar{T}_{\vec{n}} T_{\vec{n}} + \sum_{b \in \mathcal{B}^d} \frac{(\lambda\bar{\lambda})^{p(b)}}{\mathrm{Sym}(b)} N^{-(d-1)(p(b)-1) - \frac{2}{(d-2)!}\varpi(b)} \mathrm{Tr}_b[T, \bar{T}] \ , \tag{3.38}$$

where $p(b)$ denotes the number of black vertices of b, and $\mathcal{B}^d$ the set of all *connected* bubbles in dimension d. This result has been considered by the authors of [14] as the starting point of a new axiomatic definition of tensor models, based on the $\mathcal{U}(N)^{\times d}$ invariance, coming from a single tensor field but with an arbitrary number of couplings, and the recipe is the following:

- We select a subset $\bar{\mathcal{B}} \subset \mathcal{B}_d$ of $\mathcal{U}^{\times d}$-invariant interactions,
- We associate a coupling t_b for each bubble b,

such that, up to an appropriate changing of field normalization, an arbitrary tensor model is defined in this axiomatic point of view by an action of the form

$$\mathcal{S}[T,\bar{T}] := \sum_{\vec{n}\in[\![1,N]\!]^d} \bar{T}_{\vec{n}} T_{\vec{n}} + \sum_{b\in\bar{\mathcal{B}}} t_b N^{-\frac{2}{(d-2)!}\varpi(b)} \mathrm{Tr}_b[T,\bar{T}] \ , \tag{3.39}$$

and a partition function

$$\mathcal{Z} = \int dT d\bar{T} e^{-N^{d-1}\mathcal{S}[T,\bar{T}]} . \tag{3.40}$$

As a result, we obtain an extended tensorial space, well defined by the internal symmetry $\mathcal{U}(N)^{\times d}$, allowing to construct arbitrary models for freely adjustable interactions. This new class of statistical models can be studied perturbatively, by expanding the corresponding partition function in a power of the couplings $\{t_b\}$:

$$\mathcal{Z} = \sum_{\mathcal{G}} \frac{1}{s(\mathcal{G})} \left(\prod_{b\in\mathcal{G}} (-t_b) \right) \mathcal{A}_{\mathcal{G}}. \tag{3.41}$$

The graphs $\mathcal{G}$ labeling the amplitude $\mathcal{A}_{\mathcal{G}}$ are made of several interaction bubbles playing the role of effective vertices, connected together by dotted lines, such that Wick contractions pair black and white vertices. An example of such a Feynman graph is pictured in Figure 3.16. Note that this kind of graph is therefore a $(d+1)$-colored one. Taking into account that each dotted line provides a factor $N^{-(d-1)}$, each face of colors $(0c)$, $c \in [\![1,d]\!]$ provides a factor N, and that each vertex bubble b comes with a factor $N^{d-1-\frac{2}{(d-2)!}\varpi(b)}$, the amplitude $\mathcal{A}_{\mathcal{G}}$ writes as:

$$\mathcal{A}_{\mathcal{G}} = N^{(d-1)|V(\mathcal{G})| - \frac{2}{(d-2)!}\sum_{\rho\in V(\mathcal{G})}\varpi(b_\rho) - (d-1)|L(\mathcal{G})| + \sum_c |F_{0c}(\mathcal{G})|} , \tag{3.42}$$

where V, L and F_{0c} are respectively the sets of vertex bubbles, dotted lines and faces of colors $0c$. Using Proposition 2, this amplitude matches exactly with the amplitude 3.16. Then, the power counting makes sense for the extended axiomatic formalism of uncolored tensor models.

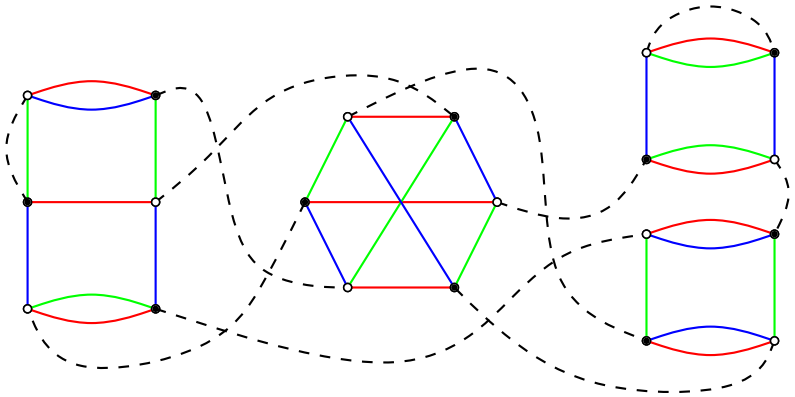

Figure 3.16: A vacuum Feynman graph with $d = 3$.

The uncolored tensor models have been actively investigated since 2012, especially for quartic melonic truncation, for which a double-scaling limit has been studied [11]. Phase transitions have also been studied, and in particular the symmetry breaking aspects in [9], where the authors link continuum phase transition to a break of the symmetry $\mathcal{U}(N)^{\times d}$. Finally, a constructive program has been started in [7] and is currently in active development for several models [16], providing a deep definition of such models at the non-perturbative level.

I conclude this section by some discussion of the terminology. At this stage, the word *vertex* refers to the black and white nodes of the colored graph and to the interaction bubbles of the uncolored formalism. In order to avoid any ambiguity, we save the word "vertex" for the interaction bubbles in the rest of this thesis, and we denote by *node* the black and white vertices in the colored extension shown in Figure 3.16.

3.2.2 Tensorial Group Field Theories

The $\mathcal{U}(N)^{\times d}$ invariance, say *tensor invariance*, highlights the fundamental mistake of the earliest tensor models, and, as explained in this chapter, the color structure of the Feynman graphs makes the topology and the combinatorics tractable. For this reason it has been argued that tensor invariance seems to be a good prescription for the GFTs interactions, instead of the usual simplicial prescription. This new class of GFTs corresponds to the so-called *tensorial group field theories* (TGFTs), to which a large part of this thesis is dedicated. At the classical level, a TGFT is a group field theory for a single complex field φ in dimension d, defined by:

• The choice of a group manifold $\mathbf{G}$ on which the field is defined: $\varphi : \mathbf{G}^d \to \mathbb{C}$,

• A kinetic action $\mathcal{S}_{kin}[\varphi, \bar{\varphi}]$,

$$\mathcal{S}_{kin}[\varphi, \bar{\varphi}] = \int_{\mathbf{G}^{2d}} d\mathbf{g} d\mathbf{g}' \bar{\varphi}(\mathbf{g}) \mathcal{K}(\mathbf{g}, \mathbf{g}') \varphi(\mathbf{g}') \ , \tag{3.43}$$

• An interaction action $\mathcal{S}_{int}[\varphi, \bar{\varphi}]$, which is a sum of tensorial bubbles, weighted by different couplings $\{\lambda_b\}$:

$$\mathcal{S}_{int}[\varphi, \bar{\varphi}] = \sum_b \frac{\lambda_b}{\mathrm{Sym}(b)} \mathrm{Tr}_b[\varphi, \bar{\varphi}] \ , \tag{3.44}$$

• The choice of a set of constraints or *gauge symmetries* acting on the group variables. The most popular, and the only used in this thesis, is the *closure constraint*:

$$\varphi(g_1 h, ..., g_d h) = \varphi(g_1, ..., g_d) \quad \forall h \in \mathbf{G} \ . \tag{3.45}$$

The structure of the interaction bubbles is exactly the same as for tensors, up to the replacement of sums by integration. As an example, for the bubble of Figure 3.14, the corresponding interaction term writes as:

$$\mathrm{Tr}_{b_1}[\varphi, \bar{\varphi}] = \int_{\mathbf{G}^{2d}} d\mathbf{g} d\mathbf{g}' \varphi(g_1, g_2, g_3) \bar{\varphi}(g_1, g_2', g_3') \varphi(g_1', g_2', g_3') \bar{\varphi}(g_1', g_{2,3}) . \tag{3.46}$$

As discussed in Chapter 1, at the quantum level, the gauge symmetries, and especially the closure constraint, have to be implemented in the definition of the covariance, or equivalently of the Gaussian measure $d\mu_C$:

$$\int d\mu_C[\varphi, \bar{\varphi}] \varphi(\mathbf{g}) \bar{\varphi}(\mathbf{g}') = (\hat{P} \mathcal{K} \hat{P})(\mathbf{g}, \mathbf{g}') \ , \tag{3.47}$$

where $\hat{P}$ is the projector into the gauge invariant fields. The quantum theory is then defined by the partition function

$$\mathcal{Z}_{TGFT} = \int d\mu_C[\varphi, \bar{\varphi}] e^{-\mathcal{S}_{int}[\varphi,\bar{\varphi}]} \ . \tag{3.48}$$

To conclude, we introduce the usual notation T^n_d, and we refer to the "T^n_d-model" for the TGFT in dimension d whose higher valent interaction bubbles have valence n.

For the topics of this thesis, which treats essentially of renormalization aspects of TGFTs, the tensor invariance will play an important role, because it provides a notion of locality, the *traciality*, well-adapted to the renormalization procedure. We shall explore it in detail in the third chapter. However, we shall dedicate the end of this section to an important point, closely related with the renormalization procedure, concerning the choice of the kinetic action. Up to now, for all the models that we have considered in this chapter, the kinetic kernel $\mathcal{K}$ reduces to the identity operator, hence to a product of Kronecker deltas, and the propagator to the quantum theory given by $\hat{P}$ for topological models. There are nevertheless some arguments in favor of a different choice. Firstly, as mentioned at the end of Chapter 1, for the Boulatov-Ooguiri models, radiative corrections of the 2-points functions [17] generate a Laplacian contribution, which therefore should be also included in the definition of the classical action. Secondly, such a Laplace operator provides a notion of scale, which is a good point for renormalization. Thirdly, recent results [18] about GFT condensates seem to indicate that Friedman's equation can be recovered only for kinetic terms including a Laplacian. For the purpose of this thesis, the second point remains the most relevant, and is quite flexible, in the sense that models with lower order differential operators can be also considered. This will be the case in Chapter 6.

Finally, note that, when the power of this differential operator is smaller or equal to that of the Laplacian, we may hope for some analog of Osterwalder-Schrader positivity to hold [19]. This hope at the moement just relies on an analogy with the ordinary quantum field theory case, in which the (Euclidean) OS positivity axiom requires precisely such a bound on the degree of the kinetic term. Remember OS positivity is the key Euclidean property which ensures continuation to Minkovski time. Without such an OS condition, divergence-free quantum field theories could be built easily by simply using a high power of the Laplacian to suppress any ultraviolet problem. But we know that such "cheap" constructions violate OS positivity, hence have no continuation to Minkovski time. We feel a similar selection rule probably will be needed also in the pregeometric tensor models, to ensure not just a random geometric simulation of the Euclidean world, but ultimately a real time interpretation. It is however a deep problem far from a complete understanding at this point.

In conclusion the TGFT framework appears as a very flexible framework, and a large variety of models, depending on the choice of the kinetic kernel and bubbles interactions, can be considered. As for standard quantum field theories, renormalizability, studied in the next chapters of this thesis, and probably other conditions in the future, analog to OS positivity, should drastically restrict this family.

Bibliography

[1] R. Gurau, "Lost in Translation: Topological Singularities in Group Field Theory," Class. Quant. Grav., 27:235023, 2010, arXiv:1006.0714 [hep-th];

[2] A. Baratin, F. Girelli and D. Oriti, "Diffoomorphisms in group field theories," Phys. Rev., D83:104051, 2011, arXiv: 1101.0590. ;

F. Girelli and E. Livine, "A Deformed Poincaré Invariance fro Group Field Theories" arXiv:1001.2919 [gr-qc];

[3] R. Gurau, "A generalization of the Virasoro algebra to arbitrary dimensions," Nucl. Phys., B852:592-614, 2011, 1105.6072. ;

[4] R. Gurau, "Colored Group Field Theory," Commun. Math. Phys., 304:69-93, 2011, 0907.2582.;

[5] R. Gurau and J.P. Ryan, "Colored Tensor Models - a review," SIGMA, 8:020, 2012, 1109.4812. ;

[6] J.P. Ryan, "Tensor Models and embedded Riemann surfaces," Phys. Rev., D85:024010, 2012, 1104.5471.;

[7] R. Gurau, "The 1/N expansion of colored tensor models," Annales Henri Poincaré **12**, 829 (2011) [arXiv:1011.2726 [gr-qc]].

R. Gurau and V. Rivasseau, "The 1/N expansion of colored tensor models in arbitrary dimension," Europhys. Lett. **95**, 50004 (2011), [arXiv:1101.4182 [gr-qc]].

R. Gurau, "The complete 1/N expansion of colored tensor models in arbitrary dimension," Annales Henri Poincaré **13**, 399 (2012) [arXiv:1102.5759 [gr-qc]].

V. Bonzom, R. Gurau, and V. Rivasseau, "Random tensor models in the large N limit: Uncoloring the colored tensor models," Phys. Rev. **D85**, 084037 (2012), [arXiv:1202.3637 [hep-th]].

R. Gurau and J. P. Ryan, "Melons are branched polymers," Annales Henri Poincaré **15** no. 11, (2014) 2085, [arXiv:1302.4386 [math-ph]];

[8] V. Bonzom, R. Gurau, A. Riello and V. Rivasseau, "Critical behavior of colored tensor models in the large N limit," Nucl. Phys. B **853** (2011) 174 [arXiv:1105.3122 [hep-th]].

[9] T. Delepouve and R. Gurau, "Phase Transition in Tensor Models," JHEP **1506**, 178 (2015) [arXiv:1504.05745 [hep-th]].

D. Benedetti and R. Gurau, "Symmetry breaking in tensor models," arXiv:1506.08542 [hep-th].

[10] R. Gurau and G. Schaeffer "Regular colored graphs of positive degree",arXiv:1307.5279, to appear in Annales Institut Henri Poincaré D.

[11] S. Dartois, R. Gurau and V. Rivasseau, "Double scaling in tensor models with a quartic interaction," JHEP **1309** (2013) 088 [arXiv:1307.5281 [hep-th]];

R. Gurau, A. Tanasa and D.R. Youmans. "The double scaling limit of the multi-orientable tensor model. 2015.

[12] W. Kaminski, D. Oriti and J.P. Ryan, "Towards a double-scaling limit for tensor models: probing sub-dominant orders," New J.Phys., 16:063048, 2014.;

[13] A. Baratin, S. Carrozza, D. Oriti, J.P. Ryan and M. Smerlak, "Melonic phase transition in group field theory," 2013, 1307.5026. ;

[14] V. Bonzom, R. Gurau and V. Rivasseau. "Random tensor models in the large N limit: Uncoloring the colored tensor models," Phys. Rev., D85:084037, 2012.;

[15] R. Gurau, "The $1/N$ Expansion of Tensor Models Beyond Perturbation Theory." 2013, 1304.2666. ;

[16] V. Rivasseau, "Constructive Tensor Field Theory," arXiv:1603.07312 [math-ph].

[17] J. Ben Geloun and V. Bonzom, "Radiative corrections in the Boulatov-Ooguri tensor model: The 2-point function," Int. J. Theor. Phys. **50**, 2819 (2011) [arXiv:1101.4294 [hep-th]];

[18] D. Oriti, R. Pereira and L. Sindoni, "Coherent states for quantum gravity: towards collective variables," arXiv:1202.0526 [gr-qc], Class.Quant.Grav. 29 (2012) 135002.

D. Oriti, L. Sindoni and E. Wilson-Ewing, "Emergent Friedmann dynamics with a quantum bounce from quantum gravity condensates," arXiv:1602.05881 [gr-qc];

S. Gielen and D. Oriti, "Quantum cosmology from quantum gravity condensates: cosmological variables and lattice-refined dynamics," arXiv:1407.8167 [gr-qc], New J.Phys. 16 (2014) no.12, 123004;

S. Gielen, D. Oriti and L. Sindoni, "Homogeneous cosmologies as group field theory condensates," arXiv:1311.1238 [gr-qc], JHEP 1406 (2014) 013;

[19] V. Rivasseau, "The Tensor Track: An Update." 2012, 1209.5284. ;

Chapter 4

Perturbative renormalization: The $U(1) - T_d^4$

This chapter is devoted to the perturbative renormalization of TGFTs. It performs a transition between the description of the state of the art in TGFTs, given in Chapters 1 and 2, and the specific models studied in this thesis. Indeed, this chapter has two entangled objectives. It provides a presentation of the key notions for renormalization in the TGFT context (which differs essentially from the renormalization in standard field theory by the non-locality of their interactions) on a concrete example, the melonic Abelian T_d^4 model with closure constraint. Although we focus our attention on this model, which will be our favorite example for the rest of this thesis, some of the results of this chapter are common to all the Abelian models, and in the leading sector, to the non-Abelian models. We then indicate for each key result whether it is a specific aspect of the T_d^4 or a general one. Some aspects of this chapter are based on [1]. The general reference on renormalization via multiscale analysis which we use is [2]. More details on renormalization in the TGFT context can be found in [3, **?**, 12, 6].

4.1 Definition of the model

Let us focus our attention on the Abelian T_d^4 melonic model. More precisely, in order to study simultaneously the effect of the dimension of the space and of the group manifold, and to give the more general treatment, we consider the $U(1)^D - T_d^4$ melonic model, described by the classical action:

$$\mathcal{S}_{kin}[T,\bar{T}] = \sum_{\vec{\mathbf{p}}\in(\mathbb{Z}^D)^d} \bar{T}_{\vec{\mathbf{p}}}(\vec{\mathbf{p}}^{\,2}+m^2)T_{\vec{\mathbf{p}}} \ , \tag{4.1}$$

$$\mathcal{S}_{int}[T,\bar{T}] = \lambda \sum_{i=1}^{d} \sum_{\{\vec{\mathbf{p}}_c, c=1,\dots,4\}} \mathcal{W}^{(i)}_{\vec{\mathbf{p}}_1,\vec{\mathbf{p}}_2,\vec{\mathbf{p}}_3,\vec{\mathbf{p}}_4} T_{\vec{\mathbf{p}}_1}\bar{T}_{\vec{\mathbf{p}}_2}T_{\vec{\mathbf{p}}_3}\bar{T}_{\vec{\mathbf{p}}_4} \ . \tag{4.2}$$

In these definition, $\vec{\mathbf{p}}$ denotes a set of d-vectors of size D: $\vec{\mathbf{p}} := (\mathbf{p}_1, ..., \mathbf{p}_d)$, $\vec{\mathbf{p}}^{\,2}$ denotes the usual norm on $(\mathbb{Z}^D)^d$: $\vec{\mathbf{p}}^{\,2} := \sum_{i=1}^{d}\sum_{k=1}^{D} p_{ki}^2$, $T_{\vec{\mathbf{p}}}$ corresponds to the Fourier components of the field $\varphi : (U(1)^D)^{\times d} \to \mathbb{C}$, and the symbols $\mathcal{W}^{(i)}_{\vec{\mathbf{p}}_1,\vec{\mathbf{p}}_2,\vec{\mathbf{p}}_3,\vec{\mathbf{p}}_4}$ are products of delta functions whose indices follow the pattern corresponding to the quartic melon pictured in Figure 4.1. Explicitly:

$$\mathcal{W}^{(i)}_{\vec{\mathbf{p}}_1,\vec{\mathbf{p}}_2,\vec{\mathbf{p}}_3,\vec{\mathbf{p}}_4} := \delta_{\vec{\mathbf{p}}_{1i}\vec{\mathbf{p}}_{4i}}\delta_{\vec{\mathbf{p}}_{2i}\vec{\mathbf{p}}_{3i}} \prod_{j\neq i} \delta_{\vec{\mathbf{p}}_{1j}\vec{\mathbf{p}}_{2j}}\delta_{\vec{\mathbf{p}}_{3j}\vec{\mathbf{p}}_{4j}} \ . \tag{4.3}$$

Finally, note that we have chosen the same coupling λ for each of the interaction bubbles. Moreover, the "melonicity" of the interaction is obvious, indeed, it is easy to see that the interaction pictured in Figure 4.1 is obtained from the mother of melons in dimension d by insertion of an elementary melon on the line of color i.

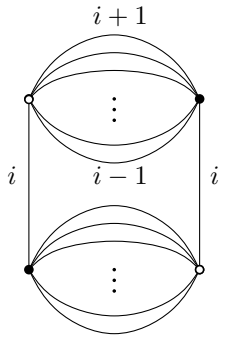

Figure 4.1: Melonic interaction corresponding to the symbol $\mathcal{W}^{(i)}_{\vec{\mathbf{p}}_1,\vec{\mathbf{p}}_2,\vec{\mathbf{p}}_3,\vec{\mathbf{p}}_4}$.

The corresponding quantum field theory is then described by the generating functional:

$$\mathcal{Z}_{U(1)^D-T_d^4} := \int d\mu_{C_\Lambda}[T,\bar{T}] e^{-\mathcal{S}_{int}[T,\bar{T}]+\bar{J}\cdot T+\bar{T}\cdot J} \ , \tag{4.4}$$

where J, $\bar{J}$ denote the *external sources*, and where we have used the shorthand notation

$$\bar{J}\cdot T := \sum_{\vec{\mathbf{p}}\in(\mathbb{Z}^D)^d} \bar{J}_{\vec{\mathbf{p}}}T_{\vec{\mathbf{p}}}. \tag{4.5}$$

The subscript Λ in the covariance refers to the ultra-violet (UV) cut-off, introduced in order to circumvent the apparition of eventual UV divergences in the perturbative Feynman expansion. In the Schwinger scheme, our covariance writes as:

$$\int d\mu_{C_\Lambda}[T,\bar{T}]T_{\vec{\mathbf{p}}}\bar{T}_{\vec{\mathbf{p}}'} = \delta_{\vec{\mathbf{p}}\vec{\mathbf{p}}'}\int_{1/\Lambda^2}^{+\infty} d\alpha e^{-\alpha(\vec{\mathbf{p}}^{\,2}+m^2)} \int_{[-\pi,\pi[^D} \frac{d\beta}{(2\pi)^D} e^{i\sum_{k=1}^{D}\beta_k\left(\sum_{i=1}^{d} p_{ki}\right)} \ , \tag{4.6}$$

where $\beta = (\beta_1, ...\beta_D) \in [-\pi, \pi[^D$, and where we have used the integral representation of the Kronecker delta, implementing the closure constraint. Moreover : $\delta_{\vec{\mathbf{p}}\vec{\mathbf{p}}'} := \prod_{i=1}^{d} \prod_{k=1}^{D} \delta_{p_{ki} p'_{ki}}$. More than the partition function $Z(J = \bar{J} = 0)$ and its vacuum amplitudes, the objects of interest for this chapter are the connected N-point functions, or Schwinger functions, S_N, which can be expanded as a Feynman series in power of the coupling λ:

$$S_N = \sum_{\mathcal{G} \in G_N} \frac{1}{\mathrm{Sym}(\mathcal{G})} (-\lambda)^{V(\mathcal{G})} \mathcal{A}_{\mathcal{G}} \ , \tag{4.7}$$

where G_N denotes the set of connected Feynman diagrams with N external lines and $V(\mathcal{G})$ the number of vertices. A typical Feynman diagram is pictured on Figure 4.2. Using Feynman rules, the amplitude $\mathcal{A}_{\mathcal{G}}$ takes the form:

$$\begin{aligned} \mathcal{A}_{\mathcal{G}} = \prod_{e \in \mathcal{L}(\mathcal{G})} \int_{1/\Lambda^2}^{+\infty} d\alpha_e e^{-\alpha_e m^2} \int_{[-\pi,\pi[^D} \frac{d\beta_e}{(2\pi)^D} \prod_{f \in \mathcal{F}(\mathcal{G})} \sum_{\mathbf{p}_f \in \mathbb{Z}^D} e^{-\alpha_f \mathbf{p}_f^2 + i \sum_{k=1}^{D} (\beta_f)_k p_{fk}} \\ \times \prod_{f \in \mathcal{F}_{ext}(\mathcal{G})} e^{-\alpha_f \mathbf{p}_f{}^2 + i \sum_{k=1}^{D} (\beta_f)_k p_{fk}} \end{aligned} \tag{4.8}$$

where $\alpha_f := \sum_{e \in \partial f} \alpha_e$, $(\beta_f)_k := \sum_{e \in \partial f} \epsilon_{fe} (\beta_e)_k$, $\mathcal{L}(\mathcal{G}), \mathcal{F}(\mathcal{G})$ and $\mathcal{F}_{ext}(\mathcal{G})$ are respectively the sets of lines, internal and external faces, with $L(\mathcal{G})$, $F(\mathcal{G})$ and $F_{ext}(\mathcal{G})$ denoting their cardinals.

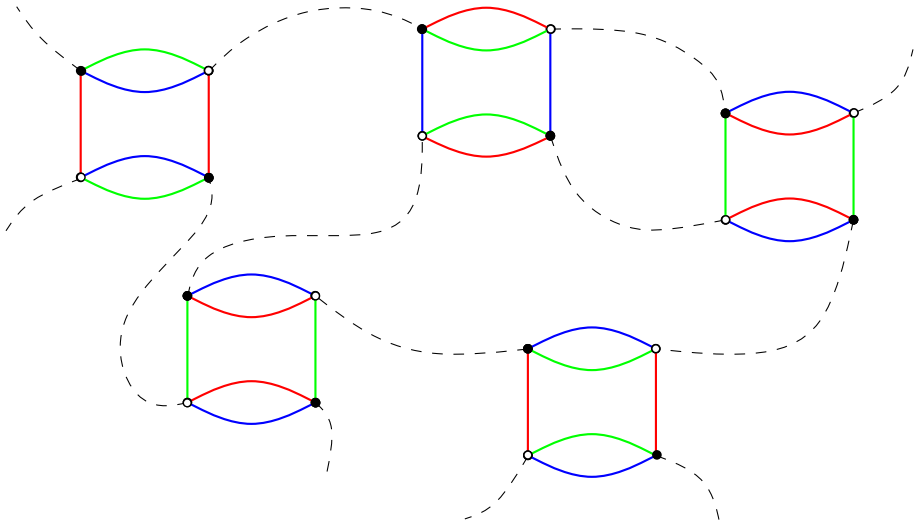

Figure 4.2: An example of Feynman graph with 6-external lines and five vertices in dimension 3.

4.2 One-loop computations and renormalization

In order to understand the behavior of physical quantities, and to introduce the formalism of renormalization for TGFTs, we now compute the leading order contributions of the correlation functions. We limit our attention to the 2 and 4-point functions, respectively at order λ and λ^2. Finally, we shall use these examples to discuss the general procedure for renormalization of TGFTs.

4.2.1 Divergences of 2 and 4-point functions at one-loop

The 2-point functions at order λ

At first order in λ, the one-particule irreductible (1PI) 2-point function, say Γ_2^{1-loop}, with external momentum $\vec{\mathbf{p}}$ has the following structure:

$$\Gamma_2^{1-loop}(\vec{\mathbf{p}}) = -2\lambda \sum_{i=1}^{d} \sum_{m=1,2} \mathcal{A}_{\mathcal{G}_{i,m}}(\vec{\mathbf{p}}) \ , \tag{4.9}$$

where the two graphs $\mathcal{G}_{i,m}$ for a fixed i correspond to the two Wick contractions pictured on Figure 4.3 below, and the factor 2 in front of the right hand side comes from the fact that we have two contractions giving the same diagram $\mathcal{G}_{im}$. Using the Feynman rules, the computation of the two amplitudes is straightforward, and we get:

$$\mathcal{A}_{\mathcal{G}_{i,1}}(\vec{\mathbf{p}}) := \sum_{\mathbf{q}_j \in \mathbb{Z}^D, j\neq i} \int_{[-\pi,\pi[^D} \frac{d\beta}{(2\pi)^D} \int_{1/\Lambda^2}^{+\infty} d\alpha e^{-\alpha(\vec{\mathbf{q}}^{\,2}+m^2)} e^{i\sum_{k=1}^{D}\beta_k\left(\sum_{i=1}^{d} q_{ki}\right)}\Big|_{\mathbf{q}_i=\mathbf{p}_i} \ , \tag{4.10}$$

$$\mathcal{A}_{\mathcal{G}_{i,2}}(\vec{\mathbf{p}}) := \sum_{\mathbf{q}_i \in \mathbb{Z}^D} \int_{[-\pi,\pi[^D} \frac{d\beta}{(2\pi)^D} \int_{1/\Lambda^2}^{+\infty} d\alpha e^{-\alpha(\vec{\mathbf{q}}^{\,2}+m^2)} e^{i\sum_{k=1}^{D}\beta_k\left(\sum_{i=1}^{d} q_{ki}\right)}\Big|_{\mathbf{q}_j=\mathbf{p}_j, j\neq i} \ . \tag{4.11}$$

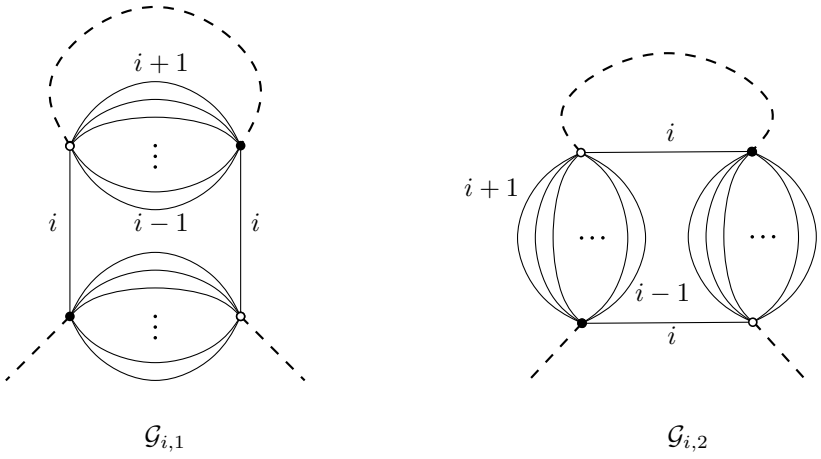

$\mathcal{G}_{i,1}$ $\mathcal{G}_{i,2}$

Figure 4.3: The two Wick contractions $\mathcal{G}_{i,m}$.

Note that the first diagram $\mathcal{G}_{i,1}$ corresponds to a melonic insertion on the line of color i of the d+1-elementary melon with external edges of colors 0. Such a diagram is therefore called *melonic*. In contrast the second diagram $\mathcal{G}_{i,2}$ is not melonic. Remark also that due to the closure constraint, the momentum running over the single face of the second contribution 4.11 is completely fixed by the external momenta. The sum is therefore trivial in this case:

$$\mathcal{A}_{\mathcal{G}_{i,2}}(\vec{\mathbf{p}}) = \frac{1}{\sum_{j\neq i}\mathbf{p}_j^2 + (\sum_{j\neq i}\mathbf{p}_j)^2 + m^2}. \tag{4.12}$$

The first contribution 4.10 involves sums of the type $\sum_{p\in\mathbb{Z}} e^{-\alpha p^2 + i\beta p}$, which can be exactly computed as

$$\sum_{p\in\mathbb{Z}} e^{-\alpha p^2+i\beta p} = \left(\frac{\pi}{\alpha}\right)^{1/2} \sum_{n\in\mathbb{Z}} e^{\frac{|\beta+2\pi n|^2}{4\alpha}} = \left(\frac{\pi}{\alpha}\right)^{1/2} e^{-\frac{\beta^2}{4\alpha}} \left(1 + 2\sum_{n>0} e^{-\frac{\pi^2 n^2}{\alpha}} \cosh\left(\frac{\pi n \beta}{\alpha}\right)\right) \ , \tag{4.13}$$

and the amplitude $\mathcal{A}_{\mathcal{G}_{i,1}}$ writes as

$$\mathcal{A}_{\mathcal{G}_{i,1}}(\vec{\mathbf{p}}) := \int \frac{d\beta}{(2\pi)^D} \int_{1/\Lambda^2}^{+\infty} d\alpha e^{-\alpha m^2} \left(\frac{\pi}{\alpha}\right)^{(d-1)D/2} \times e^{-\frac{(d-1)D\beta^2}{4\alpha}} \left(1 + 2\sum_{n>0} e^{-\frac{\pi^2 n^2}{\alpha}} \cosh\left(\frac{\pi n\beta}{\alpha}\right)\right)^{(d-1)D} e^{-\alpha \mathbf{p}_i^2 + i\sum_{k=1}^D \beta_k p_{k,i}} . \tag{4.14}$$

We are interested by the UV-divergences, occurring in the vicinity of $\alpha = 0$. In order to isolate the potentially divergent contributions, i.e. the part of the expression 4.14 having potentially singular behavior in the limit $\alpha \to 0$, we use the distributional identity:

$$e^{-\theta^2/4\alpha} = \sum_n \frac{\sqrt{4\pi}}{n!} [\alpha]^{n+\frac{1}{2}} \delta^{2n}(\theta) . \tag{4.15}$$

Then, taking into account the bounds

$$\sum_{n>0} e^{-\frac{\pi^2 n^2}{\alpha}} \leq \int_1^\infty dx e^{-\frac{\pi^2 x^2}{\alpha}} \leq \frac{1}{2}\sqrt{\frac{\alpha}{\pi}} e^{-\frac{\pi^2}{\alpha}} , \tag{4.16}$$

we deduce that the second term in the sum 4.13 converges in the limit $\alpha \to 0$. Therefore, the divergent part of the amplitude 4.14 writes as:

$$\mathcal{A}^{\infty}_{\mathcal{G}_{i,1}}(\vec{\mathbf{p}}) := \sum_{n_1,\dots,n_D} \frac{(-1)^{\sum_k n_k}}{(D(d-1))^{D/2}} \frac{(4\pi)^{D/2}}{\prod_{k=1}^D n_k!} \frac{\pi^{(d-1)D/2}}{(2\pi)^D} \times \int_{1/\Lambda^2}^{+\infty} d\alpha e^{-\alpha(\mathbf{p}_i^2 + m^2)} \alpha^{\sum_k n_k - \frac{(d-2)D}{2}} \prod_{k=1}^D \left[\frac{p_{i,k}^2}{D(d-1)}\right]^{n_k} \tag{4.17}$$

$$= \frac{\pi^{(d-2)D/2}}{(D(d-1))^{D/2}} \int_{1/\Lambda^2}^{+\infty} d\alpha e^{-\alpha((1+\frac{1}{D(d-1)})\mathbf{p}_i^2 + m^2)} \alpha^{-\frac{(d-2)D}{2}} . \tag{4.18}$$

At this stage, we find a condition on d and D if we want that the Laplacian kinetic term remains stable. Indeed, if $d > 2 + 4/D$, singular contributions with higher derivative couplings have to be introduced. As a result, it seems that the dimensions of the group manifold and space-time cannot be chosen too large in a consistent model of this type. We shall return to this perturbative argument in Section 4.4, in which we shall make it more precise and rigorous.

The 4-point function at order λ^2

At zero-loop order, the 1PI 4-point function, for which a typical contribution is pictured on Figure 4.4, involves only one vertex, and has the following structure:

$$\Gamma_4^{1-loop}(\vec{\mathbf{p}}_1, \vec{\mathbf{p}}_2, \vec{\mathbf{p}}_3, \vec{\mathbf{p}}_4) = -4\lambda \sum_{i=1}^d \frac{1}{2} \mathrm{Sym}\mathcal{W}^{(i)}_{\vec{\mathbf{p}}_1,\vec{\mathbf{p}}_2,\vec{\mathbf{p}}_3,\vec{\mathbf{p}}_4} , \tag{4.19}$$

where the factor 4 in front of the right-hand-side counts the number of contractions for the external fields (there are 2 ways for contracting the T, and 2 for contracting the $\bar{T}$), and:

$$\mathrm{Sym}\mathcal{W}^{(i)}_{\vec{\mathbf{p}}_1,\vec{\mathbf{p}}_2,\vec{\mathbf{p}}_3,\vec{\mathbf{p}}_4} := W^{(i)}_{\vec{\mathbf{p}}_1,\vec{\mathbf{p}}_2,\vec{\mathbf{p}}_3,\vec{\mathbf{p}}_4} + W^{(i)}_{\vec{\mathbf{p}}_3,\vec{\mathbf{p}}_2,\vec{\mathbf{p}}_1,\vec{\mathbf{p}}_4} . \tag{4.20}$$

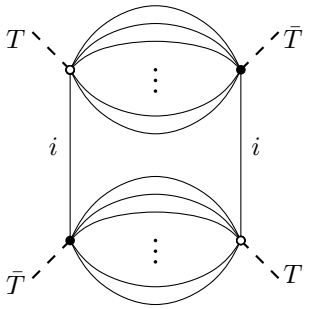

Figure 4.4: Contributions to the 1PI 4-point function at zero-loop order.

At one-loop order, the 1PI 4-point Γ_4^{1-loop} receives many contributions, corresponding to all the Wick contractions. But as for the 2-point function, some of these contributions are trivial, due to the closure constraint. For instance, the momentum running along the internal face of the diagram pictured on Figure 4.5a is completely determined by external momenta. As a result, only the contribution corresponding to the diagram pictured on Figure 4.5b may be divergent in the UV. Moreover, note that, in the case $i \neq j$, the sum:

$$I_1(\mathbf{p}_1, \mathbf{p}_2) := \sum_{\mathbf{q}_m, m\neq i,j} \frac{\prod_{k=1}^D \delta(\sum_{i=1}^d q_{ki})}{(\vec{\mathbf{q}}^2 + m^2)^2}\Big|_{(\mathbf{q}_i,\mathbf{q}_j)=(\mathbf{p}_1,\mathbf{p}_2)} , \tag{4.21}$$

is absolutely convergent if the condition $d \leq 2 + 4/D$ is satisfied. Therefore, only the diagrams with $i = j$ may be singular in the limit $\alpha \to 0$, which scales as $\Lambda^{(d-2)D-4}$. One more time, note that these contributions are melonic, in the sense that they correspond to melonic insertions from the original interaction[1]. Hence, Γ_4^{1-loop} has the following structure:

$$\Gamma_4^{1-loop}(\vec{\mathbf{p}}_1, \vec{\mathbf{p}}_2, \vec{\mathbf{p}}_3, \vec{\mathbf{p}}_4) = \sum_{i=1}^d \Delta\Gamma^{(i)}_{melo}(\mathbf{p}_{4i}) \frac{1}{2} \mathrm{Sym} \mathcal{W}^{(i)}_{\vec{\mathbf{p}}_1,\vec{\mathbf{p}}_2,\vec{\mathbf{p}}_3,\vec{\mathbf{p}}_4} + \Gamma^{1-loop}_{4,NLO}(\vec{\mathbf{p}}_1, \vec{\mathbf{p}}_2, \vec{\mathbf{p}}_3, \vec{\mathbf{p}}_4) , \tag{4.22}$$

where $\Gamma^{1-loop}_{4,NLO}$ gathers all the non-melonic, UV-convergent contributions, and

$$\Delta\Gamma^{(i)}_{melo}(\mathbf{p}) := 8\lambda^2 \sum_{\mathbf{q}_j \in \mathbb{Z}^D, 0<j\leq d} \int_{1/\Lambda^2}^\infty d\alpha_1 d\alpha_2 e^{-(\alpha_1+\alpha_2)(\mathbf{p}^2+m^2)} \prod_{j\neq i} e^{-(\alpha_1+\alpha_2)\mathbf{q}_j^2} \times \int_{[-\pi,\pi[^D} \frac{d\beta}{(2\pi)^D} e^{i\sum_{k=1}^D \beta_k (p_k + \sum_{i=2}^d q_{ki})} . \tag{4.23}$$

As for the zero-loop contribution, the factor 8 in front of the right hand arises because we have 4 ways to contract the fields between the two vertices in a melonic diagram, 4 ways to contract the external lines, and an additional factor 1/2 coming from the expansion of the exponential. Computing the sums with 4.13, we find for the divergent contribution

$$\Delta\Gamma^{(i)\infty}_{melo}(\mathbf{p}) := \frac{8\lambda^2 \pi^{(d-2)D/2}}{(D(d-2))^{D/2}} \int_{1/\Lambda^2}^\infty d\alpha_1 d\alpha_2 e^{-(\alpha_1+\alpha_2)((1+\frac{1}{D(d-1)})\mathbf{p}^2+m^2)} (\alpha_1+\alpha_2)^{-\frac{D(d-2)}{2}} .$$

Note that some convergent contributions do not have the same structure as the melonic interaction. It is in particular the case of the contribution 4.5b, for $i \neq j$.

[1] We shall give a precise definition of melonic diagrams in Section 4.4

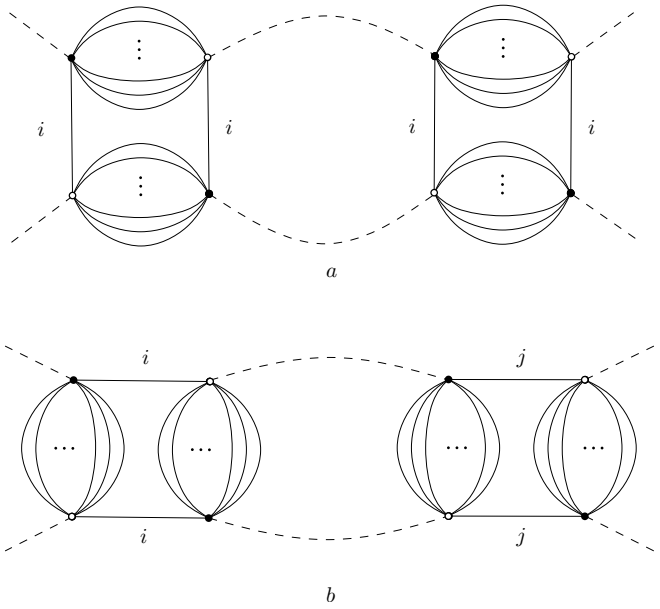

Figure 4.5: Contributions to the 1PI 4-point function at one-loop order.

4.2.2 Counter-terms and renormalization

If the condition $d \leq 2 + 4/D$ is satisfied, only the terms up to $\mathbf{p}^2$ in 4.18 may be UV divergent, and:

$$\mathcal{A}^{\infty}_{\mathcal{G}_{i,1}}(\vec{\mathbf{p}}) = \frac{\pi^{(d-2)D/2}}{(D(d-1))^{D/2}} \left[\mathcal{I}_{\Lambda}(d,D) - \mathcal{J}_{\Lambda}(d,D) \left(1 + \frac{1}{D(d-1)} \right) \mathbf{p}_i^2 \right] + convergent, \tag{4.24}$$

with the definitions:

$$\mathcal{I}_{\Lambda}(d,D) := \int_{1/\Lambda^2}^{+\infty} d\alpha e^{-\alpha m^2} \alpha^{-\frac{(d-2)D}{2}}, \tag{4.25}$$

$$\mathcal{J}_{\Lambda}(d,D) := \int_{1/\Lambda^2}^{+\infty} d\alpha e^{-\alpha m^2} \alpha^{1-\frac{(d-2)D}{2}}. \tag{4.26}$$

The extraction of the divergent part of the 4-point contribution $\Delta\Gamma^{(i)\infty}_{melo}$ requires more precautions. We have to isolate the contributions in each of the two *Hepp's sector* $\alpha_1 \leq \alpha_2$ and $\alpha_1 \geq \alpha_2$. Due to their symmetry, the contributions of each Hepp sector are the same, and we only need to extract the divergences of the first one $\alpha_1 \geq \alpha_2$. Performing the change of variables $(\alpha_1, \alpha_2) \to (\alpha, x)$, defined as

$$\alpha_1 = \alpha, \tag{4.27}$$

$$\alpha_2 - \frac{1}{\Lambda^2} = x \left(\alpha_1 - \frac{1}{\Lambda^2} \right), \tag{4.28}$$

and such that $\alpha \in [1/\Lambda^2, \infty]$, $x \in [0,1]$, $d\alpha_1 d\alpha_2 = (\alpha - 1/\Lambda^2) d\alpha dx$, we get

$$\Delta\Gamma^{(i)\infty}_{melo}(\mathbf{p}) = \frac{8\lambda^2 \pi^{(d-1)D/2}}{(D(d-2))^{D/2}} \mathcal{J}_{\Lambda}(d,D) + UV - convergent\ . \tag{4.29}$$

The basic idea of renormalization comes from the observation that in one-loop graphs the divergences amount to shifts in the parameters of the action, spliting the classical action as a

renormalized part, involving renormalized couplings, and a *counter action*, involving counter-terms, whose values are adjusted in order to cancel the one-loop divergences as $\Lambda \to \infty$. More precisely:

$$\mathcal{S}_{kin}[T_r, \bar{T}_r] = \sum_{\vec{\mathbf{p}} \in (\mathbb{Z}^D)^d} \bar{T}_{r,\vec{\mathbf{p}}} (\vec{\mathbf{p}}^{\,2} + m_r^2) T_{r,\vec{\mathbf{p}}} \ , \tag{4.30}$$

$$\begin{aligned} \mathcal{S}_{int}[T_r, \bar{T}_r] &= (\lambda_r + \delta\lambda) \sum_{i=1}^{d} \sum_{\{\vec{\mathbf{p}}_c, c=1,\dots,4\}} \mathcal{W}^{(i)}_{\vec{\mathbf{p}}_1,\vec{\mathbf{p}}_2,\vec{\mathbf{p}}_3,\vec{\mathbf{p}}_4} T_{r,\vec{\mathbf{p}}_1} \bar{T}_{r,\vec{\mathbf{p}}_2} T_{r,\vec{\mathbf{p}}_3} \bar{T}_{r,\vec{\mathbf{p}}_4} \\ &+ \sum_{\vec{\mathbf{p}} \in (\mathbb{Z}^D)^d} \bar{T}_{r,\vec{\mathbf{p}}} (\delta Z \vec{\mathbf{p}}^{\,2} + \delta m^2) T_{r,\vec{\mathbf{p}}} \ . \end{aligned} \tag{4.31}$$

This form of the action is useful in doing perturbation theory. We treat the terms involving counter-terms as interactions, and expand the counter-terms in infinite series, each term cancelling the divergences of one specific graph. Indeed, with this new parametrization, and assuming that all the *counter-terms* $\delta\lambda$, δZ and δm^2 are of order λ_r^2, the 2 and 4-point functions computed above become:

$$\Gamma^{1-loop}_{2,ren}(\vec{\mathbf{p}}) = -2\lambda_r \sum_{i=1}^{d} \sum_{m=1,2} \mathcal{A}_{\mathcal{G}_{i,m}}(\vec{\mathbf{p}}) - (\delta Z \vec{\mathbf{p}}^{\,2} + \delta m^2) \ , \tag{4.32}$$

$$\Gamma^{1-loop}_{4,ren}(\vec{\mathbf{p}}_1, \vec{\mathbf{p}}_2, \vec{\mathbf{p}}_3, \vec{\mathbf{p}}_4) = \sum_{i=1}^{d} \Delta\Gamma^{(i)}_{melo}(\mathbf{p}_{4i}) \frac{1}{2} \mathrm{Sym} \mathcal{W}^{(i)}_{\vec{\mathbf{p}}_1,\vec{\mathbf{p}}_2,\vec{\mathbf{p}}_3,\vec{\mathbf{p}}_4} + \Gamma^{1-loop}_{4,NLO}(\vec{\mathbf{p}}_1, \vec{\mathbf{p}}_2, \vec{\mathbf{p}}_3, \vec{\mathbf{p}}_4) \tag{4.33}$$

$$- 4\delta\lambda \sum_{i=1}^{d} \frac{1}{2} \mathrm{Sym} \mathcal{W}^{(i)}_{\vec{\mathbf{p}}_1,\vec{\mathbf{p}}_2,\vec{\mathbf{p}}_3,\vec{\mathbf{p}}_4} \ , \tag{4.34}$$

where we use the subscript "ren" for renormalized. Then, at one-loop, with the choices:

$$\delta Z = \frac{2\lambda_r \pi^{(d-2)D/2}}{(D(d-1))^{D/2}} \mathcal{J}_\Lambda(d, D) \left(1 + \frac{1}{D(d-1)}\right) , \tag{4.35}$$

$$\delta m^2 = -\frac{2d\lambda_r \pi^{(d-2)D/2}}{(D(d-1))^{D/2}} \mathcal{I}_\Lambda(d, D) \, , \tag{4.36}$$

$$\delta\lambda = \frac{2\lambda_r^2 \pi^{(d-1)D/2}}{(D(d-2))^{D/2}} \mathcal{J}_\Lambda(d, D) \, , \tag{4.37}$$

all the one-loop renormalized amplitudes become UV-finite. We now extend this procedure to all orders in the next subsection.

4.2.3 Running coupling constant

In standard notations, the relationship between the initial - also called *bare* - and the renormalized parameters of the action may be rewritten as follows:

$$T = Z^{1/2} T_r \, , \quad \lambda = Z^{-2} Z_\lambda \lambda_r \, , \quad m^2 = Z^{-1} Z_m m_r^2 \, , \tag{4.38}$$

where, as usually, Z_m and Z_λ are the mass and coupling renormalizations and Z is the field-strength renormalization. They are related to the counter-terms δm^2, $\delta\lambda$ and δZ by

$$\delta Z := Z - 1 \, , \quad \delta\lambda = (Z_\lambda - 1)\lambda_r \, , \quad \delta m^2 = (Z_m - 1) m_r^2 \, . \tag{4.39}$$

Since each counter-term depends explicitly on the UV cut-off, the bare couplings inherit this dependence. Moreover, the renormalized couplings do not depend on the UV cut-off. The dependence of Λ is therefore entirely contained in the factor $Z^{-2}Z_\lambda$. At one-loop:

$$\begin{aligned} Z^{-2}Z_\lambda &= \frac{1+\frac{2\lambda_r\pi^{(d-2)D/2}}{(D(d-1))^{D/2}}\mathcal{J}_\Lambda(d,D)}{\left[1+\frac{2\lambda_r\pi^{(d-2)D/2}}{(D(d-1))^{D/2}}\mathcal{J}_\Lambda(d,D)\left(1+\frac{1}{D(d-1)}\right)\right]^2} \\ &\approx 1-\frac{4\lambda_r\pi^{(d-2)D/2}}{(D(d-1))^{D/2}}\mathcal{J}_\Lambda(d,D)\left(\frac{1}{2}+\frac{1}{D(d-1)}\right). \end{aligned} \tag{4.40}$$

The *beta-function* $\beta(\lambda)$ describes the way in which the coupling constant depends on the fundamental scale Λ,

$$\beta(\lambda) := \Lambda\frac{d\lambda}{d\Lambda}\,. \tag{4.41}$$

At one-loop, we find:

$$\beta(\lambda) = -\frac{8\lambda^2\pi^{(d-2)D/2}}{(D(d-1))^{D/2}}\left(\frac{1}{2}+\frac{1}{D(d-1)}\right)\Lambda^{(d-2)D-4}\,. \tag{4.42}$$

In analogy with standard quantum field theory, the factor $\Lambda^{(d-2)D-4}$ seems to indicate that we can associate a dimension $4-(d-2)D$ to the corresponding operator[2]. Then, defining the *dimensionless coupling* $\bar\lambda$ as $\lambda = \Lambda^{4-(d-2)D}\bar\lambda$, the corresponding beta function $\bar\beta(\bar\lambda) := \Lambda d\bar\lambda/d\Lambda$ is:

$$\bar\beta(\bar\lambda) = [(d-2)D-4]\bar\lambda - \frac{8\bar\lambda^2\pi^{(d-2)D/2}}{(D(d-1))^{D/2}}\left(\frac{1}{2}+\frac{1}{D(d-1)}\right). \tag{4.43}$$

The beta function admits a fixed point for the value :

$$\bar\lambda_* = \frac{((d-2)D-4)(D(d-1))^{D/2}}{8\pi^{(d-2)D/2}\left(\frac{1}{2}+\frac{1}{D(d-1)}\right)}\,. \tag{4.44}$$

We shall return to this non-trivial fixed point in Chapter 5, and focus our attention on a special model. In a quantum gravity perspective, we are essentially interested in the small dimensions, and the canonical dimension vanishes for :

$$d=6, D=1\,; \quad d=4, D=2\,; \quad d=3, D=4\,. \tag{4.45}$$

The second case has the most interesting value $d=4$ for a model of quantum gravity, but the dimension of the group is too small from a standard group field theory perspective. The most interesting toy model, allowing to study combinatorial and qualitative aspects of the theory, seems then to be the first one, in dimension 6 and with $D=1$. The vanishing of the canonical dimension seems to indicate that the theory is just-renormalizable, a statement that we shall establish rigorously in the next section, and which agrees with the one-loop computations above. (It is easy to check that Green functions with more than four external lines are superficially convergent: only the 2 and 4-point functions show divergences, respectively square and logarithmically divergent with the cutoff). For this model, the one-loop beta function writes as:

$$\beta(\lambda) = -\frac{28\pi^2}{5\sqrt{5}}\lambda^2\,, \tag{4.46}$$

[2]We shall give another, more systematic, definition of the *canonical dimension* in Chapter 5.

and in this context, it is interesting to comment the sign in front of this equation. The minus sign means that the theory is *asymptotically free*. This is very good news for a field theory! Indeed, the coupling decreases with the fundamental scale, and the perturbation theory is then well defined in the UV (we do not crash on a *Landau-pole* in the UV). At this stage of our knowledge of particle physics, asymptotic freedom is indeed an essential aspect of the standard model. It is a property of all non-Abelian gauge theories without too many Fermionic matter fields, hence it holds both for the weak and strong interactions and may be communicated to the electromagnetic and Higgs sector in case of some grand unification scheme. Moreover, this property is generally associated to very interesting physics, in particular to phase transitions which can be dynamically generated in the infrared. In the case of QCD the confinement from quarks to hadrons is such a phase transition and it is fundamental for nuclear physics. To find such a property in this toy model of quantum gravity is very encouraging from the physical perspective of emergent effective space-time which motivates this thesis. Note that this phenomena seems to be quite general for TGFTs, see [4].

Finally, note that, as in the standard quantum field framework, the independence of the renormalized quantities on the fundamental scale can be translated into a dynamical equation, the *Callan-Symanzik* equation, describing how any change of scale modifies the parameters of the theory. For a 1PI vertex function Γ_N with N external lines, this equation writes

$$\left[\Lambda\frac{\partial}{\partial\Lambda}+\beta(\lambda)\frac{\partial}{\partial\lambda}+(m^2\gamma_{m^2}+\delta_{m^2})\frac{\partial}{\partial m^2}-\frac{N}{2}\gamma\right]\Gamma_N=0\,. \tag{4.47}$$

The derivation of this equation is quite standard, and will not be reproduced here. However, note that, at one-loop, this equation is verified for the value 5.86, and for:

$$\gamma=-\frac{24\pi^2\lambda}{5\sqrt{5}}\,, \tag{4.48}$$

$$\gamma_{m^2}=\frac{24\pi^2\lambda}{\sqrt{5}}\,, \tag{4.49}$$

$$\delta_{m^2}=-\frac{12\pi^2\lambda}{\sqrt{5}}\Lambda^2\,. \tag{4.50}$$

4.2.4 Why does renormalization make sense?

In the previous section we illustrated at one-loop order the mechanism of renormalization but we shall now show that it is more general. Our formulas 4.32 and 4.34 for renormalized one-loop amplitudes take the general form:

$$\mathcal{A}_{\mathcal{G},ren}(\lambda_r,m_r)(\mathbf{p}_{ext})=\mathcal{A}_{\mathcal{G}}(\lambda_r,m_r)(\mathbf{p}_{ext})-\tau^*_{\mathcal{H}}\mathcal{A}_{\mathcal{G}}(\lambda_r,m_r)(\mathbf{p}_{ext})\,, \tag{4.51}$$

where $\mathbf{p}_{ext}$ refers in both cases to the external momentum running along the external face of the divergent subgraph $\mathcal{H}$ (see below). Such a structure is very familiar in standard quantum field theory, where the $*$-operator $\tau_{\mathcal{H}}$ replaces in the graph $\mathcal{G}$ the subgraph $\mathcal{H}$ by its local approximation. However, contrary to the standard quantum field theory, the interactions for TGFTs are non-local over the group manifold $\mathbf{G}^d$ that we consider. The one-loop computations are then also interesting at this level. They shall allow us to understand what is the general principle that plays the role of locality in the TFGT framework.

On the way to our understanding of this principle, we first need some material. More precisely, we have to define what a subgraph is and what its *contraction* means.

Definition 9. ***(Subgraph)*** *A subgraph $\mathcal{H}$ of a graph $\mathcal{G}$ is a subset of (dotted) lines. Therefore any $\mathcal{G}$ has exactly $2^{L(\mathcal{G})}$ subgraphs. $\mathcal{H}$ is then completed by first adding all the vertices to which these lines hook. The closed faces in $\mathcal{G}$ are those which go only through lines of $\mathcal{H}$ and are also called internal faces. The external faces of $\mathcal{H}$ are the maximal open connected pieces of either open or closed faces of $\mathcal{G}$ that pass through at least one line of $\mathcal{H}$. Finally, the external half-lines of $\mathcal{H}$ are the ones that connect to one of its vertices.*

Definition 10. ***(Contraction)***. *Let b an interaction bubble with $L(b)$ dash-dotted lines. Let $L_0 = \{l_i\} \subset L(b)$ an ordered subset of dash-dotted lines in b. The contracted graph b/L_0 is obtained from b by:*
• *Deleting the line $l_i \in L_0$ and its two (black and white) end vertices and all the colored lines joining these two vertices.*
• *Identifying the colored line linked to the deleted black vertex with the line of corresponding color linked to the white vertex.*
• *Repeat for l_{i+1}.*

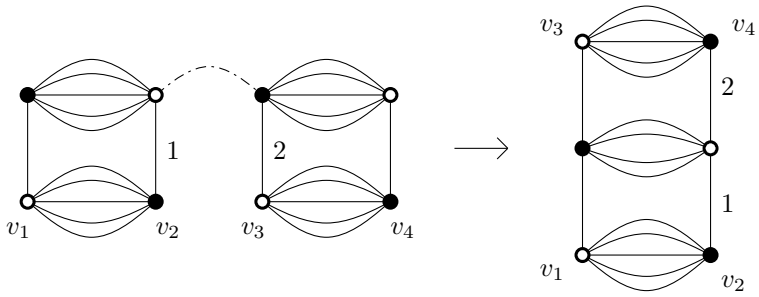

Figure 4.6: Contraction of a dotted line between two vertices with $d = 6$. Some black and white vertices are labeled as v_i in order to facilitate the understanding of the picture.

Now we observe more closely the structure of the one-loop graphs, and especially why in both cases the amplitude depends on a single external momentum $\mathbf{p}_{ext}$. For instance, consider the (leading) one-loop correction to the interaction bubble. We can summarize the expression 4.22, skipping several details, as

$$\mathcal{M}^{(i)}_{\vec{\mathbf{p}}_1,\vec{\mathbf{p}}_2,\vec{\mathbf{p}}_3,\vec{\mathbf{p}}_4} := \sum_{\vec{\mathbf{p}},\vec{\mathbf{p}}'} \mathcal{W}^{(i)}_{\vec{\mathbf{p}}_1,\vec{\mathbf{p}}_2,\vec{\mathbf{p}},\vec{\mathbf{p}}'} \mathcal{W}^{(i)}_{\vec{\mathbf{p}},\vec{\mathbf{p}}',\vec{\mathbf{p}}_3,\vec{\mathbf{p}}_4} C(\vec{\mathbf{p}}') C(\vec{\mathbf{p}}) \tag{4.52}$$

where $C(\vec{\mathbf{p}})$ denotes the propagator of the theory. Firstly, note that, due to structure of the vertex coefficients $\mathcal{W}^{(i)}$, the internal sum can be splitted into a sum over d internal faces. Explicitly:

$$\mathcal{M}^{(i)}_{\vec{\mathbf{p}}_1,\vec{\mathbf{p}}_2,\vec{\mathbf{p}}_3,\vec{\mathbf{p}}_4} = \delta_{\vec{\mathbf{p}}_{1i}\vec{\mathbf{p}}_{4i}} \delta_{\vec{\mathbf{p}}_{2i}\vec{\mathbf{p}}_{3i}} \prod_{j\neq i} \delta_{\vec{\mathbf{p}}_{1j}\vec{\mathbf{p}}_{2j}} \delta_{\vec{\mathbf{p}}_{3j}\vec{\mathbf{p}}_{4j}} \sum_{\mathbf{q}_j\, j\neq i} C(\mathbf{q}_1, ..., \mathbf{p}_{1i}, ...\mathbf{q}_d) C(\mathbf{q}_1, ..., \mathbf{p}_{2i}, ...\mathbf{q}_d)\,. \tag{4.53}$$

It seems at this stage that we have two external momenta, $\mathbf{p}_{1i}$ and $\mathbf{p}_{1i}$. However, an additional constraint occurs in the propagators themselves. Indeed, they share a delta function $\delta(\sum_{j\neq i} \mathbf{q}_j + \mathbf{p}_{ki})$, $k = 2, 4$, implying $\mathbf{p}_{2i} = \mathbf{p}_{4i}$, hence

$$\mathcal{M}^{(i)}_{\vec{\mathbf{p}}_1,\vec{\mathbf{p}}_2,\vec{\mathbf{p}}_3,\vec{\mathbf{p}}_4} = \delta_{\vec{\mathbf{p}}_{1i}\vec{\mathbf{p}}_{4i}} \delta_{\vec{\mathbf{p}}_{2i}\vec{\mathbf{p}}_{3i}} \prod_{j\neq i} \delta_{\vec{\mathbf{p}}_{1j}\vec{\mathbf{p}}_{2j}} \delta_{\vec{\mathbf{p}}_{3j}\vec{\mathbf{p}}_{4j}} \sum_{\mathbf{q}_j\, j\neq i} C^2(\mathbf{q}_1, ..., \mathbf{p}_{1i}, ...\mathbf{q}_d)\,. \tag{4.54}$$

The fact that the 4-point amplitude only depends on one external momentum is therefore due as much to the melonic structure of the vertices of the Feynman graphs than to the closure

constraint. The property of the theory responsible for this fact is called *traciality*. It is essential for renormalization. In standard QFT, for the scalar ϕ^4 theory for instance, a 4-point loop such as Figure 4.7 only depends of one external momentum $P = q_1 + q_2 = q_3 + q_4$, providing a factor $e^{-\alpha P^2}$. This factor occurs because the ϕ^4 theory is *local* in space-time, implying conservation of the momentum at each vertex. It allows to approximate the complete graph by a sequence of local approximations, obtained by expanding around $P = 0$ the exponential factor in power of α. The *counter-terms* in this context are nothing but the first UV divergent terms in this expansion into local approximations.

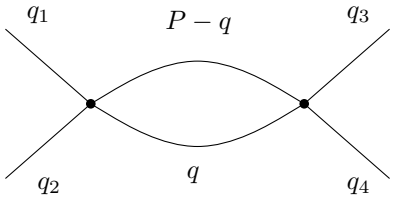

Figure 4.7: One-loop contribution to the 4-point function in scalar ϕ^4 theory

As a result, the fact that the divergent amplitudes only depend on one momentum implies that such a factor $e^{-\alpha \mathbf{p}_{ext}^2}$ occurs also for the TGFTs amplitudes, as we have seen in the one-loop computations. Therefore, each amplitude can be expanded around $\mathbf{p}_{ext} = 0$, which is naturally understood as a kind of generalization of a local approximation. For instance, for the $U(1) - T_6^4$ model, the one-loop 4-point amplitude is logarithmically divergent, meaning that all the terms in $\mathbf{p}_{ext}^n$ with $n > 0$ are convergent in the UV. Hence, the first term, which is:

$$\mathcal{M}^{(i)}_{\vec{\mathbf{p}}_1,\vec{\mathbf{p}}_2,\vec{\mathbf{p}}_3,\vec{\mathbf{p}}_4} = \delta_{\vec{\mathbf{p}}_{1i}\vec{\mathbf{p}}_{4i}}\delta_{\vec{\mathbf{p}}_{2i}\vec{\mathbf{p}}_{3i}} \prod_{j\neq i} \delta_{\vec{\mathbf{p}}_{1j}\vec{\mathbf{p}}_{2j}}\delta_{\vec{\mathbf{p}}_{3j}\vec{\mathbf{p}}_{4j}} \left(\sum_{\mathbf{q}_j\, j\neq i} C^2(\mathbf{q}_1, ..., \mathbf{p}_{1i} = 0, ...\mathbf{q}_d) \right), \tag{4.55}$$

contains all the UV singularities. Note that the product of deltas is nothing but $\mathcal{W}^{(i)}$, meaning that the first term of the local approximation corresponds to the original vertex multiplied by a factor corresponding to the divergent subgraph $\mathcal{H}$ whose external faces are discarded (see Figure 4.8). This is exactly the action of the operator $\tau_{\mathcal{H}}$, and the factor corresponds to the counter-term. For the 2-point function, the first term of the expansion corresponds to a mass counter-term. But pushing the expansion one step further is required to cancel the stronger UV divergence. This further step generates a deviation to exact locality, proportional to $\mathbf{p}_{ext}^2$, which is nevertheless again a counter-term for the initial action, which corresponds to the wave-function renormalization.

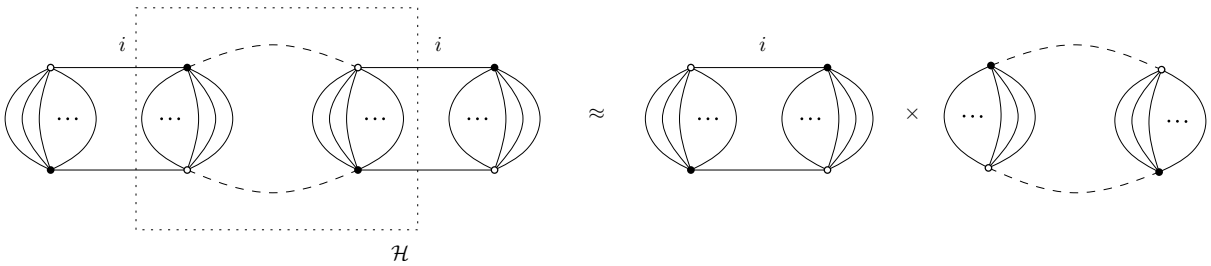

Figure 4.8: Local approximation of the melonic one-loop 4-point graph.

This picture illustrates the general mechanism for renormalization, and points out the role of traciality, which provides a good notion of locality. We shall give a more general definition in the next Section. But we insist at this stage on the fact that renormalization in such models succeeds because the melonic sector contains all the divergences, and because all melonic graphs

display the traciality property[3]. A similar although slightly different phenomenon occurs in the Grosse-Wulkenhaar matrix model, in which the renormalization mechanism can work only because the divergent graphs are all *planar with a single external face* [13].

To summarize this section, since the divergent sector is made only of tracial graphs, the formula 4.51 can be generalized at all orders in λ by the standard BPHZ method using *Zimmermann's divergent forests*. It is the subject of Section 4.5.1, where we shall show a uniform bound for renormalized amplitudes of given order and divergent forest structure.

4.3 Hubbard-Stratanovic decomposition

The Hubbard-Stratanovic (or intermediate field) decomposition is a standard trick in field theory. For tensor models, this trick, first introduced in [14], leads to a convenient reorganization of the set of graphs with respect to their scaling in N. For instance, the melonic graphs discussed in the second chapter become exactly the trees of this new representation. Moreover, this intermediate field representation is at the core of the *loop vertex expansion* in constructive theory [15], and has many other virtues, as confirmed by the large number of recent publications which use it [16]. These benefits apply particularly well to the melonic quartic TGFTs, as we shall see in this chapter and in Chapter 7. However, in this section, we only give the recipe of the decomposition.

We start with the original action 4.2, and introduce the d Hermitian matrices $\mathbb{M}^i$, $i = 1, ..., d$ with elements

$$\mathbb{M}^i_{mn} := \sum_{\{\vec{\mathbf{p}}_1, \vec{\mathbf{p}}_2\}} \prod_{j \neq i} \delta_{\mathbf{p}_{1j}\mathbf{p}_{2j}} \delta_{\mathbf{p}_{1i}\mathbf{n}} \delta_{\mathbf{p}_{2i}\mathbf{m}} T_{\vec{\mathbf{p}}_1} \bar{T}_{\vec{\mathbf{p}}_2}, \quad \mathbf{m}, \mathbf{n} \in \mathbb{Z}^D \,, \tag{4.56}$$

so that the action 4.2 can be rewritten in terms of these matrices $\mathbb{M}^i$:

$$S_{int} = \lambda \sum_{i=1}^{d} \mathrm{tr}(\mathbb{M}^i)^2 \tag{4.57}$$

where "tr" means the trace over indices of the matrices $\mathbb{M}^i$. The intermediate field decomposition arises as an application of the well-known properties of Gaussian integration to the partition function 4.4:

$$\mathcal{Z}_{U(1)^D - T^4_d}[J, \bar{J}] = \int d\mu_C(T, \bar{T}) e^{-\lambda \sum_{i=1}^d \mathrm{tr}(\mathbb{M}^i)^2 + \langle \bar{J}, T\rangle + \langle \bar{T}, J\rangle} \tag{4.58}$$

$$= \frac{\int \prod_{i=1}^d \sigma_i e^{-\mathrm{tr}(\sigma_i)^2}}{\int \prod_{i=1}^3 d\sigma'_i e^{-\mathrm{tr}(\sigma'_i)^2}} \int d\mu_C(T, \bar{T}) e^{i\sqrt{2\lambda} \sum_{i=1}^d \mathrm{tr}(\sigma_i \mathbb{M}^i) + \langle \bar{J}, T\rangle + \langle \bar{T}, J\rangle} \tag{4.59}$$

$$= \int d\nu_{\mathbb{I}}(\sigma) e^{-\mathrm{Tr}\ln(1 - i\sqrt{2\lambda} C\Sigma) - \bar{J}RJ}, \tag{4.60}$$

where in the last line the integration over $\bar{T}, T$ has been performed. $R := (1 - i\sqrt{2\lambda}C\Sigma)^{-1}C$ is the *resolvent matrix*, $d\nu_{\mathbb{I}}(\sigma)$ is the normalized Gaussian integration over the σ_i with covariance the identity matrix $\mathbb{I}$ (Gaussian unitary ensemble), and:

$$\Sigma := \sum_{i=1}^{d} \mathbb{I}^{\otimes i-1} \otimes \sigma_i \otimes \mathbb{I}^{d-i} \,. \tag{4.61}$$

[3]Traciality also occurs in some non-melonic graphs, but in contrast with locality in ordinary quantum field theory, it is definitely not a property of *all* Feynman graphs.

In perturbation theory, we expand the big trace of the logarithm and the resolvents as

$$\mathrm{Tr}\ln(1-i\sqrt{2\lambda}C\Sigma)=\sum_n\frac{1}{n}\mathrm{Tr}(i\sqrt{2\lambda}C\Sigma)^n\,;\quad (1-i\sqrt{2\lambda}C\Sigma)^{-1}C=\sum_n(i\sqrt{2\lambda}C\Sigma)^nC. \tag{4.62}$$

Following the standard nomenclature in the literature, we call the interactions $\mathrm{Tr}(i\sqrt{2\lambda}C\Sigma)^n$ *loop vertices*, and the resolvents $(i\sqrt{2\lambda}C\Sigma)^nC$ *ciliated vertices* [14]. The graphical representation of the intermediate field Feynman graphs are the following. A loop vertex $\mathrm{Tr}(i\sqrt{2\lambda}C\Sigma)^n$ is pictured as a grey disk with n half colored wavy lines. A ciliated vertex $(i\sqrt{2\lambda}C\Sigma)^nC$ is pictured as a lighter grey disk with n half colored wavy lines and one dotted cilium (which can be thought of either as representing an intermediate field external half-line, or as a conjugate pair of tensor sources). The propagators of the intermediate fields are represented by colored wavy lines, joining the half wavy lines of the grey disks, accordingly to each color (see [6]). Figure 4.9 gives an example of Feynman graph in this intermediate field representation for $d=3$. Note that the dotted lines of the original representation 4.4 are in a one-to-one correspondence with the *arcs* of the grey disks in the intermediate field decomposition.

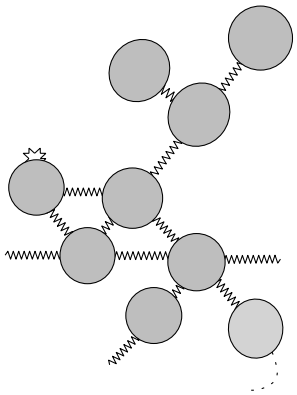

Figure 4.9: Example of a Feynman graph in intermediate field representation with one ciliated vertex for $d=3$. Note that in this graph, the half wavy-lines are think to be connected to the rest of the graph.

We conclude this section by underlining an important simplification coming from gauge invariance, first pointed out in [1]. If we call $\tau_i(\mathbf{p}_i):=(\sigma_i)_{\mathbf{p}_i\mathbf{p}_i}$ the *diagonal part* of the matrix σ_i, we have:

$$\mathrm{Tr}(i\sqrt{2\lambda}C\Sigma)^n=(i\sqrt{2\lambda})^n\sum_{\vec{\mathbf{p}}\in(\mathbb{Z}^D)^d,\vec{k}\in\mathbb{N}^d|\sum_i k_i=n}\frac{n!}{\prod_i k_i!}\frac{\prod_{l=1}^D\delta\big(\sum_i p_{li}\big)}{(\vec{\mathbf{p}}^{\,2}+m^2)^n}\prod_{i=1}^d[\tau_i(\mathbf{p}_i)]^{k_i}, \tag{4.63}$$

and a similar result holds for the ciliated vertices [6]. Hence, only the diagonal part of the intermediate field contributes effectively, so that we can reduce our three intermediate field matrices σ_i to three *intermediate vector fields* τ_i. Therefore 4.58 writes:

$$\begin{aligned}\mathcal{Z}_{U(1)^D-T^4_d}[J,\bar{J}] &= \int d\nu_{\mathbb{I}}(\tau)e^{-\sum_{\vec{\mathbf{p}}\in\mathcal{P}}\ln(1-i\sqrt{2\lambda}C_0(\vec{\mathbf{p}})\Gamma(\vec{\mathbf{p}}))}\\ &\quad e^{-\sum_{\vec{\mathbf{p}}\in\mathcal{P}}\bar{J}(\vec{p})(1-i\sqrt{2\lambda}C_0(\vec{\mathbf{p}}))\Gamma(\vec{\mathbf{p}}))^{-1}C_0(\vec{\mathbf{p}})J(\vec{\mathbf{p}})},\end{aligned} \tag{4.64}$$

where $C_0(\vec{\mathbf{p}}):=(\vec{\mathbf{p}}^{\,2}+m^2)^{-1}$, $\mathcal{P}:=\{\vec{\mathbf{p}}\in(\mathbb{Z}^D)^d|\sum_i p_{ki}=0\,,1\le k\le D\}$, $\Gamma(\vec{\mathbf{p}}):=\sum_i\tau_i$, and $d\nu_{\mathbb{I}}(\tau)$ is the Gaussian measure of the three vector fields, defined as:

$$\int d\nu_{\mathbb{I}}(\tau)\tau_i(\mathbf{p})\tau_j(\mathbf{p}'):=\delta_{ij}\delta_{\mathbf{p}\mathbf{p}'}. \tag{4.65}$$

4.4 Power-counting and Abelian classification

4.4.1 Multi-scale decomposition

We move on to a more systematic analysis provided by the *multi-scale expansion* [2]. It attributes a scale to each line $e \in \mathcal{L}(\mathcal{G})$ of any amplitude of any Feynman graph $\mathcal{G}$, and allows to deduce power-counting in a more systematic and rigorous way. Moreover, it renormalizes any graph in a sequence of successive steps, providing a concrete implementation of Wilson' ideas directly at the graphical level.

For convenience, we choose the UV-regulator Λ so that $\Lambda = M^{-2\rho}$, and the complete propagator $C_\Lambda \equiv C^\rho$ is then given by:

$$C^\rho = \sum_{i=0}^{\rho} C_i. \tag{4.66}$$

A corresponding sharp momentum cut-off $\chi_{\leq\rho}(\vec{\mathbf{p}})$ is 1 if $|\vec{\mathbf{p}}|^2 \leq M^{2\rho}$ and zero otherwise. The theory with cut-off ρ is defined by using the covariance

$$C^\rho(\vec{\mathbf{p}}) = C(\vec{\mathbf{p}})\chi_{\leq\rho}(\vec{\mathbf{p}}). \tag{4.67}$$

Then we slice the theory according to

$$C^\rho(\vec{\mathbf{p}}) = \sum_{i=1}^{\rho} C_i(\vec{\mathbf{p}}),\ C_i(\vec{\mathbf{p}}) = C(\vec{\mathbf{p}})\chi_i(|\vec{p}|^2) \tag{4.68}$$

where χ_1 is 1 if $|\vec{\mathbf{p}}|^2 \leq M^2$ and zero otherwise and for $i \geq 2$ χ_i is 1 if $M^{2(i-1)} < |\vec{\mathbf{p}}\,|^2 \leq M^{2i}$ and zero otherwise.

4.4.2 Power-counting Theorem

Let us start by establishing general power counting via a multi-scale analysis, following the notations and general strategy of [2]. We can perform this analysis both with parametric or sharp cut-offs, ending with the same conclusions. In this subsection we prefer to use sharp cut-offs since thanks to the closure constraint and melonicity of the interaction, they attribute the same scale to all arcs of any loop vertex or chain, hence a single scale to any loop vertex of the intermediate field representation.

The amplitude of a graph $\mathcal{G}$, $\mathcal{A}(\mathcal{G})$, with fixed external momenta, is thus divided into the sum of all the scale attributions $\mu = \{i_e, e \in \mathcal{L}(\mathcal{G})\}$, where i_e is the scale of the momentum p of line e:

$$\mathcal{A}(\mathcal{G}) = \sum_{\mu} \mathcal{A}_\mu(\mathcal{G}). \tag{4.69}$$

At fixed scale attribution μ, we can identify the power counting in powers of M. The essential role is played by the subgraph $\mathcal{G}_i$ formed by the subset of lines of $\mathcal{G}$ with scales higher than i. By the momentum conservation rule along any loop vertex, this subgraph is automatically a PI subgraph which decomposes into $k(i)$ connected PI components : $\mathcal{G}_i = \cup_{k=1}^{k(i)} \mathcal{G}_i^{(k)}$. These connected components form, when (i,k) take all possible values, an abstract tree for the inclusion relation (the famous Gallavotti-Nicolò tree [12]). We have

Theorem 1. *The amplitude $\mathcal{A}_\mu(\mathcal{G})$ is bounded by:*

$$|\mathcal{A}_\mu(\mathcal{G})| \leqslant K^{L(\mathcal{G})} \prod_i \prod_{k=1}^{k(i)} M^{\omega(\mathcal{G}_i^k)},\ K > 0, \tag{4.70}$$

and the divergence degree $\omega(\mathcal{H})$ of a connected subgraph $\mathcal{H}$ is given by:

$$\omega(\mathcal{H}) = -2L(\mathcal{H}) + D(F(\mathcal{H}) - R(\mathcal{H})), \tag{4.71}$$

where $L(\mathcal{H})$ and $F(\mathcal{H})$ are respectively the number of lines and internal faces of the subgraph $\mathcal{H}$, and $R(\mathcal{H})$ is the rank of the adjacency matrix ϵ_{ef} for the lines and faces of $\mathcal{H}$.

Proof: Obviously we have (for $K = M^2$)

$$|C_i(\vec{\mathbf{p}})| \leq K\delta(\sum_c \mathbf{p}_c) M^{-2i} \chi_{\leq i}(\vec{\mathbf{p}}). \tag{4.72}$$

Fixing the external momenta of all external faces of the Feynman amplitude, we obtain the bound

$$|A_\mu(\mathcal{G})| \leq \left[\prod_{e\in\mathcal{L}(\mathcal{G})} K M^{-2i_e}\right] \prod_{f\in F_{int}(\mathcal{G})} \sum_{\mathbf{p}_f\in\mathbb{Z}} \prod_{e\in\partial f} \chi_{\leq i_e}(\vec{\mathbf{p}}) \prod_{e\in\mathcal{L}(\mathcal{G})} \delta(\sum_c \mathbf{p}_c^\ell). \tag{4.73}$$

The key to multiscale power counting is to attribute the powers of M to the $\mathcal{G}_i^{(k)}$ connected components. For this, we first remark that $M^i = M^{-1}\prod_{j=0}^{i} M$, a trivial but useful identity which allows e.g. to rewrite $\prod_{e\in L(G)} M^{-2i_e} = M^2 \prod_{e\in L(G)} \prod_{i=0}^{i_e} M^{-2}$. Then, inverting the order of the double product leads to

$$\prod_{e\in L(\mathcal{G})} M^{-2i_e} = \prod_i \prod_{e\in\mathcal{L}(\cup_{k=1}^{k(i)}\mathcal{G}_i^k)} M^{-2} = \prod_i \prod_{k=1}^{k(i)} \prod_{l\in\mathcal{L}(\mathcal{G}_i^k)} M^{-2} = \prod_i \prod_{k=1}^{k(i)} M^{-2L(\mathcal{G}_i^k)}. \tag{4.74}$$

The goal is now to optimize the cost of the sum over the momenta p_f of the internal faces. Summing over $\mathbf{p}_f$ with a factor $\chi_{\leq i}(\vec{\mathbf{p}})$ leads to a factor KM^i, hence we should sum with the smallest values $i(f)$ of slices i for the lines $e \in \partial f$ along the face f. This is exactly the value at which, starting form i large and going down towards $i = 0$ the face becomes first internal for some $\mathcal{G}_i^k$. Hence in this way we can bound the sums $\prod_{f\in F_{int}(\mathcal{G})} \sum_{\mathbf{p}_f\in\mathbb{Z}}$ by

$$\prod_i \prod_{k=1}^{k(i)} M^{DF(\mathcal{G}_i^k)}. \tag{4.75}$$

However this can still be improved, because we have not yet taken into account the gauge factor $\prod_{e\in\mathcal{L}(\mathcal{G})} \delta(\sum_c \mathbf{p}_c)$. It clearly tells us that some sums over $\mathbf{p}_f$ do not occur at all. Their amount obviously depends on the *rank* R of the incidence matrix ϵ_{ef}. Indeed rewriting the delta functions in terms of the $\mathbf{p}_{f(e,c)}$ we have

$$\prod_{e\in\mathcal{L}(\mathcal{G})} \delta(\sum_c \mathbf{p}_c^\ell) = \prod_{e\in\mathcal{L}(\mathcal{G})} \delta(\sum_f \epsilon_{ef}\mathbf{p}_f). \tag{4.76}$$

Hence writing the linear system of L equations $\sum_f \epsilon_{ef} \mathbf{p}_f = 0$ corresponding to the delta functions we can solve for R momenta $\mathbf{p}_f$ in terms of $L-R$ others. It means that in the previous argument we should pay only for $F-R$ sums over internal face momenta instead of F [4].
This argument can be made more precise and rigorous and distributed over all scales. Starting from the leaves of the Gallavotti-Nicolò tree (the smallest subgraphs $\mathcal{G}_i^k$) and progressing towards the root we can select faces such that the restricted sub-matrix ϵ_{ef} still has maximal rank $R(\mathcal{G}_i^k)$ in each $\mathcal{G}_i^k$. We discard all decay factors for other faces. Then we can select lines in order to find a restricted *square* submatrix $\epsilon_{\ell f}$ with maximal rank $R(\mathcal{G}_i^k)$ in each $\mathcal{G}_i^k$. This leads to

$$|A_\mu(\mathcal{G})| \leq K^{L(\mathcal{G})} \prod_i \prod_{k=1}^{k(i)} M^{-2L(\mathcal{G}_i^k)+D(F(G_i^k)-R(\mathcal{G}_i^k))} = K^{L(G)} \prod_i \prod_{k=1}^{k(i)} M^{\omega(\mathcal{G}_i^k)}. \tag{4.77}$$

This equation completes the proof, and the exponent $\omega(\mathcal{G}_i^k) = -2L(\mathcal{G}_i^k) + D(F(\mathcal{G}_i^k) - R(\mathcal{G}_i^k))$ identifies the divergence degree.

□

For the rest of this Chapter, we set $D = 1$.

4.4.3 Leading sector and classification

The intermediate field formalism is particularly suitable to understand the leading order sector. Indeed, we have the following result:

Proposition 4. *Let $\mathcal{G}$ be a vacuum leading order Feynman graph, $H(\mathcal{G})$ its intermediate field decomposition. Then, if $d \geq 3$, $H(\mathcal{G})$ is a tree.*

Proof. The proof proceed by recursion in the number of wavy lines. With one wavy-line, it is not hard to see that the only divergent configuration is pictured on Figure 4.10, and has $\omega = 2d-8$.

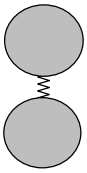

Figure 4.10: The leading configuration with one wavy line

Now, starting with a graph $H(\mathcal{G})$ with ℓ wavy lines, we have only two types of moves for adding a new wavy line. The first one is pictured on Figure 4.11. We can add a leaf on a grey disk or replace a wavy line by a grey disc with two external wavy lines.

[4] Note that the remaining product of unused or redundant δ functions is simply bounded by 1 because the p_f variables are discrete, hence the δ functions are simply Kronecker symbols, all bounded by 1; of course this would not be true for continuous variables as a product of redundant Dirac δ distributions in the continuum is ill-defined.

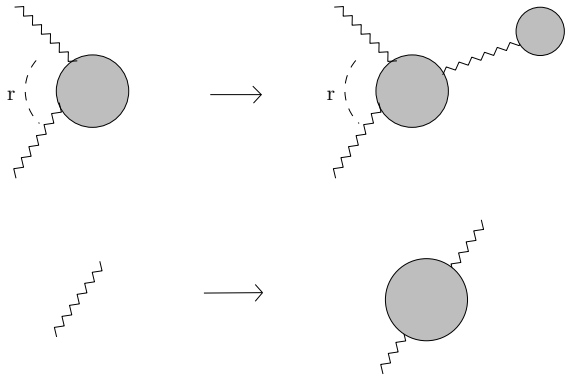

Figure 4.11: The first two moves: we add a leaf on a grey disk or replace a wavy line by a grey disk with two external wavy lines.

These moves add two dotted lines in the original representation and they create $d-1$ faces. Moreover, in both cases, the rank increases by one, and the variation of the divergent degree is:

$$\delta\omega = -2\delta L + \delta F - \delta R = d - 6\,. \tag{4.78}$$

For $d < 6$, the move cost at least -1, and the convergence increases quickly. The second possibility is pictured in Figure 4.12: we can add a wavy line between two grey disks or add a self wavy loop on a single grey disk.

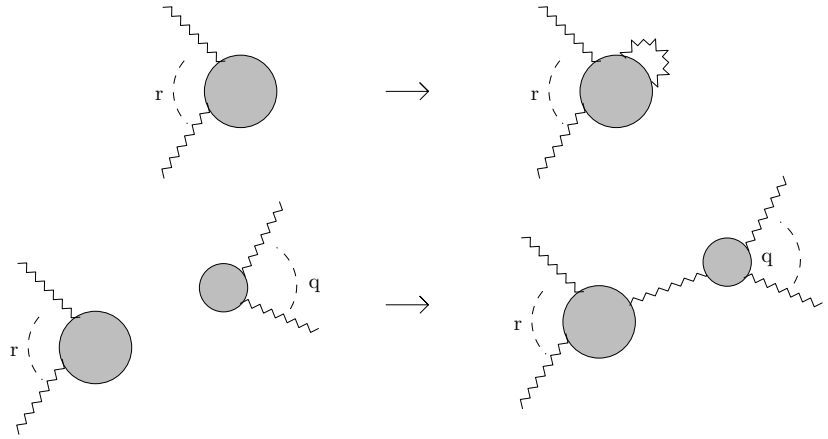

Figure 4.12: The second two moves: we add a wavy line between two grey disks or a self-loop on a single grey disk.

In both cases $\delta L = 2$. Adding a self-loop increases by one the number of faces (i.e. the face running in the internal arc), and by one the rank of ϵ_{ef}. If we add a wavy line, say of color i between two grey disks, either it connects together two disconnected faces of color i, and then $\delta F = -1$, $\delta R = 0, -1$, or it disconnects a face of color i, and $\delta F = 1$, $\delta R = 1$. In both cases, we conclude that

$$\delta\omega \leq -2 \times 2 + (1-1) = -4\,. \tag{4.79}$$

Therefore, if $d \geq 3$, the trees are the leading order graphs.

□

Now, consider first the case of a vacuum subgraph which is *particle irreducible* (PI) in terms of the propagators of the initial representation, hence in terms of the arcs of the intermediate field representation. If it is a tree with $\mathcal{B}$ grey disks, it has $L = 2(n-1)$ arcs, $(d-1)\mathcal{B}+1$

faces (since each wavy line glues two faces) and it is easy to check by induction (adding leaves one by one from a root) that the rank R of the ϵ matrix is maximal, namely n. Hence $\omega = -4(\mathcal{B}-1)+(d-1)\mathcal{B}+1-n = (d-6)\mathcal{B}+5$ in this case. Next let us consider the case of a PI tree subgraph with n external wavy lines, hence $2n$ external arcs.

- if $n=1$ the subgraph is a 1-point function[5] and the single external wavy line adds one arc, suppresses one face and does not change the rank, hence $\omega = (d-6)\mathcal{B}+2$ in this case.

- if $n=2$ the subgraph is a 4-point function and the two external wavy lines add two arcs. If they have different colors, or have the same color i and hook to two components of the tree not connected by lines of color i, then they open two different faces and do not change the rank, so that $\omega = -1$. However there is a special case, when the two external wavy lines have same color and hook to the same loop vertex or to different loop vertices joined by a path in the tree made of wavy lines all of the same color i. In that case and only in that case, the wavy lines open only the single face of color i common to all loop vertices along this path, the rank again has not changed and $\omega = (d-6)\mathcal{B}$.

- if $n>2$, each new external line turning L into $L+1$, can either keep F unchanged (if it hits a face already opened), in which case R is also unchanged, or change F to $F-1$, in which case either R is unchanged or goes to $R-1$; hence ω decreases at least by 1. As a result, for $d \leq 6$, this proves

$$\omega(\mathcal{G}) \leq -(n-2) \text{ if } n>2. \tag{4.80}$$

Finally we still have to study the case of non-vacuum, non-PI graph. Since they add at least one new arc to a PI graph, it is easy to check that they have $\omega < 0$, except in two particular cases corresponding both to one-particle reducible graphs:

- a chain of arcs joining PI two-point trees, with one of them at both ends. Such subgraphs are one-particle reducible two-point subgraphs of the initial theory with $\omega = 2$.

- a chain of arcs joining PI two-point trees, with one of them at a single of its two ends. Such subgraphs are one-particle reducible four-point subgraphs of the initial theory, with $\omega = 0$.

Translated into the original representation, this result shows that for leading graphs the divergent degree is:

$$\omega(\mathcal{G}) = (d-2) - (6-d)V(\mathcal{G}) - (d-4)\frac{N(\mathcal{G})}{2}, \tag{4.81}$$

where we used the fact that each wavy line corresponds to a bubble vertex in the original representation, that each arc corresponds to a dotted line, and that the rank is exactly the number of grey disks. We can then classify the theory, from $d=3$ to $d=6$:

• For $d=3$, the divergent degree is reduced to $\omega = 1-3V+N/2$. Hence, because the number of external lines of a graph with $V(\mathcal{G})$ vertices is bounded by $N_{max} = 2(V(\mathcal{G})+1)$, when the graph is a tree, without faces, the divergent degree is strictly smaller than $\omega_{max} = 2(1-V(\mathcal{G})) \leq 0$, which is strictly smaller than 0 for $V>1$. For $V=1$ our bound could indicate a logarithmic

[5]Hence a two-point function in the original representation.

divergence, but a direct calculation shows that the divergent degree of a melonic graph with one vertex, as depicted below, is :

$$\omega_{melo}(V=1) = -2+2-1 = -1,$$

so that the model is in fact divergence free, at least for non-vacuum graphs. The vacuum graphs are not directly concerned by our purpose in this chapter, but our conclusion about the finiteness of the model can be complete only if these graphs are finite as well; and it is not hard to see that it is the case. Indeed, for these graphs, the bound [12](saturated for melonic graphs) can be established:

$$F(\mathcal{G}_{vac}) - R(\mathcal{G}_{vac}) \leq L(\mathcal{G}_{vac}) - V(\mathcal{G}_{vac}) + 2 \tag{4.82}$$

so that

$$\omega_{melo}(\mathcal{G}_{vac}) = 2 - 3V(\mathcal{G}_{vac}) < 0. \tag{4.83}$$

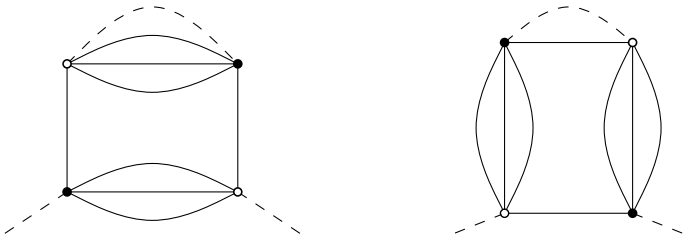

a b

Figure 4.13: The two configurations for tadpole graphs

• For $d = 4$, it reduces to $\omega = 2(1-V)$, and the theory becomes *super-renormalizable*. ω is negative for $V > 1$. For $V = 1$, the degree vanishes, so that such a graph with one vertex diverges at least logarithmically. The two possible diagrams are pictured in Figures 4.13a and 4.13b. But by direct inspection, it can be shown that the graph of Figure 4.13b is finite, with divergent degree $\omega = -2+1-1 = -2$. The melonic tadpole of Figure 4.13a however has a vanishing divergent degree $\omega = -2+3-1 = 0$, so that it diverges logarithmically. Hence, the only divergent graphs in that model are *melopoles* [12] whose definition we now recall[6].

Definition 11. *In a graph $\mathcal{G}$, a melopole is a tadpole (or single-vertex) subgraph $\mathcal{H}$, such that there is at least one ordering (or "Hepp's sector") of its k-dotted lines as $e_1, ..., e_k$ such that $\{e_1, ..., e_i\}/\{e_1, ..., e_{i-1}\}$ is a d-dipole for $1 \leq i \leq k$.*

• For $d = 5$, the degree becomes $\omega = 3 - V - N/2$, and the theory remains *super-renormalizable*. The divergences come only from the 2-point graphs. However, in this case, divergences occur not only for melopole graphs, with one vertex and divergent degree $\omega = 1$, but also for melonic graphs with two vertices, and divergent degree $\omega = 0$.
• For $d = 6$, the divergent degree $\omega = 4 - N$ becomes independent of the number of vertices number and the theory is called *just-renormalizable*: There are infinitely many divergent graphs. However all the divergences can be removed with counter-terms of valence zero, two and four.

It is easy to see that the leading graphs are nothing but melonic graphs. The tree structure reflects the recursive definition of the melons. Therefore:

Proposition 5. *The T^4_6 model with closure constraint is just-renormalizable. All the divergences of the 2 and 4-point functions. are restricted to the melonic sector.*

[6]The finiteness of the number of divergent graphs is a characteristic of super-renormalizable theories.

Definition 12. *In a graph $\mathcal{G}$, a melonic subgraph is a face-connected subgraph $\mathcal{H}$ containing at least one maximal spanning tree $\mathcal{T}$ such that $\mathcal{H}/\mathcal{T}$ is a melopole.*

In this definition the concept of face-connectivity refers to the factorization of the incidence matrix ϵ_{ef} as rectangular blocks. A face-connected component is then defined as the subset of lines of such a block, and a graph is *face-connected* if it has a single face-connected component. Note that in the rest of this chapter, we call "melonic" any leading order graph with 0, 2 or 4 external lines.

4.4.4 Locality and traciality

The remaining question concerns the locality principle suitable for the TGFTs. We have discussed this principle, called traciality in Section 4.2.4, and we shall give in this section a general definition of this concept, and a minimal discussion of the way it works. In the original representation, and in term of the group variables (the notations are those of Chapter 3), a graph is said to be *tracial* if it is contractible, and the resulting graph is connected. The notion of *contractibility* is the following:

Definition 13. *Let $\mathcal{G}$ be a vertex-connected graph, and $\mathcal{H}$ be one of its face-connected subgraphs.*

• *If $\mathcal{H}$ is a tadpole, $\mathcal{H}$ is contractible if, for any group element assignments $\{h_e, e \in \mathcal{L}(\mathcal{H})\}$:*

$$\forall f \in \mathcal{F}(\mathcal{H}), \overrightarrow{\prod_{e\in f}} h_e^{\epsilon_{ef}} = \mathbb{I} \Rightarrow \forall e \in \mathcal{L}(\mathcal{H}), h_e = \mathbb{I}\,. \tag{4.84}$$

• *In general, $\mathcal{H}$ is contractible if it admits a spanning tree $\mathcal{T}$ such that $\mathcal{H}/\mathcal{T}$ is a contractible tadpole.*

In order to understand the meaning of this concept in momentum space and intermediate field representation, let us consider a melonic graph in the intermediate field representation, with 2 external wavy lines of the same color, say 1. An example is pictured on Figure 4.14 below, in which the path surrounding the external faces of color 1 has been shown. We denote by p_{ext} the momentum running along these faces.

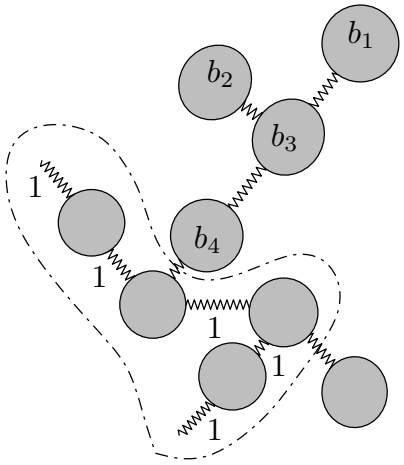

Figure 4.14: A leading graph with two external wavy lines in the intermediate field representation. The grey disks sharing the external faces have been surrounded.

For such a graph, the corresponding amplitude $\mathcal{A}_\mathcal{G}$ is:

$$\mathcal{A}_\mathcal{G} = \prod_{e\in\mathcal{L}(\mathcal{G})}\int_{1/\Lambda^2}^{+\infty} d\alpha_e e^{-\alpha_e m^2}\prod_{b\in\mathbb{B}}\delta\Big(\sum_i p_{bi}\Big)\prod_{f\in\mathcal{F}(\mathcal{G})}\sum_{p_f\in\mathbb{Z}} e^{-\alpha_f p_f^2}e^{-\alpha_{ext}p_{ext}^2}\,, \tag{4.85}$$

where $\mathbb{B}$ (for "blobs") denotes the set of grey disks, $\vec{p}_b$ the momentum running along the strands of the grey disk b, and α_{ext} is the sum of Schwinger parameters along the external faces. Expanding the delta functions in Fourier components, the previous expression becomes:

$$\mathcal{A}_\mathcal{G} = \prod_{e\in\mathcal{L}(\mathcal{G})}\int_{1/\Lambda^2}^{+\infty} d\alpha_e e^{-\alpha_e m^2}\prod_{b\in\mathbb{B}}\int_{-\pi}^{\pi}\frac{d\beta_b}{2\pi}\prod_{f\in\mathcal{F}(\mathcal{G})}\sum_{p_f\in\mathbb{Z}} e^{-\alpha_f p_f^2+i\beta_f p_f}e^{-\alpha_{ext}p_{ext}^2+i\beta_{ext}p_{ext}}\,, \tag{4.86}$$

where $\alpha_f := \sum_{e\in\partial f}\alpha_e$ and $\beta_f := \sum_{b\in\partial f}\epsilon_{bf}\beta_b$, $\epsilon_{bf} := \frac{1}{|\partial f\cap b|}\sum_{e\in\partial f\cap b}\epsilon_{ef}$. Computing the sums using 4.13, the amplitude behaves as:

$$\mathcal{A}_\mathcal{G} \propto \prod_{e\in\mathcal{L}(\mathcal{G})}\int_{1/\Lambda^2}^{+\infty} d\alpha_e e^{-\alpha_e m^2}\prod_{b\in\mathbb{B}}\int_{-\pi}^{\pi}\frac{d\beta_b}{2\pi}\prod_{f\in\mathcal{F}(\mathcal{G})}\frac{1}{\alpha_f^{1/2}}e^{-\beta_f^2/4\alpha_f}e^{-\alpha_{ext}p_{ext}^2+i\beta_{ext}p_{ext}}\,. \tag{4.87}$$

Now, consider the vicinity of the point $\alpha_e = 0\,\forall e$. As for the one-loop computations, the Gaussian $e^{-\beta_f^2/4\alpha_f}$ must be expanded as a distribution $\prod_f e^{-\beta_f^2/4\alpha_f} \sim \prod_f\sum_{n_b} a_{n_b}\delta^{(2n_b)}(\beta_f)$. But it is easy to see that, due to the melonic structure :

Lemma 1. *For any melonic graphs in the intermediate field representation:*

$$\forall f\ ,\beta_f = 0 \Rightarrow \forall b\ ,\beta_b = 0\,, \tag{4.88}$$

which is nothing but the translation of Formula 4.84. The proof can be easily checked recursively on the number of (internal) wavy lines from the tree structure of the melonic graph, using the operations pictured in Figure 4.11. Obviously, the two-point graph with two external wavy lines and one grey disk

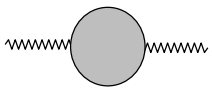

verifies 4.88. Now, starting with a graph with ℓ internal wavy lines, we can either add a leaf or replace a wavy line by a two-point grey disk (the first case corresponds to the grey disks b_1 and b_2 on the Figure 4.14, the second to the grey disk labeled b_4). In both cases, we introduce at least 4 internal faces running into the added bubbles, meaning that the relation 4.88 remains true.

As a result, $\prod_f e^{-\beta_f^2/4\alpha_f} \sim \prod_b\sum_{n_b} a_{n_b}\delta^{(2n_b)}(\beta_b)$. Moreover, each grey disk sharing external faces (surrounded in Figure 4.14) makes contact with internal faces. Therefore, the amplitude 4.87 can be consistently expanded in powers of p_{ext}, as in the one-loop case of Section 4.2.1. The factorized part corresponds as in Figure 4.8, to the original amplitude whose external faces have been discarded. Then, our claim is the following:

Proposition 6. *Any melonic subgraph $\mathcal{H}$ is tracial.*

It will entail that we shall be able to renormalize it.

4.5 Systematic renormalization of T_6^4

4.5.1 Bound of the renormalized amplitudes

In this section we truly prove that T_6^4 is a just-renormalizable theory, to all orders in perturbation theory. We introduce a systematic renormalization leading to a well-defined renormalized series, with finite renormalized amplitudes at all orders. The best way to prove that they are finite is to do more, and to give precise explicit bounds on any renormalized amplitudes. It will depend of their *Zimmermann forest structure*. We begin by a uniform bound for convergent graphs, which is an adapted version of the same theorem in the ordinary field theory case [2]. Then we shall study broadly the renormalization of divergent graphs, before closing the section by a proof of finiteness of any renormalized amplitude.

Uniform Weinberg Theorem

An important aspect of the multiscale analysis is that it provides easily a uniform exponential bound on *convergent* amplitudes:

Theorem 2. *The amplitude $A(\mathcal{G})$ for a completely convergent connected graph $\mathcal{G}$ (i.e. a graph for which $\omega(\mathcal{H}) < 0 \, \forall \mathcal{H} \subset \mathcal{G}$) is uniformly bounded in terms of its size, i.e. there exists a constant K such that if n is the order (number of vertices) of the graph:*

$$|\mathcal{A}(\mathcal{G})| \leq K^{n(\mathcal{G})}. \tag{4.89}$$

Proof. We assume that $N(\mathcal{G}) \geq 1$, so that $\forall \mathcal{H} \subset \mathcal{G}, N(\mathcal{H}) \geq 1$ (the vacuum case $N(\mathcal{G}) = 0$ is an easy extension left to the reader). (4.80) implies that for a convergent PI graph with $2N > 4$ external arcs

$$\omega(\mathcal{H}) \leq -N(\mathcal{H})/3 = -2N(\mathcal{H})/6. \tag{4.90}$$

This is also true if $\mathcal{H}$ is convergent with $N = 1$ or 2, since we saw that in this case $\omega \leq -1 \leq -N(\mathcal{H})/3$. For a ϕ^4 graph of order $V = n$ with $2N$ external legs, we have $2L = 4V + 2N$. Therefore (4.77) implies that for another constant K

$$\mathcal{A}(\mathcal{G}) \leq K^n \sum_{\mu} \prod_{i} \prod_{k=1}^{k(i)} M^{-2N(\mathcal{G}_i^k)/6}. \tag{4.91}$$

Let us now define

$$i_v(\mu) = \sup_{e \in L_v(\mathcal{G})} i_e(\mu) \ , \ e_v(\mu) = \inf_{e \in L_b(\mathcal{G})} i_e(\mu), \tag{4.92}$$

where v denotes a vertex $v \in \mathcal{G}$, and $L_v(\mathcal{G})$ the set of its external (half)-lines. v is external to a high subgraph $\mathcal{G}_i^k$ if and only if $e_b < i \leq i_b$, and then it is hooked to at least one of the $2N(\mathcal{G}_i^k)$ external half-lines of $\mathcal{G}_i^k$. Therefore

$$\prod_{i,k} M^{-2N(\mathcal{G}_i^{(k)})/6} \leq \prod_{i,k} \prod_{v \in \mathcal{G}_i^{(k)} | e_v < i \leq i_v} M^{-1/6}. \tag{4.93}$$

Using the fact that there are at most 4 half-lines, and thus $6 = 4 \times 3/2$ pairs of half-lines hooked to a given vertex, and that, for two external lines e and e' of a vertex v, $|e_v - i_v| \geq |i_e - i_{e'}|$, we obtain:

$$\mathcal{A}(\mathcal{G}) \leq K^n \sum_{\mu} \prod_{v} \prod_{(e,e') \perp v} M^{-\frac{|i_e - i_{e'}|}{36}}, \tag{4.94}$$

where the product over $(e, e') \perp v$ means the product over all pairs of half-lines hooked to v. The bound means that there is exponential decay in scale differences between all such pairs[7]. Organizing the sum over $\mu = \{i_e\}$ along a tree of lines of $\mathcal{G}$ as in [2], it is easy to bound it by $K^{L(\mathcal{G}}$, hence to complete the proof of (4.89), hence of Theorem 2. □

Divergent graphs and renormalization

Definition 14. *Consider a non-vacuum Feynman graph $\mathcal{G}$ and let $h \subseteq \mathcal{G}$ be a subgraph of $\mathcal{G}$ with n_h external wavy lines. The subgraph h is said to be*
- *superficially convergent if $\omega(h) < 0$,*
- *superficially divergent if $\omega(h) \geq 0 \Rightarrow n_h \leq 2$.*

Definition 15. *Consider a Feynman graph $\mathcal{G}$. A Zimmermann forest $\mathbb{F}$ is a forest of connected divergent subgraphs $\{h \subseteq \mathcal{G} | \omega(h) \geq 0\}$. Here the word* forest *should be understood in the sense of inclusion relations. It simply means that taking two elements $h_1, h_2 \in \mathbb{F}$, they are either line and vertex disjoint or included one into the other. The set of all Zimmermann forests of $\mathcal{G}$ is noted $\mathcal{D}_Z(\mathcal{G})$.*

Taking into account these definitions, we shall give a general definition of the counter-terms and contraction operator $\tau_{\mathcal{H}}$ introduced in Section 4.2.4.

Let us start with the case of a 1-point subgraph in the intermediate field representation, as the graph called $\mathcal{M}$ in Figure 4.15a, with external wavy line of color 1, ℓ_1 and amplitude $\mathcal{M}_j$. The index j refers to the lower scale attribution of $\mathcal{M}_j$, and it is included in the amplitude $\mathcal{A}_{\mathcal{G},\mu}$, for a scale attribution μ. We denote by $\bar{\mathcal{A}}_{\mathcal{G},\mu}$ the part of the amplitude $\mathcal{A}_{\mathcal{G},\mu}$, amputated of $\mathcal{M}_j$ and of the two arcs hooked to the wavy line ℓ_1, and by i_1 the scale attribution of the arcs of the grey disk hooked to ℓ_1. We assume that $\mathcal{M}$ is the only divergent subgraph of $\mathcal{G}$. The amplitude $\mathcal{A}_{\mathcal{G},\mu}$ takes the form:

$$\mathcal{A}_{\mathcal{G},\mu} = \sum_{\vec{p} \in \mathbb{Z}^6} \bar{\mathcal{A}}_{\mathcal{G},\mu}(p_1, \{p_j, j \neq 1\}) C^2_{i_1}(\vec{p}) \mathcal{M}_j(p_1)\,. \tag{4.95}$$

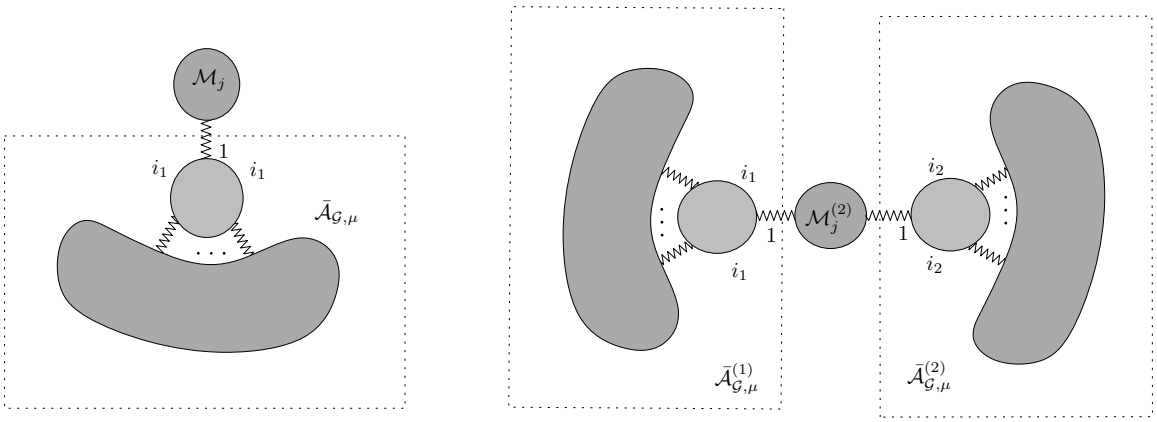

Figure 4.15: Sub-divergent 1-point graph (a) and 2-point graph (b).

[7] (4.94) is of course a very sloppy estimate, that could be easily improved. For instance we could take advantage of the momentum representation conservation rules to remark that only one pair of different scales is in fact hooked to any vertex, rather than 6, but it won't change the structure of the result, only improve numerical constants.

Now, we introduce a real parameter $t \in [0,1]$, and define:

$$\mathcal{A}_{\mathcal{G},\mu}(t) := \sum_{\vec{p}\in\mathbb{Z}^6} \bar{\mathcal{A}}_{\mathcal{G},\mu}(p_1, \{p_j, j \neq 1\}) C^2_{i_1}(\vec{p}) \mathcal{M}_j(tp_1)\,, \tag{4.96}$$

such that $\mathcal{A}_{\mathcal{G},\mu}(t=1) = \mathcal{A}_{\mathcal{G},\mu}$. The operator $\tau_{\mathcal{M}}$ acting on the sub-divergent graph $\mathcal{M}$ is

$$\tau^*_{\mathcal{M}} \mathcal{A}_{\mathcal{G},\mu} := \sum_{n=0}^{\omega(\mathcal{M})} \frac{1}{n!} \frac{d^n}{dt^n} \mathcal{A}_{\mathcal{G},\mu}(t=0)\,, \tag{4.97}$$

For instance $\omega(\mathcal{M}) = 2$ in the case considered, hence the sum over n in (4.97) has a priori three terms in this case, but by symmetry consideration the one with $n = 1$ vanishes. We shall prove that the remaining term in the Taylor expansion,

$$\mathcal{A}^R_{\mathcal{G},\mu} := (1 - \tau^*_{\mathcal{M}}) \mathcal{A}_{\mathcal{G},\mu}(t=1) = \int_0^1 dt \frac{(1-t)^{\omega(\mathcal{M})}}{\omega(\mathcal{M})!} \frac{d^{\omega(\mathcal{M})+1}}{dt^{\omega(\mathcal{M})+1}} \mathcal{A}_{\mathcal{G},\mu}(t) \tag{4.98}$$

is convergent. Obviously, it follows from the bounds 4.72 that

$$\left| \frac{d^k}{dp_i^k} C_i(\vec{p}) \right| \leq K M^{(-2-k)i} \delta(\sum_c p_c) \chi_{\leq i}(\vec{p})\,. \tag{4.99}$$

Then, the derivative in 4.98 generates a factor $M^{-(\omega(\mathcal{M})+1)j}$. Moreover, the derivative generates a factor $p_1^{\omega(\mathcal{M})+1}$, increasing the convergent degree by a factor $M^{(\omega(\mathcal{M})+1)i_1}$. As a result, if the divergent subgraph $\mathcal{M}$ is high, i.e. if $i > i_1$, the total decay factor is bounded by -1

$$\omega(\mathcal{M}) + (\omega(\mathcal{M}) + 1)(i_1 - j) < -1\,, \tag{4.100}$$

meaning that the remaining term 4.98 is convergent. In the same way, for the 2-point sub-divergent graph $\mathcal{M}^{(2)}$ pictured on Figure 4.15b, the amplitude "at time t" writes as:

$$\begin{aligned} \mathcal{A}_{\mathcal{G},\mu}(t) &:= \sum_{\vec{p}_1,\vec{p}_2} \bar{\mathcal{A}}^{(1)}_{\mathcal{G},\mu}(\vec{p}_1) C^2_{i_1}(p_{11}, \{p_{1l}, l \neq 1\}) C^2_{i_2}(\vec{p}_2) \bar{\mathcal{A}}^{(2)}_{\mathcal{G},\mu}(p_{21} \\ &= p_{11}, \{p_{2l}, l \neq 1\}) \mathcal{M}^{(2)}_j(tp_{11})\,. \end{aligned} \tag{4.101}$$

As for the 1-point function, we can introduce the operator $\tau_{\mathcal{M}^{(2)}}$, whose action is defined by 4.97, and in the same way, we prove that the remaining term is superficially convergent.

The general procedure, extending the one-loop subtraction of Section 4.2 is then the following, defining the *renormalized amplitude* $\mathcal{A}^R_{\mathcal{G}}$:

Definition 16. *The renormalized amplitude $\mathcal{A}^R_{\mathcal{G}}$ for a Feynman graph $\mathcal{G}$ with sub-divergences is defined from the bare amplitude $\mathcal{A}_{\mathcal{G}}$ through the Zimmermann (or forest) formula :*

$$\mathcal{A}^R_{\mathcal{G}} := \sum_{\mathbb{F}\subset\mathcal{D}_Z(\mathcal{G})} \prod_{h\in\mathbb{F}} (-\tau^*_h) \mathcal{A}_{\mathcal{G}}\,, \tag{4.102}$$

where $\mathcal{D}_Z(\mathcal{G})$ is the set of Zimmermann forests.

The form of the counters-terms ensures the stability of the original classical action. Indeed:

• For a one point function graph, because $\mathcal{M}$ only depends on one external momenta, the zero-derivative with respect to $\mathcal{A}_{\mathcal{G},\mu}(t)$ generates a mass counter-term:

$$\tau^{1\,*}_{\mathcal{M}}\mathcal{A}_{\mathcal{G},\mu} := \mathcal{M}_j(0) \times \mathcal{A}_{\mathcal{G}/\mathcal{M}}\,. \tag{4.103}$$

where $\mathcal{G}/\mathcal{M}$ corresponds to the contraction operation defined in Definition 10.
• The first derivative with respect to t vanishes, because of the structure of the amplitude (see 4.87). Indeed, $\mathcal{M}_j \propto e^{-\alpha_{ext}p_1^2+i\beta_{ext}p_1}$, and the first derivative with respect to t generates a factor $i\beta_{ext}$.
• The last derivative, involving two derivatives with respect to t, generates a wave-function counter-terms. Indeed,

$$\tau^{2\,*}_{\mathcal{M}}\mathcal{A}_{\mathcal{G},\mu} := \left(\frac{1}{2}\frac{d^2}{dp^2}\mathcal{M}_j(p)\Big|_{p=0}\right) \times \sum_{\vec{p}\in\mathbb{Z}^6} p_1^2 \bar{\mathcal{A}}_{\mathcal{G},\mu}(p_1,\{p_j, j\neq 1\})C^2_{i_1}(\vec{p}) \tag{4.104}$$

• Finally, for the 2-point graphs, for which $\omega = 0$, there is only a zero-derivative term which generates a coupling constant counter-term

$$\tau^{*}_{\mathcal{M}^{(2)}}\mathcal{A}_{\mathcal{G},\mu} = \mathcal{M}^{(2)}_j(0) \times \mathcal{A}_{\mathcal{G}/\mathcal{M}^{(2)},\mu}. \tag{4.105}$$

Again, $\mathcal{G}/\mathcal{M}^{(2)}$ corresponds to the connected contracted graph, pictured on Figure 4.16.

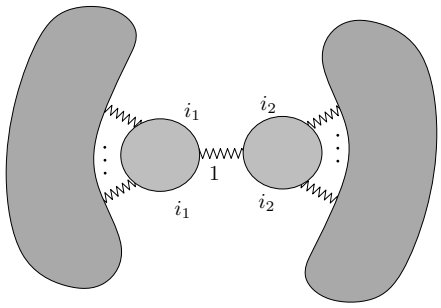

Figure 4.16: The graph $\mathcal{G}/\mathcal{M}^{(2)}$.

Bounds of the renormalized amplitudes

The finiteness of the renormalized amplitude can be proved rigorously, and we do this in this section, following closely [2]. In fact, we shall prove like in [2] that, when the graph contains some subdivergences, the renormalized amplitude $\mathcal{A}^R_{\mathcal{G}}$ is finite, but can increase dramatically with its size, as a *factorial* of the maximal number of elements in a Zimmermann forest. Proving this theorem requires to define precisely the so-called "dangerous" and "safe" divergent forests:

Definition 17. Dangerous and safe forests *Consider a fixed graph $\mathcal{G}$ and a fixed attribution μ. Let $\mathcal{A}_{\mathcal{G},\mu}$ be the corresponding amplitude for the scale attribution μ, and $\mathbb{F} \in \mathcal{D}_Z(G)$ a Zimmermann forest. Consider then $h \subset \mathbb{F}$. We define i_h and e_h as:*

$$i_h = \inf\{i_l | l \in h/\mathbb{A}_{\mathbb{F}}(h)\} \quad e_h = \sup\{i_l | l \in L_h \cap \mathbb{B}_{\mathbb{F}}(h)\}$$

where L_h is the set of external lines of h, $\mathbb{B}_{\mathbb{F}}(h)$ is the ancestor of h in $\mathbb{F}$ and $\mathbb{A}_{\mathbb{F}}(h)$ the union of all its immediate descendants (for the inclusion relation).

The set $D_\mu(\mathbb{F})$ of dangerous or "high" subgraphs in $\mathbb{F}$ with respect to the scale assignment μ is defined as made of all $h \in \mathbb{F}$ with $i_h > e_h\}$. The safe forest $S_\mu(\mathbb{F})$ is then its complement in $\mathbb{F}$.

A key property is that taking the safe part of a forest is a projector, namely $S_\mu \mathrm{o} S_\mu = S_\mu$. More explicitly, for any Zimmermann forest $S_\mu(S_\mu(\mathbb{F})) = S_\mu(\mathbb{F})$. This identity is not obvious and a general proof can be found in [2].

Let us define safe forests as the fixed points under this projection. The forests which project onto a given safe forest S have then a simple structure: they are exactly the forest including S and included in an other Zimmermann forest, $S \cup H_\mu(S)$. $H_\mu(S)$ can be though of as the maximal set of high subgraphs compatible with S.

In particular the cardinal of $S_\mu^{-1}(S)$ is always a power of 2. This is not true in general for the full set $\mathcal{D}_Z(G)$, because of the famous problem of *overlapping divergencies* [2]. This particular structure of any $S_\mu^{-1}(S)$ allows to reorganize in any attribution μ the renormalized amplitude as a sum indexed by safe forest, and in each safe forest contribution to factorize a product of $(1 - \tau_h^*)$ operators, using a binomial identity. This is the essential point which in turn will allow to subtract any dangerous high subgraph in any attribution. More precisely

$$\mathcal{A}^R_{\mathcal{G},\mu} = \sum_{S \,\text{safe for}\, \mu} \mathcal{A}^R_{\mathcal{G},\mu,S} \ , \tag{4.106}$$

with:

$$\mathcal{A}^R_{\mathcal{G},\mu,S} := \prod_{h \in S} (-\tau_h^*) \prod_{h \in H_\mu(S)} (1 - \tau_h^*) \mathcal{A}_{\mathcal{G},\mu} \ . \tag{4.107}$$

Beginning with the contractions over the safe forest S, we obtain, after appropriate organization of the successive contractions a series of terms each associated to a subgraph g of $\mathcal{G} \cup S$ reduced by its descendants in S.

$$\mathcal{A}^R_{\mathcal{G},\mu} = \prod_{g \in S \cup \{\mathcal{G}\}} \mathcal{A}^R_\mu(g/\mathbb{A}_S(g)) \ . \tag{4.108}$$

Note that all these terms are not exactly disconnected, because the contraction of the 2-point graphs reveals a non-local operator, which acts on another contracted component. Using a Taylor remainder formula for each $(1 - \tau_h^*)\mathcal{A}_{\mathcal{G},\mu}$ piece, we can cure every high divergent subgraph in each of the contracted pieces $g/\mathbb{A}_S(g)$ It follows then from the multiscale analysis, in the same way than in the previous subsection, that the renormalized amplitude for that attribution is bounded by

$$\Big| \prod_{g \in S \cup \{\mathcal{G}\}} \mathcal{A}^R_\mu(g/\mathbb{A}_S(g)) \Big| \leq \prod_{g \in S \cup \{\mathcal{G}\}} \prod_{i,\rho} M^{\omega' \left[(g/\mathbb{A}_S(g))^\rho_i \right]} \ . \tag{4.109}$$

where :

$$\omega' \left[(g/\mathbb{A}_S(g))^\rho_i \right] := \inf \left(-1, \omega \left[(g/\mathbb{A}_S(g))^\rho_i \right] \right) \ .$$

From the decay factor of equation (4.109), we can extract the factor $M^{-\delta i_{max}(\mu)}$, where $i_{max}(\mu) := \sup(\mu)$. With the rest of the decay, we can sum over each component $g/\mathbb{A}_S(g)$, as in the proof of the uniform Weinberg theorem. Because of the following bound:

$$\prod_{g \in S \cup \{G\}} K^{|V(g/\mathcal{A}_S(g))|} \leq {K'}^{|V(G)|} \ , \tag{4.110}$$

the sum over all internal scale assignments in each $g/\mathbb{A}_S(g)$ is bounded by ${K'}^{|V(g)|}$, and from the convergence we can always spare a decay factor at least $M^{-\delta i_{max}}$ for some $\delta > 0$, where i_{max} is the maximal scale for the whole attribution μ.

However for any safe element $h \in S$ it remains to sum over one scale, say i_h, which is only bounded by some external line scale of h, hence by e_h. In the worst case we may have up to $|S|$

different such sums one for all the $i_h, h \in S$ indices to perform, and only a single decay $M^{-\delta i_{max}}$ factor for all of them. Now since

$$\sum_{i_{max}} M^{-\delta i_{max}} \prod_{h \in S} \sum_{i_h \leq i_{max}} 1 = \sum_{i_{max}} (i_{max})^{|S|} M^{-\delta i_{max}} \simeq |S|! K^{|S|} \quad , \tag{4.111}$$

where $|S|$ is the cardinality of S, it is impossible to conclude to a uniform bound of type (2) for the *renormalized* amplitudes. Indeed in a graph with n vertices, there can be forests with almost n elements, and they can be safe for some attributions. We finally deduce the following theorem [2]:

Theorem 3. (BPH uniform) *Consider a Feynman graph G of order $|V(\mathcal{G})|$. The renormalized amplitude $\mathcal{A}^R_{\mathcal{G}}$ has the following bound:*

$$|\mathcal{A}^R_{\mathcal{G}}| \leq K^{|V(\mathcal{G})|} d(\mathcal{G})!, \ K \in \mathbb{R}^+ \quad , \tag{4.112}$$

where $d(\mathcal{G}) := \sup_{\mathcal{F} \in \mathcal{D}_Z(\mathcal{G})} |\mathcal{F}|$ is the maximum cardinal of any Zimmermann forest of $\mathcal{G}$.

As announced, the amplitude is finite but can increase dramatically with the maximal size of divergent forests. This is the well-known problem of *renormalons*. It is a *second source* of divergence of the full renormalized perturbative series (4.102), completely independent of the much better known *first source*, which exists for any model, and is the large (factorial) growth in n of the number of Feynman graphs at order n.

To see why this problem exists also in our model, and even in its melonic approximation, we consider the 2-point subgraph of Figure 4.17; made of an arbitrarily large monocolor chain of n simple loop vertices with two arcs, ending on a leaf with a single arc. All wavy lines have the same color i and carry the same momentum p_i.

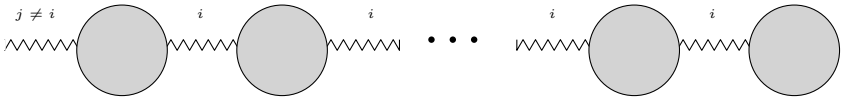

Figure 4.17: Typical melonic graph with renormalon effect

Because the renormalized 4-point function, i.e the renormalized loop vertex with two arcs, behaves as $\log(p_i)$ at large p_i, inserting such a chain on a convergent loop in a convergent melonic vertex function will lead to a very large sum over p_i which typically can behave at large n as

$$\sum_{p_i \in \mathbb{Z}} [\log p_i]^n \frac{1}{p_i^2 + m^2} \sim K^n n! \tag{4.113}$$

for some constant K. This is the renormalon problem.

Typically nobody knows how to resum rigorously the renormalon problem when the theory is neither asymptotically free nor asymptotically safe. One must then perhaps rely on computer simulations to search for an eventual ultraviolet fixed point. But our model *is* asymptotically free. Continuing along the strategy of [2] we can pass to the effective series, defined in the next section, which reshuffles the renormalized power series as a series in many effective couplings, all related through a flow equation. This effective series is renormalon-free (although of course the *first source* of diveregnce, the large number of graphs still remains). Asymptotic freedom, proved at the one loop order, is enough to control the flow equation. This result indicates that the effective series should be convergent and the renormalized series Borel-summable, although a full proof would require constructive techniques beyond the scope of this thesis.

4.5.2 The effective series

The effective series is a more physical way to compute perturbation theory, and a natural solution to the renormalon problem when the theory is asymptotically free [2]. The basic idea is to renormalize in the Wilsonian spirit, namely step by step, expanding in a whole sequence of effective couplings rather than in the single renormalized coupling. Consider a graph $\mathcal{G}$ and its bare amplitude $A_\mu(\mathcal{G})$ with scale attribution μ as defined in the previous section. There are some $\mathcal{G}_i^k$ subgraphs which are divergent ($\omega(\mathcal{G}_i^k) \geq 0$). They form a forest $H_\mu(\mathcal{G})$ (because it is a subset of the Gallavotti-Nicolò tree containing all $\mathcal{G}_i^k$ high subgraphs). [8]. The effective amplitude $\mathcal{A}^{eff}(\mathcal{G})$ is defined by

$$\mathcal{A}^{eff}(\mathcal{G}) = \sum_\mu \mathcal{A}_\mu^{eff}(\mathcal{G}), \;\; \mathcal{A}_\mu^{eff}(\mathcal{G}) := \prod_{h \in H_\mu(\mathcal{G})} (1 - \tau_h^*) A_\mu(\mathcal{G}). \tag{4.114}$$

Theorem 4. (Existence of the effective expansion): *Consider the formal (bare) power series defined by:*

$$S_N^\Lambda = \sum_{\mathcal{G},\mu} \frac{1}{s(\mathcal{G})} \left(\prod_{v \in \mathcal{V}(\mathcal{G})} \Big(- \lambda_v^{(\Lambda)} \Big) \right) \mathcal{A}_\mu(\mathcal{G}) \quad , \tag{4.115}$$

where $\lambda_v^{(\Lambda)}$ designates the coupling constant of the vertex v. This series can be rewritten in a more convenient form in terms of the effective amplitudes:

$$S_N^\Lambda = \sum_{\mathcal{G},\mu} \frac{1}{s(G)} \left(\prod_{b \in \mathcal{V}(\mathcal{G})} \big(- \lambda_{v,e_v(\mathcal{G},\mu)}^{(\Lambda)} \big) \right) \mathcal{A}_\mu^{eff}(\mathcal{G}) \quad , \tag{4.116}$$

where the $\lambda_{v,e_v(\mathcal{G},\mu)}^{(\Lambda)}$ are the effective couplings, generated by the local part of the high divergent subgraphs. They obey the following inductive relation

$$\begin{aligned} -\lambda_{v,i}^{(\Lambda)} \;\; = \;\; & -\lambda_{v,i+1}^{(\Lambda)} + \sum_{\substack{(\mathcal{H},\mu,\hat{S})\hat{S} \neq \emptyset \\ \phi_i(\mathcal{H},\mu,\hat{S}) = (v,\mu,\emptyset)}} \frac{1}{s(\mathcal{H})} \left(\prod_{v' \in \mathcal{V}(\mathcal{H})} \big(- \lambda_{v',i'_v(\mathcal{H},\mu)}^{(\Lambda)} \big) \right) \\ & \times \left(\prod_{h \in H_\mu^{i+1} \setminus \hat{S}} (1 - \tau_h^*) \right) \prod_{M \in \hat{S}} \tau_M^* \mathcal{A}_\mu(\mathcal{H}) \; , \end{aligned} \tag{4.117}$$

with $e_v = \sup\{\mu_l, l \,\text{hooked to}\, v\}$. The notation introduced above will be defined precisely in the proof, for which we give only the main steps, referring to [2, 12] for details.

Proof. The basic idea is to introduce an intermediate step between the bare and the effective series as follows. We consider a slice i and define:

$$S_N^\Lambda = \sum_{\mathcal{G},\mu} \frac{1}{s(\mathcal{G})} \left(\prod_{v \in \mathcal{V}(\mathcal{G})} (-\lambda_{v,sup(i,i_v(\mathcal{G},\mu))}^{(\Lambda)}) \right) \mathcal{A}_\mu^{eff,i}(\mathcal{G}) \; , \tag{4.118}$$

where

$$\mathcal{A}_\mu^{eff,i}(\mathcal{G}) := \prod_{h \in H_\mu^i} (1 - \tau_h^*) \mathcal{A}_\mu(\mathcal{G}) \; , \tag{4.119}$$

[8] This forest exactly corresponds also to $H_\mu(\emptyset)$ associated to the empty safe forest in the previous subsection.

and

$$H_\mu^{i+1}(\mathcal{G}) = \{h \in H(\mathcal{G}) | i_h > i\} \quad i_h := \inf\{\mu_l, l \,\text{hooked to}\, v\} \ .$$

It is obvious that, if $i = \rho$, where $\Lambda = M^\rho$, the effective series reduces to the bare one. Assuming this is true at scale $i+1$, we can prove it at scale i by induction, by multiplying the effective amplitude at scale $i+1$ by a suitable form of the identity, adding and subtracting the counter-terms in $H_\mu^i(\mathcal{G}) \setminus H_\mu^{i+1}(\mathcal{G}) = \{h \in H(\mathcal{G}) | i_h = i+1\}$, which changes $\mathcal{A}_\mu^{eff,i+1}(\mathcal{G})$ into $\mathcal{A}_\mu^{eff,i}(\mathcal{G})$,

$$\mathcal{A}_\mu^{eff,i}(\mathcal{G}) := \prod_{\substack{S \subseteq H_\mu^i \setminus S_\mu^{i+1} \\ S \neq \emptyset}} \prod_{M \in S} (1 - \tau_M^* + \tau_M^*) \prod_{h \in H_\mu^i} (1 - \tau_h^*) \mathcal{A}_\mu(\mathcal{G}) \ .$$

The completely subtracted piece changes $\mathcal{A}_\mu^{eff,i+1}(\mathcal{G})$ into $\mathcal{A}_\mu^{eff,i}(\mathcal{G})$, and the second one is developed as a sum over S as follows:

$$S_N^\Lambda = \sum_{\substack{(\mathcal{G},\mu,S) \\ S \subseteq H_\mu^i \setminus H_\mu^{i+1}}} \frac{1}{s(\mathcal{G})} \left(\prod_{v \in \mathcal{V}(\mathcal{G})} (-\lambda^{(\Lambda)}_{b,sup(i+1,i_v(\mathcal{G},\mu))}) \right) \mathcal{A}_{\mu,S}^{eff,i}(\mathcal{G}) \ ,$$

with

$$\mathcal{A}_{\mu,S}^{eff,i} := \prod_{M \in S} (-\tau_M^*) \prod_{h \in H^i \setminus S} (1 - \tau_h^*) \mathcal{A}_\mu(\mathcal{G}) \ ,$$

and in particular $\mathcal{A}_{\mu,\emptyset}^{eff,i} = \mathcal{A}_\mu^{eff,i}$. A subtlety appears in this case because the 2-point divergent graphs (with degree $\omega = 2$) introduce two counter-terms, one for the mass and one for the wave-function. For this reason we change the previous definition of S, and introduce the new definition:

$$\hat{S} = \{(M, k_M) | M \in S, k_M \in 0, 2, k_M \leq \omega(M)\} \quad .$$

Secondly, we introduce the *collapse* ϕ_i which sends the triplet $(G, \mu, \hat{S})$ to its contracted version $(\mathcal{G}', \mu', \emptyset)$, such that the previous sum can be rewritten as a sum on $\mathcal{G}'$

$$S_N^\Lambda = \sum_{\mathcal{G}',\mu'} \sum_{\substack{\{(G,\mu,S)\} = \\ \phi_i^{-1}(\mathcal{G}',\mu',\emptyset)}} \frac{\mathcal{A}_{\mu,S}^{eff,i}(\mathcal{G})}{s(\mathcal{G})} \left(\prod_{v \in \mathcal{V}(G)} (-\lambda^{(\Lambda)}_{v,sup(i+1,i_v(G,\mu))}) \right) \quad . \tag{4.120}$$

Decomposing

$$\prod_{M \in \hat{S}} (-\tau_M^*) = \prod_{v' \in \mathcal{V}(G)} \left(\prod_{M \in \hat{S},\, M \subset \phi_i^{-1}(v')} (-\tau_M^*) \right)$$

in the sum (4.120), we find that it gives exactly the effective sum at scale i given by (4.118), if the coupling satisfies the recursive relation of the theorem.

□

Remark also that such recursive equations are *non-Markovian*. By this we mean that the effective coupling λ_i is itself a multi-series in the sequence of all effective couplings $\lambda_\rho, \cdots, \lambda_{i+1}$. Any attempt to rewrite it in terms of the single coupling λ_{i+1} would automatically reintroduce the renormalon problem.

Thanks to Theorem 1 the effective expansion is therefore able to define the theory, if all couplings on the trajectory from λ_ρ to $\lambda_0 = \lambda_r$ are uniformly bounded by a small enough constant, and the number of graphs is not too big. This is the case when

- the theory is asymptotically free or asymptotically safe in the ultraviolet regime,
- the set of graphs considered does not proliferate more than exponentially with size n.

Planar "wrong sign" ϕ^4 [9] or the Grosse Wulkenhaar model [13] satisfy these two conditions. Since melonic graphs, like trees, proliferate no more than exponentially in size and since our theory is asymptotically free, its melonic approximation is a free from the *two* sources of divergence of perturbation theory discussed above. Hence the effective expansion should allow us to define rigorously and non perturbatively any Green function G^{melo}_{2N} or vertex function Γ^{melo}_{2N} in this melonic approximation.

Comparing (4.114) with (4.102), we see that such amplitudes are very different from the renormalized ones. Because in (4.114) all divergent high graphs are subtracted, effective amplitudes, like renormalized ones, have a finite limit when the ultraviolet cut-off is removed. However unlike renormalized amplitudes, effective amplitudes are free of renormalons [2]. More precisely:

Corollary 1. *The effective amplitude $\mathcal{A}_{eff}(\mathcal{G})$ for a graph $\mathcal{G}$ with $V(\mathcal{G})$ internal wavy lines is uniformly exponentially bounded in term of its size, hence for some constant K*

$$|A_{eff}(\mathcal{G})| \leq K^{V(\mathcal{G})}. \tag{4.121}$$

This result follows directely from the analysis of the previous section. The effective series correspond to the special case of an empty safe forest S, hence the factorial of its cardinal in (4.111) is simply 1.

4.6 Closed equations in the melonic sector

In this section, we establish a closed equation for the melonic two-point vertex function, and an equation expressing the melonic four-point vertex function in terms of the two-point one. Combining this with the effective bounds of the previous section we shall prove existence and unicity of the solution of these equations at small renormalized coupling.

4.6.1 Bare equations

Let us consider the $U(1) - T^4_d$ model, and $\langle\tau\rangle(p)$ the mean values of an intermediate field $\tau_i(p)$, which, due to the color symmetry, does not depend on the color i:

$$\langle\tau\rangle(p) := \frac{\sqrt{-2\lambda}}{\mathcal{Z}_{U(1)-T^4_d}} \int d\nu_{\mathbb{I}}(\tau)\tau_i(p) e^{-\sum_{\vec{\mathbf{p}}\in\mathcal{P}} \ln(1-i\sqrt{2\lambda}C_0(\vec{\mathbf{p}})\Gamma(\vec{\mathbf{p}}))}\,, \tag{4.122}$$

where we have added a factor $\sqrt{-2\lambda}$ in the definition for convenience.

Proposition 7. *Consider the melonic restriction $\langle\tau\rangle_{melo}(p)$, whose perturbative Feynman expansion contains only melon graphs, i.e. is labeled by connected trees $\mathcal{T}$ in the intermediate field representation:*

$$\langle\tau\rangle_{melo}(p) = \sqrt{-2\lambda}\sum_{\mathcal{T}}(-2\lambda)^{\ell(\mathcal{T})/2}\mathcal{A}_{\mathcal{T}}(p)\,. \tag{4.123}$$

Then, $\langle\tau\rangle_{melo}(p)$ verifies the closed equation:

$$\langle\tau\rangle_{melo}(p) = -2\lambda \sum_{q_j\in\mathbb{Z},j>1} \frac{\delta\big(p+\sum_{j=2}^{d} q_j\big)}{p^2+\sum_{j>1} q_j^2 + m^2 - \langle\tau\rangle_{melo}(p) - \sum_{j>1}\langle\tau\rangle_{melo}(q_j)}\,. \tag{4.124}$$

Proof. The formula can be established recursively in λ. Let b be the grey disk hooked to the external wavy live. At first order, this grey disk reduces to a single loop made of a single dotted line of the original representation (see Figure 4.18a). Therefore we recover the one-loop expression, and the formula works.

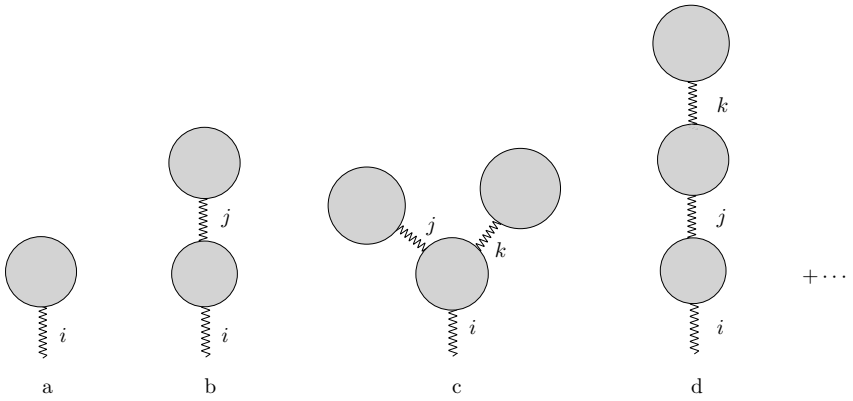

Figure 4.18: The first melonic contributions to τ_{melo}.

The first next melonic contributions are pictured on Figures 4.18b, c and d. Grouping together, orders by orders, the contributions to each hooked 1-point functions to the disc b, we build the exact $\langle\tau\rangle_{melo}$ function. As a result, the loop of the disc b corresponds to the effective propagator

$$\begin{aligned} G_{eff}(\vec{q}) &= C(\vec{q}) + \sum_i C(\vec{q})\langle\tau\rangle_{melo}(q_i)C(\vec{q}) + \cdots \\ &\quad + \sum_{i,j} C(\vec{q})\langle\tau\rangle_{melo}(q_i)C(\vec{q})\langle\tau\rangle_{melo}(q_j)C(\vec{q}) + \cdots \\ &= C(\vec{q})\left[1+\sum_{n=1}^{\infty}\left(\sum_i \langle\tau\rangle_{melo}(q_i)C(\vec{q})\right)^n\right] \\ &= C(\vec{q})\frac{1}{1-\sum_i\langle\tau\rangle_{melo}(q_i)C(\vec{q})}\,, \end{aligned} \tag{4.125}$$

where C is the bare propagator

$$C(\vec{q}) = \frac{\delta(\sum_i q_i)}{\vec{q}^{\,2}+m^2}\,. \tag{4.126}$$

Then, fixing the color of the external wavy line to 1, and taking into account $\langle\tau\rangle_{melo}(p)$ writes as:

$$\langle\tau\rangle_{melo}(p) = -2\lambda \sum_{q_j,j>1} G_{eff}(\vec{q})\big|_{q_1=p}\,, \tag{4.127}$$

which is nothing but the theorem, taking into account 4.126.

□

In the same way, we define the connected 2-point function $\langle \tau_i(p_i)\tau_j(p_j)\rangle$ as

$$\begin{aligned}\langle \tau_i(p_i)\tau_j(p_j)\rangle \;&:=\; \frac{-2\lambda}{\mathcal{Z}_{U(1)-T^4_d}}\int d\nu_{\mathbb{I}}(\tau)\tau_i(p_i)\tau_j(p_j)e^{-\sum_{\vec{\mathbf{p}}\in\mathcal{P}}\ln(1-i\sqrt{2\lambda}C_0(\vec{\mathbf{p}})\Gamma(\vec{\mathbf{p}}))}\\ &\quad +2\lambda\langle\tau(p_i)\rangle\langle\tau(p_j)\rangle\,. \end{aligned} \tag{4.128}$$

Note that in the melonic sector $i=j$ and $p_i=p_j$, and we can simplify the notation, and we denote by $\langle\tau^2\rangle_{melo}(p)$ the 2-point function in this sector. We have the following proposition:

Proposition 8. *The connected melonic 2-point function $\langle\tau^2\rangle_{melo}(p)$ verifies:*

$$\langle\tau^2\rangle_{melo}(p) = -2\lambda\frac{1}{1+2\lambda\Sigma(p)}\,, \tag{4.129}$$

with

$$\Sigma(p) := \sum_{q_j,j>1}\frac{\delta(p+\sum_{j>1}q_j)}{\left[p^2+\sum_{j>1}q_j^2+m^2-\langle\tau\rangle_{melo}(p)-\sum_{j>1}\langle\tau\rangle_{melo}(q_j)\right]^2}\,. \tag{4.130}$$

Proof. As for the 1-point function, we fix to 1 the color of the external half-wavy lines. The function $-2\lambda\Sigma$ is nothing but the 1PI-2 point version[9] of $\langle\tau^2\rangle_{melo}(p)$. The first terms of its perturbative expansion are pictured in Figure 4.19.

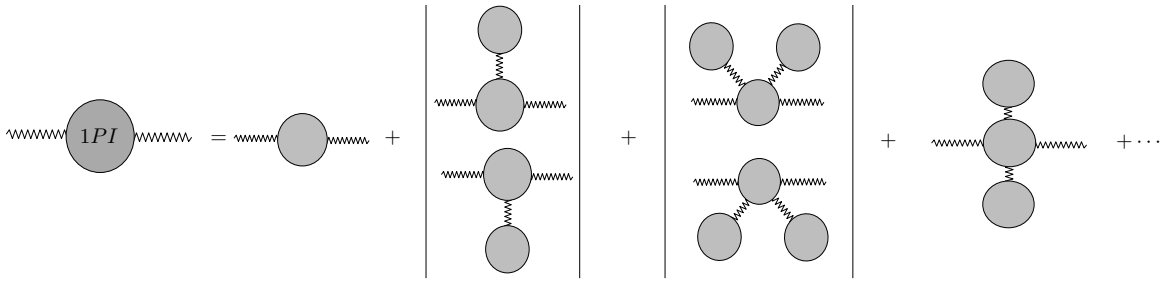

Figure 4.19: First terms of the perturbative expansion of Σ.

The complete 2-point function is then obtained as a sum of particle reductible contributions pictured in Figure 4.20.

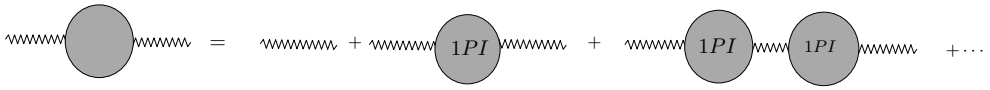

Figure 4.20: The complete 2-point function.

Then, since the propagator for the intermediate fields is the identity, the complete 2-point function is given by the simple geometric series:

$$\langle\tau^2\rangle_{melo}(p) = -2\lambda[1+(-2\lambda\Sigma(p))+(-2\lambda\Sigma(p))^2+\cdots]\,, \tag{4.131}$$

which proves the proposition.

□

[9]Here "1PI" means that we cannot find a wavy line whose cut gives two connected components with exactly two external lines

The closed equations of the two previous propositions determine the 1-point and 2-point functions of the intermediate field in the melonic sector. However in the renormalizable case $d = 6$, the sums inside the equations are divergent. The equations become therefore highly formal, and must be replaced by their analogues for renormalized functions.

Before ending this section, note that in the point of view of the original representation, the 1-point intermediate field function corresponds to the melonic 1P1 2-point function. More precisely, denoting the latter by $\Gamma_{2,melo}(\vec{p})$:

$$\Gamma_{2,melo}(\vec{p}) = \sum_{i=1}^{d} \langle \tau \rangle_{melo}(p_i) \,. \tag{4.132}$$

In the same way, the melonic 1PI 4-point function $\Gamma_{4,melo}(\vec{p}_1, \vec{p}_2, \vec{p}_3, \vec{p}_4)$ is related to the 2-point function $\langle \tau^2 \rangle_{melo}(p)$ by:

$$\Gamma_{4,melo}(\vec{p}_1, \vec{p}_2, \vec{p}_3, \vec{p}_4) = \sum_{i=1}^{d} \langle \tau^2 \rangle_{melo}(p_{4i}) \mathrm{Sym} \mathcal{W}^{(i)}_{\vec{p}_1, \vec{p}_2, \vec{p}_3, \vec{p}_4} \,. \tag{4.133}$$

4.6.2 Renormalized equations

In this section, for convenience, we assume the existence of a sharp UV cut-off Λ in momentum space. All sums are on $\mathbb{Z}_\Lambda$.

Definition 18. *The renormalized melonic* 1*-point function* $\langle \tau \rangle_{melo,R}(p)$ *is defined as:*

$$\langle \tau \rangle_{melo,R}(p) := \langle \tau \rangle_{melo}(p) - \langle \tau \rangle_{melo}(p=0) - p^2 \frac{d^2}{dp^2} \langle \tau \rangle_{melo}(p=0) \tag{4.134}$$

where the terms without index "R" are unrenormalized, and assumed to be expressed in terms of the renormalized couplings λ_r, m_r*.*

From these definitions we can extract the relation between "bare" and renormalized couplings. Indeed, the two subtracted terms are nothing but the counter-terms for mass and wave-function renormalization, then:

$$m^2 = \frac{m_r^2 + d \times \langle \tau \rangle_{melo}(p=0)}{Z} \,, \quad Z = 1 + \frac{d}{dp^2} \langle \tau \rangle_{melo}(p=0) \,. \tag{4.135}$$

From Definition 18, 4.135 and Proposition 7, we deduce the *closed equation for the renormalized* 1*-point function*[10] :

Corollary 2. *The renormalized* 1*-point function* $\langle \tau \rangle_{melo,R}(p)$ *satisfies the equation:*

$$\begin{aligned} \langle \tau \rangle_{melo,R}(p) = -2Z^2\lambda \sum_{q_j \in \mathbb{Z}_\Lambda, j>1} \Bigg[& \frac{\delta\big(p + \sum_{j=2}^d q_j\big)}{p^2 + \sum_{j>1} q_j^2 + m_r^2 - \langle \tau \rangle_{melo,R}(p) - \sum_{j>1} \langle \tau \rangle_{melo,R}(q_j)} \\ & - \frac{\delta\big(\sum_{j=2}^d q_j\big) + \frac{d}{dp^2} \delta\big(p + \sum_{j=2}^d q_j\big)\big|_{p=0}}{\sum_{j>1} q_j^2 + m_r^2 - \sum_{j>1} \langle \tau \rangle_{melo,R}(q_j)} \\ & + \frac{\delta\big(\sum_{j=2}^d q_j\big)}{\big[\sum_{j>1} q_j^2 + m_r^2 - \sum_{j>1} \langle \tau \rangle_{melo,R}(q_j)\big]^2} \Bigg] \,. \end{aligned} \tag{4.136}$$

[10] To deduce this corollary, we assume that all the sums are UV-regularized, for instance with a sharp cut-off, so that it is legal to invert the sums and the subtractions of the standard BPHZ-scheme.

In the same way, the closed equation for the bare 2-point function can be translated as a closed equation for the renormalized vertex function:

Definition 19. *We define the renormalized 1PI 2-point function Σ_R as:*

$$\Sigma_R(p) := \Sigma(p) - \Sigma(0)\,, \tag{4.137}$$

where, again, the unrenormalized function is expressed in terms of the renormalized couplings.

The 1PI version of the *renormalized* 2-point function $\langle\tau^2\rangle_{melo,R}(p)$ is then $-2Z^2\lambda\Sigma_R$, and $\langle\tau^2\rangle_{melo,R}(p)$ is obtained by summing the geometric series, as in the proof of Proposition 8. We deduce the following corollary:

Corollary 3. *The renormalized 2-point function $\langle\tau^2\rangle_{melo,R}(p)$ (i.e. the usual 2-point renormalized function multiplied by $2\lambda_r$) verifies:*

$$\langle\tau^2\rangle_{melo,R}(p) = -2\lambda_r \frac{1}{1-2\lambda_r\Sigma_R(p)}\,. \tag{4.138}$$

It is compatible with the standard definition, the renormalized coupling λ_r being related to the vertex function through

$$\lambda_r := -\frac{1}{2}\langle\tau^2\rangle_{melo,R}(p=0)\,. \tag{4.139}$$

The system is then completely determined. From Definition 19 and equation 4.39, we have $Z^2\lambda = \lambda_r + \delta\lambda$, with

$$\delta\lambda = \lambda_r^2\Sigma(0). \tag{4.140}$$

Then $Z_\lambda = 1 + \lambda_r\Sigma(0)$ and

$$Z^2\lambda = [1+\lambda_r\Sigma(0)]\lambda_r\,. \tag{4.141}$$

As a result:

Proposition 9. *The 1-point function obeys the following closed equation:*

$$\begin{aligned}\langle\tau\rangle_{melo,R}(p) = -2\lambda_r\Bigg(1+\lambda_r\sum_{q_j,j>1}\frac{\delta(\sum_{j>1}q_j)}{\big[\sum_{j>1}(q_j^2-\langle\tau\rangle_{melo,R}(q_j))+m_r^2\big]^2}\Bigg)\\ \times\sum_{q_j\in\mathbb{Z}_\Lambda,j>1}\Bigg[\frac{\delta\big(p+\sum_{j=2}^d q_j\big)}{p^2+\sum_{j>1}q_j^2+m_r^2-\langle\tau\rangle_{melo,R}(p)-\sum_{j>1}\langle\tau\rangle_{melo,R}(q_j)}\\ -\frac{\delta\big(\sum_{j=2}^d q_j\big)+\frac{d}{dp^2}\delta\big(p+\sum_{j=2}^d q_j\big)\big|_{p=0}}{\sum_{j>1}q_j^2+m_r^2-\sum_{j>1}\langle\tau\rangle_{melo,R}(q_j)}\\ +\frac{\delta\big(\sum_{j=2}^d q_j\big)}{\big[\sum_{j>1}q_j^2+m_r^2-\sum_{j>1}\langle\tau\rangle_{melo,R}(q_j)\big]^2}\Bigg]\,.\end{aligned} \tag{4.142}$$

Its solutions only depend on the renormalized couplings.

The previous closed equations define, in principle, the renormalized melonic vertex functions. Neither the existence nor the unicity of their solutions, however, are obvious at all, since the bare equations do not have an ultraviolet limit and the renormalized ones typically have zero convergence radius in λ_r because of renormalons (except at very special values such as zero external momenta). But we can expand these equations according to the multiscale expansion of Section 4.4 and reshuffle them in terms of the effective amplitudes and effective constants λ_i of

Section 4.5.1. Subtractions in loop sums will then occur only when the external momentum p_c has scale strictly lower than the one of $\vec{q}^c$ and the coupling λ_r will be replaced by the effective coupling corresponding to the scale of $\vec{q}^c$.

Expanding in a multiseries for all couplings gives therefore an effective expansion with

- at most $(K_1)^n$ graphs at order n, since it is a well-know fact that trees proliferate only exponentially in their number of vertices,
- effective melonic amplitudes bounded by $(K_2)^n$ by Theorem 1 (which applies to *any* effective amplitude, hence in particular to the melonic ones),
- effective constants all bounded by the last λ_r because of asymptotic freedom.

Hence this effective melonic expansion converges and defines a unique solution of the renormalized equations for $0 \leq \lambda_r < (K_1 K_2)^{-1}$. As usually for flow equations, the solution is in fact analytic in λ_r in a disk tangent to the real axis, with uniform Taylor remainder estimates at order s in $K^s s!$ [2]. We leave the details to the reader, but have no doubt that the unique solution sum of the effective series is therefore the *Borel sum* of the renormalized expansion for the melonic vertex functions $\Gamma^{melo}_{2N,r}$, and that this holds not just for $N = 1$ and 2 but for *any* number $2N$ of external arguments. This completes the control of the melonic sector of the theory.

Theorem 5. *The effective expansions of the renormalized melonic vertex functions converge for $0 \leq \lambda_r < K^{-1}$ to the Borel sum of their renormalized expansions.*

It is tempting to believe that like for tensor models, for $|\lambda_r|$ large enough we reach singularities at which phase transitions occur. However, the complexity of the previous equations for $d = 6$ complicates the outcome. Numerical studies for a similar model without closure constraint [11, 10] give encouraging results, but without definitive conclusion. This is why we choose to focus on non-perturbative renormalization methods for the rest of this thesis. In the next section, we introduce the renormalization group "à la Wilson", which will be our conceptual framework for the next two chapters.

4.7 Renormalization group flow

In a modern point of view, thanks to the work of Wilson in the seventies, renormalization and renormalization group are understood as a *coarse-graining* process from a microscopic theory toward an effective long-distance theory. There are in fact different implementations of this idea, depending on the context. In this section, we present a derivation of the Wilson-Polchinski equation in the TGFT context, which corresponds to an infinitesimal step of the renormalization group flow, and gives a perturbative solution at first orders. Standard reference on the approach detailed in this section may be found in [17]

4.7.1 Wilson-Polchinski equation

Theorem 6. *Let us consider two non-normalized Gaussian measures $d\mu_C$ and $d\mu_{C'}$ whose covariances C and C' are related by $C' = C + \Delta$. C, C' and Δ are all assumed positive. Then:*

$$\int d\mu_C(\bar{T}_1, T_1) d\mu_\Delta(\bar{T}_2, T_2) e^{-S_{int}(T_1+T_2, \bar{T}_1+\bar{T}_2)} = \left(\frac{\det(\Delta C)}{\det(C')}\right)^{1/2} \int d\mu_{C'}(\bar{T}, T) e^{-S_{int}(T,\bar{T})}. \quad (4.143)$$

The proof of this theorem, which links two Gaussian integrations with two propagators, relies only on the standard properties of Gaussian measures (Isserlis-Wick theorem). In a Wilsonian point of view, we shall interpret this theorem as a partial integration over rapid modes, associated to the propagator Δ. This requires the introduction of an UV-cut-off Λ playing the role of a fundamental scale. Broadly speaking, we can write the propagator as a Laplace transform:

$$C_\Lambda(\vec{p}) = \int_0^{+\infty} dt \chi(t\Lambda^2) e^{-t(\vec{p}^2+m^2)} \delta\Big(\sum_i p_i\Big)\,, \tag{4.144}$$

where the function $\chi(t)$ is chosen so that $|1-\chi(t)| \leq Ce^{-kt}$, for $C, k > 0$ and $t \to +\infty$. Here, we shall make the simpler choice $\chi(t) = \theta(t-1)$, $\theta(t)$ being the Heaviside function, defined on $\mathbb{R}$ by: $\theta(t) = 1$ for $t \geq 0$ and $\theta(t) = 0$ on the complementary $]-\infty, 0[$, so that we recover the Schwinger regularization:

$$C_\Lambda(\vec{p}) = \frac{e^{-(\vec{p}^2+m^2)/\Lambda^2}}{\vec{p}^2+m^2} \delta\Big(\sum_i p_i\Big). \tag{4.145}$$

Then, we introduce a dilatation parameter $s < 1$. This parameter will be used as a step to the gradual integration of the UV modes, and it is at this step that Theorem 6 plays a role. Indeed, defining the variation

$$\begin{aligned} \Delta_{s,\Lambda}(\vec{p}) &:= C_\Lambda(\vec{p}) - C_{s\Lambda}(\vec{p}) \\ &= \int_0^{+\infty} dt \int_{s^2}^1 dx \frac{d}{dx} \chi(tx\Lambda^2) e^{-t(\vec{p}^2+m^2)} \delta\Big(\sum_i p_i\Big), \end{aligned} \tag{4.146}$$

and its infinitesimal version $D_{s,\Lambda}(\vec{p})$, when s is close to 1:

$$\Delta_{s,\Lambda}(\vec{p}) \simeq \frac{2(1-s)}{\Lambda^2} e^{-(\vec{p}^2+m^2)/\Lambda^2} \delta\Big(\sum_i p_i\Big) =: (1-s) D_{s,\Lambda}(\vec{p})\,, \tag{4.147}$$

we can write the partition function as an integral over two fields, respectively associated to "slow" and "rapid" modes. Starting with the partition function $\mathcal{Z}_\Lambda$ at scale Λ:

$$\mathcal{Z}_\Lambda[S_{int}] := \int d\mu_{C_\Lambda}(\bar{T}, T) e^{-S_{int,\Lambda}(T,\bar{T})}\,, \tag{4.148}$$

Theorem 6 allows to decompose it into two Gaussian integrals over two fields, $T_>$ and $T_<$, the "rapid" and "slow" modes, respectively with covariances $\Delta_{s,\Lambda}$ and $C_{s\Lambda}$:

$$\mathcal{Z}_\Lambda[S_{int}] = \left(\frac{\det(\Delta_{s,\Lambda} C_{s\Lambda})}{\det(C_\Lambda)}\right)^{-1/2} \int d\mu_{C_{s\Lambda}}(\bar{T}_<, T_<) \int d\mu_{\Delta_{s,\Lambda}}(\bar{T}_>, T_>) e^{-S_{int}(T_<+\bar{T}_>, \bar{T}_<+\bar{T}_>)}\,. \tag{4.149}$$

Then, identifying the effective action $S_{int,s\Lambda}$ at scale $s\Lambda$ as:

$$e^{-S_{int,s\Lambda}(T_<,\bar{T}_<)} := \frac{1}{\sqrt{\det \Delta_{s,\Lambda}}} \int d\mu_{\Delta_{s,\Lambda}}(\bar{T}_>, T_>) e^{-S_{int}(T_<+T_>, \bar{T}_<+\bar{T}_>)}\,, \tag{4.150}$$

the decomposition 4.149 becomes:

$$\mathcal{Z}_\Lambda = \left(\frac{\det C_{s\Lambda}}{\det C_\Lambda}\right)^{-1/2} \int d\mu_{C_{s\Lambda}}(\bar{T}_<, T_<) e^{-S_{int,s\Lambda}(T_<,\bar{T}_<)}\,. \tag{4.151}$$

Now, for an infinitesimal step, keeping only the leading order terms in $1-s$ when s is very close to 1, we find:

$$e^{-\Delta S_{int,\Lambda}(T_<,\bar{T}_<)} = 1 - \mathrm{Tr}\Big[\Big(\frac{\delta^2 S_{int,\Lambda}}{\delta T \delta \bar{T}} - \frac{\delta S_{int,\Lambda}}{\delta T}\frac{\delta S_{int,\Lambda}}{\delta \bar{T}}\Big)\Delta_{s,\Lambda}\Big] + \mathcal{O}(1-s), \tag{4.152}$$

with $\Delta S_{int,\Lambda}(T_<,\bar{T}_<) := S_{int,s\Lambda}(T_<,\bar{T}_<) - S_{int\Lambda}(T_<,\bar{T}_<)$. At the same time, expanding the left hand side of 4.151 in powers of $1-s$, and identifying the power of $1-s$ leads to :

$$\frac{dS_{int,s\Lambda}}{ds} = -\mathrm{Tr}\Big\{\Big(\frac{\delta^2 S_{int,s\Lambda}}{\delta T \delta \bar{T}} - \frac{\delta S_{int,s\Lambda}}{\delta T}\frac{\delta S_{int,s\Lambda}}{\delta \bar{T}}\Big)D_{s,\Lambda}\Big\}. \tag{4.153}$$

Note that we can consider Λ not as a fundamental scale, but as an arbitrary step on the flow, meaning that equation 4.153 holds at each step of that flow. Physically, equation 4.153 tells how the couplings are affected when the fundamental scale changes, and is therefore an incarnation of the renormalization group flow and of the original Wilson's idea.
This description does not include the field renormalization, which is usually required to obtain fixed points of the renormalization group equations [17] and to ensure the regularity of the solution obtained. A pragmatic way to introduce field strength renormalization is the following. We consider a derivable parameter $Z(s)$ as well as a new field for the scale $s\Lambda$: $T = \sqrt{Z(s)}\tilde{T}$. A new functional $\tilde{S}^s_{int}$ is associated to this field such as $\tilde{S}_{int,s\Lambda}[\tilde{T},\bar{\tilde{T}}] = S_{int,s\Lambda}[T,\bar{T}]$. The equation 4.153 is then modified into (leaving out the tildes):

$$\begin{aligned}\frac{dS_{int,s\Lambda}}{ds} =& -\mathrm{Tr}\Big\{\Big(\frac{\delta^2 S_{int,s\Lambda}}{\delta T \delta \bar{T}} - \frac{\delta S_{int,s\Lambda}}{\delta T}\frac{\delta S_{int,s\Lambda}}{\delta \bar{T}}\Big)D_{s,\Lambda}\Big\} \\ &- \frac{1}{2}\gamma(s)\Big[\mathrm{Tr}\Big(\frac{\delta S_{int,s\Lambda}}{\delta T}T\Big) + \mathrm{Tr}\Big(\bar{T}\frac{\delta S_{int,s\Lambda}}{\delta \bar{T}}\Big)\Big],\end{aligned} \tag{4.154}$$

where $\gamma(s)$ is defined by

$$\gamma(s) := \frac{d}{ds}\ln Z(s). \tag{4.155}$$

In the next section we shall show how the flow equations can be solved in a perturbative way for the UV modes, and allow to recover the equations obtained in Section 4.2. In that purpose, the flow equation 4.154 has to be rewritten in a more practical way. As explained in Section 4.2, S_{int} is a sum of tensorial bubbles, which are characterized by their connectivity, their topology and their degree, which correspond to half the number of fields involved in the tensorial trace. Hence, in order to study the evolution of each interaction separately, it is more convenient to rewrite the flow equation in terms of bubble interactions. To this end, connectivity and topology do not play a role, and we label the interactions only by the valence, that is, the number of black or white nodes of the bubbles.

Let us consider the following expansion for $S_{int,s\Lambda}[T,\bar{T}]$:

$$S_{int,s\Lambda}[T,\bar{T}] = \sum_{n_l}\mathcal{V}^{(n_l)} = \sum_{n_l}\sum_{\{\vec{p}_i,\vec{\bar{p}}_i\}}\mathcal{V}^{(n_l)\,\vec{p}_1,\dots,\vec{p}_l}_{\vec{\bar{p}}_1,\dots,\vec{\bar{p}}_l}\prod_{i=1}^{l}T_{\vec{p}_i}\bar{T}_{\vec{\bar{p}}_i}, \tag{4.156}$$

where n_l denotes the number of black and white nodes in each interactions. By replacing this expression of the action in the flow equation 4.153, we obtain the set of renormalization group

equations :

$$\frac{d\mathcal{V}^{(n_l)}}{ds} = -\sum_{\vec{p}\vec{\bar{p}}} D_{s,\Lambda,\vec{p}\vec{\bar{p}}} \frac{\partial}{\partial \bar{T}_{\vec{p}}} \frac{\partial}{\partial T_{\vec{\bar{p}}}} \mathcal{V}^{(n_l+1)} + \sum_{n_m=0}^{n_l-1} \sum_{\vec{p}\vec{\bar{p}}} D_{s,\Lambda,\vec{p}\vec{\bar{p}}} \frac{\partial \mathcal{V}^{(n_m+1)}}{\partial \bar{T}_{\vec{p}}} \frac{\partial \mathcal{V}^{(n_l-n_m)}}{\partial T_{\vec{\bar{p}}}} - n_l \gamma(s) \mathcal{V}^{(n_l)} , \tag{4.157}$$

where $D_{s,\Lambda,\vec{p}\vec{\bar{p}}} = D_{s,\Lambda}(\vec{p})\delta_{\vec{p}\vec{\bar{p}}}$. In Appendix B, we show that Wilson-Polchinski equation can be turned into a Fokker-Planck equation and formally solved by a standard method [17]. The rest of this section, however, is devoted to a perturbative analysis of the flow equations.

4.7.2 Perturbative solution

Before starting the calculation, we have to precise our regime of approximation. We shall consider only the ultra-violet limit, and we assume that $s\Lambda$ and Λ are large. However, we are interested in infra-red physics much below the fundamental cut-off Λ. More precisely, our approximation can be characterized by $s\Lambda$ and Λ both large, but $s\Lambda/\Lambda$ small.

At scale Λ, and up to contributions of order λ^2, the action is assumed to be of the form

$$S_{int,s\Lambda}[\bar{T},T] = \lambda \sum_{i=1}^{6} \sum_{\{\vec{p}_i,\vec{\bar{p}}_i\}} \mathcal{W}^{(i)}_{\vec{p}_1,\vec{\bar{p}}_1;\vec{p}_2,\vec{\bar{p}}_2} T_{\vec{p}_1} T_{\vec{p}_2} \bar{T}_{\vec{\bar{p}}_1} \bar{T}_{\vec{\bar{p}}_2} + \delta m^2 \sum_{\vec{p}} \bar{T}_{\vec{p}} T_{\vec{p}} + \delta Z \sum_{\vec{p}} \vec{p}^2 \bar{T}_{\vec{p}} T_{\vec{p}}., \tag{4.158}$$

where the last two terms take into account the fact that the parameter of Gaussian measure, the mass and the Laplacian term, can be affected by the integration of the UV modes, and these counter-terms, assumed to be of order λ, take into account these modifications. Moreover, note that in this approach the corrections to the Laplacian term are not suppressed by an effective counter-term in the action, but absorbed in the wave function renormalization. It is fixed such that all the Laplacian corrections are canceled by the γ term in the RGE for $\mathcal{V}^{(1)}$.

We adopt the standard Ansatz, namely that the generic interaction of valence n are of order $\lambda^{n/2-1}$. This allows to organize systematically the perturbative solution, for which we shall construct the λ^2 order.

$\mathcal{V}^{(1)}$ at order λ

The first corrections occur at order λ for $\mathcal{V}^{(1)}$, whose flow equation write as:

$$\Big[\frac{d}{ds} + \gamma(s)\Big]\mathcal{V}^{(1)} = -4\lambda \sum_{\substack{\vec{p}_1,\vec{\bar{p}}_1 \\ \vec{p}_2,\vec{\bar{p}}_2}} D_{s\,\Lambda\,\vec{p}_1,\vec{\bar{p}}_1} \mathrm{Sym}\mathcal{W}_{\vec{p}_1,\vec{\bar{p}}_1;\vec{p}_2,\vec{\bar{p}}_2} \bar{T}_{\vec{\bar{p}}_2} T_{\vec{p}_2} \tag{4.159}$$

where $\mathrm{Sym}\mathcal{W} := \sum_i \mathrm{Sym}\mathcal{W}^{(i)}$ and $\mathcal{W} = \sum_{i=1}^{6} \mathcal{W}^{(i)}$. The r.h.s involves two typical contributions which are pictured graphically in Figure 4.21, where the contraction with $D_{s,\Lambda}$ is represented by a dotted line with a white box. These two contributions are exactly the same as the one we found in the perturbative analysis of Section 4.2.

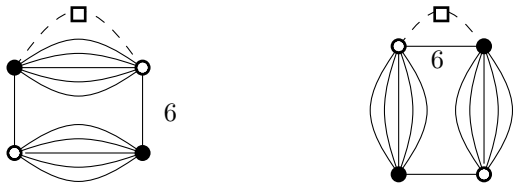

a b

Figure 4.21: Typical graph contributing to the interaction $\mathcal{V}^{(1)}$ of degree 2.

In the UV limit that we consider, the non-melonic contractions of type 4.21b, creating only one internal face (of color 6 in the Figure), can be neglected in comparison to the melonic contributions of the form of Figure 4.21a. Retaining only the melonic contractions, equation 4.159 becomes:

$$\Big[\frac{d}{ds}+\gamma(s)\Big]\mathcal{V}^{(1)} = -2\lambda \sum_{\substack{\vec{p}_1,\vec{\vec{p}}_1\\ \vec{p}_2,\vec{\vec{p}}_2}} D_{s\,\Lambda,\vec{p}_1\vec{\vec{p}}_1}\mathcal{W}_{\vec{p}_1,\vec{\vec{p}}_1;\vec{p}_2,\vec{\vec{p}}_2}\bar{T}_{\vec{\vec{p}}_2}T_{\vec{p}_2}. \tag{4.160}$$

Note that, because the propagator, and therefore $D_{s\,\Lambda} := dC_{s\Lambda}/ds$, includes a projection onto the gauge invariant space, the connectivity structure of the interaction implies that the r.h.s of the previous equation can be rewritten as follows

$$\sum_{\substack{\vec{p}_1,\vec{\vec{p}}_1\\ \vec{p}_2,\vec{\vec{p}}_2}} D_{s\,\Lambda\,\vec{p}_1,\vec{\vec{p}}_1}\mathcal{W}^{(1)}_{\vec{p}_1,\vec{\vec{p}}_1;\vec{p}_2,\vec{\vec{p}}_2}\bar{T}_{\vec{\vec{p}}_2}T_{\vec{p}_2} = \sum_{\substack{\vec{p}_1\in\mathcal{P}\\ \vec{p}_2\in\mathcal{P}}} D_{s\,\Lambda}(\vec{p}_1)\bar{T}_{\vec{\vec{p}}_2}T_{\vec{p}_2}\delta_{p_{11},p_{21}} = \sum_{\vec{p}_1\in\mathcal{P}} f(p_{11})\bar{T}_{\vec{\vec{p}}_1}T_{\vec{p}_1}, \tag{4.161}$$

where $\mathcal{P} = \{\vec{p}\in\mathbb{Z}^6 | \sum_i p_i = 0\} \subset \mathbb{Z}^6$ and $f(p_{11}) := \sum_{p_{1i}\, i\neq 1} D_{s\,\Lambda}(\vec{p}_1)$. This is nothing but a manifestation of the *traciality* of the melonic diagrams. Expanding f in power of p_{11}, we generate mass and wave function corrections, and sub-dominant corrections, involving powers of p_{11} greater than two. They correspond to the first deviation to the original form 4.158. Neglecting these sub-dominant contributions, and using the sum

$$\sum_{p_1,\dots,p_5}\frac{2}{s^3\Lambda^2}e^{-\frac{1}{(s\Lambda)^2}(\vec{p}^2+m^2)}\delta\Big(\sum_i p_i\Big) \sim \frac{2\pi^2}{\sqrt{5}}s\Lambda^2 - \frac{2\pi^2}{\sqrt{5}}\frac{1}{s}m^2 - \frac{12\pi^2}{5\sqrt{5}}\frac{1}{s}p_6^2 + \mathcal{O}(s), \tag{4.162}$$

for which we only keep the leading order terms in s, we can extract the dominant contributions to the mass and wave-function renormalization. The term in p_6^2 generates a non-local 2-point interaction of the form $-\delta Z(s)\mathrm{Tr}(\bar{T}\Delta_{\vec{g}}T)$, where Δ_g is the Laplacian on $U(1)^{\times 6}$, and the first term generates a mass correction. Summing over the six colors, we find, at first order in λ:

$$\gamma(s) = \frac{24\pi^2\lambda}{5\sqrt{5}}\frac{1}{s}. \tag{4.163}$$

$$\frac{d}{ds}\delta m^2 = -\frac{24\pi^2\lambda}{\sqrt{5}}s\Lambda^2 + \frac{24\pi^2\lambda}{\sqrt{5}}\frac{1}{s}m^2. \tag{4.164}$$

$\mathcal{V}^{(3)}$ and $\mathcal{V}^{(2)}$ at order λ^2

At order λ^2, we have to take into account the contributions of interactions of valence six, $\mathcal{V}^{(3)}$, verifying the flow equation:

$$\frac{d\mathcal{V}^{(3)\,\vec{p}_1,\vec{\vec{p}}_2,\vec{\vec{p}}_3}_{\vec{p}_1,\vec{p}_2,\vec{p}_3}}{ds} = 4\lambda^2\sum_{i,j,\vec{p},\vec{\vec{p}}}\mathcal{W}^{(i)}_{\vec{p}_1,\vec{\vec{p}}_1,\vec{p},\vec{\vec{p}}_2}\mathcal{W}^{(j)}_{\vec{p}_2,\vec{\vec{p}}_3;\vec{p}_3,\vec{\vec{p}}}D_{s,\Lambda,\vec{p}\vec{\vec{p}}}. \tag{4.165}$$

It can be easily integrated, with $D_{s,\Lambda} = dC_{s\Lambda}/ds$ and the initial condition

$$\mathcal{V}^{(3)\,\vec{p}_1,\vec{p}_2,\vec{p}_3}_{\vec{p}_1,\vec{p}_2,\vec{p}_3}(1) = 0.$$

We get:

$$\mathcal{V}^{(3)\,\vec{p}_1,\vec{p}_2,\vec{p}_3}_{\vec{p}_1,\vec{p}_2,\vec{p}_3}(s) = -\,4\lambda^2 \sum_{i,j,\vec{p},\vec{p}} \mathcal{W}^{(i)}_{\vec{p}_1,\vec{p}_1,\vec{p},\vec{p}_2} \mathcal{W}^{(j)}_{\vec{p}_2,\vec{p}_3;\vec{p}_3,\vec{p}} \big(C_\Lambda - C_{s\Lambda}\big)_{\vec{p}\vec{p}}. \tag{4.166}$$

As for the interaction of degree 1, the structure of this effective interaction can be understood as a contraction between two bubbles, as pictured in Figure 4.22, where the dotted line with a black box represents the contraction with $C_\Lambda - C_{s\Lambda}$.

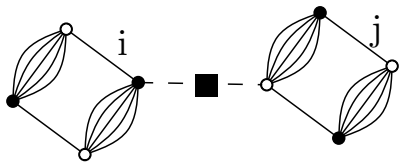

Figure 4.22: Typical graph contributing to the interaction of $\mathcal{V}^{(3)}$ of degree 6.

.

We have now all the material to build the effective coupling for the quartic melonic interaction at order λ^2, for which we shall extract the leading behavior. From the flow equations, it seems that the coupling evolution receives many contributions. The first one comes from $\mathcal{V}^{(3)}$. By deriving two times this interaction we obtain an interaction of degree two, which can be either 1PI, when the contraction with $D_{s\,\Lambda}$ links two black and white nodes of two different bubbles, or one particule reducible if the two nodes stand on the same interaction bubble. Explicitly:

$$\Big[\frac{d}{ds} + 2\gamma(s) - 4\delta m^2 \bar{D}_{s,\,\Lambda}[\{p_i\}]\Big] \lambda \mathcal{W}^{(i)}_{\vec{p}_2,\vec{p}_1;\vec{p}_3,\vec{p}_2} = 4\lambda^2 \sum_{\vec{p},\vec{p}\vec{p}',\vec{p}'} \Bigg[\bar{\mathrm{Sym}}\Big(\mathcal{W}^{(i)}_{\vec{p}',\vec{p}_1;\vec{p},\vec{p}_2} \mathcal{W}^{(i)}_{\vec{p}_2,\vec{p}';\vec{p}_3,\vec{p}}\Big) + 2\sum_j \bar{\mathrm{Sym}}\Big(\mathcal{W}^{(i)}_{\vec{p}_2,\vec{p}_1;\vec{p},\vec{p}_2} \mathcal{W}^{(j)}_{\vec{p}',\vec{p}';\vec{p}_3,\vec{p}}\Big)\Bigg] \times \big(C_\Lambda - C_{s\Lambda}\big)_{\vec{p}\vec{p}} D_{s,\Lambda,\vec{p}'\vec{p}'}\,, \tag{4.167}$$

where:

$$\bar{\mathrm{Sym}}\Big(\mathcal{W}^{(i)}_{\vec{p}',\vec{p}_1;\vec{p},\vec{p}_2} \mathcal{W}^{(j)}_{\vec{p}_2,\vec{p}';\vec{p}_3,\vec{p}}\Big) := \mathcal{W}^{(i)}_{\vec{p}',\vec{p}_1;\vec{p},\vec{p}_2} \mathcal{W}^{(j)}_{\vec{p}_2,\vec{p}';\vec{p}_3,\vec{p}} + \mathcal{W}^{(i)}_{\vec{p},\vec{p}_1;\vec{p}',\vec{p}_2} \mathcal{W}^{(j)}_{\vec{p}_3,\vec{p}';\vec{p}_2,\vec{p}}, \tag{4.168}$$

and

$$\bar{D}_{s,\,\Lambda}[\{p_i\}] := D_{s,\,\Lambda}(\vec{p}_2) + D_{s,\,\Lambda}(\vec{p}_1) + D_{s,\,\Lambda}(\vec{p}_3) + D_{s,\,\Lambda}(\vec{p}_2). \tag{4.169}$$

Equation 4.167 gives the exact behavior for the beta function at order λ^2, but it is not hard to see that it reduces to the expression 5.86 already obtained in Section 4.2 in the deep UV sector that we consider. Indeed, retaining only the melonic contributions, and noting that 1PR contributions of the r.h.s are exactly canceled by the term involving the mass correction δm in the l.h.s, we get:

$$\Big[\frac{d}{ds} + 2\gamma(s)\Big] \lambda \mathcal{W}^{(i)}_{\vec{p}_2,\vec{p}_3;\vec{p}_1,\vec{p}_2} \approx 4\lambda^2 \sum_{\vec{p},\vec{p}\vec{p}',\vec{p}'} \mathcal{W}^{(i)}_{\vec{p}',\vec{p};\vec{p}_1,\vec{p}_2} \times \mathcal{W}^{(i)}_{\vec{p}_2,\vec{p}_3;\vec{p}',\vec{p}} \big(C_\Lambda - C_{s\Lambda}\big)_{\vec{p}\vec{p}} D_{s,\Lambda,\vec{p}'\vec{p}'}. \tag{4.170}$$

The computation of the loop appearing on the r.h.s leads to

$$\sum_{p_1,\dots,p_5}\int_1^s ds' \frac{4}{s'^3 s^3 \Lambda^4} e^{-\left(\frac{1}{(s\Lambda)^2}+\frac{1}{(s'\Lambda)^2}\right)(\vec{p}^2+m^2)} \delta\Big(\sum_i p_i\Big) \sim -\frac{\pi^2}{\sqrt{5}}\frac{1}{s} + \mathcal{O}(s), \tag{4.171}$$

from which we finally deduce, using the value 4.163,

$$s\frac{d\lambda}{ds} = -\frac{28\pi^2}{5\sqrt{5}}\lambda^2 \tag{4.172}$$

which, as claimed before, is exactly the value of the one-loop beta function already obtained in the first section.

4.7.3 Toward non-perturbative renormalization

The main advantage of the Wilson-Polchinski equation is that it provides a very transparent interpretation of the renormalization group flow in the space of couplings. However, except for perturbative computations, the Wilson-Polchinski equation is more adapted to mathematical and formal proofs than to non-perturbative analysis. Going beyond the perturbative level requires another formulation of the coarse-graining renormalization group, called *Wetterich equation*, which allows usually to better capture the non-perturbative effects. The price to pay is an approximation scheme a bit more difficult to use. This non-perturbative approach to the renormalization group flow will be the subject of the next two chapters.

Appendix A

Closed melonic equation for $d = 3$

The aim of this section is to prove that our closed equation 4.124 has a unique solution for $d = 3$. We shall prove that it is the case if the coupling constant λ does not exceed a finite critical value λ_c. To this end, we shall prove that the transformation that we call $T_{\lambda,m}$, defined by its action on a sequence f_p by

$$T_{\lambda,m}[f](p) := 2\lambda \sum_{\vec{q}\in\mathbb{Z}^3} \frac{\delta(\sum_i q_i)}{\vec{q}^2 + m^2 + \sum_i f(q_i)}\bigg|_{q_1=p}, \tag{A.1}$$

admits a unique fixed point in a set of sequences that will be precisley defined below, but which include the "physical set" $\mathcal{O}_{phy}$ of such sequences. The latter is a subclass designed to include the perturbative solutions for the 1-point function. The proof is entirely based on the Banach fixed point theorem. This theorem involves the notion of contracting map, defined as:

Definition 20. ***(Contracting map)*** *Let f a map $f : E \to F$, from a metric space E with the norm $||.||$ to a subset $F = \Im(f)$ and $k \in \mathbb{R}^+$ a positive real number. This map is said to be k-lipschitz if:*

$$\forall (x, y) \in E^2 \quad ||f(x) - f(y)|| \leq k||x - y|| \tag{A.2}$$

A k-lipschitz map is said to be contracting if $k \in]0, 1[$.

The theorem states

Theorem 7. ***(Banach)*** *Let E be a complete metric vector space, i.e. a Banach space, and $f : E \to E$ a k-contractible map. There is a unique fixed point x^*, such as $f(x^*) = x^*$. In addition, the sequence defined as $x_{n+1} = f(x_n)$, verifies the bound :*

$$||x_n - x^*|| \leq \frac{k^n}{1-k}||x_0 - x_*|| \tag{A.3}$$

where $||.||$ is the norm of the metric space E.

It has the following corollary, since any closed subspace of a complete metric space is also complete for the induced norm:

Corollary 4. *Let $F \subset E$ a closed subset of a Banach space, and $f : F \to F$ a k-contractible map on F which is stable under f. The map f has a unique fixed point.*

In order to identify a large enough complete metric space, we first note that the self-energy $\tilde{\Gamma}_2^{melo}$ must be negative. It is a consistency condition ensuring that any singularity occurs for the effective 2-point function:

$$G(\vec{p}) = \frac{\delta\big(\sum_i p_i\big)}{\vec{p}^2 + m^2 - \tilde{\Gamma}_2^{melo}(\vec{p})}. \tag{A.4}$$

It implies the following bound:

$$\sigma(p) = 2\lambda \sum_{\vec{q}\in\mathbb{Z}^3} \frac{\delta\big(\sum_i q_i\big)}{\vec{q}^2 + m^2 + \sum_{j=1}^3 F(q_j)}\bigg|_{q_1=p} \leq 2\lambda \sum_{\vec{q}\in\mathbb{Z}^3} \frac{\delta\big(\sum_i q_i\big)}{\vec{q}^2 + m^2}\bigg|_{q_1=p} := \sigma_{o(\lambda)}(p) \tag{A.5}$$

where the sum defining $\sigma_{o(\lambda)}(p)$ can be computed exactly using standard complex analysis. We find:

$$\sigma_{o(\lambda)}(p) = \frac{\pi\lambda}{\sqrt{3p^2+2m^2}} \coth\left[\pi\sqrt{3p^2+2m^2}\right] \leq \frac{\pi\lambda}{\sqrt{2}m} \coth\big(\sqrt{2}\pi m\big). \tag{A.6}$$

Hence, $\sigma_{o(\lambda)}(p)$ is a positive bounded sequence. The space of bounded sequences with the norm $\sup : ||u|| := \sup|u_p|$ is a Banach space that we call traditionally ℓ_∞, and the closed subset $\ell^+_\infty := \{u \in \ell_\infty | u \geq 0\}$ of positive bounded sequences is complete for the norm inherited from ℓ_∞. On this subset, we define the map $T_{\lambda,m}$ by:

$$T_{\lambda,m} : \ell^+_\infty \to \Im[T_{\lambda,m}] \tag{A.7}$$

$$\forall u \in \ell^+_\infty \to T_{\lambda,m}[u] \tag{A.8}$$

where the sequence $T_{\lambda,m}[u]$ is defined by A.1. Clearly from this definition, $T_{\lambda,m}$ sends any positive sequence to another positive sequence, bounded by $\sigma_{o(\lambda)}$, so that $\Im[T_{\lambda,m}] \subset \ell^+_\infty$. So far, all the assumptions of Corollary 4 are verified. We have now to check if our map $T_{\lambda,m}$ is contracting. To see this, we must prove that, for any $f, g \in \ell^+_\infty$ and $k \in]0,1[$:

$$||T_{\lambda,m}[f] - T_{\lambda,m}[g]|| \leq k||f-g||. \tag{A.9}$$

In fact, we have the following lemma:

Lemma 2. *Our map $T_{\lambda,m}$ satisfies the inequality A.9 when the coupling λ does not exceed a finite critical value λ_c depending on the mass parameter m^2.*

Proof. For any $f, g \in \ell^+_\infty$, expanding $||T_{\lambda,m}[f] - T_{\lambda,m}[g]||$ with the definitions of $||.||$ and $T_{\lambda,m}[.]$, we find:

$$\begin{aligned}
d_{f,g} &:= ||T_{\lambda,m}[f] - T_{\lambda,m}[g]|| \\
&= 2\lambda \sup_{p\in\mathbb{Z}} \left| \sum_{\vec{q}\in\mathbb{Z}^3} \delta_{q_1,p} \left(\frac{\delta\big(\sum_i q_i\big)}{\vec{q}^2 + m^2 + \sum_i f_{q_i}} - \frac{\delta\big(\sum_i q_i\big)}{\vec{q}^2 + m^2 + \sum_i g_{q_i}} \right) \right| \\
&\leq 2\lambda \sup_{p\in\mathbb{Z}} \left| \sum_{\vec{q}\in\mathbb{Z}^3} \delta_{q_1,p} \frac{\sum_i (g_{q_i} - f_{q_i})}{(\vec{q}^2 + m^2)^2} \delta\Big(\sum_i q_i\Big) \right| \\
&\leq \frac{6\pi\lambda}{\sqrt{2}m} \coth\big(\sqrt{2}\pi m\big) \times ||f-g||.
\end{aligned} \tag{A.10}$$

Hence there is a non vanishing real number $k(m^2)$, depending on m^2, so that our map is contractible if $\lambda < 1/k(m^2)$, where:

$$0 < k(m^2) \leq \frac{6\pi}{\sqrt{2}m} \coth\big(\sqrt{2}\pi m\big). \tag{A.11}$$

□

Our map $T_{\lambda,m}$ satisfies all the assumptions of the Banach theorem. Hence,

Proposition 10. *The map $T_{\lambda,m}$ admits a unique fixed point on ℓ_∞ when λ does not exceed a finite critical value.*

If the coupling exceeds the finite critical value $\lambda_c := 1/k(m^2)$, the leading perturbative expansion may become ill-defined.

Appendix B

Formal solution of RG equation

The flow equation 4.153 admits a formal solution which is the generating functional of connected functions, defined as:

Definition 21. *: The generating functional of connected functions $\mathcal{W}[J,\bar{J},s]$ is*

$$e^{-\mathcal{W}[J,\bar{J},s]} := \int d\mu_{\Delta_{s,\Lambda}}(\bar{T},T)e^{-S_{int,\Lambda}(T,\bar{T})+\mathrm{Tr}(\bar{J}T)+\mathrm{Tr}(\bar{T}J)} \tag{B.1}$$

$$= e^{\mathrm{Tr}\frac{\delta}{\delta T}\Delta_{s,\Lambda}\frac{\delta}{\delta \bar{T}}}e^{-S_{int,\Lambda}(T,\bar{T})+\mathrm{Tr}(\bar{J}T)+\mathrm{Tr}(\bar{T}J)}\Big|_{T,\bar{T}=0}, \tag{B.2}$$

where the covariance $\Delta_{s,\Lambda}$, as well as the functional $S_{int,s\Lambda}$, are assumed to be derivable functions with respect to the parameter s, and the measure $d\mu_{\Delta_{s,\Lambda}}$ is normalized, hence $\int d\mu_{\Delta_{s,\Lambda}} = 1$.

Differentiating term by term, we get:

$$\frac{d\mathcal{W}}{ds}e^{-\mathcal{W}[J,\bar{J},s]} = e^{\mathrm{Tr}\frac{\delta}{\delta T}\Delta_{s,\Lambda}\frac{\delta}{\delta \bar{T}}}\mathrm{Tr}\Big(\frac{\delta}{\delta T}\frac{d\Delta_{s,\Lambda}}{ds}\frac{\delta}{\delta \bar{T}}\Big)e^{-S_{int,\Lambda}(T,\bar{T})+\mathrm{Tr}(\bar{J}T)+\mathrm{Tr}(\bar{T}J)}\Big|_{T=\bar{T}=0}, \tag{B.3}$$

leading to:

Proposition 11. *: The generating functional of correlation functions $\Xi[J,\bar{J},s] = e^{-\mathcal{W}[J,\bar{J},s]}$ verifies the following time-dependent equation of the Fokker-Planck type*

$$\frac{d\Xi}{ds} = -\mathrm{Tr}\Big[\frac{d\Theta^{(0)}_{s,\Lambda}}{ds}\frac{\delta^2\Xi}{\delta J\delta\bar{J}}\hat{P}\Big], \tag{B.4}$$

where $\Theta^{(0)}_{s,\Lambda} := (\Delta^{(0)}_{s,\Lambda})^{-1}$, $\Delta^{(0)}_{s,\Lambda} = \frac{2(1-s)}{\Lambda^2}e^{-(\vec{p}^2+m^2)/\Lambda^2}$, and $\hat{P}$ is the projector into the gauge invariant subspace.

Proof: The Gaussian integral properties allow us to demonstrate the following lemma.

Lemma 3.

$$e^{\mathrm{Tr}\frac{\delta}{\delta T}C\frac{\delta}{\delta T}}T(\vec{\theta})e^{-S_{int}(T,\bar{T})}\Big|_{T=\bar{T}=0} = e^{\mathrm{Tr}\frac{\delta}{\delta T}C\frac{\delta}{\delta T}}\int d\vec{\theta}'C(\vec{\theta},\vec{\theta}')\frac{\delta}{\delta\bar{T}(\vec{\theta}')}e^{-S_{int}(T,\bar{T})}\Big|_{T=\bar{T}=0}. \tag{B.5}$$

Besides, the definition of the operator $\hat{P}$ implies: $\Delta_{s,\Lambda} = \hat{P}\Delta^{(0)}_{s,\Lambda}\hat{P}$. From equation B.3 we get

$$\begin{aligned}
\frac{d\Xi}{ds} &= e^{\mathrm{Tr}\frac{\delta}{\delta T}\Delta_{s,\Lambda}\frac{\delta}{\delta \bar{T}}} \times \mathrm{Tr}\Big(\frac{\delta}{\delta T}\hat{P}\frac{d\Delta^{(0)}_{s,\Lambda}}{ds}\hat{P}\frac{\delta}{\delta \bar{T}}\Big)e^{-S_{int,\Lambda}(T,\bar{T})+\mathrm{Tr}(\bar{J}T)+\mathrm{Tr}(\bar{T}J)}\Big|_{T=\bar{T}=0} \qquad \text{(B.6)}\\
&= -e^{\mathrm{Tr}\frac{\delta}{\delta T}\Delta_{s,\Lambda}\frac{\delta}{\delta \bar{T}}}\mathrm{Tr}\Big(\frac{\delta}{\delta T}\hat{P}\Delta^{(0)}_{s,\Lambda}\hat{P}\frac{d\Theta^{(0)}_{s,\Lambda}}{ds}\hat{P}\Delta^{(0)}_{s,\Lambda}\hat{P}\frac{\delta}{\delta \bar{T}}\Big) \times e^{-S_{int,\Lambda}(T,\bar{T})+\mathrm{Tr}(\bar{J}T)+\mathrm{Tr}(\bar{T}J)}\Big|_{T=\bar{T}=0}\\
&= -e^{\mathrm{Tr}\frac{\delta}{\delta T}\Delta_{s,\Lambda}\frac{\delta}{\delta \bar{T}}}\mathrm{Tr}\Big(\hat{P}[\bar{T}]\frac{d\Theta^{(0)}_{s,\Lambda}}{ds}\hat{P}[T]\Big) \times e^{-S_{int,\Lambda}(T,\bar{T})+\mathrm{Tr}(\bar{J}T)+\mathrm{Tr}(\bar{T}J)}\Big|_{T=\bar{T}=0}\\
&= -\mathrm{Tr}\Big(\hat{P}\frac{\delta}{\delta J}\frac{d\Theta^{(0)}_{s,\Lambda}}{ds}\hat{P}\frac{\delta}{\delta \bar{J}}\Big)e^{\mathrm{Tr}\frac{\delta}{\delta T}\Delta_{s,\Lambda}\frac{\delta}{\delta \bar{T}}} \times e^{-S_{int,\Lambda}(T,\bar{T})+\mathrm{Tr}(\bar{J}T)+\mathrm{Tr}(\bar{T}J)}\Big|_{T=\bar{T}=0}.
\end{aligned}$$

This is nothing but the definition of the connected correlation function given by B.1, hence the proposition is proved.

□

The equation given in Proposition 11 can be formally solved by using a functional Fourier transform:

$$\Xi[J,\bar{J},s] = \int dT d\bar{T} e^{-\mathcal{H}(T,\bar{T},s)+\mathrm{Tr}(\bar{J}T)+\mathrm{Tr}(\bar{T}J)}\,, \qquad \text{(B.7)}$$

leading, from Proposition 11, to the differential equation

$$\frac{d\mathcal{H}}{ds} = \mathrm{Tr}\Big(\hat{P}[\bar{T}]\frac{d\Theta^{(0)}_{s,\Lambda}}{ds}\hat{P}[T]\Big)\,, \qquad \text{(B.8)}$$

which we can be easily integrated :

$$\mathcal{H}(T,\bar{T},s) = \mathrm{Tr}\Big(\hat{P}[\bar{T}]\Theta^{(0)}_{s,\Lambda}\hat{P}[T]\Big) + \mathcal{V}_{int}[T,\bar{T}]\,. \qquad \text{(B.9)}$$

In this solution, the interaction $\mathcal{V}_{int}[T,\bar{T}]$ does not depend on s. This equation directly gives the classical effective action at scale $s\Lambda$. The solution is unique, once the initial conditions fixed, that is the interaction and the propagator.

Bibliography

[1] V. Lahoche, D. Oriti and V. Rivasseau, "Renormalization of an Abelian Tensor Group Field Theory: Solution at Leading Order," JHEP **1504**, 095 (2015) [arXiv:1501.02086 [hep-th]].

[2] V. Rivasseau, "From perturbative to constructive renormalization," Princeton, USA: Univ. Pr. (1991) 336 p. (Princeton series in physics)

[3] L. Freidel, R. Gurau and D. Oriti, "Group field theory renormalization - the 3d case: Power counting of divergences," Phys. Rev. D **80**, 044007 (2009) [arXiv:0905.3772 [hep-th]].

J. Ben Geloun, J. Magnen and V. Rivasseau, "Bosonic Colored Group Field Theory," Eur. Phys. J. C **70**, 1119 (2010) [arXiv:0911.1719 [hep-th]].

J. Ben Geloun, T. Krajewski, J. Magnen and V. Rivasseau, "Linearized Group Field Theory and Power Counting Theorems," Class. Quant. Grav. **27**, 155012 (2010) [arXiv:1002.3592 [hep-th]];

J. Ben Geloun and V. Bonzom, "Radiative corrections in the Boulatov-Ooguri tensor model: The 2-point function," Int. J. Theor. Phys. **50**, 2819 (2011) [arXiv:1101.4294 [hep-th]];

[4] J. Ben Geloun and V. Rivasseau, "A Renormalizable 4-Dimensional Tensor Field Theory," Commun. Math. Phys. **318**, 69 (2013) [arXiv:1111.4997 [hep-th]].

J. Ben Geloun and V. Rivasseau, "Addendum to 'A Renormalizable 4-Dimensional Tensor Field Theory'," Commun. Math. Phys. **322**, 957 (2013) [arXiv:1209.4606 [hep-th]].

J. Ben Geloun and E. R. Livine, "Some classes of renormalizable tensor models," J. Math. Phys. **54**, 082303 (2013) [arXiv:1207.0416 [hep-th]].

J. Ben Geloun, "Renormalizable Models in Rank $d \geq 2$ Tensorial Group Field Theory," Commun. Math. Phys. **332**, 117–188 (2014) [arXiv:1306.1201 [hep-th]];

J. Ben Geloun and D. O. Samary, "3D Tensor Field Theory: Renormalization and One-loop β-functions," Annales Henri Poincare **14**, 1599 (2013) [arXiv:1201.0176 [hep-th]]. J. Ben Geloun, "Two and four-loop β-functions of rank 4 renormalizable tensor field theories," Class. Quant. Grav. **29**, 235011 (2012) [arXiv:1205.5513 [hep-th]].

D. O. Samary, "Beta functions of $U(1)^d$ gauge invariant just renormalizable tensor models," Phys. Rev. D **88**, 105003 (2013) [arXiv:1303.7256 [hep-th]].

[5] S. Carrozza, D. Oriti and V. Rivasseau, "Renormalization of Tensorial Group Field Theories: Abelian U(1) Models in Four Dimensions," Commun. Math. Phys. **327**, 603 (2014) [arXiv:1207.6734 [hep-th]].

S. Carrozza, D. Oriti and V. Rivasseau, "Renormalization of a SU(2) Tensorial Group Field Theory in Three Dimensions," Commun. Math. Phys. **330**, 581 (2014) [arXiv:1303.6772 [hep-th]].

S. Carrozza, "Tensorial methods and renormalization in Group Field Theories," Springer Theses, 2014 (Springer, NY, 2014), arXiv:1310.3736 [hep-th].

[6] D. O. Samary and F. Vignes-Tourneret, "Just Renormalizable TGFT's on $U(1)^d$ with Gauge Invariance," Commun. Math. Phys. **329**, 545 (2014) [arXiv:1211.2618 [hep-th]].

M. Raasakka and A. Tanasa, "Combinatorial Hopf algebra for the Ben Geloun-Rivasseau tensor field theory," Seminaire Lotharingien de Combinatoire 70 (2014), B70d [arXiv:1306.1022 [gr-qc]].

D. O. Samary, "Closed equations of the two-point functions for tensorial group field theory," Class. Quant. Grav. **31**, 185005 (2014) [arXiv:1401.2096 [hep-th]].

J. Ben Geloun, "On the finite amplitudes for open graphs in Abelian dynamical colored Boulatov-Ooguri models," J. Phys. A **46**, 402002 (2013) [arXiv:1307.8299 [hep-th]].

S. Carrozza, "Discrete Renormalization Group for SU(2) Tensorial Group Field Theory," arXiv:1407.4615 [hep-th].

[7] Dine Ousmane Samary, "Beta functions ofU(1)d gauge invariant just renormalizable tensor models", Phys.Rev. D88, 105003 (2013) [arXiv:1303.7256[hep-th]].

[8] V. Rivasseau, "Why are tensor field theories asymptotically free?", arXiv: 507.04190v1.

[9] G. 't Hooft, "Rigorous construction of planar diagram field theories in four-dimensional Euclidean space," Commun. Math. Phys. **88** (1983) 1–25; V. Rivasseau, "Construction and Borel summability of planar four-dimensional Euclidean field theory," Commun. Math. Phys. **95** (1984) 445–486.

[10] D. O. Samary, "Closed equations of the two-point functions for tensorial group field theory," Class. Quant. Grav. **31**, 185005 (2014) [arXiv:1401.2096 [hep-th]].

[11] D. O. Samary, C. I. Pérez-Sánchez, F. Vignes-Tourneret and R. Wulkenhaar, "Correlation functions of just renormalizable tensorial group field theory: The melonic approximation," arXiv:1411.7213 [hep-th].

[12] G. Gallavotti and F. Nicolò, "Renormalization theory in four-dimensional scalar fields. I", Comm. Math. Phys. **100** (1985), 545-590.

[13] H. Grosse and R. Wulkenhaar, "Renormalisation of phi**4 theory on noncommutative R**4 in the matrix base," Commun. Math. Phys. **256**, 305 (2005), arXiv:hep-th/0401128; "Progress in solving a noncommutative quantum field theory in four dimensions," arXiv:0909.1389; "Self-dual noncommutative ϕ^4-theory in four dimensions is a non-perturbatively solvable and non-trivial quantum field theory," arXiv:1205.0465; "Solvable 4D noncommutative QFT: phase transitions and quest for reflection positivity," arXiv:1406.7755 [hep-th].

[14] R. Gurau, "The 1/N Expansion of Tensor Models Beyond Perturbation Theory," Commun. Math. Phys. **330**, 973 (2014) [arXiv:1304.2666 [math-ph]];

[15] V. Rivasseau, "Constructive Matrix Theory," JHEP **0709**, 008 (2007), arXiv:0706.1224.

[16] S. Dartois, R. Gurau and V. Rivasseau, "Double Scaling in Tensor Models with a Quartic Interaction," JHEP **1309**, 088 (2013) [arXiv:1307.5281 [hep-th]];

T. Delepouve and V. Rivasseau, "Constructive Tensor Field Theory: The T^4_3 Model," arXiv:1412.5091 [math-ph];

T. Delepouve, R. Gurau and V. Rivasseau, "Borel summability and the non perturbative $1/N$ expansion of arbitrary quartic tensor models," arXiv:1403.0170, to appear in Annales Henri Poincaré, Probablités;

R. Gurau, "The 1/N Expansion of Tensor Models Beyond Perturbation Theory," Commun. Math. Phys. **330**, 973 (2014) [arXiv:1304.2666 [math-ph]];

V. A. Nguyen, S. Dartois and B. Eynard, "An analysis of the intermediate field theory of T^4 tensor model," arXiv:1409.5751 [math-ph].

V. Bonzom, L. Lionni, V. Rivasseau, "Colored triangulation of arbitrary dimensions are stuffed maps", Arxiv: 1508.03805 [math.CO];

[17] M. Le Bellac, "Quantum and statistical field theory", Clarendon Press, Oxford, 1991. ;

J. Zinn-Justin, Quantum Field Theory. "Quantum Field Theory and statistical phenomena", Oxford University Press, New York, 1989.;

J. Polchinski, Nucl. Phys. B 231, 269, 1984.;

Chapter 5

Functional Renormalization Group

From the quantum gravity point of view, one of the main challenges of (T)GFTs is to understand how the quantum degrees of freedom organize to form a geometric structure which can be identified with a semi-classical space-time [1]. In this quest, the physics of phase transitions seems to be a promising route. In the most widely admitted scenario [5], and according to recent works [6, 7], these phase transitions should correspond to the condensation of quanta corresponding to the fields involved in the GFTs. This phenomenon, very similar to the Bose-Einstein condensation, implies the spontaneous acquisition of a nonzero value by the mean field (something similar has also been explored recently in tensor models [8, 9]), and, as discussed in the Chapter 2, the physical content of such states has started to be investigated for instance in a cosmological context. In this approach, as discussed in the previous chapter, the help of the renormalization machinery, which perfectly matches with the GFTs formalism, is invaluable [2]. Several approaches have been followed, especially perturbative ones, and some characteristics of these models start to emerge. An interesting and important aspect is the presence of non-trivial fixed points, which started being explored only recently by means of the Functional Renormalization Group (FRG) [10, 11], and the ϵ-expansion [2].

In this chapter we develop the general functional renormalization group (FRG) formalism for a tensorial group field theory with closure constraint, and discuss two examples of melonic just renormalizable Abelian models over $U(1)^{\times d}$, for $d = 6$ and $d = 5$, namely respectively the T^4_6 and T^6_5 models. We begin by giving a general introduction on the non-perturbative framework applied to TGFTs, and by deriving the so-called *Wetterich's equation* for TGFTs with closure constraint. Then we focus on the melonic T^4_6-model, that we shall consider in detail. The method that we shall use allows us to obtain a closed but non-autonomous system of differential equations which describe the renormalization group flow of the couplings beyond perturbation theory. The explicit dependence of the beta functions on the running scale is due to the existence of an external scale in the model, the radius of $S^1 \simeq U(1)$. We study this system in two different approximation regimes, corresponding to the deep UV and deep IR, in which it turns to be autonomous. In both cases, we study the occurrence of non-trivial fixed points, in addition to the Gaussian one, and recover the asymptotic freedom of the model discussed in the previous chapter with the same beta function at the one-loop order. Interestingly, we show the occurrence of a non-trivial Wilson-Fisher-like fixed point with one relevant and one irrelevant direction.

[1] This is a challenge that GFTs share with loop quantum gravity [4]

5.1 Functional renormalization group for TGFTs

In ordinary quantum field theory, there are essentially two approaches to the non-perturbative renormalization group. The most popular one, that we have briefly discussed at the end of the previous chapter, is based on a local version of Wilson's ideas, called the Wilson-Polchinski equation. However, except for the derivation of formal results, or in exceptional situations, the Wilson-Polchinski equation leads to untractable computations. The functional renormalization group method is an alternative, formally equivalent implementation of the Wilson strategy, firstly proposed by C. Wetterich [20, 15, 16, 17, 18], but more suited to effective computations. As explained before, the original strategy proposed by Wilson and Kadanoff is to map actions onto other actions at large scale via a coarse-graining procedure. The effective action that we obtain by this coarse-graining procedure only concerns the modes that have not been yet integrated out in the partition function, that we call $\varphi_<$. But these actions remain very abstract, and in practice it is usually impossible to extract easily any physical information out of it. Conversely, in the FRG approach, we compute the *Gibbs free energy*, or *effective action* $\Gamma[\phi, \bar{\phi}]$ (which is the Legendre transform of the free energy). More precisely, one builds a one-parameter family of Gibbs free energies $\Gamma_k[\phi, \bar{\phi}]$ indexed by a scale k, such that:

• When $k = \Lambda$, for some UV cut-off Λ, no fluctuation has been integrated out, the effective action $\Gamma_k[\phi, \bar{\phi}]$ is therefore equal to the microscopic action.

• When $k = 0$, all fluctuations are integrated out, and $\Gamma_{k=0}$ is nothing but the effective action of the original model.

Then, when k decreases from Λ to 0, more and more fluctuations are integrated out. Interestingly, the parameter k plays the role of an IR cut-off in the FRG framework, in contrast with the role of the analogue parameter in the Wilson-Polchinski approach (where the cut-off is an UV cut-off). This distinction is due to the fact that Γ_k is the effective action for the high energy modes. Moreover, the low energy modes, which play a fundamental role in the Wislon-Polchinski formulation, are absent in the FRG method, which only describes the high energy modes. Finally, an important advantage of the FRG approach is that any information on the model, renormalization group flows, existence of a fixed point, correlations functions, etc, are all derived from the effective action.

We shall now present the FRG formalism in some generality, and then build explicitly the one parameter family Γ_k for the Abelian TGFT models.

5.1.1 Effective average action for TGFTs

Concretely, the point of the FRG is to decouple the low energy modes in the partition function, and the standard strategy is to give them a large mass. Indeed, for modes with large mass, quantum fluctuations are important only for a small range of distances. It means in particle physics language that a very heavy particle should decouple from the low energy physics. Therefore we introduce the following one-parameter family of partition functions, for which a momentum dependent mass term has been added to the original fundamental action:

$$\mathcal{Z}_s[\bar{J}, J] := \int d\mu_C(\bar{\varphi}, \varphi) e^{-S_{int}(\bar{\varphi},\varphi) - \Delta S_s[\bar{\varphi},\varphi] + \langle \bar{J},\varphi\rangle + \langle \bar{\varphi}, J\rangle}, \tag{5.1}$$

where we think about S_{int} as the action e.g. for the T_6^4 model, and $s := \ln(k)$. The added IR cutoff or "momentum-dependent mass term" ΔS_s is chosen ultralocal in the momentum representation, and formally defined as:

$$\Delta S_s[\bar{\varphi}, \varphi] := \langle \bar{\varphi}, R_s \varphi \rangle = \sum_{\vec{p} \in \mathbb{Z}^d} R_s(\vec{p}) T_{\vec{p}} \bar{T}_{\vec{p}}, \tag{5.2}$$

where as in the previous chapter, $T_{\vec{p}}$ denotes the Fourier transform (or Peter-Weyl decomposition) of the field $\varphi(\vec{\theta})$. As usual, in order to give sense to the partition function we assume that a UV regulator is also present, e.g. a sharp cutoff on the momenta $|p| \leq \Lambda$ (for the usual norm: $|p| = \sqrt{\vec{p} \cdot \vec{p}}$). We refer to Λ as the "fundamental cut-off". In practice, we often work in the limiting case $\Lambda \to \infty$, because the Wetterich equation is well defined in that limit (although not its path integral origin).

The cutoff function $R_s(\vec{p})$ is a positive definite function chosen so that:

- $R_s(\vec{p}) \geq 0$ for all $\vec{p} \in \mathbb{Z}^d$ and $s \in (-\infty, +\infty)$.

- $\lim_{s \to -\infty} R_s(\vec{p}) = 0$, implying:

$$\mathcal{Z}_{s=-\infty}[\bar{J}, J] = \mathcal{Z}[\bar{J}, J]. \tag{5.3}$$

This condition ensures that the original model is in the family (5.1). Physically, it means that the original model is recovered when all the fluctuations are integrated out.

- $\lim_{s \to \ln \Lambda} R_s(\vec{p}) = +\infty$, ensuring that all the fluctuations are frozen when $e^s = \Lambda$. As a consequence, the bare action will be represented by the initial condition for the flow at $s = \ln \Lambda$.

- For $-\infty < s < \ln \Lambda$, the cutoff R_s is chosen so that

$$R_s(|p| > e^s) \ll 1, \tag{5.4}$$

a condition ensuring that the UV modes $|p| > e^s$ are almost unaffected by the additional cutoff term, while $R_s(|p| < e^s) \sim 1$, or $R_s(|p| < e^s) \gg 1$, will guarantee that the IR modes $|p| < e^s$ are decoupled.

- $\frac{d}{d|\vec{p}|} R_s(\vec{p}) \leq 0$, for all $\vec{p} \in \mathbb{Z}^d$ and $s \in (-\infty, +\infty)$, which means that high UV modes should not be suppressed more than lower modes.

As it stands, (5.1) defines an infinite-dimensional deformation of the original partition function. However, the role of the precise cutoff function, chosen to satisfy the above requirements, is secondary with respect to the role of the parametric dependence on s. From a Wilsonian point of view, the former corresponds to a choice of coarse graining scheme, while the latter corresponds to the coarse graining scale. We are primarily interested in the scale dependence of the theory, and therefore we take the point of view that a specific cutoff function has been chosen, and view (5.1) as a one-parameter family of theories.[2] We thus obtain a one-parameter family of free

[2] In principle, physical quantities, such as critical exponents, are independent of the coarse graining scheme (see for example the universality of the one-loop beta function for marginal couplings, which we discuss in appendix C.2), but approximations generally spoil this property. Scheme dependence is thus an important issue, which has been greatly developed into a full art of optimization [24], but we shall not discuss it further here.

energies,

$$W_s := \log \mathcal{Z}_s[\bar{J}, J], \tag{5.5}$$

and by their Legendre transform, a one-parameter family of effective actions, collectively called *effective average action*. To be more precise, the effective average action Γ_s is defined as:

$$\Gamma_s[\bar{\phi}, \phi] + \langle \bar{\phi}, R_s \phi \rangle = \langle \bar{J}, \phi \rangle + \langle \bar{\phi}, J \rangle - W_s[\bar{J}, J], \tag{5.6}$$

where the source J is to be expressed as a function of the effective mean field ϕ via the solution of

$$\phi = \frac{\delta W_s}{\delta \bar{J}}. \tag{5.7}$$

The previous properties concerning the cutoff term ΔS_s ensure that:

• $\Gamma^{int}_{s=\ln \Lambda} = S_{kin} + S_{int}$, for gauge invariant fields, so that when all the fluctuations are frozen, the effective average action coincides with the initial bare action.

• $\Gamma_{s=-\infty} = \Gamma$, meaning that when all the fluctuations are integrated out, the effective average action coincides with the full effective action.

This is nothing but the desired relationships for the effective averaging action Γ_k.

Interestingly, and to make contact with the Wilson-Polchinski point of view (or to point out their differences!), the modified action appearing in (5.1) can be usually interpreted as originating from a modification of the propagator. For a standard Gaussian measure, with usual kinetic action, this property is obvious, but it is not so obvious for our model, for which the covariance has been defined without an explicit kinetic action.[3] To prove this point, we use Wick theorem. Considering the following covariance:

$$C_s(\vec{p}, \vec{p}') = \frac{\delta\Big(\sum_i p_i\Big)}{\vec{p}^2 + m^2 + R_s(\vec{p})} \delta_{\vec{p},\vec{p}'}, \tag{5.8}$$

and the two Gaussian integrations:

$$C_s(\vec{p}, \vec{p}') := \int d\mu_{C_s}(T, \bar{T}) \bar{T}(\vec{p}) T(\vec{p}') \tag{5.9}$$

$$J_s(\vec{p}, \vec{p}') := \int d\mu_C(T, \bar{T}) e^{-\sum_{\vec{p}''} R_s \bar{T}(\vec{p}'') T(\vec{p}'')} \bar{T}(\vec{p}) T(\vec{p}'), \tag{5.10}$$

where $d\mu_C$ is the normalized Gaussian integration: $\int d\mu_C = 1$. In a first step, we shall prove that $J_s \propto C_s$. This comes obviously from the Wick theorem. Using the derivative representation of a Gaussian integral:

$$\begin{aligned} J_s(\vec{p}, \vec{p}') &= \exp\left(\frac{\delta}{\delta\varphi} C \frac{\delta}{\delta\bar{\varphi}}\right) e^{-\sum_{\vec{p}} R_s \bar{T}(\vec{p}) T(\vec{p})} \bar{T}(\vec{p}) T(\vec{p}') \Big|_{T,\bar{T}=0} \\ &= \frac{d}{dx} \exp\left(\frac{\delta}{\delta\varphi} C \frac{\delta}{\delta\bar{\varphi}}\right) e^{-\langle \bar{T}, (R_s + xL) T \rangle} \Big|_{T,\bar{T},x=0} \\ &= \frac{d}{dx} e^{-\mathrm{Tr}\ln(1 + C(R_s + xL))} \Big|_{x=0} = C_s(\vec{p}, \vec{p}') \times \det\left[\frac{C_s}{C}\right], \end{aligned} \tag{5.11}$$

[3] We can define our covariance C in its momentum representation, directly via equation (5.8). In this case, we see that because of the projector $\delta(\sum_i p_i)$, the definition of the inverse C^{-1}, which usually appears in the kinetic action, is slightly subtle and we prefer to present a more formal derivation involving only C.

where the elements of the (super-) matrix L are defined as $L_{\vec{p}_1,\vec{p}_2} = \delta_{\vec{p}_1,\vec{p}}\delta_{\vec{p}_2,\vec{p}'}$. Next, consider the following Gaussian integral:

$$J'_s := \int d\mu_{C_s}(T,\bar{T}) \prod_{j=1}^{N} \bar{T}^j(\vec{p}_j) T^j(\vec{p}'_j). \tag{5.12}$$

Using the Wick theorem, and the previous result, we obtain:

$$\begin{aligned} J'_s &= \sum_{\pi_N} \prod_j \left(\int d\mu_{C'}(T,\bar{T}) \bar{T}^{\pi_N(j)}(\vec{p}_{\pi_N(j)}) T^j(\vec{p}'_j) \right) \\ &= \sum_{\pi_N} \prod_j \left(\det\left[\frac{C}{C_s}\right] \int d\mu_C(T,\bar{T}) e^{-\langle \bar{T}, R_s T\rangle} \times T^{\pi_N(j)}(\vec{p}_{\pi_N(j)}) T^j(\vec{p}'_j) \right), \end{aligned}$$

where π_N is the permutation group of N elements. Now, using the Wick theorem, the big parenthesis can be written as:

$$\begin{aligned} I_s &:= \det\left[\frac{C}{C_s}\right] \int d\mu_C(T,\bar{T}) e^{-\langle \bar{T}, R_s T\rangle} T^{\pi_N(j)}(\vec{p}_{\pi_N(j)}) T^j(\vec{p}'_j) \\ &= \sum_n \frac{(-1)^n}{n!} \det\left[\frac{C}{C_s}\right] \int d\mu_C(T,\bar{T}) \times \langle \bar{T}, R_s T\rangle^n \bar{T}^{\pi_N(j)}(\vec{p}_{\pi_N(j)}) T^j(\vec{p}'_j) \\ &= \det\left[\frac{C}{C_s}\right] \sum_n \sum_p \frac{(-1)^{n-p+p}}{n!} \frac{n!}{p!(n-p)!} \\ &\qquad \times \left\langle \langle \bar{T}, R_s T\rangle^p \right\rangle_C \left\langle \langle \bar{T}, R_s T\rangle^{n-p} \bar{T}^{\pi_N(j)}(\vec{\theta}_{\pi_N(j)}) T^j(\vec{\theta}'_j) \right\rangle_{C,NV}, \end{aligned} \tag{5.13}$$

where the brackets $\langle . \rangle_C$ mean the Gaussian contractions with covariance C, and $\langle . \rangle_{C,NV}$ with subscript NV means that we select only the non-vacuum contractions (i.e. involving external fields only). The Cauchy decomposition formula allows to rewrite the double sum as:

$$\begin{aligned} I^j_s &= \sum_p \left\langle \frac{(-1)^p}{p!} \langle \bar{T}, R_s T\rangle^p \right\rangle_C \times \sum_n \left\langle \langle \bar{T}, R_s T\rangle^n \bar{T}^{\pi_N(j)}(\vec{p}_{\pi_N(j)}) T^j(\vec{p}'_j) \right\rangle_{C,N.V} \\ &= \left\langle e^{-\langle \bar{T}, R_s T\rangle} \right\rangle_C \times \left\langle e^{-\langle \bar{T}, R_s T\rangle} \bar{T}^{\pi_N(j)}(\vec{p}_{\pi_N(j)}) T^j(\vec{p}'_j) \right\rangle_{C,N.V}. \end{aligned}$$

The first term $\left\langle e^{-\int \bar{\varphi}\Delta\varphi} \right\rangle_C$ is nothing but the trivial Gaussian integral, i.e. the normalization of the Gaussian measure $d\mu_{C_s}$:

$$\left\langle e^{-\langle \bar{T}, R_s T\rangle} \right\rangle_C = e^{-\mathrm{Tr}\ln(1+C\Delta)} = \det(1+C\Delta)^{-1} = \det\left(\frac{C_s}{C}\right),$$

implying finally:

$$I^j_s = \left\langle e^{-\langle \bar{T}, R_s T\rangle} \bar{T}^{\pi_N(j)}(\vec{p}_{\pi_N(j)}) T^j(\vec{p}'_j) \right\rangle_{C,N.V}.$$

Reporting this result into equation (5.13) for J'_s leads to:

$$J'_s = \sum_{\pi_N} \prod_j I^j_s = \det\left(\frac{C}{C_s}\right) \left\langle e^{-\langle \bar{T}, R_s T\rangle} \right\rangle_C \sum_{\pi_N} \prod_j I^j_s. \tag{5.14}$$

Finally, since the factor $\left\langle e^{-\langle \bar{T}, R_s T\rangle}\right\rangle_C$ is nothing but the vacuum contribution of the measure $d\mu_C e^{-\langle \bar{T}, R_s T\rangle}$, we find:

$$\int d\mu_{C_s}(T,\bar{T}) \prod_{j=1}^{N} \bar{T}^j(\vec{p}_j) T^j(\vec{p}'_j) = \det\left(\frac{C}{C_s}\right) \int d\mu_C(T,\bar{T}) e^{-\langle \bar{T}, R_s T\rangle} \prod_{j=1}^{N} \bar{T}^j(\vec{p}_j) T^j(\vec{p}'_j). \tag{5.15}$$

With no surprise, this result is exactly what is expected for a standard Gaussian integration with well-defined kinetic action. Hence, it follows from the properties of the Gaussian integration that the definition (5.1), with modification of the action, can be interpreted as a modification of the covariance, i.e.

$$\mathcal{Z}'_s[\bar{J}, J] := \int d\mu_{C_s}(\bar{\varphi}, \varphi) e^{-S_{int}(\bar{\varphi},\varphi) + \langle \bar{J}, \varphi\rangle + \langle \bar{\varphi}, J\rangle}. \tag{5.16}$$

In fact, the flow equations for (5.1) and (5.16) differ for vacuum terms due to the $\det(C_s)$ implicit in the measure of (5.16) (see (5.15)), but as usual such vacuum terms are completely unimportant[4]. The difference between the Wilson-Polchinski strategy can be stressed on an explicit example, and is very clear with the choice of the regulator used in Appendix C.2, where the role of k as an IR regulator is explicit.

Let us remind in this context the definitions of the projector into the gauge invariant field $\hat{P}$, introduced in Chapter 2:

$$\hat{P} : \varphi \to \hat{P}[\varphi](\theta_1, ..., \theta_d) = \int \frac{d\eta}{2\pi} \varphi(\theta_1 + \eta, ..., \theta_d + \eta), \tag{5.17}$$

and of the invariant field subspace as $\mathbb{G} = \ker(\hat{P} - \mathbb{I})$, where $\mathbb{I}$ means the identity in the space of fields. Interestingly, because of the projection in the propagator, the gauge symmetry is implemented, at the graphical level, at each colored line hooked to a black or white node. Hence the mean field ϕ, defined by (5.7), lives in $\mathbb{G}$. The gauge symmetry is then dynamically implemented by the propagator, and affects each N-point function : $G_N \in \mathbb{G}^{\otimes N}$.

Using the Legendre transform (5.6) and the definition (5.1), we obtain formally the so-called Wetterich equation, describing the evolution of the effective average action. We have:

Proposition 12. (Wetterich equation)
For a given cutoff R_s, the effective average action Γ_s satisfies the following partial differential equation:

$$\begin{aligned} \partial_s \Gamma_s =& \sum_{\vec{p} \in \mathbb{Z}^d} \partial_s R_s(\vec{p}) \cdot \left[\Gamma_s^{(2)} + R_s\right]^{-1}(\vec{p}, \vec{p})\, \delta\left(\sum_{i=1}^{d} p_i\right) \\ =& \mathrm{Tr}\left[\hat{P} \frac{\partial_s R_s}{\Gamma_s^{(2)} + R_s}\right], \end{aligned} \tag{5.18}$$

where Tr *is the super-trace, meaning the trace over the block-indices, and* $\Gamma_s^{(2)} \equiv \frac{\delta^2 \Gamma_s}{\delta\bar{\phi}\delta\phi}$. *The presence of* $\hat{P}$ *restricts the sums over the subspace of* $\mathbb{Z}^d$ *which we denote by* $\mathcal{P}$ *and define by :* $\mathcal{P} = \{\vec{p} \in \mathbb{Z}^d | \sum_i p_i = 0\}$.

[4]Note that in the pregeometric interpretation of tensor models, vacuum terms are completely unrelated to the cosmological constant.

Proof: The proof is rather standard [20, 21], but it is useful to review it because of the TGFT context and the appearance of the projector $\hat{P}$ in the equation. Applying the operator ∂_s on the two members of the equation (5.6), we have

$$\partial_s \Gamma_s = \langle \partial_s \bar{J}, \phi \rangle + \langle \bar{\phi}, \partial_s J \rangle - \partial_s W_s - \langle \partial_s \bar{J}, \frac{\delta W_s}{\delta \bar{J}} \rangle - \langle \frac{\delta W_s}{\delta J}, \partial_s J \rangle - \langle \bar{\phi}, \partial_s R_s \phi \rangle. \tag{5.19}$$

The term $\partial_s W_s$ can be easily computed from the definitions (5.1) and (7.2.1):

$$\partial_s W_s = - \sum_{\vec{p} \in \mathbb{Z}^d} \partial_s R_s(\vec{p}) \left(\frac{\delta^2 W_s}{\delta J_{\vec{p}} \delta \bar{J}_{\vec{p}}} + \frac{\delta W_s}{\delta J_{\vec{p}}} \frac{\delta W_s}{\delta \bar{J}_{\vec{p}}} \right). \tag{5.20}$$

Using (5.7), many terms cancel in (5.19), and we are left with

$$\partial_s \Gamma_s = \sum_{\vec{p} \in \mathbb{Z}^d} \partial_s R_s(\vec{p}) \frac{\delta^2 W_s}{\delta J_{\vec{p}} \delta \bar{J}_{\vec{p}}}. \tag{5.21}$$

Deriving (5.7) with respect to J we find

$$\frac{\delta^2 W_s}{\delta J \delta \bar{J}} = \frac{\delta \phi}{\delta J}, \tag{5.22}$$

while deriving (5.6) with respect to ϕ and then $\bar{\phi}$ gives

$$\frac{\delta^2 \Gamma_s}{\delta \bar{\phi} \delta \phi} = \frac{\delta J}{\delta \phi} - R_s. \tag{5.23}$$

Therefore we obtain, in matrix notation:

$$\frac{\delta^2 W_s}{\delta J \delta \bar{J}} \left[\frac{\delta^2 \Gamma_s}{\delta \bar{\phi} \delta \phi} + R_s \right] = \mathbb{I}. \tag{5.24}$$

The second functional derivative $W_s^{(2)}$ is the 2-point function which, as the effective mean field $\phi = W_s^{(1)}$, is gauge invariant: $W_s^{(2)} \in \mathbb{G} \otimes \mathbb{G}$. Hence, the previous equation (5.24) means that $\Gamma^{(2)} + R_s$ is the inverse of $\mathcal{W}^{(2)}$ on the subspace $\mathcal{P}$ only. Finally, using (5.24) in (5.21), and the fact that, because $\mathcal{W}^{(2)}$ is a gauge invariant matrix, $\mathcal{W}^{(2)} \in \mathbb{G} \otimes \mathbb{G} \to \hat{P} \mathcal{W}^{(2)} \hat{P} = \mathcal{W}^{(2)}$, we find the Wetterich equation (5.18).

□

The Wetterich equation is nothing but a renormalization group equation, governing how the couplings change under a change of scale, and it is an *exact equation*. Moreover, in contrast with perturbation theory, where l-loop diagrams require l d-dimensional integrals, the Wetterich equation has a one-loop structure, and then, only one integral has to be computed, which is an important point in practice.

5.1.2 Canonical dimension of a tensorial bubble

In order to investigate the influence of the dimension d on the occurrence of fixed points in the FRG analysis, we need to work with dimensionless quantities, as in usual quantum or statistical field theories. In the present case, there is an external scale L (the radius of $S^1 \simeq U(1)$) which we have set to 1, thus implicitly making all quantities dimensionless in the usual sense. In fact, as pointed out in [10], and as usual in the presence of an external scale [23], this is the reason why we shall obtain non-autonomous RG flow equations. However, what matters for our purpose is how such quantities scale with the cutoff. We need therefore to compute what we refer to as their *scaling dimension*. Such scaling dimensions appear quite naturally in the perturbative calculations. For instance, in Schwinger regularization and in dimension d, we have shown at the beginning of Chapter 4 that, at the dominant order, the 2 and 4-point functions behave as:

$$\Sigma_{1\,loop,\infty} = \lambda \Lambda^{(d-4} K_1 \tag{5.25}$$

$$\Gamma^{(4)}_{1\,loop,\infty} = 24\big(-\lambda + \lambda^2 \Lambda^{d-6} K_2\big), \tag{5.26}$$

where K_1 and K_2 are two numerical constants independent of λ, Λ or m. The exponent of Λ in the above expressions is in general a universal number, meaning that it does not depend on the chosen renormalization (for example, we find the same exponent by regularizing the theory by means of a momentum cutoff). We therefore define the (canonical[5]) scaling dimension $[X]$ of a quantity X in such a way that by redefining $X = \bar{X}\Lambda^{[X]}$ we obtain an homogeneous expression in Λ for the renormalization of X. The equation (5.26) then shows that the scaling dimension of λ is $[\lambda] = 6-d$, so that both summands have the same dimension. Inserting this result in (5.25), we find $[\Sigma_{1\,loop,\infty}] = 2$, implying that $[m] = 1$, since $\Sigma_{1\,loop,\infty}$ gives the radiative corrections of the mass term.

We can easily check the coherence of these definitions at all orders, noting that the exponent of Λ appearing in (5.25) and (5.26) is nothing else but the divergence degree ω of the corresponding graph. The divergent degree has been studied in Chapter 4, and we have show that the leading order graphs correspond to the so-called melonic graphs. Due to their recursive definition, it is not hard to see that it obeys[6]:

$$F(\mathcal{G}) - R(\mathcal{G}) = (d-2)(L(\mathcal{G}) - V(\mathcal{G}) + 1), \tag{5.27}$$

where $V(\mathcal{G})$ is the number of vertices in the $\mathcal{G}$ graph. The equation (5.27), together with the combinatorial relation $L(\mathcal{G}) = 2V(\mathcal{G}) - N_{ext}(\mathcal{G})/2$, leads to

$$\omega(\mathcal{G}) = (d-6)V(\mathcal{G}) + \Big[(d-2) + \frac{4-d}{2} N_{ext}(\mathcal{G})\Big]. \tag{5.28}$$

We limit ourselves to the interactions that we can find in the initial theory. A 1PI graph with four external legs has, *a priori* the same dimension as the coupling constant λ. That is to say:

$$(d-6+[\lambda])\big(V(\mathcal{G})-1\big) + (d-6) + \Big[(d-2) + \frac{4-d}{2} \times 4\Big] = 0,$$

implying $[\lambda] = 6-d$. The same argument applied to an 1PI function with two external legs justifies $[m] = 1$:

$$(d-6+[\lambda])V(\mathcal{G}) + \Big[(d-2) + \frac{4-d}{2} \times 2\Big] = 2. \tag{5.29}$$

[5] At a non-trivial fixed point the scaling dimension will in general be anomalous, i.e. different from the canonical one.

[6] See the discussion at the begining of Chapter 6.

Note that, for the ordinary scalar field theory with $\lambda_4\phi^4$ interaction, the local nature of the interaction leads to $[\lambda_4] = 4 - d$. Therefore, the tensorial nature of the interaction leads to a shift in the critical dimension, from 4 to 6. The same argument can be extended to a general melonic coupling t_b with n_b-external points, and we get:

$$[t_b] = (d-2) + \frac{1}{2}(4-d)n_b \ . \tag{5.30}$$

5.2 The truncation procedure for T_6^4

One of the many advantages of the FRG is the possibility to make an approximation directly at the level of the effective average action. The latter is in principle a complicated functional, containing infinitely many terms, and therefore an exact solution of the Wetterich equation is generally beyond reach. One of the most common approximation method, besides perturbation theory, consists in truncating the space of functionals in which Γ_s is defined, retaining only a finite-dimensional subspace, or a simple infinite-dimensional one. This allows to obtain a closed and tractable system of differential equations, which can be analytically studied in some cases, or numerically integrated for most cases. As an organizational principle for such truncations, we usually start off by Taylor expanding the effective average action in powers of $\vec{p}$. Truncating such expansion to some given order is expected to be a valid approximation in a context where we are interested in the long distance physics. Subsequently, we can proceed to expand each order in powers of the fields, and truncate that expansion too, thus leading to a finite-dimensional subspace of functionals. The main idea is that by systematically expanding such subspace one should observe some convergence pattern in the values of physical quantities, such as the critical exponents. This justifies a posteriori the approximation procedure. A nice example of this method is provided by the Ising universality class, associated to the Wilson-Fisher fixed point in three dimensions [25]. However, when applying the FRG in a new context, before reaching such advanced level of systematization, it is often necessary to start from the simplest possible approximation in such a class of truncations, to work out the formalism and understand possible outcomes. In our case, the simplestand most obvious truncation boils down to write Γ_s exactly in the same form as the bare action we have in mind, but with coupling, mass and wave function normalization depending on s. This is the approximation we shall now adopt.

More precisely, we henceforth consider the following simple truncation:

$$\begin{aligned}\Gamma_s[\phi,\bar{\phi}] = &\int d\vec{\theta}\bar{\phi}(\vec{\theta})\big[-Z_s\Delta_{\vec{\theta}} + m_s^2\big]\phi(\vec{\theta}) \\ &+ \lambda_s \sum_i \int \left(\prod_{j=1}^{4} d\vec{\theta}_j\right) \mathcal{W}^{(i)}_{\vec{\theta}_1,\vec{\theta}_2,\vec{\theta}_3,\vec{\theta}_4}\phi(\vec{\theta}_1)\bar{\phi}(\vec{\theta}_2)\phi(\vec{\theta}_3)\bar{\phi}(\vec{\theta}_4),\end{aligned} \tag{5.31}$$

where $\Delta_{\vec{\theta}}$ is the Laplacian operator on $U(1)^{\times d}$, λ_s and m_s are the effective coupling and mass at the scale s, and Z_s is the field strength normalization. Furthermore, as explained below equation (5.17), the fields $\phi \in \mathbb{G}$ appearing in (5.31), are gauge invariant fields. We can give a qualitative critera for the consistency of this truncation, based on the anomalous dimension $\eta := \partial_s \ln(Z)$. Indeed, at the vicinity of a fixed point, η can reach a non-zero value η_*. As a result, the effective propagator becomes:

$$\frac{Z^{-1}}{\vec{p}^2 + (m_s^2/Z)} \approx \frac{e^{-\eta_* s}}{\vec{p}^2 + m_*^2} \ . \tag{5.32}$$

This modifies the perturbative power counting, which becomes in the melonic sector (all the star-quantities refer to the non-Gaussian fixed point that we consider):

$$\omega_*(\mathcal{G}) = -(2+\eta_*)L(\mathcal{G}) + (F(\mathcal{G}) - R(\mathcal{G})) = (d-6-2\eta_*)V(\mathcal{G}) + \left[(d-2) + \frac{4+\eta_*-d}{2}N_{ext}(\mathcal{G})\right]. \tag{5.33}$$

As a result, the canonical dimension 5.30 turns to be

$$[t_b]_* = (d-2) + \frac{1}{2}(4-d+\eta_*)n_b = [t_b] + \frac{1}{2}\eta_* n_b \ , \tag{5.34}$$

from which we can argue that, as long as $\eta_* \ll 1$, the classification in terms of essential, inessential and marginal couplings remains unchanged, and the truncation around marginal couplings with respect to the perturbative power counting makes sense.

Evaluating the second derivative of (5.31), we get, in momentum representation:

$$\Gamma^{(2)}_s(\vec{p},\vec{p}') = \left[Z_s\vec{p}^{\,2} + m_s^2\right]\hat{P}_{\vec{p},\vec{p}'} + 2\lambda_s \sum_{\{\vec{p}_i\}} \hat{P}_{\vec{p},\vec{p}_1}\hat{P}_{\vec{p}',\vec{p}_2}\mathrm{Sym}\mathcal{W}_{\vec{p}_1,\vec{p}_2,\vec{p}_3,\vec{p}_4}T_{\vec{p}_3}\bar{T}_{\vec{p}_4}, \tag{5.35}$$

where we recall that

$$\mathrm{Sym}\mathcal{W}_{\vec{p}_1,\vec{p}_2,\vec{p}_3,\vec{p}_4} := \mathcal{W}_{\vec{p}_1,\vec{p}_2,\vec{p}_3,\vec{p}_4} + \mathcal{W}_{\vec{p}_3,\vec{p}_2,\vec{p}_1,\vec{p}_4}. \tag{5.36}$$

and

$$\hat{P}_{\vec{p}_1,\vec{p}_2} = \delta_{\vec{p}_1,\vec{p}_2}\delta\left(\sum_{i=1}^{d} p_i\right). \tag{5.37}$$

Let us also define:

$$F_s(\vec{p},\vec{p}') := 2\sum_{\{\vec{p}_i\}} \hat{P}_{\vec{p},\vec{p}_1}\hat{P}_{\vec{p}',\vec{p}_2}\mathrm{Sym}\mathcal{W}_{\vec{p}_1,\vec{p}_2,\vec{p}_3,\vec{p}_4}T_{\vec{p}_3}\bar{T}_{\vec{p}_4} \tag{5.38}$$

and

$$K_s(\vec{p}) := \left(Z_s\vec{p}^{\,2} + m_s^2 + R_s(\vec{p})\right). \tag{5.39}$$

The next step is the choice of the regulator R_s, for which we adopt Litim's cutoff [24]:

$$R_s(\vec{p}) = Z_s(e^{2s} - \vec{p}^{\,2})\Theta(e^{2s} - \vec{p}^{\,2}), \tag{5.40}$$

where Θ stands for the Heaviside step function. The special dependence on $\vec{p}^{\,2}$ and the inclusion of a wave function renormalization will lead to substantial simplifications. Applying the derivative operator on R_s, we find:

$$\partial_s R_s(\vec{p}) = \left\{\partial_s Z_s(e^{2s} - \vec{p}^{\,2}) + 2Z_s e^{2s}\right\}\Theta(e^{2s} - \vec{p}^{\,2}). \tag{5.41}$$

Using the equations (5.35) and (5.41) in the flow equation (5.18), we shall obtain the renormalization group flow equations, which are the subject of the next section.

5.2.1 Renormalization group flow equations

Using our Ansatz (5.31) in the Wetterich equation (5.18), expanding its r.h.s. of in power of ϕ, and truncating at order ϕ^4, we find:

$$r.h.s. = \sum_{\vec{p}\in\mathcal{P}} \frac{\partial_s R_s}{K_s(\vec{p})} \left[1 - \lambda_s \frac{F_s(\vec{p},\vec{p})}{K_s(\vec{p})} + \lambda_s^2 \sum_{\vec{p}'\in\mathcal{P}} \frac{F_s(\vec{p},\vec{p}')F_s(\vec{p}',\vec{p})}{K_s(\vec{p})K_s(\vec{p}')} + \mathcal{O}(\phi^6) \right].$$

The RG flow equations for coupling, mass and wave function renormalization can be obtained from this expansion, identifying the corresponding powers of $\bar{\phi}\phi$.

- **Equations for m_s and Z_s.** Identifying the terms of order $\bar{\phi}\phi$ leads to:

$$\sum_{\vec{p}\in\mathcal{P}} (\partial_s m_s^2 + \partial_s Z_s \vec{p}^{\,2}) T_{\vec{p}} \bar{T}_{\vec{p}} = -2\lambda_s \sum_{\substack{\vec{p}\in\mathcal{P} \\ |\vec{p}|\leq e^s}} \frac{\left(\partial_s Z_s (e^{2s} - \vec{p}^{\,2}) + 2 Z_s e^{2s}\right)}{(Z_s e^{2s} + m_s^2)^2} \times \sum_{\vec{q}_1,\vec{q}_2} \mathrm{Sym}\mathcal{W}_{\vec{p},\vec{p},\vec{q}_1,\vec{q}_2} T_{\vec{q}_1} \bar{T}_{\vec{q}_2}. \tag{5.42}$$

We start the analysis with some considerations about the r.h.s.. Because of the form of the interaction matrices $\mathcal{W}^{(i)}$ and $T_{\vec{p}} \in \mathbb{G}$:

$$\sum_{\vec{p}\in\mathcal{P}} \sum_{\vec{q}_1,\vec{q}_2} f(\vec{p}^{\,2}) \mathcal{W}^{(i)}_{\vec{p},\vec{p},\vec{q}_1,\vec{q}_2} T_{\vec{q}_1} \bar{T}_{\vec{q}_2} = \sum_{\vec{p},\vec{p}'\in\mathcal{P}} f(\vec{p}^{\,2}) T_{\vec{p}'} \bar{T}_{\vec{p}'} \delta_{p_i,p_i'}. \tag{5.43}$$

Defining $\vec{p}_\perp$ to be the set $(p_1,\ldots,p_{i-1},p_{i+1},\ldots,p_d)$, and

$$\tilde{f}(p_i^2) = \sum_{\vec{p}_\perp} f(\vec{p}^{\,2})\, \delta\left(\sum_{j=1}^{d} p_j\right), \tag{5.44}$$

equation (5.43) can be rewritten as:

$$\sum_{\vec{p}\in\mathcal{P}} \sum_{\vec{q}_1,\vec{q}_2} f(\vec{p}^{\,2}) \mathcal{W}^{(i)}_{\vec{p},\vec{p},\vec{q}_1,\vec{q}_2} T_{\vec{q}_1} \bar{T}_{\vec{q}_2} = \sum_{\vec{p}\in\mathcal{P}} \tilde{f}(p_i^2)\, T_{\vec{p}} \bar{T}_{\vec{p}}. \tag{5.45}$$

In the same way, because of the closure constraint,

$$\sum_{\vec{p}\in\mathcal{P}} \sum_{\vec{q}_1,\vec{q}_2} f(\vec{p}^{\,2}) \mathcal{W}^{(i)}_{\vec{q}_1,\vec{p},\vec{p},\vec{q}_2} T_{\vec{q}_1} \bar{T}_{\vec{q}_2} = \sum_{\vec{p}\in\mathcal{P}} f(\vec{p}^{\,2}) T_{\vec{p}} \bar{T}_{\vec{p}}. \tag{5.46}$$

We can therefore rewrite (5.42) as

$$\sum_{\vec{p}\in\mathcal{P}} (\partial_s m_s^2 + \partial_s Z_s \vec{p}^{\,2}) T_{\vec{p}} \bar{T}_{\vec{p}} = -2\lambda_s \sum_{\vec{p}\in\mathcal{P}} \left(\sum_{i=1}^{d} \tilde{f}(p_i^2) + d\, f(\vec{p}^{\,2}) \right) T_{\vec{p}} \bar{T}_{\vec{p}}, \tag{5.47}$$

where

$$f(\vec{p}^{\,2}) = \left(A + B\,\vec{p}^{\,2}\right) \theta(e^{2s} - \vec{p}^{\,2}), \tag{5.48}$$

and we have defined

$$A := \frac{\big(\partial_s Z_s + 2Z_s\big)e^{2s}}{(Z_s e^{2s} + m_s^2)^2}, \tag{5.49}$$

$$B := -\frac{\partial_s Z_s}{(Z_s e^{2s} + m_s^2)^2}. \tag{5.50}$$

We want to satisfy (5.47) up to order $\vec{p}^{\,2}$, meaning that we want to expand

$$\sum_{i=1}^{d} \tilde{f}(p_i^2) + d\, f(\vec{p}^{\,2}) = d\,\Big(\tilde{f}(0) + f(0)\Big) + \vec{p}^{\,2}\,\Big(\tilde{f}'(0) + d\, f'(0)\Big) + O(\vec{p}^{\,4}), \tag{5.51}$$

equating the coefficients of $\vec{p}^{\,0}$ and $\vec{p}^{\,2}$,

$$\partial_s m_s^2 = -2\lambda_s\, d\,\Big(\tilde{f}(0) + f(0)\Big), \tag{5.52}$$

$$\partial_s Z_s = -2\lambda_s\,\Big(\tilde{f}'(0) + d\, f'(0)\Big) \tag{5.53}$$

and discarding the rest. The expansion of $f(\vec{p}^{\,2})$ is trivial, as the step function is equal to one at all orders of the Taylor expansion, and we thus have $f(0) = A$ and $f'(0) = B$. The expansion of $\tilde{f}(p_i^2)$ is instead slightly more involved. We can first write $\tilde{f}(p_i^2)$ as

$$\tilde{f}(p_i^2) = A S_1(p_i^2) + B S_2(p_i^2), \tag{5.54}$$

where

$$S_1(k^2) := \sum_{\vec{p}_\perp} \delta\left(k + \sum_{l\neq i} p_l\right)\theta(e^{2s} - k^2 - \vec{p}_\perp{}^2), \tag{5.55}$$

$$S_2(k^2) := \sum_{\vec{p}_\perp} (k^2 + \vec{p}_\perp^{\,2})\delta\left(k + \sum_{l\neq i} p_l\right)\theta(e^{2s} - k^2 - \vec{p}_\perp{}^2), \tag{5.56}$$

so that

$$\partial_s m_s^2 = -2\lambda_s\, d\,\left(A\,(1 + S_1(0)) + B\, S_2(0)\right), \tag{5.57}$$

$$\partial_s Z_s = -2\lambda_s\,\left(A\, S_1'(0) + B\,(d + S_2'(0))\right). \tag{5.58}$$

Since we shall be mostly interested in the large-s limit (the small-s case will be treated separately), we can approximate the sums by integrals, replacing the Kronecker deltas by Dirac deltas. The support of the integrals is in the intersection of the hyperplane of equation $k + \sum_{l\neq i} p_l = 0$ and the $(d-1)$-ball of radius $\sqrt{e^{2s} - k^2}$. Note that the Kronecker delta of the closure constraint can be rewritten as $k + \vec{p}_\perp \cdot \vec{n} = 0$, where $\vec{n} = (1, 1, ...1)$ is the vector with all components equal to 1 in $\mathbb{R}^{d-1}$. Using the rotational invariance of our integral, we can choose one of our coordinate axis to be in the direction $\vec{n}$. If we choose the axis 2 in this direction, our constraint writes as $\delta(k + p_2'|\vec{n}|) = \delta(k + p_2'\sqrt{d-1}) = \delta(k/\sqrt{d-1} + p_2')/\sqrt{d-1}$, and we find the following integral approximation:

$$S_1(k^2) \simeq \frac{1}{\sqrt{d-1}}\Omega_{d-2}\left[e^{2s} - \frac{dk^2}{d-1}\right]^{\frac{d-2}{2}} =: \tilde{S}_1(k^2) \tag{5.59}$$

$$S_2(k^2) \simeq \frac{1}{\sqrt{d-1}}\Big[\frac{dk^2}{d-1} + \frac{d-2}{d}\left(e^{2s} - \frac{dk^2}{d-1}\right)\Big]\Omega_{d-2}\left(e^{2s} - \frac{dk^2}{d-1}\right)^{\frac{d-2}{2}} =: \tilde{S}_2(k^2), \tag{5.60}$$

where $\Omega_d := \pi^{d/2}/\Gamma(d/2+1)$ is the volume of the unit d-ball. The integral approximations are easily expanded to yield:

$$I_1 := \tilde{S}_1(0) = \frac{1}{\sqrt{d-1}}\Omega_{d-2}e^{(d-2)s}, \tag{5.61}$$

$$I_2 := \tilde{S}_2(0) = \frac{1}{\sqrt{d-1}}\frac{d-2}{d}\Omega_{d-2}e^{ds}, \tag{5.62}$$

$$I_3 := \tilde{S}_1'(0) = -\frac{1}{\sqrt{d-1}}\frac{d(d-2)}{2(d-1)}\Omega_{d-2}e^{(d-4)s}, \tag{5.63}$$

$$I_4 := \tilde{S}_2'(0) = -\frac{1}{\sqrt{d-1}}\frac{d(d-4)}{2(d-1)}\Omega_{d-2}e^{(d-2)s}. \tag{5.64}$$

Therefore we obtain

$$\partial_s m_s^2 = -2\lambda_s\, d\, \left(A\,(1+I_1) + B\, I_2\right), \tag{5.65}$$

$$\partial_s Z_s = -2\lambda_s\, \left(A\, I_3 + B\,(d+I_4)\right), \tag{5.66}$$

which, using (5.49)-(5.50) and (5.61)-(5.64), can be translated into

$$\boxed{\partial_s m_s^2 = -2\lambda_s Z_s \frac{\left(2\frac{\Omega_{d-2}}{\sqrt{d-1}}e^{ds} + de^{2s}\right)\eta_s + 2d\left(\frac{\Omega_{d-2}}{\sqrt{d-1}}e^{ds} + e^{2s}\right)}{(Z_s e^{2s} + m_s^2)^2},} \tag{5.67}$$

and

$$\boxed{\eta_s = \frac{2d(d-2)}{(d-1)^{3/2}}\frac{\lambda_s\Omega_{d-2}e^{(d-2)s}}{(Z_s e^{2s}+m_s^2)^2 - 2\lambda_s\left[\frac{d}{(d-1)^{3/2}}\Omega_{d-2}e^{(d-2)s} + d\right]},} \tag{5.68}$$

where we have defined

$$\eta_s := \frac{\partial}{\partial s}\log(Z_s). \tag{5.69}$$

• **Equation for λ_s.** In order to obtain the equation describing the running coupling constant flow, we must identify the correct melonic structure among the terms of order $(\bar{\phi}\phi)^2$ in the r.h.s. of the flow equation, i.e. in

$$\sum_{\vec{p}\in\mathcal{P}}\frac{\partial_s R_s}{K_s(\vec{p})}\lambda_s^2\sum_{\vec{p}'\in\mathcal{P}}\frac{F_s(\vec{p},\vec{p}')F_s(\vec{p}',\vec{p})}{K_s(\vec{p})K_s(\vec{p}')}.$$

The expression above involves a term of the form

$$\mathrm{Sym}\mathcal{W}_{\vec{p},\vec{p}',\vec{p}_1,\vec{p}_2}\mathrm{Sym}\mathcal{W}_{\vec{p},\vec{p}',\vec{p}_1',\vec{p}_2'},$$

giving three types of contributions,

$$\mathcal{W}^i_{\vec{p},\vec{p}',\vec{p}_1,\vec{p}_2}\mathcal{W}^j_{\vec{p},\vec{p}',\vec{p}_1',\vec{p}_2'},$$

$$\mathcal{W}^i_{\vec{p}_1,\vec{p}',\vec{p},\vec{p}_2}\mathcal{W}^j_{\vec{p},\vec{p}',\vec{p}_1',\vec{p}_2'},$$

$$\mathcal{W}^i_{\vec{p}_1,\vec{p}',\vec{p},\vec{p}_2}\mathcal{W}^j_{\vec{p}_1',\vec{p}',\vec{p},\vec{p}_2'},$$

all depicted in Figure 5.1 below.

The connectivity of the original melonic interaction induces a selection rule for the interactions generated by the r.h.s of the flow equation. This selection rule is based on the study of the "ultra-local" version of the interactions depicted in Figures 5.1a, 5.1b and 5.1c, i.e. the interactions obtained by replacing the propagators with Kronecker delta functions, or equivalently, by the contraction of the dotted lines following the contraction procedure of the Chapter4. Indeed, this contraction procedure is just to allow us to obtain the connectivity structure of an interaction, and therefore we do not keep track of the black square (the insertion of the cutoff operator) in the definition above and in the figures. Of course we shall keep track of that once we have identified the correct structures.

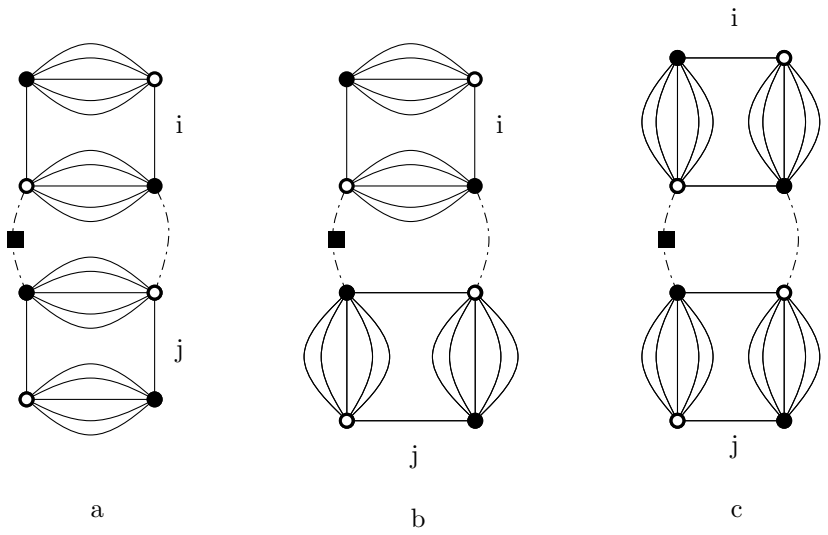

Figure 5.1: Interactions involved in the r.h.s of the Wetterich equation. The dash-dotted line represents a contraction involving the operator K_s^{-1}, and the dash-dotted line with a square represents a contraction involving the propagator $\hat{P}\partial_s R_s\, K_s^{-2}\hat{P}$.

As an example of contraction, we can consider the interaction depicted in 5.1a, for which we obtain, after contraction over the two dash-dotted lines, the result depicted in Figure 5.2.

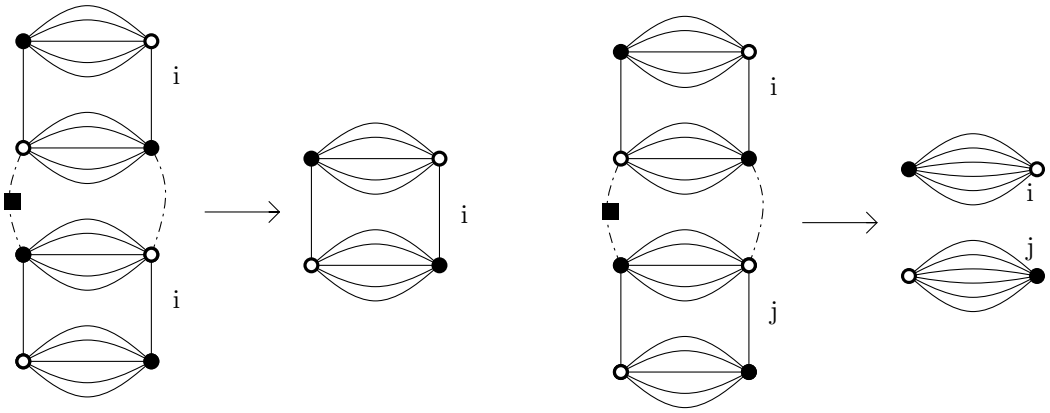

Figure 5.2: Connecting structure of the interactions 5.1a.

We observe that the first contraction gives exactly a vertex of the original form, while the second contraction gives a disconnected vertex corresponding to the square of a mass-term, which is outside of our truncation, and thus will be discarded. As a second example, the case $i = 1$ and $j = 2$ for the last 5.1c case gives, after contraction of its two dash-dotted lines, the result

depicted in Figure 5.3, showing that the interaction does not have the connectivity structure of a melonic bubble, and will also be discarded.

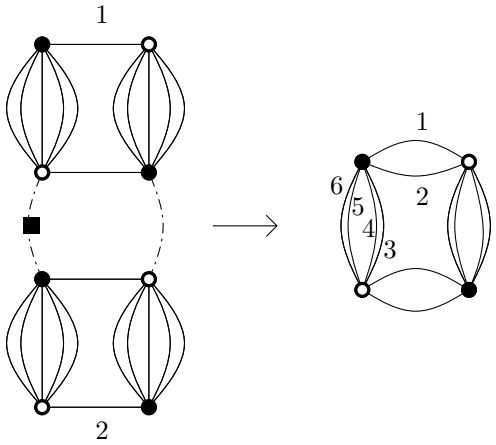

Figure 5.3: Connecting structure of the interactions 5.1c with $i \neq j$

Of all the possible interactions, only those of type 5.1a and 5.1c with $i = j$, and 5.1b with $i \neq j$, respect the connectivity of the original melonic interaction. Therefore, we retain only such terms for the computation of $\partial_s \lambda_s$, i.e. we make the approximation

$$\begin{aligned}\mathrm{Sym}\mathcal{W}_{\vec{p},\vec{p}',\vec{p}_1,\vec{p}_2}\mathrm{Sym}\mathcal{W}_{\vec{p}',\vec{p},\vec{p}_3,\vec{p}_4} \simeq \sum_{i=1}^{d}\Bigg[&\mathcal{W}^{(i)}_{\vec{p},\vec{p}',\vec{p}_1,\vec{p}_2}\mathcal{W}^{(i)}_{\vec{p}',\vec{p},\vec{p}_3,\vec{p}_4} + \mathcal{W}^{(i)}_{\vec{p}_1,\vec{p}',\vec{p},\vec{p}_2}\mathcal{W}^{(i)}_{\vec{p}_3,\vec{p},\vec{p}',\vec{p}_4} \\ &+ \mathcal{W}^{(i)}_{\vec{p},\vec{p}',\vec{p}_1,\vec{p}_2}\sum_{j\neq i}\mathcal{W}^{(j)}_{\vec{p}_3,\vec{p},\vec{p}',\vec{p}_4}\Bigg] \\ =:& \left(\bar{\mathrm{Sym}}^2\mathcal{W}\right)_{\vec{p},\vec{p}',\vec{p}_1,\vec{p}_2,\vec{p}_3,\vec{p}_4},\end{aligned} \tag{5.70}$$

after which we obtain the equation

$$\begin{aligned}\partial_s\lambda_s\,\mathcal{W}_{\vec{p}_1,\vec{p}_2,\vec{p}_3,\vec{p}_4}T_{\vec{p}_1}\bar{T}_{\vec{p}_2}T_{\vec{p}_3}\bar{T}_{\vec{p}_4} =& 4\lambda_s^2\sum_{\vec{p},\vec{p}'\in\mathcal{P}}\frac{\left(\partial_s Z_s(e^{2s}-\vec{p}^{\,2})+2Z_s e^{2s}\right)}{(Z_s e^{2s}+m_s^2)^3}\theta\left(e^{2s}-\vec{p}^{\,2}\right) \\ &\times\left(\bar{\mathrm{Sym}}^2\mathcal{W}\right)_{\vec{p},\vec{p}',\vec{p}_1,\vec{p}_2,\vec{p}_3,\vec{p}_4}T_{\vec{p}_1}\bar{T}_{\vec{p}_2}T_{\vec{p}_3}\bar{T}_{\vec{p}_4}.\end{aligned} \tag{5.71}$$

As before, we want to satisfy this equation to the desired order in $\vec{p}_i^{\,2}$, in this case meaning to zeroth order. The easiest way to accomplish that is to project the equation onto the field $T^{(0)}_{\vec{p}} = \prod_{i=1}^d \delta^0_{p_i}$, leading to the equation:

$$d\partial_s\lambda_s = 4\lambda_s^2\sum_{\vec{p},\,|\vec{p}|\leq e^s}\sum_{\vec{p}'}\frac{\left(\partial_s Z_s(e^{2s}-\vec{p}^{\,2})+2Z_s e^{2s}\right)}{(Z_s e^{2s}+m_s^2)^3}\times\delta\left(\sum_{i=1}^d p_i\right)\left(\bar{\mathrm{Sym}}^2\mathcal{W}\right)_{\vec{p},\vec{p}',\vec{0},\vec{0},\vec{0},\vec{0}}.$$

Taking into account the closure constraint $\sum_i p_i = 0$, we find $\mathcal{W}^{(i)}_{\vec{0},\vec{p},\vec{p}',\vec{0}} = \prod_{i=1}^d \delta^0_{p_i}\prod_{j=1}^d \delta_{p_j,p'_j}$ and $\mathcal{W}^{(i)}_{\vec{p},\vec{p}',\vec{0},\vec{0}} = \delta_{p_i,0}\delta\big(\sum_{j\neq i}p_j\big)\prod_{j=1}^d\delta_{p_j,p'_j}$, and as a consequence:

$$\delta\left(\sum_{i=1}^d p_i\right)\left(\bar{\mathrm{Sym}}^2\mathcal{W}\right)_{\vec{p},\vec{p}',\vec{0},\vec{0},\vec{0},\vec{0}} = \left(d^2\prod_{i=1}^d\delta^0_{p_i} + \sum_{i=1}^d\delta^0_{p_i}\delta\left(\sum_{j\neq i}p_j\right)\right)\delta_{\vec{p},\vec{p}'}. \tag{5.72}$$

As for the mass and anomalous dimension, the flow of λ_s can be expressed in terms of S_1 and S_2, defined in (5.55) and (5.56), giving

$$\partial_s \lambda_s = 4\lambda_s^2 \frac{\Big(de^{2s} + e^{2s}S_1(0) - S_2(0)\Big)\partial_s Z_s + 2e^{2s}\Big(d + S_1(0)\Big)Z_s}{(Z_s e^{2s} + m_s^2)^3}, \tag{5.73}$$

or, in terms of the integral approximations (5.61) and (5.62):

$$\boxed{\partial_s \lambda_s = 4\lambda_s^2 \frac{\Big(de^{2s} + \frac{2}{d}\frac{\Omega_{d-2}}{\sqrt{d-1}}e^{ds}\Big)\partial_s Z_s + 2\Big(de^{2s} + \frac{\Omega_{d-2}}{\sqrt{d-1}}e^{ds}\Big)Z_s}{(Z_s e^{2s} + m_s^2)^3}.} \tag{5.74}$$

5.2.2 RG equations for dimensionless parameters

The RG flow equation obtained above describes the evolution of the couplings in our truncation with respect to the scale/time s. But, as in the quantum field theory or condensed matter models, a trivial contribution to the evolution comes from the dimension of the operator associated to these couplings. We define the dimensionless parameters $\bar{\lambda}_s$ and $\bar{m}_s$ as

$$\lambda_s = e^{(6-d)s}\bar{\lambda}_s, \qquad m_s = e^s \bar{m}_s, \tag{5.75}$$

using the results on the dimension of the local operators introduced in Section 1.2. The flow equations for the dimensionless couplings are easily deduce from the previous ones. The equation for η_s is unchanged, and the equations for λ_s and m_s become:

$$\partial_s \bar{m}_s^2 = -2\bar{m}_s^2 - 2\bar{\lambda}_s \frac{\Big(2\frac{\Omega_{d-2}}{\sqrt{d-1}} + de^{(2-d)s}\Big)\partial_s Z_s + 2d\Big(\frac{\Omega_{d-2}}{\sqrt{d-1}} + e^{(2-d)s}\Big)Z_s}{(Z_s + \bar{m}_s^2)^2},$$

$$\partial_s \bar{\lambda}_s = (d-6)\bar{\lambda}_s + 4\bar{\lambda}_s^2 \frac{\Big(d\,e^{(2-d)s} + \frac{2}{d}\frac{\Omega_{d-2}}{\sqrt{d-1}}\Big)\partial_s Z_s + 2\Big(d\,e^{(2-d)s} + \frac{\Omega_{d-2}}{\sqrt{d-1}}\Big)Z_s}{(Z_s + \bar{m}_s^2)^3}.$$

Another more physical redefinition concerns the relations between the different renormalization parameters. The couplings λ_s and m_s which appear in the original model are not the effective mass and effective coupling at the scale s. Indeed, the evolution of the wave function renormalization Z_s, from 1 to an arbitrary value, modifies the effective couplings, which become: $\bar{\lambda}_s = Z_s^2 \bar{\lambda}_s^r$, $\bar{m}_s = \sqrt{Z_s}\bar{m}_s^r$. Hence, from the two previous equations, we finally deduce:

$$\partial_s \bar{m}_s^{r\,2} = -2\Big(1 + \frac{\eta_s}{2}\Big)\bar{m}_s^{r\,2} - 2\bar{\lambda}_s^r \frac{\Big(2\frac{\Omega_{d-2}}{\sqrt{d-1}} + de^{(2-d)s}\Big)\eta_s + 2d\Big(\frac{\Omega_{d-2}}{\sqrt{d-1}} + e^{(2-d)s}\Big)}{(1 + \bar{m}_s^{r\,2})^2}, \tag{5.76}$$

$$\partial_s \bar{\lambda}_s^r = (d - 6 - 2\eta_s)\bar{\lambda}_s^r + 4\bar{\lambda}_s^{r\,2} \frac{\Big(d\,e^{(2-d)s} + \frac{2}{d}\frac{\Omega_{d-2}}{\sqrt{d-1}}\Big)\eta_s + 2\Big(d\,e^{(2-d)s} + \frac{\Omega_{d-2}}{\sqrt{d-1}}\Big)}{(1 + \bar{m}_s^{r\,2})^3}, \tag{5.77}$$

with:

$$\eta_s = \frac{2d(d-2)}{(d-1)^{3/2}} \frac{\Omega_{d-2}\bar{\lambda}_s^r}{(1 + \bar{m}_s^{r\,2})^2 - 2\bar{\lambda}_s^r\Big[\frac{d}{(d-1)^{3/2}}\Omega_{d-2} + de^{(2-d)s}\Big]}. \tag{5.78}$$

Note that, similarly to what was found in [10], the system of differential equations we just obtained is not autonomous, in the sense that even after switching to dimensionless couplings it maintains an explicit dependence on the RG scale s. This was interpreted in [10] (based on more general cases in which a similar phenomenon takes place, e.g. [23]) as consequence of the implicit scale set by the compactness of the group, i.e. the radius of $S^1 \simeq U(1)$, an interpretation corroborated by the recent results of [11], where autonomous equations are obtained in the non-compact limit $U(1) \to \mathbb{R}$.

In the next section we examine the flow equation in the large-s approximation, or in the UV limit. In this sector, the equations are much simpler, since they become autonomous, and thus it is possible to find fixed points, and their relevant or irrelevant perturbations.

5.2.3 Large s approximation, vicinity of the Gaussian fixed point

In the UV regime, corresponding to the large-s limit, the previous equations (5.76), (5.77), and (5.78), for $d > 2$, reduce to:

$$\partial_s \bar{m}_s^{r\,2} = -2\Big(1 + \frac{\eta_s}{2}\Big)\bar{m}_s^{r\,2} - 2\bar{\lambda}_s^r \frac{\Omega_{d-2}}{\sqrt{d-1}} \frac{2\eta_s + 2d}{(1+\bar{m}_s^{r\,2})^2}, \tag{5.79}$$

$$\partial_s \bar{\lambda}_s^r = (d - 6 - 2\eta_s)\bar{\lambda}_s^r + 4\bar{\lambda}_s^{r\,2} \frac{\Omega_{d-2}}{\sqrt{d-1}} \frac{\frac{2}{d}\eta_s + 2}{(1+\bar{m}_s^{r\,2})^3}, \tag{5.80}$$

$$\eta_s = \frac{2d(d-2)\Omega_{d-2}\bar{\lambda}_s^r}{(d-1)^{3/2}(1+\bar{m}_s^{r\,2})^2 - 2d\Omega_{d-2}\bar{\lambda}_s^r}. \tag{5.81}$$

Note that, unsurprisingly, only the melonic contributions survive in the large cut-off limit. These equation form an autonomous system, whose fixed points can be studied with standard methods. A trivial fixed point occurs for $m_s^r = \lambda_s^r = 0$, corresponding to the so-called Gaussian fixed point (GFP). In order to study the stability of this fixed point, we expand the previous RGEs around this fixed point, at second order in the coupling constant. We obtain the following system (we limit the development of η_s to the first order in λ_s, because the anomalous dimension appears always as a quantum correction):

$$\partial_s \bar{m}_s^{r\,2} = -2\bar{m}_s^{r\,2} + 2d\frac{\Omega_{d-2}}{\sqrt{d-1}}\frac{3d-2}{(d-1)}\bar{\lambda}_s^r\bar{m}_s^{r\,2} - 4d\frac{\Omega_{d-2}}{\sqrt{d-1}}\bar{\lambda}_s^r - \frac{8d(d-2)}{(d-1)^2}\Omega_{d-2}^2\bar{\lambda}_s^{r\,2} \tag{5.82}$$

$$\partial_s \bar{\lambda}_s^r = (d-6)\bar{\lambda}_s^r - 4\left[\frac{d(d-2)}{d-1} - 2\right]\frac{\Omega_{d-2}}{\sqrt{d-1}}\bar{\lambda}_s^{r\,2}, \tag{5.83}$$

$$\eta_s = \frac{2d(d-2)}{(d-1)^{3/2}}\Omega_{d-2}\bar{\lambda}_s^r. \tag{5.84}$$

At $d = 6$ the coupling $\bar{\lambda}_s^r$ becomes marginal, and using $\Omega_4 = \pi^2/2$ we obtain:

$$\partial_s \bar{m}_s^{r\,2} = -2\bar{m}_s^{r\,2} + \frac{96\pi^2}{5\sqrt{5}}\bar{\lambda}_s^r\bar{m}_s^{r\,2} - \frac{12}{\sqrt{5}}\pi^2\bar{\lambda}_s^r - \frac{48}{5\sqrt{5}}\pi^2\bar{\lambda}_s^{r\,2} \tag{5.85}$$

$$\partial_s \bar{\lambda}_s^r = -\frac{28\pi^2}{5\sqrt{5}}\bar{\lambda}_s^{r\,2}, \tag{5.86}$$

$$\eta_s = \frac{24\pi^2}{5\sqrt{5}}\bar{\lambda}_s^r. \tag{5.87}$$

Then, we recover the (perturbative) asymptotic freedom already obtained at the beginning of Chapter 4. We insist on the fact that it is not an accident, due to the choice of our regulator. A general argument, given in Appendix C.1 shows that the one-loop computation is *universal*, and therefore does not dependent on the choice of R_s.

For $d > 6$, the theory is perturbatively non-renormalizable, but the equations (5.82) and (5.83) show the existence of a non-trivial fixed point for $\bar{\lambda}_s$ and $\bar{m}$ at:

$$\bar{\lambda}^* = \frac{1}{4}\frac{(d-6)(d-1)^{3/2}}{(d^2-4d+2)\Omega_{d-2}}, \tag{5.88}$$

$$\bar{m}^{*2} = \frac{d(d-6)(d-1)}{d^2-4d+2}\,\frac{3d^2-16d+16}{d(d-6)(3d-2)-4(d^2-4d+2)}. \tag{5.89}$$

For $d = 6$ the fixed point merges with the GFP, and for small $\epsilon = d-6$ it occurs at small values of the couplings. Therefore the use of the expansion (5.82) and (5.83) is justified (but note that the mass grows rapidly and diverges at $d \simeq 6.65$). In order to analyze the stability of this fixed point, we compute the first derivative, at the point $(\bar{m}^{2\,*}, \bar{\lambda}^*) \equiv (g_1^*, g_2^*)$ of the functions β_i defined by (5.82) and (5.83), where the index i labels the couplings $(\bar{m}^{r\,2}, \bar{\lambda}^r) \equiv (g_1, g_2)$. These derivatives build the *stability matrix* $\beta_{ij}^* = \partial\beta_i(g^*)/\partial g_j$, whose expression for general d is not particularly enlightening. More important are its eigenvalues (which, up to a sign, correspond to the so-called *critical exponents*), which, at leading order in ϵ, are $-2+24\epsilon/7$ and $-\epsilon$, respectively, meaning that we have two relevant perturbations (an operator is said to be relevant if it becomes important in the IR limit, irrelevant if it disappears in the IR limit, and marginal for vanishing critical exponent). Therefore, for small $\epsilon > 0$ we have asymptotic safety. Whether this survives or not at $\epsilon = 1$ is a question that we shall not address here.

For $d = 6$, (5.82) and (5.83) admit only the GFP, and the stability matrix reads:

$$\beta_{ij}^{*\,diag} := \begin{pmatrix} -2 & -\frac{12\pi^2}{\sqrt{5}} \\ 0 & 0 \end{pmatrix}, \tag{5.90}$$

with eigenvalues $(-2, 0)$ (for the GFP the critical exponents coincide with the canonical dimension of the associated operators), and eigenvectors

$$h_1 = \begin{pmatrix} 1 \\ 0 \end{pmatrix}, \qquad h_2 = \begin{pmatrix} -\frac{6\pi^2}{\sqrt{5}} \\ 1 \end{pmatrix}. \tag{5.91}$$

The first direction is associated to a relevant operator (the mass), and the second one is marginal. To decide whether the marginal coupling is marginally relevant (i.e. asymptotically free) or marginally irrelevant (i.e. trivial) we have to go to the next order in the expansion, as we did in (5.86).

Rather than expanding (5.82) and (5.83) in powers of the couplings, the flow can be studied numerically, and this is the subject of the next section (for the case $d = 6$).

5.2.4 Non-Gaussian fixed point at d=6

At $d = 6$, the autonomous system (5.79), (5.80), (5.81) has other non trivial fixed points than the trivial GFP. After a simple analysis of the equations, we find two fixed points, for the values:

$$\{\bar{\lambda}^*_\pm, \bar{m}^*_\pm\} = \left\{ \frac{\sqrt{5}(43309 \mp 79\sqrt{1141})}{2135484\pi^2}, \frac{-175 \pm \sqrt{1141}}{234} \right\}. \tag{5.92}$$

As for the Gaussian fixed point, we can study the stability of these fixed points by computing the eigenvalues of the stability matrix, i.e. the critical exponents. Diagonalizing the stability matrix at the two fixed points, we find:

$$\beta^{(+)\,diag}_{ij} \approx \begin{pmatrix} 4.86 & 0 \\ 0 & -0.9 \end{pmatrix}, \tag{5.93}$$

$$\beta^{(-)\,diag}_{ij} \approx \begin{pmatrix} 262.8 & 0 \\ 0 & 7 \end{pmatrix}, \tag{5.94}$$

showing that the fixed point $\{\bar{\lambda}_{*+}, \bar{m}_{*+}\}$ has one relevant and one irrelevant direction, whereas the other one has only irrelevant directions.

The result is very similar to the one obtained in [10] for a TGFT of rank-3 without closure constraint. As for that model, we find the existence of non-trivial fixed points (one of which carrying one relevant eigen-direction) in the critical dimension at which the model is asymptotically free. Note that, as we have seen in Section 5.2.3, moving infinitesimally away from the critical dimension implies the loss of asymptotic freedom, but a new non-trivial fixed point emerges from the Gaussian one. Such merging or splitting of fixed points near the critical dimension are standard phenomena, but have nothing to do with the fixed points (5.92), which appear precisely at the critical dimension. On the contrary, this is not a standard phenomenon, and it has to be attributed to the non-local structure of the TGFT interaction.

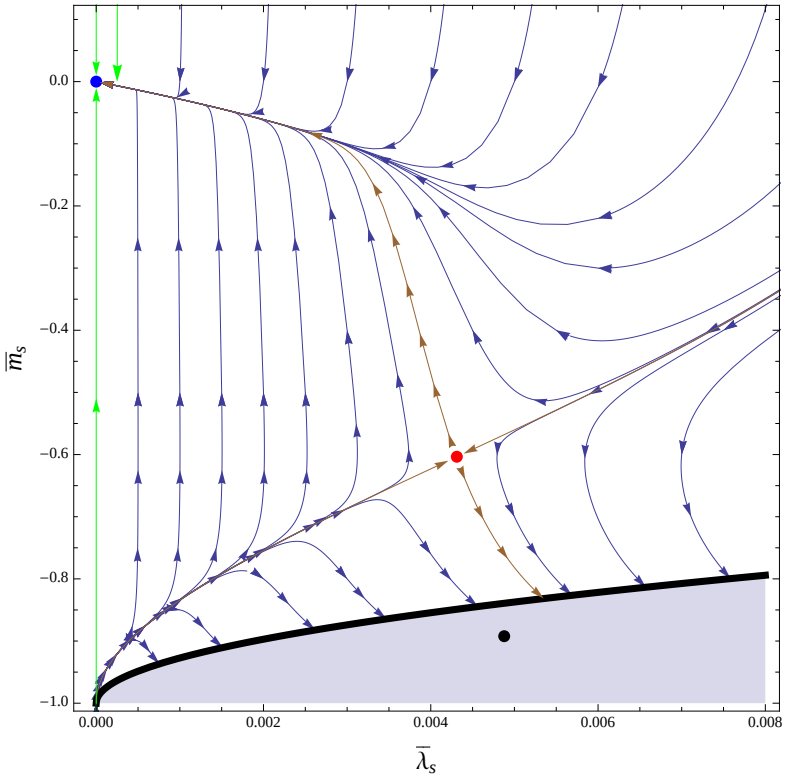

Figure 5.4: The flow diagram at large cutoff. The blue dot is the GFP, while the red and black are the non trivial ones, labelled with + and −, respectively. The black line corresponds to the singularity of the flow equations, which disconnects the shaded region from the GFP. In green and brown are respectively the eigen-perturbation for the GFP and the NGFP.

The numerical integration of the large-s flow leads to the phase diagram of Figure 5.4, which shows again a strong resemblance to the one found in [10]. Note that, due to our choice of truncation (5.31) and parametrization, and in particular due to the choice of the regulator (5.40), the flow equations (5.79), (5.80), and (5.81) have singularities at $\bar{\lambda}^r = 5^{3/2}(1+\bar{m}^{r\,2})^2/6\pi^2$. A similar singularity was found in [10], where its origin is discussed in more details. As a consequence of that singular line, the fixed point $\{\bar{\lambda}_{*-}, \bar{m}_{*-}\}$ is disconnected from $\{\bar{\lambda}_{*+}, \bar{m}_{*+}\}$ and the GFP.

The non-Gaussian fixed point $\{\bar{\lambda}_{*+}, \bar{m}_{*+}\}$ is a reminiscence of the Wilson-Fisher fixed point. It appears as an IR fixed point associated to a broken phase, with positive coupling and negative mass. More precisely, as discussed in [10], the region above the irrelevant trajectory at the NGFP can be interpreted as a symmetric phase, with coupling and mass of the same sign, and the region below this irrelevant trajectory has a broken phase, with negative mass and positive coupling.

Within the present truncation, our conclusion about the existence of such non-trivial fixed point is only valid in the large cutoff limit, i.e. in the UV limit. Therefore, the occurrence of a non-trivial behavior associated to the broken phase rests upon the survival of such fixed points in the IR, and this is why we need to look at the counterpart of the regime studied in this section, the small cutoff limit, in the next section.

Finally, computing the anomalous dimension for the two non-trivial fixed points, we find:

$$\eta_+ \approx 0.68, \qquad \eta_- \approx -7.27\ . \tag{5.95}$$

As a result, the qualitative criteria that we have discussed in the Section 5.2 seems to be failed. Indeed, it can be easily cheeked from equation 5.34 that, with $\eta_* = 0.68$, the truncation have to include interactions of valence six, which become essentials. Then, the dependence of our result on the choice of the truncation becomes unclear. We will return on this question in the next Chapter, where other pathological effects will occur.

5.2.5 Small-s limit

When the cutoff becomes very small, $e^s < 1$, all the sums in 5.2.1 reduce to a single element, the zero mode $\vec{p} = \vec{0}$. In this limit, for the sums defined in (5.55) and (5.56), we find $S_1 = 1$ and $S_2 = 0$, independently of $k < e^s$. Therefore, from equations (5.57), (5.58), and (5.73), we find that the anomalous dimension vanishes, implying that we are free to choose $Z_s = 1$, and that the beta function becomes, in $d = 6$:

$$\partial_s m_s^2 = -48\lambda_s \frac{e^{2s}}{(e^{2s}+m_s^2)^2}, \tag{5.96}$$

$$\partial_s \lambda_s = 56\lambda_s^2 \frac{e^{2s}}{(e^{2s}+m_s^2)^3}. \tag{5.97}$$

Using the rescaling $m_s = e^s \bar{m}_s$ and $\lambda_s = e^{4s}\bar{\lambda}_s$ leads to the following autonomous system:

$$\partial_s \bar{m}_s^2 = -2\bar{m}_s^2 - 48\frac{\bar{\lambda}_s}{(1+\bar{m}_s^2)^2}, \tag{5.98}$$

$$\partial_s \bar{\lambda}_s = -4\bar{\lambda}_s + 56\frac{\bar{\lambda}_s^2}{(1+\bar{m}_s^2)^3}. \tag{5.99}$$

In addition, as in the previous case, the system admits again a GFP, and a NGFP for the values:

$$\bar{\lambda}^* = \frac{49}{13718}, \qquad \bar{m}^* = -\frac{12}{19}. \tag{5.100}$$

In order to study the stability of these fixed points, we compute the matrix β_{ij} as before. For the Gaussian fixed point, we find:

$$\beta_{ij}^{GFP} = \begin{pmatrix} -2 & -48 \\ 0 & -4 \end{pmatrix}, \tag{5.101}$$

whose eigenvalues $(-4, -2)$ correspond to the two relevant eigen-directions.

For the non-Gaussian fixed point, we find the matrix:

$$\beta_{ij}^{NG} = \begin{pmatrix} \frac{34}{7} & -\frac{17328}{49} \\ -\frac{42}{361} & 4 \end{pmatrix}, \tag{5.102}$$

with eigenvalues $(76/7, -2)$, corresponding to one relevant and one irrelevant direction. As in the large s limit case, the numerical integration of these flow equations gives Figure 5.5 below.

Note that in this IR regime the rescaling for the mass and coupling constant does not correspond to the canonical one defined in Section 5.1.2. Again, this is a consequence of the fact that at small s our model is essentially a zero dimensional field theory, and our rescaling matches exactly with the one expected for such a theory, by fixing to zero the dimension of the (effective) action, and to 1 the dimension of the mass parameter. Indeed, by direct inspection of our truncation (5.31), we find $[\lambda] = 4$. This is an essential indication of the symmetric phase restoration in our model, as ultimately expected for a field theory on a compact space. Indeed phase transitions strictly speaking only occur in an infinite volume limit[7]. that is in the *thermodynamic limit* or, in other words, for a non-compact manifold. This limit, in our case, can be approached by restoring in our expressions the radius L of $S^1 \simeq U(1)$, here always fixed to 1, and by sending this radius to infinity. Such a non-compact limit has been recently studied in [11], confirming that in this limit we recover a picture identical to the large-s regime, and thus a non-trivial phase transition.

We have not extended our results in the intermediate cutoff regime, between small and large cutoff, but the two asymptotic regimes being qualitatively very similar to the ones in [10], we expect the intermediate regime to add no new qualitative insight with respect to the analysis performed there.

[7]For a related discussion on effective dimensional reduction and symmetry restoration see also [26].

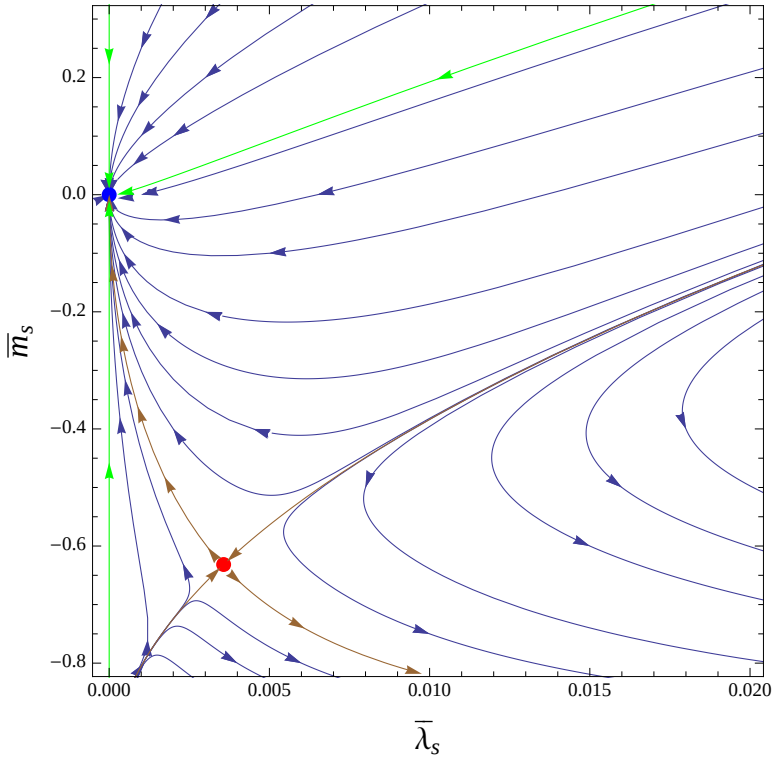

Figure 5.5: The flow diagram at small cutoff. The color rules are the same as in Figure 5.4. Ordinary trajectories are in blue, eigen-perturbations of the GFP are in green, and eigen-perturbation of the NGFP are in brown.

5.3 Discussion

Among the many results obtained with the renormalization group, two of the most famous are certainly the asymptotic freedom of QCD and the non-trivial IR behavior of scalar field theories below the critical dimension, due to the presence of a Wilson-Fisher fixed point. However, the two phenomena are hard to find in the same system: the non-trivial IR behavior of QCD is due to confinement, not to an IR fixed point, and the marginal couplings of scalar field theories do not go to zero in the UV, running instead into Landau poles. One example of coexistence is provided by gauge theories with N_f massless fermions, with N_f close to the critical number above which asymptotic freedom is lost: in such cases we find the so-called Banks-Zaks fixed point [1]. However, such a fixed point is not a generic feature of gauge theories, it exists only for a restricted "fine-tuned" range of parameters. The result obtained in this chapter is interesting in this respect, since it provides an explicit example of coexistence of asymptotic freedom with a Wilson-Fisher fixed point. Moreover it is quite general, as this coexistence has been stressed for other TFGTs, for instance in [10].

For quantum gravity, the main lessons of this non-perturbative analysis can be summarized as follows. First, we have shown that the presence of the closure constraint can be incorporated in the FRG formalism without too much pain. We have thus obtained a Wetterich equation for this class of TGFTs.

Second, in the UV limit, we have found a non-Gaussian fixed point, of which we have studied the stability, and identified the critical directions. Interestingly, this non-trivial fixed point has qualitatively similar characteristics as the Wilson-Fisher one, and is associated to a phase

transition in the flow diagram.

Lastly, in the IR sector, due to the compactness of the group manifold, we have obtained an effective zero-dimensional theory, with symmetry restoration in the deep IR. This is not surprising, given the compact nature of the manifold. The compactness of space can be seen as an additional regularization, to be removed in order to study the non-compact limit [11], or otherwise we can see the latter as the UV approximation, as we did here. In the non-compact limit we are left with just the large-s regime of the analysis (because $s = \ln(kL)$, if L is the radius of S^1 and k the dimensionful RG scale), and thus with a non-trivial IR fixed point associated to a phase transition between a broken and a symmetric phase.

Overall, the above picture is strikingly similar to the one obtained in [10], and in part to the one in [11], despite the models having essential differences. The model in [10] is in three dimensions, whereas our is in six; the model in [10] has no closure constraint, whereas our does; and the model in [10] has a kinetic term linear in momentum, whereas our is quadratic. These are all important differences. Nevertheless the fact that the final result is so similar points towards the conclusion that the non-local tensorial melonic nature of the interaction is the most important feature responsible for this similarity between the two models. We are therefore tempted to conjecture that renormalizable TGFTs with melonic quartic interactions enjoy in quite some generality not only asymptotic freedom, but also a Wilson-Fisher-like fixed point. Of course, the approximation we used here is the simplest one, and making our result more solid will require to study larger truncations. Also more models should be studied in order to understand whether our conjecture applies to all asymptotically free TGFTs or only to some specific sub-class. Grasping also at a more qualitative level how this common feature arises is also an open question. Ideally we should try to relate it to some kind of universal argument just as asymptotic freedom in quartic TGFTs was understood to simply arise from the combinatorics of wave function versus coupling constant renormalization in [29]). We are just at the beginning of the FRG investigations of TGFTs and hopefully these and other aspects will be clarified soon. The models that we study in the rest of this thesis already allow to identify some general aspects. However, some additional material seems to be required to come to the claim that "there exists a Wilson-Fisher fixed point" and to make it a solid result. For the original Wilson-Fisher fixed point, the claim is supported by a ϵ-expansion, which allows to keep control on the distance between the non-trivial fixed-point and the Gaussian one. More concretely, the expansion of the beta function for the coupling g of the ϕ^4-theory leads to:

$$\beta(g) = -\epsilon g + \frac{3}{16\pi^2} g^2 + \mathcal{O}(g^3, \epsilon g^2) \,, \tag{5.103}$$

which shows a fixed point for $g^* = 16\pi^2\epsilon/3$. Unfortunately, in the TGFT context, such an expansion is yet unknown. But a promising way to investigate this question is based on a modification of the propagator so that the coupling constant remains marginal in any dimension [28]. The hope is that such a modified theory may have a well-defined $1/d$ expansion, allowing to gain control over the distance between fixed points, as in the standard ϵ-expansion.

Appendix C

Universality of the one-loop beta function

In this section we review a well-known argument explaining why the one-loop beta function does not depend on the choice of the regularization, and we give an explicit example of this result for the computation of the beta function for T_6^4 with the FRG method around the Gaussian fixed point using a different regulator than the one used in the main part of the paper. Note that a similar regulation will be used in the next chapter for a non-Abelian TGFT.

C.1 A standard argument for one-loop universality

Different computational schemes result from physical predictions being made in terms of different couplings. Suppose that in some scheme we have a dimensionless coupling λ, whose flow equation reads

$$\partial_s \lambda = b_1 \lambda^2 + b_2 \lambda^3 + b_3 \lambda^4 + \dots \,. \tag{C.1}$$

In a different scheme we have a different coupling λ' with flow

$$\partial_s \lambda' = b'_1 \lambda'^2 + b'_2 \lambda'^3 + b'_3 \lambda'^4 + \dots \,. \tag{C.2}$$

At tree level the two couplings are the same, because tree level does not involve any ambiguity, thus the relation between the two couplings must be of the form

$$\lambda' = \lambda + C_1 \lambda^2 + C_2 \lambda^3 + \dots \,. \tag{C.3}$$

Now write

$$\begin{aligned} \partial_s \lambda' &= \frac{\partial \lambda'}{\partial \lambda} \partial_t \lambda \\ &= (1 + 2C_1\lambda + 3C_2\lambda^2 + \dots)(b_1\lambda^2 + b_2\lambda^3 + b_3\lambda^4 + \dots) \\ &= b_1\lambda^2 + (2C_1 b_1 + b_2)\lambda^3 + (3C_2 b_1 + 2C_1 b_2 + b_3)\lambda^4 + \dots \\ &= b_1\lambda'^2 + b_2\lambda'^3 + (b_3 - 2C_1 b_2 - C_1^2 b_1 + C_2 b_1)\lambda'^4 + \dots \,, \end{aligned} \tag{C.4}$$

where in the last row we used the inverse of (C.3),

$$\lambda = \lambda' - C_1 \lambda'^2 - (C_2 - 2C_1^2)\lambda'^3 + \dots \,, \tag{C.5}$$

and we assumed that $\partial_t C_1 = 0$. Therefore, under these assumptions, b_1 and b_2, i.e. the one- and two-loop coefficients of the beta function, are scheme independent.

Note that if $\partial_s C_1 \neq 0$, the flow of λ' is not autonomous, unless $C_1 = as + b$, or unless the s-dependence of C_1 is related to the beta function of another coupling. This is precisely what happens in general within the FRG, which is a mass-dependent renormalization scheme [27]. However, when expanding the beta functions around zero mass, the above argument must hold true also for the FRG.

C.2 Example with a different regulator

As we mentioned in section 5.2.3, the choice of a cutoff function corresponds to a choice of coarse graining scheme. Different choices thus affect the flow, but we expect that physical quantities, such as the critical exponents, will not depend on it. As we argued above, one such quantity is the one-loop coefficient of the beta function for the marginal coupling. To illustrate this point more explicitly, we choose here a different regulator:

$$R'_s(\vec{p}) = \frac{Z_s\vec{p}^2 + m_s^2}{\exp\left[\frac{Z_s\vec{p}^2+m_s^2}{Z_s e^{2s}}\right] - 1}, \tag{C.6}$$

and study the large cutoff limit ($s \gg 1$) of the flow equations around the Gaussian fixed point, in order to compare them with the ones obtained in section 5.2.3. At the leading order inλ_s, i.e. discarding the derivative of Z_s, the derivative of the regulator writes as:

$$\partial_s R'_s(\vec{p}) \simeq \frac{2}{e^{2s}Z_s}\left[\frac{Z_s\vec{p}^2 + m_s^2}{e^{(Z_s\vec{p}^2+m_s^2)/Z_s e^{2s}}}\right]^2 \left(1 - e^{-(Z_s\vec{p}^2+m_s^2)/Z_s e^{2s}}\right)^2. \tag{C.7}$$

Following the same procedure as in section 5.2.1, we find the three equations:

$$\partial_s m_s^2 \simeq -\frac{4\lambda_s}{Z_s}\sum_{\vec{p}\in\mathbb{Z}^6} e^{-2s} e^{-\frac{Z_s\vec{p}^2+m_s^2}{e^{2s}}} \delta\Big(\sum_i p_i\Big) \times \mathrm{Sym}\mathcal{W}_{\vec{p},\vec{p},\vec{0},\vec{0}}, \tag{C.8}$$

$$\partial_s Z_s \simeq -\frac{4\lambda_s}{Z_s}\frac{d}{dk^2}\left[\sum_{\vec{p}\in\mathbb{Z}^6} e^{-2s} e^{-\frac{Z_s\vec{p}^2+m_s^2}{e^{2s}}} \delta\Big(\sum_i p_i\Big) \times \mathrm{Sym}\mathcal{W}_{\vec{p},\vec{p},\vec{k},\vec{k}}\right]_{k=0}$$

$$\partial_s \lambda_s \simeq \frac{8\lambda_s^2}{Z_s e^{2s}}\sum_{\vec{p}\in\mathbb{Z}^6} \frac{e^{-\frac{Z_s\vec{p}^2+m_s^2}{Z_s e^{2s}}} - e^{-\frac{Z_s\vec{p}^2+m_s^2}{Z_s e^{2s}/2}}}{Z_s\vec{p}^2 + m_s^2} \delta_{p_i,0}\delta\Big(\sum_i p_i\Big). \tag{C.9}$$

For each of these equations the leading order can be easily extracted. Using the following sum formula

$$\begin{aligned}\sum_{n\in\mathbb{Z}} e^{-\alpha n^2} e^{i\beta n} &= \left(\frac{\pi}{\alpha}\right)^{1/2} \sum_{n\in\mathbb{Z}} e^{-\frac{|\beta+2\pi n|^2}{4\alpha}} \\ &= \left(\frac{\pi}{\alpha}\right)^{1/2} e^{-\frac{\beta^2}{4\alpha}} \left(1 + 2\sum_{n>0} e^{-\frac{\pi^2 n^2}{\alpha}} \cosh\left(\frac{\pi n\beta}{\alpha}\right)\right),\end{aligned} \tag{C.10}$$

the Fourier decomposition of $\delta\Big(\sum_i p_i\Big)$ and the distributional identity:

$$e^{-\beta^2/4\alpha} = \sum_n \frac{\sqrt{4\pi}}{n!}[\alpha^{1/2}]^{2n+1}\delta^{(2n)}(\beta), \tag{C.11}$$

we find:

$$\partial_s m_s^2 \simeq -\frac{24\pi^2}{\sqrt{5}}\frac{\lambda_s}{Z_s^2}e^{2s}, \tag{C.12}$$

$$\eta(s) \simeq \frac{24\pi^2}{5\sqrt{5}} \frac{\lambda_s}{Z_s^2}, \tag{C.13}$$

$$\partial_s \lambda_s \simeq \frac{4\pi^2}{\sqrt{5}} \frac{\lambda_s^2}{Z_s^2}. \tag{C.14}$$

Using both equations (C.13) and (C.14), we find for the effective coupling $\lambda_s/Z_s^2 := \lambda_s^r$:

$$\partial_s \lambda_s^r \simeq -\frac{28\pi^2}{5\sqrt{5}} \lambda_s^{r\,2}, \tag{C.15}$$

in agreement with our results of section 5.2.3, and with the universality argument.

Bibliography

[1] T. Banks and A. Zaks, "On the Phase Structure of Vector-Like Gauge Theories with Massless Fermions," Nucl. Phys. B **196**, 189 (1982).

[2] V. Rivasseau, "Quantum Gravity and Renormalization: The Tensor Track," AIP Conf. Proc. **1444**, 18 (2011) [arXiv:1112.5104 [hep-th]].

V. Rivasseau, "The Tensor Track: an Update," arXiv:1209.5284 [hep-th].

V. Rivasseau, "The Tensor Track, III," Fortsch. Phys. **62**, 81 (2014) [arXiv:1311.1461 [hep-th]].

[3] M. P. Reisenberger and C. Rovelli, "Space-time as a Feynman diagram: The Connection formulation," Class. Quant. Grav. **18**, 121 (2001) [gr-qc/0002095].

[4] B. Dittrich, "The continuum limit of loop quantum gravity - a framework for solving the theory," to appear in A. Ashtekar and J. Pullin ed., "100 Years of General Relativity", World Scientific [arXiv:1409.1450 [gr-qc]].

[5] D. Oriti, "Group field theory as the microscopic description of the quantum spacetime fluid: A New perspective on the continuum in quantum gravity," PoS QG **-PH**, 030 (2007) [arXiv:0710.3276 [gr-qc]].

[6] S. Gielen, D. Oriti and L. Sindoni, "Cosmology from Group Field Theory Formalism for Quantum Gravity," Phys. Rev. Lett. **111** (2013) 3, 031301 [arXiv:1303.3576 [gr-qc]].

[7] S. Gielen, D. Oriti and L. Sindoni, "Homogeneous cosmologies as group field theory condensates," JHEP **1406** (2014) 013 [arXiv:1311.1238 [gr-qc]].

[8] T. Delepouve and R. Gurau, "Phase Transition in Tensor Models," JHEP **1506**, 178 (2015) [arXiv:1504.05745 [hep-th]].

[9] D. Benedetti and R. Gurau, "Symmetry breaking in tensor models," arXiv:1506.08542 [hep-th].

[10] D. Benedetti, J. Ben Geloun and D. Oriti, "Functional Renormalisation Group Approach for Tensorial Group Field Theory: a Rank-3 Model," JHEP **1503**, 084 (2015) [arXiv:1411.3180 [hep-th]].

[11] J. Ben Geloun, R. Martini and D. Oriti, "Functional Renormalisation Group analysis of a Tensorial Group Field Theory on $\mathbb{R}^3$," arXiv:1508.01855 [hep-th].

[12] S. Carrozza, "Group field theory in dimension $4 - \epsilon$," Phys. Rev. D **91**, 065023 (2015) [arXiv:1411.5385 [hep-th]].

[13] J. Berges, N. Tetradis and C. Wetterich, "Nonperturbative renormalization flow in quantum field theory and statistical physics," Phys. Rept. **363**, 223 (2002) [hep-ph/0005122].

[14] C. Bagnuls and C. Bervillier, "Exact renormalization group equations. An Introductory review," Phys. Rept. **348**, 91 (2001) [hep-th/0002034].

[15] B. Delamotte, "An introduction to the nonperturbative renormalization group," Lect. Notes Phys. **852**, 49 (2012) [arXiv:cond-mat/0702365].

[16] O. J. Rosten, "Fundamentals of the Exact Renormalization Group," Phys. Rept. **511**, 177 (2012) [arXiv:1003.1366 [hep-th]].

[17] J. P. Blaizot, "Nonperturbative renormalization group and Bose-Einstein condensation," Lect. Notes Phys. **852**, 1 (2012) [arXiv:0801.0009].

[18] H. Gies, "Introduction to the functional RG and applications to gauge theories," Lect. Notes Phys. **852**, 287 (2012) [arXiv:hep-ph/0611146].

[19] M. Reuter and F. Saueressig, "Quantum Einstein Gravity," New J. Phys. **14**, 055022 (2012) [arXiv:1202.2274].

[20] C. Wetterich, "Exact evolution equation for the effective potential," Phys. Lett. B **301**, 90 (1993).

[21] T. R. Morris, "The Exact renormalization group and approximate solutions," Int. J. Mod. Phys. A **9**, 2411 (1994) [hep-ph/9308265].

[22] A. Eichhorn and T. Koslowski, "Continuum limit in matrix models for quantum gravity from the Functional Renormalization Group," Phys. Rev. D **88**, 084016 (2013) [arXiv:1309.1690 [gr-qc]].

A. Eichhorn and T. Koslowski, "Towards phase transitions between discrete and continuum quantum spacetime from the Renormalization Group," Phys. Rev. D **90**, no. 10, 104039 (2014) [arXiv:1408.4127 [gr-qc]].

[23] D. Benedetti, "Critical behavior in spherical and hyperbolic spaces," J. Stat. Mech. **1501** (2015) 1, P01002 [arXiv:1403.6712 [cond-mat.stat-mech]].

[24] D. F. Litim, "Optimized renormalization group flows," Phys. Rev. D **64**, 105007 (2001) [hep-th/0103195].

[25] L. Canet, B. Delamotte, D. Mouhanna and J. Vidal, "Nonperturbative renormalization group approach to the Ising model: A Derivative expansion at order ∂^4," Phys. Rev. B **68**, 064421 (2003) [hep-th/0302227].

[26] M. Guilleux and J. Serreau, "Quantum scalar fields in de Sitter space from the nonperturbative renormalization group," arXiv:1506.06183 [hep-th].

[27] A. Codello, M. Demmel and O. Zanusso, "Scheme dependence and universality in the functional renormalization group," Phys. Rev. D **90**, 027701 (2014) [arXiv:1310.7625 [hep-th]].

[28] D. Benedetti and V. Lahoche, "$1/d$-expansion for TGFT without closure constraint", [In preparation].

[29] V. Rivasseau, "Why are tensor field theories asymptotically free?", arXiv: 507.04190v1.

Chapter 6

Flowing rank-3 TGFTs in the UV

In this chapter, we address the issue of the non-perturbative technique developed in the previous chapter for rank-3 TGFTs with Laplacian kinetic operator. It has been established that just-renormalizable models support group manifold of dimension 3 and 4, for which we can thinks about $SU(2)$ and $SU(2) \times U(1)$. These group manifolds, and in particular $SU(2)$, are interesting in a quantum gravity perspective, and the existence of just-renormalizable models is already an interesting point. However, as far as we know, we do not have for the moment any satisfactory physical understanding of this term in a quantum gravity perspective. Yet, the results of the previous chapter seem to be improving this situation, as shown by the occurrence of IR attractive fixed points with non-zero mass. Ultimately, in the deep IR, the effect of the Laplacian becomes irrelevant, and the theory becomes essentially ultralocal, as required for spin foams amplitudes. In this point of view, the Laplacian operator can be understood as a deep UV property of the GFT, needed for the UV completion but for which no quantum gravity interpretation is required. In this point of view, a non perturbative analysis is interesting in a physical perspective. But it is also interesting for another deep reason. The model based on the group manifold $SU(2)$, which is the most interesting, involves interactions of valence six. It has been studied in perturbation theory [1], and the beta functions as well as the qualitative picture of the phase space around the Gaussian fixed point have been obtained. In particular, the author of [1] shows that, despite the domination of the wave function renormalization, large domains of the phase space are incompatible with asymptotic freedom. As a result, the consistency of the theory in the UV is not guaranteed, as for the asymptotically free quartic models studied in Chapter 4. The natural question is then to investigate the existence of non-trivial fixed points whose properties provide a natural UV completion, and make the theory at least *asymptotically safe*. Generally, this question is difficult, and requires non-perturbative methods. The problem is in fact very close to the situation in standard Euclidean field theory in dimension 3, and the most popular and simpler way to discuss the occurrence of non-Gaussian fixed points is to define a formal continuation in dimension $4-\epsilon$, interpolating between the ϕ^4 model in dimension 4 and the ϕ^6 model in dimension 3. The same trick has been used successfully in the TGFT context [2]. Indeed, defining an analytic continuation on the group manifold $SU(2) \times U(1)^{D-3}$ with respect to the parameter $\epsilon = 4 - D$, we interpolate between a quartic asymptotically free model and the ϕ^6 model for $D = 3$. The author of [2] shows that this ϵ-expansion implies the existence of a non-trivial fixed point very similar to the Wilson-Fisher fixed point, and suggests that the theory is indeed asymptotically safe. However, as for standard Euclidean field theory, this conclusion may be supported by a non-perturbative analysis, which is the aim of this chapter. The results that we shall discuss here rely primarily on [3, 4] (works in preparation), as well as on references [1, 2, 8], and on other yet unpublished results. In fact, we shall focus on the Abelian version

of the model, on $(U(1)^D)^{\times 3}$, the non-Abelian case being discussed in [3]. The interest of this approximation is essentially motivated by simplicity. Indeed, the Abelian version can be easily treated analytically using Litim's regulator. Moreover, the two versions of the theory have the same gauge invariance, the same interactions, and we claim that they are in the same *universality class*. This chapter is then essentially a spoiler of the results of the corresponding papers in preparation.

The organization of the chapter is the following. We start by a short overview of the classification of just-renormalizable models in dimension 3, which can be understood as an addendum to Chapter 4. Then, we move on to the quartic model in dimension $D = 4$, for which we deduce the flow equation in a quartic truncation, and show that the phase space has essentially the same structure as for the T_6^4 studied in Chapter 5. We then extend our flow equations into arbitrary dimension D, and perform an analytic continuation from $D = 4$ to $D = 3$. We show the occurrence of a new fixed point whose characteristics match with the ones obtained in the perturbative ϵ-expansion, and we show its persistence for large values of ϵ. Finally, we discuss the case $D = 3$ in a truncation around the marginal ϕ^6 interactions, and find non-trivial fixed points which both valid the ϵ-expansion and provide a new argument in favor of asymptotic safety. Note that we restrict our attention to the UV limit, essentially because we are ultimately interested by the UV completion of the theory.

6.1 Just-renormalizable models in dimension 3

The power counting Theorem obtained in Chapter 4 does not depend on the specific family of models that we have considered, and there are no reference to the specific form of the interactions in the proof. Moreover, this is also true for our conclusions about the leading order sector, and it is not hard to see [5, 6] that for any non-vacuum Feynman graph $\mathcal{G}$:

$$F(\mathcal{G}) - R(\mathcal{G}) = (d-2)(L(\mathcal{G}) - V(\mathcal{G}) + 1) + \rho(\mathcal{G}) \,, \tag{6.1}$$

where ρ is bounded by 0, for melonic graphs, and strictly negative when $\mathcal{G}$ is not melonic. A proof of this property can be found in [5, 6], but intuitively comes directly from the definition of melonic graphs. Indeed, after contraction of a spanning tree, the remaining $L - V + 1$ lines must be ordered such that each contraction of a line costs exactly $d-2$ (the contraction deletes $d-1$ internal faces, and decreases the rank by 1). Moreover, it is easy to check that this way is optimal, so that any deviation to the melonicity costs at least one unit at a given step with respect to the optimal configuration.

In full generalities, we consider a model with interactions of maximal valence $2p_{max}$. Then, the number of vertices of a graph $\mathcal{G}$ writes as: $V(\mathcal{G}) = \sum_{p=1}^{p_{max}} V_p(\mathcal{G})$, and using the topological relation :

$$2L(\mathcal{G}) = \sum_p 2pV_p(\mathcal{G}) - N(\mathcal{G}) \,, \tag{6.2}$$

where $N(\mathcal{G})$ denotes the number of external lines of $\mathcal{G}$, the divergent degree $\omega_{melo}(\mathcal{G})$ for the melonic graphs writes as:

$$\omega_{melo}(\mathcal{G}) = D(d-2) - \frac{N(\mathcal{G})}{2}[D(d-2)-2] + \sum_p [D(d-2)(p-1) - 2p]V_p \,. \tag{6.3}$$

We recall that for a renormalizable theory the power counting does not increase with the number of vertices. Setting $d = 3$, we find two just-renormalizable models with melonic interactions:

• For $D = 4$, with melonic interactions of maximal valence $p_{max} = 4$, of the same type as we have considered in Chapter 4.

• For $D = 3$, with melonic interaction of maximal valences $p_{max} = 6$.

The last category will be considered in Section 6.3. First we shall have a look at the quartic melonic model, as in Chapter 5. More precisely, we shall perform our analysis for arbitrary D, and we shall see that the resulting beta functions can be analytically continued to non-integer values of D. In a second time, we shall discuss a truncation up to melonic interactions of valence six for $D = 3$, and compare the fixed points with the analytic continuation in D.

The canonical dimension of the melonic interaction comes directly from the expression 6.1 as a simple extension of our discussion of Chapter 5. Hence, for arbitrary D and $d = 3$, the canonical dimension of the coupling λ_b, associated to a bubble b of valence n_b, is:

$$[\lambda_b] := D - \frac{n_b}{2}(D-2)\,. \tag{6.4}$$

Note that, as in standard quantum field theory, we recover that renormalizable interactions have positive or null dimensions.

6.2 FRG for Quartic model with $3 < D \leq 4$ in the deep UV

In this Section we discuss the application of the FRG method to the quartic model in dimension D. We shall see that the resulting system of differential equations supports an analytic continuation from $D = 4$ to $D = 3$, and we shall explore the behavior of the phase space between these two limits.

6.2.1 Truncation and β-functions

The theory has essentially the same structure as the one studied in Chapter 5, and we can transpose our method in this case. The first step is to choose a regulator and a truncation. In the notation of Chapters 4 and 5, we consider the IR Litim's regulator:

$$R_s(\vec{\mathbf{p}}) = Z(s)(e^{2s} - \vec{\mathbf{p}}^{\,2})\Theta(e^{2s} - \vec{\mathbf{p}}^{\,2})\,, \tag{6.5}$$

and the following truncation around the quartic melonic interactions:

$$\begin{aligned}\Gamma_s[\bar{T},T] = &\sum_{\vec{\mathbf{p}}\in\mathbb{Z}^{D\times d}} Z(s)\bar{T}_{\vec{\mathbf{p}}}\left(\vec{\mathbf{p}}^{\,2} + \bar{m}^2(s)e^{2s}\right)T_{\vec{\mathbf{p}}} \\ &+ e^{(4-D)s}Z^2(s)\bar{\lambda}_1(s)\sum_{\ell=1}^{3}\sum_{\{\vec{\mathbf{p}}_i\}}\sum_{i=1,\dots,4}\mathcal{W}^{(\ell)}_{\vec{\mathbf{p}}_1,\vec{\mathbf{p}}_2,\vec{\mathbf{p}}_3,\vec{\mathbf{p}}_4}T_{\vec{\mathbf{p}}_1}\bar{T}_{\vec{\mathbf{p}}_2}T_{\vec{\mathbf{p}}_3}\bar{T}_{\vec{\mathbf{p}}_4}\,,\end{aligned} \tag{6.6}$$

in which we used the dimensionless renormalized couplings $\bar{m}^2(s)$ and $\bar{\lambda}_1$ instead of the bare couplings. Except for the dimension of the group manifold and the value of the rank of the

tensors, the *Wetterich equation* derived in the previous chapter remains structurally unchanged:

$$\partial_s \Gamma_s = \sum_{\vec{\mathbf{p}} \in \mathbb{Z}^{3D}} \partial_k R_k(|\vec{\mathbf{p}}|) \cdot \left[\Gamma_k^{(2)} + R_s\right]^{-1}(\vec{\mathbf{p}}, \vec{\mathbf{p}}) \delta\Big(\sum_{i=1}^{3} \mathbf{p}_i\Big) \,. \tag{6.7}$$

Thus, our results of Chapter 5 can be directly translated in this case with minor modifications. We recall that, in the UV limit, which is the sector in which we focus in this chapter, only the melonic diagrams are relevant. Then, in the same notations as in the previous chapter, we find:

$$(\partial_s + 2 + \eta(s))\bar{m}^s = -6\bar{\lambda}(s) e^{-(2+D)s} \frac{\eta(s)[S_1(0)e^{2s} - S_2(0)] + 2S_1(0)e^{2s}}{(1+\bar{m}^2(s))^2} \,, \tag{6.8}$$

$$(\partial_s + 4 - D + 2\eta(s))\bar{\lambda} = 4\bar{\lambda}^2(s) e^{-(2+D)s} \frac{\eta(s)[S_1(0)e^{2s} - S_2(0)] + 2S_1(0)e^{2s}}{(1+\bar{m}^2(s))^3} \,, \tag{6.9}$$

$$\eta(s) = -\frac{4\bar{\lambda} S_1'(0) e^{(2-D)s}}{(1+\bar{m}^2(s))^2 + 2\bar{\lambda} e^{-Ds}[S_1'(0)e^{2s} - S_2'(0)]} \,, \tag{6.10}$$

where the sums involved in these expressions are the following:

$$S_1(\mathbf{k}^2) = \sum_{\mathbf{p}_1, \mathbf{p}_2} \Theta(e^{2s} - \mathbf{p}_1^2 - \mathbf{p}_2^2 - \mathbf{k}^2) \delta(\mathbf{p}_1 + \mathbf{p}_2 + \mathbf{k}) \,, \tag{6.11}$$

$$S_2(\mathbf{k}^2) = \sum_{\mathbf{p}_1, \mathbf{p}_2} (\mathbf{p}_1^2 + \mathbf{p}_2^2 + \mathbf{k}^2) \Theta(e^{2s} - \mathbf{p}_1^2 - \mathbf{p}_2^2 - \mathbf{k}^2) \delta(\mathbf{p}_1 + \mathbf{p}_2 + \mathbf{k}) \,. \tag{6.12}$$

As announced in the first section and in the introduction, we shall limit our attention to the UV sector, in which the sums can be legally replaced by their integral approximations. Following the same strategy and in the same notations as in the previous chapter, it is not hard to find:

$$S_1(\vec{\mathbf{k}}^2) \approx I_1(\vec{\mathbf{k}}^2) := \frac{\Omega_D}{(\sqrt{2D})^D} \left(e^{2s} - \frac{2D+1}{2D}\mathbf{k}^2\right)^{D/2} \,, \tag{6.13}$$

$$S_2(\mathbf{k}^2) \approx I_2(\mathbf{k}^2) := I_1(\mathbf{k})\mathbf{k}^2 + \frac{\Omega_D}{(\sqrt{2D})^D} \frac{D}{D+2} \left(e^{2s} - \frac{2D+1}{2D}\mathbf{k}^2\right)^{\frac{D+2}{2}} \,, \tag{6.14}$$

leading to the autonomous system of differential equations:

$$\begin{cases} \beta_m &= -(2+\eta)\bar{m}^2 - \frac{12\Omega_D \bar{\lambda}}{(2D)^{D/2}} \frac{1+\frac{\eta}{2+D}}{(1+\bar{m}^2)^2} \,, \\ \beta_\lambda &= -(4-D+2\eta)\bar{\lambda} + \frac{8\Omega_D \bar{\lambda}^2}{(2D)^{D/2}} \frac{1+\frac{\eta}{2+D}}{(1+\bar{m}^2)^3} \,, \\ \eta &= \frac{2D+1}{(2D)^{D/2}} \frac{\Omega_D \bar{\lambda}}{(1+\bar{m}^2)^2 - 2\frac{\Omega_D}{(2D)^{D/2}}\bar{\lambda}} \,. \end{cases} \tag{6.15}$$

As announced, the beta functions are analytic functions which can be formally continued analytically to non-integer values. This is the starting point of the standard ϵ-expansion.

6.2.2 D=4: RG-flows and fixed points

We start our analysis by the case $D = 4$. In this case, our flow equations reduce to the following autonomous system:

$$\begin{cases} \beta_m & = -(2+\eta)\bar{m}^2 - \frac{\pi^2\bar{\lambda}}{64}\frac{6+\eta}{(1+\bar{m}^2)^2}\,, \\ \beta_\lambda & = -2\eta\bar{\lambda} + \frac{\pi^2\bar{\lambda}^2}{96}\frac{6+\eta}{(1+\bar{m}^2)^3}\,, \\ \eta(s) & = \frac{9}{128}\frac{\pi^2\bar{\lambda}}{(1+\bar{m}^2)^2 - \frac{\pi^2}{64}\bar{\lambda}}\,. \end{cases} \tag{6.16}$$

The behavior of the system is quite similar to the T_6^4 studied in the previous chapter. In particular, in addition to the trivial UV-stable Gaussian fixed point, we find two non-Gaussian fixed points, and one of them is reminiscent of the Wilson-Fisher fixed point.

• *Gaussian fixed point.* The previous system admits a trivial fixed point for the values $\bar{\lambda} = \bar{m} = 0$, around which it reduces to:

$$\begin{cases} \beta_m & \approx -2\bar{m}^2 - \frac{3\pi^2}{32}\bar{\lambda}\,, \\ \beta_\lambda & \approx -\frac{5\pi^2}{64}\bar{\lambda}^2\,, \\ \eta(s) & \approx \frac{9\pi^2}{128}\bar{\lambda}\,. \end{cases} \tag{6.17}$$

Hence, as for the model studied in Chapter 5, the Gaussian fixed point is UV-stable, and the model is perturbatively asymptotically free. Without surprise, the computation of the stability matrix β_{ij} shows that we have one relevant and one marginal direction, respectively for the eigenvalues -2 and 0. Moreover, note that we recover the values computed at the one-loop order at the beginning of Chapter 4, in accordance with the *universality argument* discussed in the Appendix of Chapter 5.

• *Non-Gaussian fixed points.* As spoiled before, in addition to the Gaussian fixed point, we have two non-Gaussian fixed points, for the values $(\bar{\lambda}, \bar{m}^2)$:

$$FP_1 \approx (0.32; -0.59) \qquad FP_2 \approx \mathrm{diag}(0.58; -0.80)\,. \tag{6.18}$$

The computation of the eigenvalues of their respective stability, which are the opposite values of the critical exponents, leads to:

$$\beta_{FP_1} \approx \mathrm{diag}(5.31, -2.24)\,, \qquad \beta_{FP_2} \approx (64, 82, 7.90)\,. \tag{6.19}$$

The fixed point FP_1 has then one relevant (UV-attractive) direction and one irrelevant (UV repulsive) direction, whereas the fixed point FP_2 has two irrelevant directions. Moreover, this fixed point is under the singularity line defined by the zeros of the denominator of the anomalous dimensions :$(1+\bar{m}^2)^2 - \frac{\pi^2}{64}\bar{\lambda} = 0$. The situation is then very reminiscent of the UV-behavior of the T_6^4 model. The system can be numerically integrated, providing the phase diagram pictured in Figure 6.1.

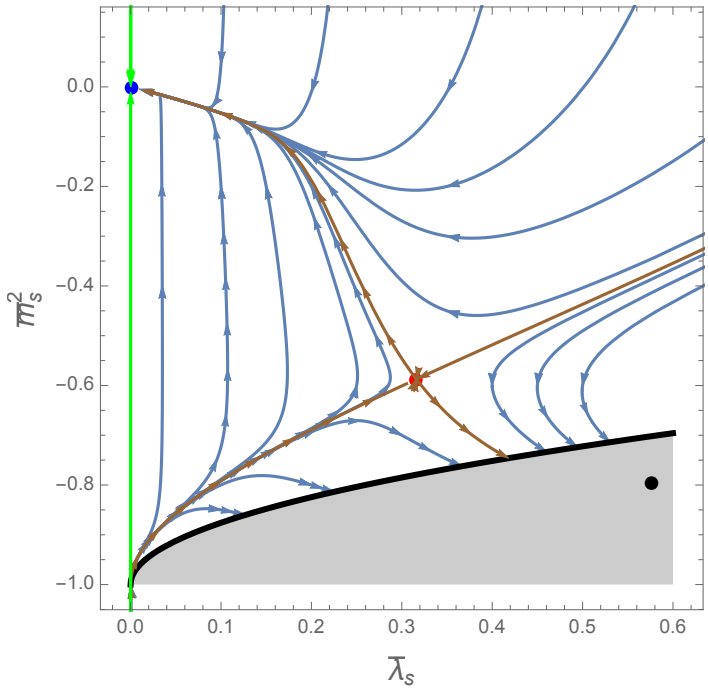

Figure 6.1: *Flow of the theory in the deep UV with* $D = 4$. The blue, red and black points are respectively the Gaussian fixed points, and the two non-Gaussian FP_1 and FP_2. The green and brown lines are respectively the eigenperturbations around the Gaussian and the FP_1 fixed points. The thick black line is the sigularity of the flow.

We recover in this case a *large river effect* [7], meaning that along the eigendirections connecting the three fixed points, the trajectories in a neighborhood of these eigendirections get closer and closer in the UV, and reach the corresponding fixed point. Then, the relevant directions of the non-Gaussian fixed point FP_1 appear as a critical surface separating the lines reaching the Gaussian fixed point of the lines reaching the singularity line. Once more, this scenario suggests a phase transition between a symmetric and a broken phase, with non-zero expectation value of the field operator. Finally, computing the value of the anomalous dimension, we find $\eta_{FP_1} \approx 1.80$. The effect of the neglected irrelevant couplings is then highly enhanced in the vicinity of this point.

6.2.3 Analytic continuation in D, from 4 to 3

We now move on to the essential purpose of this section, which is the study of the behavior of the analytic continuation in D, interpolating between $D = 3$ and $D = 4$. We introduce the interpolation parameter $\epsilon := 4 - D$. First, we can consider ϵ as an infinitesimal parameter, and perform a perturbative expansion both in the couplings and ϵ. The system 6.2.1 reduces to:

$$\begin{cases} \beta_m & \approx -2\bar{m}^2 - \frac{3\pi^2}{32}\bar{\lambda}\,, \\ \beta_\lambda & \approx -\epsilon\bar{\lambda} - \frac{5\pi^2}{64}\bar{\lambda}^2\,, \\ \eta(s) & \approx \frac{9\pi^2}{128}\bar{\lambda}\,. \end{cases} \tag{6.20}$$

As a result, in addition to the Gaussian fixed point, the flow equations admit a non-Gaussian fixed point, which occurs at the perturbative level for the values:

$$\bar{\lambda}_* = -\frac{64}{5\pi^2}\epsilon\,, \qquad \bar{m}_*^2 = \frac{3}{5}\epsilon\,, \tag{6.21}$$

leading to eigenvalues for the stability matrix:

$$\beta_* = \mathrm{diag}\left(-2 - \frac{3}{2}\epsilon, \epsilon \right). \tag{6.22}$$

Once again, the characteristics of this fixed point are quite similar to the Wilson-Fisher fixed point, and the qualitative phase diagram is pictured on Figure 6.2. We have one UV-attractive and one UV-repulsive direction, and the ϵ-expansion allows to keep an analytic control on the distance separating this fixed point from the Gaussian one. Moreover, the universality of the one-loop computations ensures that our conclusions do not depend on the choice of the regulator. The only particularity of this fixed point is that it has "wrong signs". The mass is positive, and the coupling $\bar{\lambda}$ is negative, a result which has already been pointed out by the author in [2]. This result may be pathological, because it breaks down the convergence of the path integral in the definition of the partition function. However, we note that our analytic continuation is highly formal, and no real models have non-integer values for D.

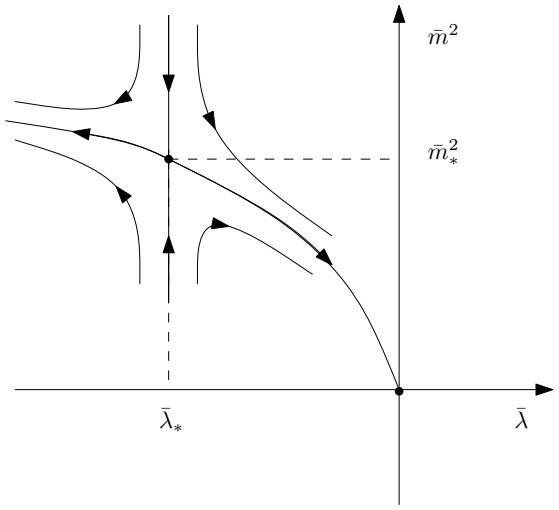

Figure 6.2: Qualitative phase space around the Gaussian fixed point for small ϵ.

More precisely, we are only interested by the continuity of the path from $\epsilon = 0$ to $\epsilon = 1$, and at this stage we have *a priori* no problem of convergence on the boundaries of this path. Indeed, for $\epsilon = 0$, the non-Gaussian fixed point disappears, and for $\epsilon = 1$, a negative value for $\bar{\lambda}$ is not necessarily a problem because the just-renormalizable truncation receives at least marginal interactions of valence six, which enforce the convergence of the path integral if their couplings are positive.

The FRG formalism allows to go beyond the ϵ-expansion, and to track the evolution of this new fixed point from $\epsilon = 0$ to $\epsilon = 1^-$. Figure 6.3 shows the phase space obtained by numerical integration for the values $D = 3.9$, $D = 3.5$ and $D = 3.1$. The new fixed point, that we call FP_3, deviates more and more from the Gaussian fixed point when we increase the value of ϵ, but the qualitative structure of the phase space remains unchanged.

Fixed Points	$\bar{\lambda}$	$\bar{m}^2$	η	θ^+	θ^-
$FP_1(D = 3.9)$	0.27	-0.60	1.75	-5.55	2.24
$FP_3(D = 3.9)$	-0.13	0.06	-0.09	2.26	-0.17
$FP_1(D = 3.5)$	0.14	-0.60	1.70	-6.62	2.24
$FP_3(D = 3.5)$	-0.69	0.38	-0.40	2.53	-0.34
$FP_1(D = 3.1)$	0.08	-0.61	1.35	-7.73	2.24
$FP_3(D = 3.1)$	-1.55	0.87	-0.67	2.71	-0.47

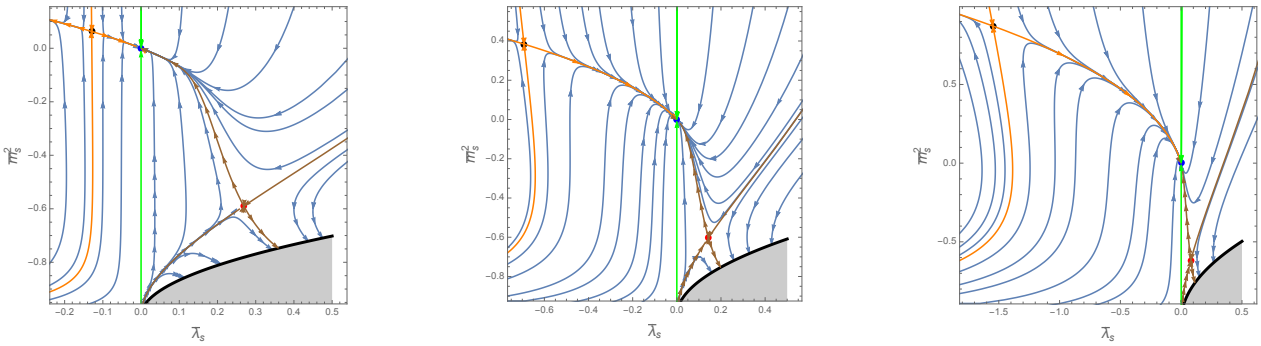

Figure 6.3: *From left to right: flow equation in the deep UV with* $D = 3.9, D = 3.5$, *and* $D = 3.1$. The black points correspond to the non-Gaussian fixed point FP_3, and the orange lines correspond to its eigenperturbations.

Figure 6.4: Summary of the properties of the non-Gaussian fixed points FP_1 and FP_3 for three values of the dimension D. The critical exponents $\theta^{\pm}$ are the opposite values of the eigenvalues of the stability matrix: $\beta_* =: \mathrm{diag}(-\theta_*^+, -\theta_*^-)$.

Again, our conclusions about phase transitions hold. We observe the splitting of the phase space in connected regions (i.e. which are not connected by any flow trajectory) separated by relevant eigenperturbations around the fixed points FP_1 and FP_3. We summarize the properties of the fixed points for the three values of D considered on Figure 6.3 and on Table 6.4.

6.3 RG-flows of the $D = 3$ model

6.3.1 Truncation and β-functions

With $D = 3$, we have to keep melonic interactions of valence six in order to make a truncation around marginal couplings. As a result, we consider a truncation of the form:

$$\begin{aligned}
\Gamma_s[\bar{T}, T] = &\sum_{\vec{\mathbf{p}}} Z(s)\Big(\vec{\mathbf{p}}^2 + e^{2s}\bar{m}^2(s)\Big) T_{\vec{\mathbf{p}}}\bar{T}_{\vec{\mathbf{p}}} \\
&+ Z^2(s)e^s\bar{\lambda}_4(s)\sum_{\ell=1}^{3}\sum_{\{\vec{\mathbf{p}}_i\}}\sum_{i=1,\dots,4} \mathcal{W}^{(\ell)}_{\vec{\mathbf{p}}_1,\vec{\mathbf{p}}_2,\vec{\mathbf{p}}_3,\vec{\mathbf{p}}_4} T_{\vec{\mathbf{p}}_1}\bar{T}_{\vec{\mathbf{p}}_2}T_{\vec{\mathbf{p}}_3}\bar{T}_{\vec{\mathbf{p}}_4} + \\
&+ Z^3(s)\bar{\lambda}_{6,1}(s)\sum_{\ell=1}^{3}\sum_{\{\vec{\mathbf{p}}_i\}}\sum_{i=1,\dots,6} \mathcal{X}^{(\ell)}_{\vec{\mathbf{p}}_1,\vec{\mathbf{p}}_2,\vec{\mathbf{p}}_3,\vec{\mathbf{p}}_4,\vec{\mathbf{p}}_5,\vec{\mathbf{p}}_6} T_{\vec{\mathbf{p}}_1}\bar{T}_{\vec{\mathbf{p}}_2}T_{\vec{\mathbf{p}}_3}\bar{T}_{\vec{\mathbf{p}}_4}T_{\vec{\mathbf{p}}_5}\bar{T}_{\vec{\mathbf{p}}_6} \\
&+ Z^3(s)\bar{\lambda}_{6,2}(s)\sum_{\ell=1}^{3}\sum_{\{\vec{\mathbf{p}}_i\}}\sum_{i=1,\dots,6} \mathcal{Y}^{(\ell)}_{\vec{\mathbf{p}}_1,\vec{\mathbf{p}}_2,\vec{\mathbf{p}}_3,\vec{\mathbf{p}}_4,\vec{\mathbf{p}}_5,\vec{\mathbf{p}}_6} T_{\vec{\mathbf{p}}_1}\bar{T}_{\vec{\mathbf{p}}_2}T_{\vec{\mathbf{p}}_3}\bar{T}_{\vec{\mathbf{p}}_4}T_{\vec{\mathbf{p}}_5}\bar{T}_{\vec{\mathbf{p}}_6}\,. \qquad (6.23)
\end{aligned}$$

The interaction bubbles involved in the action $\Gamma_s[\bar{T}, T]$ are associated to the following bubbles:

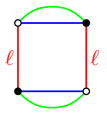

$$\longleftrightarrow \sum_{\{\vec{\mathbf{p}}_i\}\, i=1,\dots,4} \mathcal{W}^{(\ell)}_{\vec{\mathbf{p}}_1,\vec{\mathbf{p}}_2,\vec{\mathbf{p}}_3,\vec{\mathbf{p}}_4} T_{\vec{\mathbf{p}}_1} \bar{T}_{\vec{\mathbf{p}}_2} T_{\vec{\mathbf{p}}_3} \bar{T}_{\vec{\mathbf{p}}_4} \tag{6.24}$$

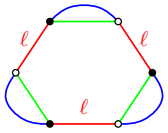

$$\longleftrightarrow \sum_{\{\vec{\mathbf{p}}_i\}\, i=1,\dots,6} \mathcal{X}^{(\ell)}_{\vec{\mathbf{p}}_1,\vec{\mathbf{p}}_2,\vec{\mathbf{p}}_3,\vec{\mathbf{p}}_4,\vec{\mathbf{p}}_5,\vec{\mathbf{p}}_6} T_{\vec{\mathbf{p}}_1} \bar{T}_{\vec{\mathbf{p}}_2} T_{\vec{\mathbf{p}}_3} \bar{T}_{\vec{\mathbf{p}}_4} T_{\vec{\mathbf{p}}_5} \bar{T}_{\vec{\mathbf{p}}_6} \tag{6.25}$$

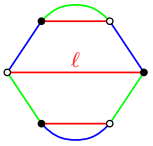

$$\longleftrightarrow \sum_{\{\vec{p}_i\}\, i=1,\dots,6} \mathcal{Y}^{(\ell)}_{\vec{\mathbf{p}}_1,\vec{\mathbf{p}}_2,\vec{\mathbf{p}}_3,\vec{\mathbf{p}}_4,\vec{\mathbf{p}}_5,\vec{\mathbf{p}}_6} T_{\vec{\mathbf{p}}_1} \bar{T}_{\vec{\mathbf{p}}_2} T_{\vec{\mathbf{p}}_3} \bar{T}_{\vec{\mathbf{p}}_4} T_{\vec{\mathbf{p}}_5} \bar{T}_{\vec{\mathbf{p}}_6}\,, \tag{6.26}$$

where the index ℓ runs from 1 to 3 and characterizes each bubble (up to automorphisms). Note that we have used the notations $\bar{\lambda}_4, \bar{\lambda}_{6,1}, \bar{\lambda}_{6,2}$ for the coupling constant, in accordance with the standard conventions in the literature. Moreover, for the rest of this chapter we shall freely substitute bubble drawings for the interactions they represent.

We have now all the material to move on to the extraction of the truncated flow equations for the couplings from the full Wetterich equation 6.2.1. We write the second derivative of Γ_s as:

$$\begin{aligned} \Gamma^{(2)}_s[\bar{T}, T](\vec{\mathbf{p}}, \vec{\mathbf{p}}') &= Z(s)\left(-\Delta + e^{2s}\bar{m}^2(s)\right)\hat{P}(\vec{\mathbf{p}}, \vec{\mathbf{p}}') \\ &\quad + F_{s,(1)}[\bar{T}, T](\vec{\mathbf{p}}, \vec{\mathbf{p}}') + F_{s,(2)}[\bar{T}, T](\vec{\mathbf{p}}, \vec{\mathbf{p}}')\,, \end{aligned} \tag{6.27}$$

in such a way that all the field-dependent terms of order $2n$ are in $F_{s,(n)}$, and where we have introduced:

$$\hat{P}(\vec{\mathbf{p}}, \vec{\mathbf{p}\prime}) := \delta\Big(\sum_{i=1}^{3} \mathbf{p}_i\Big) \prod_{i=1}^{d} \delta_{\mathbf{p}_i \mathbf{p}'_i}\,, \tag{6.28}$$

coming from the fact that the mean fields T and $\bar{T}$ involved in the truncation are assumed to be gauge invariant. We can pictorially represent them as:

$$F_{s,(1)}[\bar{T}, T](\mathbf{g}, \mathbf{g}') = 2Z(s)^2\, \lambda_4(k) \sum_{\ell=1}^{3}$$

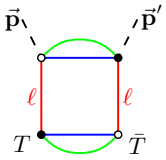

$$+ \cdots \tag{6.29}$$

and

$$F_{s,(2)}[\bar{T}, T](\vec{\mathbf{p}}, \vec{\mathbf{p}}') = 3Z(s)^3\, \lambda_{6,1}(s) \sum_{\ell=1}^{3}$$

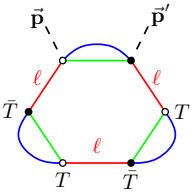

$$+ Z(s)^3\, \lambda_{6,2}(s) \sum_{\ell=1}^{3}$$

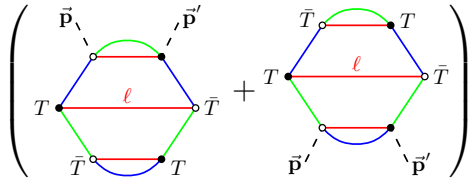

$$+ \cdots \tag{6.30}$$

where the external variables $\vec{\mathbf{p}}$ and $\vec{\mathbf{p}}'$ are represented as dashed half-lines, and will be traced over in the Wetterich equation. We furthermore only represented those diagrams which will eventually contribute in the large s limit, that is those which will yield melonic 1-loop Feynman graphs.

Expanding the right-hand side of the Wetterich equation (**??**), and denoting by $\Gamma_{s,(n)}$ the field-dependent terms of order $2n$ in our Ansatz (5.31), the identification of terms with the same order gives the following equations (in matricial notation):

$$\partial_s \Gamma_{s,(1)} = -\mathrm{Tr}\big[\partial_s R_s \mathcal{K}_s^{-1} F_{k,(1)} \mathcal{K}_s^{-1} \hat{P}\big]\,, \tag{6.31}$$

$$\partial_s \Gamma_{s,(2)} = -\mathrm{Tr}\big[\partial_s R_s \mathcal{K}_s^{-1} F_{s,(2)} \mathcal{K}_s^{-1} \hat{P}\big] + \mathrm{Tr}\big[\partial_s R_s \mathcal{K}_s^{-1} (F_{s,(1)} \mathcal{K}_s^{-1})^2 \hat{P}\big]\,, \tag{6.32}$$

$$\begin{aligned}\partial_s \Gamma_{s,(3)} = {} & \mathrm{Tr}\big[\partial_s R_s \mathcal{K}_s^{-1} F_{s,(1)} \mathcal{K}_s^{-1} F_{s,(2)} \mathcal{K}_s^{-1} \hat{P}\big] + \mathrm{Tr}\big[\partial_s R_s \mathcal{K}_s^{-1} F_{s,(2)} \mathcal{K}_k^{-1} F_{s,(1)} \mathcal{K}_s^{-1} \hat{P}\big] \\ & - \mathrm{Tr}\big[\partial_s R_s \mathcal{K}_s^{-1} (F_{s,(1)} \mathcal{K}_s^{-1})^3 \hat{P}\big]\,,\end{aligned} \tag{6.33}$$

where the operator $\mathcal{K}_s$ has been defined in the previous chapter:

$$\mathcal{K}_s(\vec{\mathbf{p}}, \vec{\mathbf{p}}') = \big[Z(s)(\vec{\mathbf{p}}^{\,2} + \bar{m}^2) + R_s(\vec{\mathbf{p}})\big]\delta_{\vec{\mathbf{p}}\vec{\mathbf{p}}'}\,. \tag{6.34}$$

We furthermore need to project back the right-hand side on the finite dimensional subspace corresponding to our ansatz, and identify terms according to their combinatorial structure. For instance, we have to extract the β-functions of both $\lambda_{6,1}$ and $\lambda_{6,2}$ from equation (**??**).

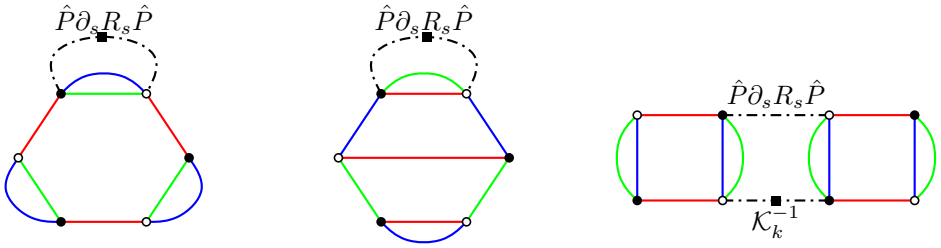

Figure 6.5: Typical melonic graphs contributing to the flow of λ_4.

The beta function β_m for the mass parameter, as well as the anomalous dimensions, receive only contributions of the quartic interactions, and their expressions remain unchanged. In the contrary, in addition to the contributions pictured on Figure 6.5c, the beta function β_{λ_4} receives contributions of the six-valent interactions, whose typical diagrams are pictured on Figure 6.5a and 6.5b. It is easy to see by contraction of the dotted lines that they have the same connectivity structure that a quartic interaction. As a result, in our graphical picture, we obtain the following equation for β_{λ_4}:

$$\partial_s \left(Z(s)^2 \frac{\lambda_4(s)}{2} \right) \sum_{\ell=1}^{3}$$

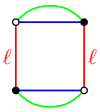

$$\approx -Z(s)^3\, \lambda_{6,1}(s) \sum_{\ell=1}^{3}$$

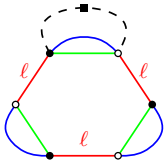

$$- Z(s)^3\, \lambda_{6,2}(s) \sum_{\ell=1}^{3}$$

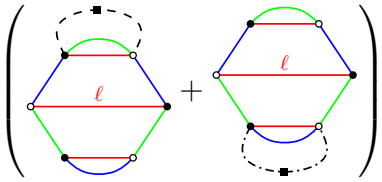

$$+ \big(Z(s)^2 \lambda_4(s)\big)^2 \sum_{\ell=1}^{3}$$

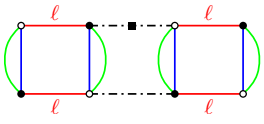

. (6.35)

Since we did not include any derivative coupling in our truncation, we need to evaluate each diagram appearing on the right-hand side at zeroth order in a Taylor expansion with respect to its external variables. The diagrams appearing in the first two lines of (6.35) have the same loop structure as the mass counter-terms computed in the previous subsection. Hence we may proceed identically. We find for instance:

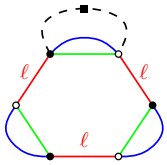

$$\approx \frac{1}{Z(s)} e^{-(2+D)s} \frac{\eta(s)[S_1(0)e^{2s} - S_2(0)] + 2S_1(0)e^{2s}}{(1+\bar{m}^2(s))^2} \times$$

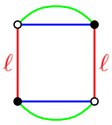

$$. \tag{6.36}$$

In the same way, listing all the melonic contractions contributing to the right-hand-sides of the equation 6.33, and separating the contractions with the connectivity of the interactions of type $6,1$ to the contractions with connectivity of the interactions of type $6,2$, we get:

$$\partial_k \left(Z(s)^3 \lambda_{6,2}(s) \right) \sum_{\ell=1}^{3}$$

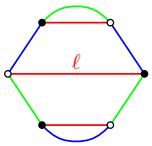

$$\approx 4Z(k)^5 \, \lambda_4(s) \lambda_{6,2}(s) \sum_{\ell=1}^{3}$$

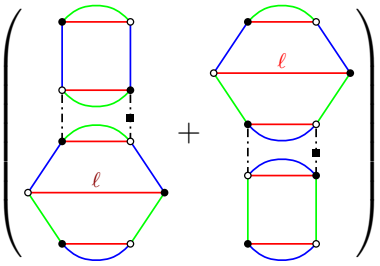

$$. \tag{6.37}$$

$$\partial_k \left(Z(s)^3 \lambda_{6,1}(s) \right) \sum_{\ell=1}^{3}$$

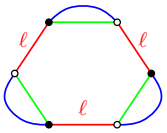

$$\approx 12 Z(s)^5 \, \lambda_4(k) \lambda_{6,1}(s) \sum_{\ell=1}^{3}$$

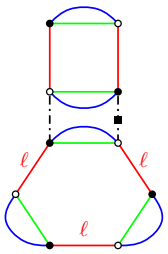

$$- Z(s)^6 \, \lambda_4(s)^3 \sum_{\ell=1}^{3}$$

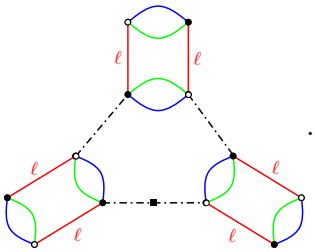

$$. \tag{6.38}$$

One more time, some local approximations of the diagrams appearing in the right-hand-side are known. This is in fact the case of all diagrams involving a loop of length 2, occurring in the computation of the beta function β_λ. For instance:

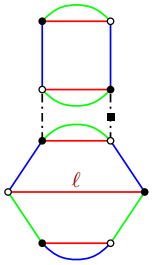

$$\approx \frac{1}{Z(s)^2} e^{-(2+D)s} \frac{\eta(s)[S_1(0)e^{2s} - S_2(0)] + 2S_1(0)e^{2s}}{(1+\bar{m}^2(s))^3} \times$$

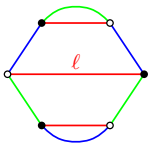

$$. \tag{6.39}$$

The real novelty is the appearance of diagrams with loop of length 3 in the right-hand-side of equation 6.38. Following the same method as for the loops of lengths one and two, we find:

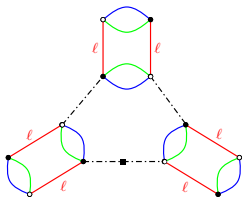

$$\approx \frac{1}{Z(s)^3} e^{-(2+D)s} \frac{\eta(s)[S_1(0)e^{2s} - S_2(0)] + 2S_1(0)e^{2s}}{(1+\bar{m}^2(s))^4} \times$$

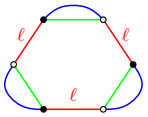

. (6.40)

To summarize, using the integral approximations for the sums, we find the autonomous system :

$$\begin{cases} \beta_m &= -(2+\eta)\bar{m}^2 - \sqrt{\frac{2}{3}}\frac{4\pi\bar{\lambda}}{15}\frac{5+\eta}{(1+\bar{m}^2)^2}\,, \\ \beta_{\lambda_4} &= -(1+2\eta)\bar{\lambda}_4 + \sqrt{\frac{2}{3}}\frac{8\pi\bar{\lambda}_4^2}{45}\frac{5+\eta}{(1+\bar{m}^2)^3} - \sqrt{\frac{2}{3}}\frac{2\pi(3\bar{\lambda}_{6,1}+2\bar{\lambda}_{6,2})}{45}\frac{5+\eta}{(1+\bar{m}^2)^3}\,, \\ \beta_{\lambda_{6,1}} &= -3\eta\bar{\lambda}_{6,1} - \sqrt{\frac{2}{3}}\frac{16\pi\bar{\lambda}_4^3}{45}\frac{5+\eta}{(1+\bar{m}^2)^4} + \sqrt{\frac{2}{3}}\frac{12\pi\bar{\lambda}_4\bar{\lambda}_{6,1}}{45}\frac{5+\eta}{(1+\bar{m}^2)^3}\,, \\ \beta_{\lambda_{6,2}} &= -3\eta\bar{\lambda}_{6,2} + \sqrt{\frac{2}{3}}\frac{8\pi\bar{\lambda}_4\bar{\lambda}_{6,2}}{45}\frac{5+\eta}{(1+\bar{m}^2)^3}\,, \end{cases} \tag{6.41}$$

where the anomalous dimension η is:

$$\eta(s) = \frac{7\sqrt{6}\pi}{27}\frac{\bar{\lambda}_4(s)}{(1+\bar{m}^2(s))^2 - \frac{2\pi\sqrt{6}}{27}\bar{\lambda}_4(s)}\,. \tag{6.42}$$

6.3.2 RG-flows and fixed points

As for the quartic melonic model, we shall study the behavior of the renormalization group equations 6.41. More precisely, we shall focus on the fixed point and the local characteristic of the flow in their vicinity.

• *Gaussian fixed points.* In the vicinity of the Gaussian fixed point, the system 6.41 reduces to:

$$\begin{cases} \beta_m &\approx -2\bar{m}^2 - \sqrt{\frac{2}{3}}\frac{4\pi\bar{\lambda}}{3}\,, \\ \beta_{\lambda_4} &\approx -\bar{\lambda}_4 - \sqrt{\frac{2}{3}}\frac{2\pi}{9}(3\bar{\lambda}_{6,1} + 2\bar{\lambda}_{6,2})\,, \\ \beta_{\lambda_{6,1}} &\approx -\pi\sqrt{\frac{2}{3}}\bar{\lambda}_4\bar{\lambda}_{6,1}\,, \\ \beta_{\lambda_{6,2}} &\approx -\frac{13\pi}{9}\sqrt{\frac{2}{3}}\bar{\lambda}_4\bar{\lambda}_{6,2}\,. \end{cases} \tag{6.43}$$

Interestingly, the system admits a non-trivial line of fixed points, of equation: $\bar{m} = \bar{\lambda}_4 = 0$, $\bar{\lambda}_{6,1} = -2/3\bar{\lambda}_{6,2}$. This line of fixed points is not a manifestation of the perturbative limit, because it occurs also in the non-perturbative system 6.41. However, such a line of fixed points is usually a pathological manifestation of the truncation rather than a real effect, which disappears when using a higher truncation. This analysis has been made for a similar model in dimension 5 [4], and the authors have pointed out the disappearance of the line of fixed points where interactions of valence 8 are taken into account in the truncation. For this reason, we ignore this line of fixed points in our current discussion. But the issue of this line of fixed points in the context of a non-Abelian rank-3 model will be discussed in [3], in preparation.

Returning to the system 6.43, we observe that all coefficients are positive. One more time, this is due, in particular for the terms in $\bar{\lambda}_4\bar{\lambda}_{6,1}$ and $\bar{\lambda}_4\bar{\lambda}_{6,2}$, to the enhancement of the anomalous

dimension which dominates the positive vertex contributions. However, as pointed out by the author in [1], despite the positivity of the coefficients, the model is not really asymptotically free. Indeed, we can easily find a trajectory which can approach arbitrarily close to the Gaussian fixed point, but which is ultimately repelled in the $e^s \to \infty$ limit. This phenomenon is extensively discussed in [1, 2] (for the non-Abelian version of this model, but the conclusion holds for the Abelian version). As an illustration, one can restrict our attention to the stable subspace $\bar{\lambda}_{6,2} = 0$[1]. The numerical integration of the system 6.43 is pictured on Figure 6.6, on the plane $(\bar{\lambda}_4, \bar{\lambda}_{6,1})$, and shows explicitly that there are no trajectories with $\bar{\lambda}_{6,1} > 0$ which are asymptotically free.

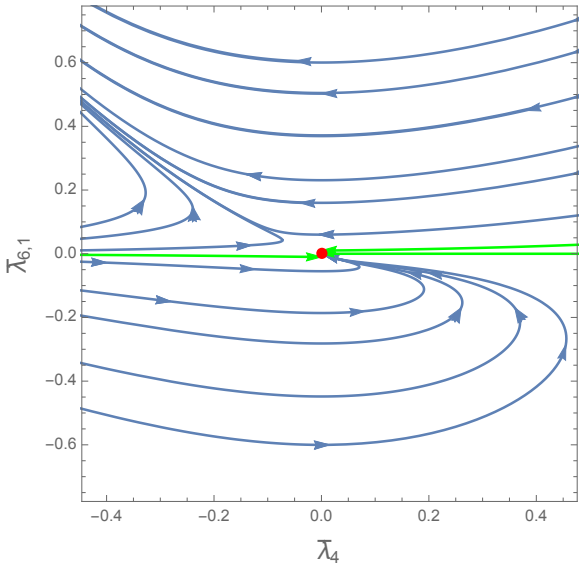

Figure 6.6: Numerical integration of the flow trajectories in the stable subspace $\bar{\lambda}_{6,2} = 0$.

This phenomenon is in fact quite common for the ϕ^6 interactions, for which the asymptotic freedom is complicated because of the back-reaction of the ϕ^4 super-renormalizable coupling. It has a non trivial influence on the flow of the ϕ^6 interaction.

• *Non-Gaussian fixed points.* The fact that a theory is not asymptotically free is not necessarily the end of the story. But the analysis of its consistency in the UV becomes a difficult question to investigate, and requires a non-perturbative analysis to show the existence of non-trivial fixed points. The standard ϵ-expansion is the simplest method, and the most popular to keep control over the distance between the Gaussian fixed point and the non-Gaussian one, and it allowa to use perturbative computations at small ϵ. Following [2], we have discussed such an ϵ-expansion for the quartic model in the previous section, and stressed a path from $D = 4$ to $D = 3$. In these considerations, we have found a fixed point with the same characterization as the Wilson-Fisher fixed point, up to a global sign. Even if it has the wrong sign, and if it survives in the limit $D = 3$, this fixed point may be nice for the UV completion of the theory. Indeed, the trajectories away from the Gaussian fixed point in Figure 6.6 reach a region with negative $\bar{\lambda}_4$, where we have found the fixed point in the ϵ-expansion. A strong argument in favor of this scenario is that we have shown that this fixed point survives to a non-perturbative analysis, for non-infinitesimal values of ϵ. But the most solid confirmation comes from the computation of the fixed points of the system 6.43. We find six fixed points (in addition to the Gaussian one and to the line of

[1]Note that, due to the form of the equation, it is obvious to see that the sign of the couplings $\bar{\lambda}_{6,i}\, i = 1, 2$ is invariant.

fixed points, which we discard of our analysis), whose properties are summarized in the Table 6.7 below.

Fixed Points	$\bar{\lambda}_{6,1}$	$\bar{\lambda}_{6,2}$	$\bar{\lambda}_4$	$\bar{m}^2$	η	θ^1	θ^2	θ^3	θ^4
FP_1	-0.71	0.	-0.43	-0.68	-5.90	-72.75	-16.44	-12.08	-5.03
FP_2	0.02	0.	0.02	-0.80	2.53	-6.87-59i	-6.87+59i	-7.93	0.30
FP_3	0.14	-0.18	0.07	-0.87	-6.5	-105.35	42.08	-18.0	-6.26
FP_4	-0.03	0.	0.09	-0.23	0.31	2.45	0.90	-0.70	0.49
FP_5	-1.62	0.	-2.69	1.26	-0.80	2.82	-2.14	-1.97	-0.47

Figure 6.7: Summary of the properties of the non-Gaussian fixed points for $D = 3$. Again, the critical exponents θ^i are the opposite values of the eigenvalues of the stability matrix: $\beta_* =: \mathrm{diag}(-\theta^1_*, -\theta^2_*, -\theta^3_*, -\theta^4_*)$.

Among all these fixed points, only FP_2, FP_4 and FP_5 give a positive value for $(1 + \bar{m}^2(s))^2 - \frac{2\pi\sqrt{6}}{27}\bar{\lambda}_4(s)$, the denominator of η. Among these three fixed points, FP_2 seems to be a novelty of the new terms in the truncation. It has three irrelevant and one relevant direction, and corresponds to an IR fixed point, with three dimensional separatrix (or IR-critical surface) spanned by the irrelevant directions. The two imaginary eigenvalues provide some oscillations for the trajectories in this sub-manifold, and the trajectories, repelled by the fixed point in the UV, make it a focal point. Once more, this picture suggests a phase transition in the IR.

The fixed points FP_4 and FP_5 however are very reminiscent of the non-Gaussian fixed points that we have called FP_1 and FP_3 in the previous section (see Table 6.4). In both cases, the values for $\bar{m}$ and λ_4 obtained for FP_4 and FP_5 are close to the ones obtained for $FP_1(D = 3.1)$ and $FP_3(D = 3.1)$ respectively. Moreover, the signs of the corresponding critical exponents are in agreement with this interpretation. This is especially true for the fixed point FP_5. As $FP2$, it corresponds to an IR fixed point, with three relevant directions and one irrelevant direction in the IR, suggesting a phase transition. Finally, for the fixed point FP_4 the sign of the second critical exponent is positive, and the value of the anomalous dimension is quite improved with respect to the previous truncation. It has three relevant directions in the UV. Then, the set of all points that flow towards the fixed point in the UV span a three dimensional UV-critical surface. This fixed point is interesting, and even if it does not correspond to the fixed point considered in the previous section, it seems to confirm our intuition concerning the UV completion of the theory. The critical surface has a controllable UV behavior, and is predictive, which corresponds to an asymptotically safe theory. One more time, however, the question of the bad sign of this fixed point holds. The problem could have been solved by the sign of the coupling $\bar{\lambda}_{6.1}$, but it has also the wrong sign. Note that it is also the case of the fixed point FP_5, and seems to be the sign of a failure of the truncation approximation, and a truncation with higher valence interactions could have positive couplings for these fixed points (if they resist to higher truncation!). At this stage, we can assert that the FRG method supports the perturbative argument about the UV completion of the theory, and we claim that:

Claim 1. *The rank-3 Abelian tensorial group field theory with Laplacian kinetic term and closure constraint is asymptotically safe in the UV.*

The discussion of the introduction of this Chapter seems to indicate that this property must be shared by the non-Abelian version. The fact that in the UV limit the non-commutative

structure of the group should not play an important role, and that this is essentially its dimension which is relevant is a strong argument which should be supported by a similar analysis for the non-Abelian case, currently in preparation.

Bibliography

[1] S. Carrozza, "Discrete Renormalization Group for SU(2) Tensorial Group Field Theory," Ann. Inst. Henri Poincaré Comb. Phys. Interact. 2 (2015), 49-112 doi:10.4171/AIHPD/15 [arXiv:1407.4615 [hep-th]].

[2] S. Carrozza, "Group field theory in dimension $4 - \epsilon$," Phys. Rev. D **91**, 065023 (2015) [arXiv:1411.5385 [hep-th]].

[3] S. Carrozza and V. Lahoche, "Functional renormalization group for a non-Abelian rank-3 Tensorial Group Field Theory in the deep UV", in preparation;

[4] D. Samary-Ousmane, V. Lahoche, "Functional renormalization group for the T_5^6 TGFT with closure constraint", in preparation;

[5] J. Ben Geloun, "Renormalizable Models in Rank $d \geq 2$ Tensorial Group Field Theory," Commun. Math. Phys. **332**, 117 (2014) doi:10.1007/s00220-014-2142-6 [arXiv:1306.1201 [hep-th]].

[6] S. Carrozza, D. Oriti and V. Rivasseau, "Renormalization of a SU(2) Tensorial Group Field Theory in Three Dimensions," Commun. Math. Phys. **330**, 581 (2014) doi:10.1007/s00220-014-1928-x [arXiv:1303.6772 [hep-th]].

[7] B. Delamotte, "An introduction to the nonperturbative renormalization group," Lect. Notes Phys. **852**, 49 (2012) [arXiv:cond-mat/0702365].

[8] J. Ben-Geloun, R. Martini and D. Oriti, "Functional Renormalization Group analysis of Tensorial Group Field Theories on $\mathbb{R}^d$", arXiv:1601.08211 [hep-th];

J. Ben-Geloun, T. A. Koslowski, "Nontrivial UV behavior of rank-4 tensor field models for quantum gravity", arXiv: 1606.04044 [gr-qc].

Chapter 7

Constructive methods for TGFTs

Constructive field theory is a set of techniques allowing to resum perturbative quantum field theory in order to obtain a rigorous definition of quantities such as Schwinger functions for interacting models [6]. The Loop Vertex Expansion (LVE) is such a constructive technique [7, 8, 9], improving the traditional constructive tools in order to treat more general models with non-local interactions and/or more general geometries. Following [10], it can be described as a reorganization of the perturbative series, combining an intermediate field decomposition with replicas and a forest formula. It allows to write the connected Schwinger functions as convergent sums indexed by spanning trees rather than as divergent sums indexed by Feynman graphs. Indeed a connected Schwinger function S is usually expanded in term of a Feynman series as

$$S = \sum_{\mathcal{G}} \mathcal{A}_{\mathcal{G}}, \tag{7.1}$$

where $\mathcal{A}_{\mathcal{G}}$ is the Feynman amplitude associated to the graph $\mathcal{G}$. However, even if each of these amplitudes is ultra-violet convergent, the sum is generally badly divergent, because of the very large number of graphs of large size. As a result the perturbative expansion has zero radius of convergence in the coupling(s), hence

$$\sum_{\mathcal{G}} |\mathcal{A}_{\mathcal{G}}| = \infty. \tag{7.2}$$

The LVE allows to circumvent this difficulty. The first step is to consider, for any pair made of a connected graph $\mathcal{G}$ and of a spanning tree $\mathcal{T} \subset \mathcal{G}$ in it, a universal *non trivial weight* $w(\mathcal{G}, \mathcal{T})$, which is the percentage of Hepp's sectors of G in which T is leading, in the sense of Kruskal *greedy algorithm* (see [10] for details). These weights, being by definition *percentages*, are normalized:

$$\sum_{\mathcal{T} \subset \mathcal{G}} w(\mathcal{G}, \mathcal{T}) = 1. \tag{7.3}$$

They allow to rewrite the Feynman expansion as a sum indexed by spanning trees:

$$S = \sum_{\mathcal{G}} \mathcal{A}_{\mathcal{G}} = \sum_{\mathcal{G}} \sum_{\mathcal{T} \subset \mathcal{G}} w(\mathcal{G}, \mathcal{T}) \mathcal{A}_{\mathcal{G}} = \sum_{\mathcal{T}} \mathcal{A}_{\mathcal{T}}, \tag{7.4}$$

where:

$$\mathcal{A}_{\mathcal{T}} := \sum_{\mathcal{G} \supset \mathcal{T}} w(\mathcal{G}, \mathcal{T}) \mathcal{A}_{\mathcal{G}}. \tag{7.5}$$

Since trees do not proliferate as fast as Feynman graphs, in good cases it can be shown that:

$$\sum_{\mathcal{T}} |\mathcal{A}_{\mathcal{T}}| < \infty \tag{7.6}$$

at least in a certain domain that we call the *summability domain*. Strictly speaking, such a program can be achieved with standard Feynman graphs only for Fermionic theories, because of the Pauli principle, since in that case amplitudes of same order combine into a determinant implying nice compensations [11]. Such compensations do not occur at fixed order for Bosonic theories, hence the sum (7.6) does not converge, even if it is repacked as a tree expansion. Fortunately the loop vertex expansion overcomes this difficulty by working in another representation, called intermediate field, or Hubbard-Stratonovic. This representation amounts to a clever exchange of the roles of propagators and vertices. The program summarized by equations (7.5)-(7.6) then works, but *for the graphs of the intermediate field representation*, and the corresponding sum (7.6) converges absolutely to the *Borel sum* of the initial expansion.

In this Chapter, based on research papers [4] and [5] we shall discuss constructive aspects for the Abelian T^4_d model with closure constraints. More precisely, we shall apply the Loop Vertex Expansion (LVE) to the T^4_3 and T^4_4 models, which are the two simplest non trivial models of rank 3 and 4, respectively UV-divergent free and super-renormalizable.

7.1 BKAR Forest formula and Borel summability

7.1.1 The "constructive swiss knife"

The BKAR (Brydges-Kennedy-Abdesselam-Rivasseau) forest interpolation formula [15], nicknamed the "constructive swiss knife", is the heart of the LVE. A forest formula expands a quantity defined on n points in terms of forests built on these points, and is a multi-variable Taylor expansion with integral remainder. There are in fact many forest formulas, but the BKAR formula seems to be the only one which is both *symmetric* under permutation of the n points and *positive* [7].

Let $[1, \cdots, n]$ be the finite set of points considered above. An edge l between two elements $i, j \in [1, \cdots, n]$ is a couple (i, j) for $1 \leq i < j \leq n$, and the set of such edges can be identified with the set of lines of K_n, the complete graph with n vertices. Consider the vector space S_n of $n \times n$ symmetric matrices, whose dimension is $n(n+1)/2$ and the *compact and convex* subset PS_n of *positive* symmetric matrices whose diagonal coefficients are all equal to 1, and off-diagonal elements are between 0 and 1. Any $X \in PS_n$ can be parametrized by $n(n-1)/2$ elements X_l, where l runs over the edges of the complete graph K_n [7]. Let us consider a smooth function f defined in the interior of PS_n with continuous extensions to PS_n itself. The BKAR forest formula states that:

Theorem 8. ***(The BKAR forest formula)***

$$f(\mathbf{1}) = \sum_{\mathcal{F}} \int dw_{\mathcal{F}} \partial_{\mathcal{F}} f[X^{\mathcal{F}}(w_{\mathcal{F}})] \tag{7.7}$$

where $\mathbf{1}$ *is the matrix with all entries equal to* 1*, and:*

• *The sum is over the forests $\mathcal{F}$ over n labeled vertices, including the empty forest.*

• *The integration over $dw_{\mathcal{F}}$ means integration from 0 to 1 over one parameter for each edge of the forest. Note that there are no integrations for the empty forest since by convention an empty product is 1.*

• *$\partial_{\mathcal{F}} := \prod_{l \in \mathcal{F}} \partial_l$ means a product of partial derivatives with respect to the variables X_l associated to the edge l of $\mathcal{F}$.*

• *The matrix $X^{\mathcal{F}}(w_{\mathcal{F}}) \in PS_n$ is such that $X^{\mathcal{F}}_{ii}(w_{\mathcal{F}}) = 1 \, \forall i$, and for $i \neq j$ $X^{\mathcal{F}}_{ij}(w_{\mathcal{F}})$ is the infimum of the w_l variables for l in the unique path from i to j in $\mathcal{F}$. If no such path exists, by definition $X^{\mathcal{F}}_{ij}(w_{\mathcal{F}}) = 0$.*

7.1.2 Borel summability

The third key ingredient is *Borel summability*, and a helpful theorem is [16]:

Theorem 9. ***(Nevanlinna)*** *A series $\sum_n \frac{a_n}{n!} \lambda^n$ is Borel summable to a function $f(\lambda)$ if the following conditions are met:*

• *$f(\lambda)$ is analytic in a disk $Re(\lambda^{-1}) > R^{-1}$ with $R \in \mathbb{R}^+$.*

• *$f(\lambda)$ admits a Taylor expansion at the origin:*

$$f(\lambda) = \sum_{k=0}^{r-1} f_k \lambda^k + R_r f(\lambda), \qquad |R_r f(\lambda)| \leq K \sigma^r r! |\lambda|^r, \tag{7.8}$$

for some constants K and σ independent of N.

If $f(\lambda)$ is Borel summable in λ, then:

$$\mathcal{B}(t) = \sum_{n=0}^{\infty} \frac{1}{n!} f_n t^n \tag{7.9}$$

is an analytic function for $|t| < \sigma^{-1}$ which admits an analytic continuation in the strip $\{z | \, |Im(z)| < \sigma^{-1}\}$ such that $|\mathcal{B}(t)| \leq B e^{t/R}$ for some constant B and $f(\lambda)$ is represented by the absolutely convergent integral:

$$f(\lambda) = \frac{1}{\lambda} \int_0^{+\infty} dt \mathcal{B}(t) e^{-t/\lambda}. \tag{7.10}$$

The aim of the rest of this chapter is to combine the intermediate field representation with the forest formula in order to obtain a tree expansion for the free energy and Schwinger functions of our theory. This expansion will be shown to converge in a cardioid domain [8, 9], larger than the one of the Nevanlinna theorem. Bound (7.8) can also be proven, hence Borel summability follows.

7.2 Convergence and summability for T^4_3

This section is devoted to the proof of convergence and to the analyticity theorem for T^4_3 using the LVE. We begin with the free energy, then extend to connected Schwinger functions. For the

convenience of the reader, two lemmas with their respective proofs are reported at the end of the first subsection.

We first recall the Hubbard-Stratonovic decomposition of the T_3^4-model, already obtained in dimension d in Chapter 4. It writes

$$\mathcal{Z}[J,\bar{J}] = \int d\nu_{\mathbb{I}}(\tau) e^{-\sum_{\vec{p}\in\mathcal{P}} \ln(1-i\sqrt{2\lambda}C_0(\vec{p})\Gamma(\vec{p})) - \sum_{\vec{p}\in\mathcal{P}} \bar{J}(\vec{p})(1-i\sqrt{2\lambda}C_0(\vec{p}))\Gamma(\vec{p}))^{-1} C_0(\vec{p}) J(\vec{p})}, \tag{7.11}$$

where $C_0(\vec{p}) := (\vec{p}^2 + m^2)^{-1}$, $\mathcal{P} := \{\vec{p} \in \mathbb{Z}^3 | \sum_i p_i = 0\}$, $\Gamma(\vec{p}) := \sum_i \tau_i$, and $d\nu_{\mathbb{I}}(\tau)$ is the Gaussian measure of the three vector fields, defined as:

$$\int d\nu_{\mathbb{I}}(\tau)\tau_i(p)\tau_j(p') := \delta_{ij}\delta_{pp'}. \tag{7.12}$$

Moreover, we recall that the divergence degree is strictly negative for any Feynman graph (vacuum or not) $\omega(\mathcal{G}) < 0\,, \forall \mathcal{G}$, meaning that the model is well defined in the UV.

7.2.1 Free energy

We start with the partition function 7.77 and we expand to infinity the exponential of the interaction (note that sources are discarded):

$$Z(\lambda) = \int d\nu(\tau) \sum_{n=0}^{\infty} \frac{1}{n!}(-W(\tau))^n, \tag{7.13}$$

where: $W := \sum_{\vec{p}\in\mathcal{P}} \ln(1 - i\sqrt{2\lambda}C_0(\vec{p})\Gamma(\vec{p}))$. The first step is to introduce a *replica trick* for the Bosonic intermediate fields. We duplicate the intermediate field into copies, so that:

$$(-W(\tau))^n \to \prod_{m=1}^{n} (-W_m(\tau_m)) \tag{7.14}$$

and at the same time we replace the single variable covariance by $\mathbf{1}_n$, the $n \times n$ matrix with all entries equals to 1, so that our measure write as: $d\nu_{\mathbf{1}}(\tau_m)$. Indeed this does not change the value of the integral, as can be checked using Wick Theorem. Exchanging sum and Gaussian integration, 7.13 becomes

$$Z(\lambda) = \sum_{n=0}^{\infty} \frac{1}{n!} \int d\nu_{\mathbf{1}_n}(\tau_m) \prod_{m=1}^{n} (-W_m(\tau_m)). \tag{7.15}$$

In order to apply the forest formula, we introduce the *coupling parameters* x_{mp}, so that $x_{mp} = x_{pm}$, $x_{pp} = 1$ between the replicas. Hence

$$Z(\lambda) = \sum_{n=0}^{\infty} \frac{1}{n!} \int \prod_{i,m} d\tau_{i,m} e^{-\frac{1}{2}\sum_{m,p=1}^{n} x_{mp}\tau_{i,m}\tau_{i,p}} \prod_{m=1}^{n} (-W_m(\tau_m)) \Big|_{x_{pm}=1} \tag{7.16}$$

where the first indice of $\tau_{i,m}$ is the color index (running from 1 to 3), and the second is the replica index (running from 1 to n). Note that in our notation, the sum over momenta in the

expression of the Gaussian measure is implied. Applying the BKAR forest formula, we find, in the derivative representation of Gaussian integration [7]:

$$Z(\lambda) = \sum_{n=0}^{\infty} \frac{1}{n!} \sum_{\mathcal{F}_n} \int_0^1 \left(\prod_{l \in \mathcal{F}_n} dw_l \right) \left[e^{\frac{1}{2} \sum_{m,p=1}^{n} X_{mp}(w_l) \frac{\partial}{\tau_{i,m}} \frac{\partial}{\tau_{i,p}}} \right. \tag{7.17}$$

$$\left. \times \prod_{l \in \mathcal{F}} \left(\frac{\partial^2}{\partial \tau_{is(l)} \partial \tau_{it(l)}} \right) \prod_{m=1}^{n} (-W_m(\tau_m)) \right]_{\tau_{im}=0}$$

where $s(t)$ and $t(l)$ are respectively the replica indices for source and target of the edge l. As well-known in quantum and statistical field theory, the *free energy* $F := \ln(Z)$ expands as a sum over amplitudes labeled by *connected* Feynman graphs. Because the expansion (7.17) factorizes over the connected components of the forest and since the connected version of a forest is a tree, we obtain the following tree expansion for the free energy F:

$$F - F_0 = \sum_{\mathcal{T}} \frac{1}{V(\mathcal{T})!} \int_0^1 \left(\prod_{l \in \mathcal{T}} dw_l \right)$$

$$\left[\int d\nu_{X(w_l)}(\tau) \prod_{l \in \mathcal{T}} \prod_{i=1}^{3} \left(\frac{\partial^2}{\partial \tau_{is(l)} \partial \tau_{it(l)}} \right) \prod_{m=1}^{V(\mathcal{T})} (-W_m(\tau_m)) \right] \tag{7.18}$$

where the sum runs over non-empty trees (with at least one edge), $V(\mathcal{T}) \geq 2$ is the number of vertices of the tree $\mathcal{T}$, and F_0 is the contribution of the trivial "empty" tree with no edges and $V(\mathcal{T}) = 1$, namely:

$$F_0 := \int d\nu_{X(w_l)}(\tau) \sum_{\vec{p} \in \mathcal{P}} \ln(1 - i\sqrt{2\lambda} C_0(\vec{p}) \Gamma(\vec{p})). \tag{7.19}$$

Note that the replica indices run now from 1 to $V(\mathcal{T})$. The derivatives can be performed, leading to:

$$F - F_0 = \sum_{\mathcal{T}} \frac{(-2\lambda)^{V(\mathcal{T})-1}}{V(\mathcal{T})!} \int_0^1 \left(\prod_{l \in \mathcal{T}} dw_l \right) \left[\int d\nu_{X(w_l)}(\tau) \prod_{m=1}^{V(\mathcal{T})} \right. \tag{7.20}$$

$$\left. \times \sum_{\vec{p}_m \in \mathcal{P}} (c(m) - 1)! R(\vec{p}_m)^{c(m)} \prod_{l \in \mathcal{T}} \left(\sum_{i=1}^{3} \delta_{p_{t(l)i} p_{s(l)i}} \right) \right] \tag{7.21}$$

where $c(m)$ is the set of *arcs* of the vertex m and $R(\vec{p})$ is the resolvent of section 7.3.3 (in momentum representation):

$$R(\vec{p}) = \frac{C_0(\vec{p})}{1 - i\sqrt{2\lambda} C_0(\vec{p}) \Gamma(\vec{p})}. \tag{7.22}$$

Each contribution to the sum over trees 7.20 can be pictured as in Figure 7.2.1 below, where each *disk* or vertex represents a product over arc-resolvents with the same variable $\vec{p}_m$, and the labeled $1, 2, 3$ lines represent the identification of internal index between two (necessarily different) vertices, coming from the Kronecker deltas $\delta_{p_{t(l)i} p_{s(l)i}}$. The labels of the lines refer to the color i of these Kronecker delta, and the number of lines starting from a given vertex m equals the number of *arcs* $c(m)$ of this vertex.

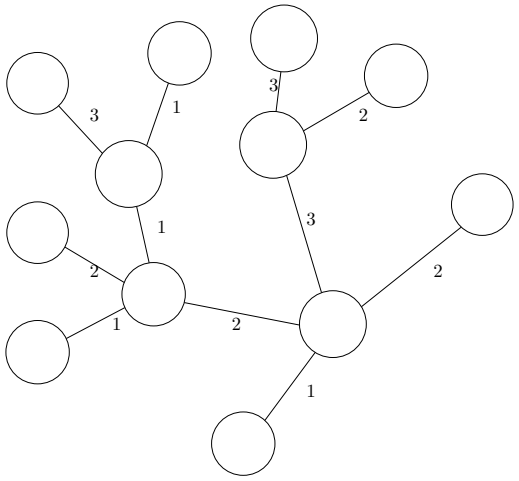

Figure 7.1: A tree contributing to the sum 7.20.

We close this section with two useful lemmas:

Lemma 4. *For $c(\mathcal{V}) > 1$, and with the parametrization $\lambda = \rho e^{i\phi}$, $\phi \in [0, \pi/2[$, we have the bound:*

$$\left| \sum_{\vec{p}\in\mathcal{P}} \left(\frac{C_0(\vec{p})}{1 - i\sqrt{2\lambda} C_0(\vec{p})\Gamma(\vec{p})} \right)^{c(m)} \right| \leq K_1(m) \left| \frac{1}{\cos(\phi/2)} \right|^{c(m)} \tag{7.23}$$

where $K_1(m)$ is a positive constant, depending on the mass parameter in a way that we shall precise in the proof.

Proof. Observe that we have not precised the domain of λ. Choosing the parametrization $\lambda = \rho e^{i\phi}$, $\phi \in [0, \pi/2[$, and because $C_0(\vec{p})\Gamma(\vec{p})$ is real:

$$\left| \frac{1}{1 - i\sqrt{2\lambda} C_0(\vec{p})\Gamma(\vec{p})} \right| \leq \left| \frac{1}{\cos(\phi/2)} \right|, \tag{7.24}$$

implying:

$$\begin{aligned} \left| \sum_{\vec{p}\in\mathcal{P}} \left(\frac{C_0(\vec{p})}{1 - i\sqrt{2\lambda} C_0(\vec{p})\Gamma(\vec{p})} \right)^{c(m)} \right| &\leq \left| \frac{1}{\cos(\phi/2)} \right|^{c(m)} \sum_{\vec{p}\in\mathcal{P}} \left| \frac{1}{\vec{p}^2 + m^2} \right|^{c(m)} \\ &\leq \left| \frac{1}{\cos(\phi/2)} \right|^{c(m)} \sum_{\vec{p}\in\mathcal{P}} \left| \frac{1}{\vec{p}^2 + m^2} \right|^{2}. \end{aligned} \tag{7.25}$$

Since the last sum converges, the lemma is proved.

□

Lemma 5. *The sequence $\mathcal{W}_p$ verifies the bound:*

$$|\mathcal{W}_p| \leq \left| \frac{1}{\cos(\phi/2)} \right| K_2(m) \tag{7.26}$$

where $K_2(m)$ is a positive constant.

Proof. From the definition

$$|\mathcal{W}_p| = \sum_{\vec{p}\in\mathcal{P}} \left| \frac{C_0(\vec{p})}{1 - i\sqrt{2\lambda} C_0(\vec{p})\Gamma(\vec{p})} \delta_{pp_1} \right| \leq \left| \frac{1}{\cos(\phi/2)} \right| \sum_{\vec{p}\in\mathcal{P}} \frac{\delta_{0p_1}}{\vec{p}^2 + m^2}, \tag{7.27}$$

one more time, because the last sum converges, the lemma is proved[1].

□

Convergence

The presence of the Kronecker deltas $\delta_{p_{t(l)i}p_{s(l)i}}$ in 7.20 gives to the sums the form of a multi-product. More precisely, each loop vertex with k external wavy lines can be represented as a multi-indexed operator $\mathcal{W}_{p_1,\ldots,p_k}$, containing an internal sum over non-external momenta. Then, formula 7.20 can be written in the form:

$$F - F_0 = \sum_{\mathcal{T}} \frac{(-2\lambda)^{V(\mathcal{T})-1}}{V(\mathcal{T})!} \mathcal{N}(\mathcal{T}) \int_0^1 \left(\prod_{l\in\mathcal{T}} dw_l \right) \left[e^{\frac{1}{2}\sum_{m,p=1}^{n} X_{mp}(w_l) \frac{\partial}{\tau_{i,m}} \frac{\partial}{\tau_{i,p}}} \right. \tag{7.28}$$
$$\left. \times \prod_{m=1}^{V(\mathcal{T})} (c(m)-1)! \sum_{\{p_{mi}\}} \prod_{m=1}^{V(\mathcal{T})} \mathcal{W}^{(m)}_{p_{m1},\ldots,p_{mk(m)}} \right]_{\tau_{im}=0},$$

where $\mathcal{N}(\mathcal{T})$ is the number of trees with the same structure but different colors for their intermediate field lines. We distinguish the *leaves* of the tree from the rest. A leaf is a terminal loop vertex involving only one resolvent, and with only one external wavy line attaching it to trhe rest of the tree. It can be represented by a function of a single variable $\mathcal{W}_p$, so that we can write the last term of the previous equation 7.28 as:

$$\sum_{\{p_{mi}\}} \prod_{m=1}^{V(\mathcal{T})} \mathcal{W}^{(m)}_{p_{m1},\ldots,p_{mk(m)}} = \sum_{\vec{P}\in\mathbb{Z}^{l(\mathcal{T})}} \mathcal{A}_{\vec{P}}(\mathcal{T}) \prod_{a=1}^{l(\mathcal{T})} \mathcal{W}_{P_a}, \tag{7.29}$$

where $l(\mathcal{T})$ is the number of leaves in $\mathcal{T}$, and the big vector $\vec{P}$ lives in the space of external momenta of the leaves : $\mathbb{Z}^{l(\mathcal{T})}$. $\mathcal{A}_{\vec{P}}(\mathcal{T})$ is the rest of the amplitude, for the tree without its leaves. Thanks to Lemma 5, the previous sum obeys the bound:

$$\left| \sum_{\{p_{mi}\}} \prod_{m=1}^{V(\mathcal{T})} \mathcal{W}^{(m)}_{p_{m1},\ldots,p_{mk(m)}} \right| \leq K_2^{l(\mathcal{T})} \left| \frac{1}{\cos(\phi/2)} \right|^{l(\mathcal{T})} \times \left| \sum_{\vec{P}\in\mathbb{Z}^{l(\mathcal{T})}} \mathcal{A}_{\vec{P}}(\mathcal{T}) \right|. \tag{7.30}$$

The remaining sum is :

$$\left| \sum_{\vec{P}\in\mathbb{Z}^{l(\mathcal{T})}} \mathcal{A}_{\vec{P}}(\mathcal{T}) \right| = \left| \sum_{\{p_{mi}\}} \prod_{m=1}^{V(\mathcal{T})-l(\mathcal{T})} \mathcal{W}^{(m)}_{p_{m1},\ldots,p_{mk(m)}} \right| \leq \left| \prod_{m=1}^{V(\mathcal{T})-l(\mathcal{T})} \sum_{\{p_{m1},\ldots,p_{mk(m)}\}} \mathcal{W}^{(m)}_{p_{m1},\ldots,p_{mk(m)}} \right| \tag{7.31}$$

$$= \left| \prod_{m=1}^{V(\mathcal{T})-l(\mathcal{T})} \sum_{\vec{p}_m\in\mathcal{P}} R(\vec{p}_m)^{c(m)} \right| \tag{7.32}$$

[1]Note that the sums involved in the proofs of Lemmas 4 and 5 can be computed exactly. For example, using standard complex analysis, we can show that :

$$\sum_{\vec{p}\in\mathcal{P}} \frac{\delta_{pp_1}}{\vec{p}^2 + m^2} = \frac{\pi/2}{\sqrt{3p^2 + 2m^2}} \coth\left[\pi\sqrt{3p^2 + 2m^2}\right] \leq \frac{\pi/2}{\sqrt{2}m} \coth\left(\sqrt{2}\pi m\right).$$

and thanks to Lemma 4,

$$\Big|\sum_{\vec{P}\in\mathbb{Z}^{l(\mathcal{T})}}\mathcal{A}_{\vec{P}}(\mathcal{T})\Big| \leq K_1(m)^{V(\mathcal{T})-l(\mathcal{T})}\left|\frac{1}{\cos(\phi/2)}\right|^{\sum_{\{V\in\bar{\mathcal{T}}\}}c(m)}. \tag{7.33}$$

$\sum_{\{V\in\bar{\mathcal{T}}\}}c(m)$ is the number of arcs in the tree $\bar{\mathcal{T}}$, amputated of its leaves. Note that the number of arcs is equal to the number of half wavy lines, or two times the number of wavy lines. Since the number of lines of a tree with V vertices is $V-1$, we finally deduce that:

$$\sum_{\{V\in\bar{\mathcal{T}}\}}c(m) = 2V(\mathcal{T}) - 2 - l(\mathcal{T}). \tag{7.34}$$

Grouping together the results 7.30 and 7.33, and defining $\mathcal{N}'(\mathcal{T}) = \mathcal{N}(\mathcal{T})\times\prod_{m=1}^{V(\mathcal{T})}(c(m)-1)!$, we obtain the following bound:

$$\begin{aligned}|F-F_0| &\leq \left|\sum_{\mathcal{T}}\frac{(-2\lambda)^{V(\mathcal{T})-1}}{V(\mathcal{T})!}\mathcal{N}'(\mathcal{T})\big[\sup\big(K_1,K_2\big)\big]^{V(\mathcal{T})}\times\left|\frac{1}{\cos^2(\phi/2)}\right|^{V(\mathcal{T})-1}\right| \\ &= \left|\frac{2\lambda}{\cos(\phi/2)}\right|^{-1}\left|\sum_{n=2}^{\infty}\Omega(n)\frac{(2\lambda)^n}{n!}\big[\sup\big(K_1,K_2\big)\big]^n\times\frac{1}{\cos^{2n}(\phi/2)}\right|\end{aligned} \tag{7.35}$$

where $\Omega(n)$ is a number depending only on n, and defined as:

$$\Omega(n) = 3^{n-1}\sum_{\substack{\{c(m)\}\\ \sum_{m=1}^n c(m)=2n-2}}\Omega(n,\{c(m)\})\prod_{m=1}^{n}(c(m)-1)! \tag{7.36}$$

where $\Omega(n,\{c(m)\})$ counts the number of trees with n labeled vertices and coordination numbers $\{c(m)\}$, and the factor 3^{n-1} corresponds to the three possible choices for the color of each intermediate field line, From *Cayley's theorem*, we have

$$\Omega(n,\{c(m)\}) = \frac{n!}{\prod_{m=1}^n(c(m)-1)!} \tag{7.37}$$

hence

$$\Omega(n) = 3^{n-1}n!\sum_{\substack{\{c(m)\}\\ \sum_{m=1}^n c(m)=2n-2}}1. \tag{7.38}$$

The remaining constrained sum can be easily bounded by the area of the $n-1$ sphere with radius $\sqrt{2n-2}$, which, by Stirling's formula, obeys the bound:

$$\frac{2\pi^{n/2}}{\big(\frac{n}{2}-1\big)!}(2n-2)^{\frac{n-1}{2}} \leq 2\sqrt{2e}\left(2\sqrt{\frac{\pi}{e}}\right)^{n-1}, \tag{7.39}$$

so that:

$$\Omega(n) \leq 2\sqrt{2e}\,3^{n-1}\left(2\sqrt{\frac{\pi}{e}}\right)^{n-1}n! \tag{7.40}$$

and 7.35 becomes

$$\begin{aligned}|F-F_0| &\leq 2\sqrt{2e}\left|\frac{12\sqrt{\pi/e}\lambda}{\cos^2(\phi/2)}\right|^{-1}\left|\sum_{n=2}^{\infty}(12\sqrt{\pi/e}\lambda)^n\big[\sup\big(K_1,K_2\big)\big]^n\times\frac{1}{\cos^{2n}(\phi/2)}\right| \\ &\leq \left(\frac{6|\lambda|}{\cos^2(\phi/2)}\right)^{-1}\sum_{n=2}^{\infty}(|\lambda|K)^n,\end{aligned} \tag{7.41}$$

with:

$$K := \frac{12\sqrt{\pi/e}\sup\left(K_1, K_2\right)}{\cos^2(\phi/2)}. \tag{7.42}$$

Finally, the first term F_0 is trivially bounded. Indeed, with integral representation of logarithm and a partial integration over intermediate fields, we find:

$$\left| \int d\nu_{X(w_l)}(\tau) \sum_{\vec{p}\in\mathcal{P}} \ln(1 - i\sqrt{2\lambda}C_0(\vec{p})\Gamma(\vec{p})) \right| \tag{7.43}$$

$$= \left| \int d\nu_{X(w_l)}(\tau) \int_0^1 dt \sum_{\vec{p}\in\mathcal{P}} \frac{-i\sqrt{2\lambda}C_0(\vec{p})\Gamma(\vec{p})}{1 - i\sqrt{2\lambda}tC_0(\vec{p})\Gamma(\vec{p})} \right| \tag{7.44}$$

$$= 3\left| \int d\nu_{X(w_l)}(\tau) \int_0^1 dt \sum_{\vec{p}\in\mathcal{P}} \frac{2\lambda[C_0(\vec{p})]^2 t}{(1 - i\sqrt{2\lambda}tC_0(\vec{p})\Gamma(\vec{p}))^2} \right|,$$

so that using Lemma 4, convergence is easy. Hence, we have proved the first result of this chapter:

Theorem 10. *The free energy expansion is absolutely convergent for a small enough coupling. More precisely, the analyticity domain is defined by the equation $|\lambda| < \frac{1}{K}$, which, with definition 7.42 for K, corresponds to the interior of a cardioid in the complex plane.*

Borel summability

After the convergence, we now move on to the Borel summability of the perturbative expansion. The previous result shows that the first requirement of Theorem 7.1.2 is satisfied, because we can find a disk inside of the cardioid in which the series converge, and we shall establish the second point in this section. Calling $R_rF(\lambda)$ the Taylor remainder of order r for the free energy F:

$$R_rF(\lambda) := \lambda^{r+1} \int_0^1 \frac{(1-t)^r}{r!} F^{(r+1)}(t\lambda)dt. \tag{7.45}$$

Expanding with the tree formula, we get:

$$R_rF(\lambda) := \sum_{n=1}^{\infty} \frac{2^{n-1}}{n!} \sum_{\mathcal{T}_n} \int_0^1 \left(\prod_{l\in\mathcal{T}_n} dw_l \right) \int d\nu_{X(w_l)}(\tau) R_r[\mathcal{Y}_{\mathcal{T}_n}], \tag{7.46}$$

where:

$$\mathcal{Y}_{\mathcal{T}_n} := (-\lambda)^{n-1} \prod_{m=1}^{n} \sum_{\vec{p}_m\in\mathcal{P}} \prod_{m=1}^{n} (c(m)-1)! R(\vec{p}_m)^{c(m)} \prod_{l\in\mathcal{T}_n} \left(\sum_{i=1}^{3} \delta_{p_{t(l)i}p_{s(l)i}} \right). \tag{7.47}$$

When $n - 2 \geq r$, $R_r[\mathcal{Y}_{\mathcal{T}_n}] = \mathcal{Y}_{\mathcal{T}_n}$. In this case, each term of the sum has a bound of the form $K^n|\lambda|^n$, and the sum converges absolutely for small enough coupling. For $n-2 < r$, however, the remainder is obtained by a Taylor expansion of the resolvents involved in $\mathcal{Y}_{\mathcal{T}}$. We can extract the factor λ^{n-1} in front of $\mathcal{Y}_{\mathcal{T}}$, and write: $\mathcal{Y}_{\mathcal{T}_n} = \lambda^{n-1}\bar{\mathcal{Y}}_{\mathcal{T}_n}$, so that: $R_r[\mathcal{Y}_{\mathcal{T}_n}] = \lambda^{n-1}R_{r-n+1}[\bar{\mathcal{Y}}_{\mathcal{T}_n}]$. Introducing $z = i\sqrt{2\lambda}$, since

$$r_z(\vec{p}) = \frac{1}{1 - z(C_0\Gamma)(\vec{p})}, \tag{7.48}$$

we have

$$\frac{\partial^n}{\partial z^n} r_z(\vec{p}) = (C_0\Gamma)^n(\vec{p}) n! r_z^{n+1}(\vec{p}), \tag{7.49}$$

and the Taylor expansion of formula 7.47 in powers of z leads to:

$$\bar{\mathcal{Y}}_{\mathcal{T}_n} = \sum_{k=0}^{\infty} \frac{z^k}{k!} \prod_{m=1}^{n} \sum_{\{k_l\}|\sum_{k_l}=k} \frac{k!}{\prod_{l=1}^{n} k_l!} \tag{7.50}$$

$$\sum_{\vec{p}_m} \left[(C_0\Gamma)^{k_m} C_0^{c(m)} \right] (\vec{p}_m)(c(m)+k_m)! \prod_{l\in\mathcal{T}_n} \left(\sum_{i=1}^{3} \delta_{p_{t(l)i} p_{s(l)i}} \right). \tag{7.51}$$

From formula 7.45 we then find:

$$R_{r-n+1}[\bar{\mathcal{Y}}_{\mathcal{T}_n}] = z^{2(r-n)} \int_0^1 dt \frac{(1-t)^{2r-2n+2}}{(2r-2n+2)!} \sum_{\{k_l\}|\sum_{k_l}=2r-2n+3} \frac{(2r-2n+3)!}{\prod_{l=1}^{n} k_l!} \prod_{m=1}^{n} \tag{7.52}$$

$$\sum_{\vec{p}_m} \left[(C_0\Gamma)^{k_m} C_0^{c(m)} \right] (\vec{p}_m) r_{tz}^{c(m)+k_m} (\vec{p}_m)(c(m)+k_m)! \prod_{l\in\mathcal{T}_n} \left(\sum_{i=1}^{3} \delta_{p_{t(l)i} p_{s(l)i}} \right).$$

We can now report this expression in equation 7.46. First, note that because $C_n^p \leq 2^n$, the factor $c(m)(c(m)+k_m)!/[k_m!c(m)!]$ is bonded by $e^{\ln(c(m))} 2^{c(m)+k_m} \leq (2e)^{c(m)} 2^{k_m}$, and the product over m gives a factor $(2e)^{2n-2} 2^{2r-2n+3}$. Secondly, we can perform the Gaussian integration. Because there are $2r-2n$ fields, the number of Wick contractions is $(2(r-n)!! = 2^{r-n}(r-n)! \leq 2^r r!$. These contractions add many intermediate loop lines to the original tree. A typical contribution to the Wick contractions can be pictured as in Figure 7.2.1 below.

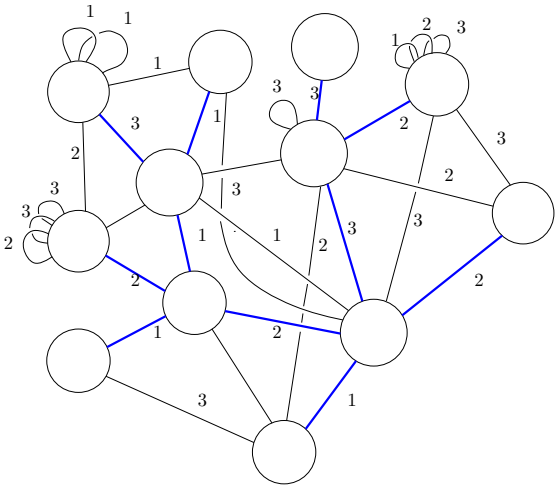

Figure 7.2: Typical contribution of the sum 7.52, with loops and tadpoles. The *root tree* lines are pictured in blue.

In this picture, which is based on the tree of Figure 7.2.1, that we call *root tree*, the original tree in blue is enriched with additional loop lines coming from the Wick contraction of the intermediate fields which were hidden in the tree resolvents. Each vertex has coordination $c(m)+k_m$, where $c(m)$ is the original number of arcs. The k_m intermediate fields of a given vertex m can be contracted together, giving tadpoles, or with the intermediate fields of others vertices, forming the loops. From Lemma 4, it follows that $|r_{tz}| \leq |\cos(\phi/2)|^{-1}$. Moreover, the contribution of the intermediate fields is twofold. The $C^{k_m}(\vec{p}_m)$ decreases the weight of each vertex, and the additional lines can be seen as constraints on the sums over $\vec{p}_m$. As a result, all the contributions are bounded by the one of the rooted tree, giving the bound:

$$(2r-2n)!! \big[\sup(K_1, K_2) \big]^n \left| \frac{1}{\cos(\phi/2)} \right|^{4n-2+2r-2n} \leq 2^r r! \left[\frac{\sup(K_1,K_2)}{\cos^2(\phi/2)} \right]^n \left| \frac{1}{\cos^2(\phi/2)} \right|^{r-1}. \tag{7.53}$$

Finally, the remaining integration over t gives $\int_0^1 (1-t)^{2r-2n+2} = 1/(2r-2n+3)$, which together with the denominator $(2r-2n+2)!$ exactly compensates the combinatorial factor $(2r-2n+3)!$. As in the previous section, using Cayley's theorem for the number of trees with n vertices and Stirling's formula, as in 7.2.1, we find a bound of the form: $AB_1^n B_2^r r!$ for some constants A, B_1 and B_2. Because $n-2 < r$, summing over n, we find the final bound : $A'|\lambda|^r B^r r!$ for the contributions in 7.46 for which $n-2 < r$. As explained before, the contributions for $n-2 \geq r$ are all bounded by bounds of the form : $|\lambda|^n K^n$, and the sum behaves as : $A''|\lambda|^r K^r$. Ultimately, because, for positive constants k_1 and k_2, $k_1 r! + k_2 \leq (k_1+k_2)r!$, we find that $|R_r F(\lambda)| \leq A''(B')^r |\lambda|^r r!$, which corresponds to the second condition of Theorem 7.1.2. It completes the proof of Borel summability.

7.2.2 Schwinger functions

Schwinger functions, or connected correlation functions are obtained from the logarithm of 7.77 by functional derivatives with respect to the sources J and $\bar{J}$. More precisely, the connected function $S_{2N}(\{\vec{p}_i, \vec{\bar{p}}_i\})$ with $2N$ external lines and external momenta $\vec{p}_i$ and $\vec{\bar{p}}_i$, $i = 1, ..., N$, is given by:

$$S_{2N}(\{\vec{p}_i, \vec{\bar{p}}_i\}) := \prod_{i=1}^{N} \frac{\partial}{\partial J(\vec{p}_i)} \frac{\partial}{\partial \bar{J}(\vec{p}_i)} \ln\left(\mathcal{Z}[J, \bar{J}]\right)\big|_{J,\bar{J}=0}. \tag{7.54}$$

Expanding $\ln\left(\mathcal{Z}[J, \bar{J}]\right)$ with the help of the forest formula, as in the previous section for the free energy, we find that the term that we called W includes the source term involved in 7.77. Because of 7.54, only the terms with N such source terms give a non-zero contribution. Each such source term corresponds to an additional resolvent. The remaining terms, involving the logarithm are then derived, but the connectivity imposes that the resolvent factors coming from the derivative of the source terms are derived at least one time with respect to the τ_i. Once more, using Lemma 4, each resolvent or derivative of resolvent can be bounded by a constant in the cardioid domain, in the same way as for the free energy, and the absolute convergence of the expansion of any Schwinger function follows.

7.3 Multi-scale loop vertex expansion for T_4^4

In case of super-renormalizable theories, requiring subtraction of a finite set of divergent graphs, a simple LVE is not enough. Indeed, even in the simplest quartic case, with only one divergent tadpole, the LVE breaks down because of the divergences of the leaves in each trees. These divergences are compensated by counter-terms, whose proliferation introduces a spurious divergence of the perturbative expansion. The multi-scale loop vertex expansion (MLVE) is an improved method based on two successive Forest decompositions, and which expands higher and higher orders of perturbation theory only when they contain higher and higher ultraviolet scales [13]. The MLVE has been successfully applied to matrix theory [1] and tensors [2, 9], and in this final section, after a short overview on the two-levels jungle expansion, we will use MLVE to prove the convergence of the perturbative free energy for the $U(1) - T_4^4$ with closure constraint.

7.3.1 List of divergent graphs

We start our investigation by listing the divergent graphs. For a non-vacuum graph, we have seen in Chapter 4 that the divergent degree writes as:

$$\omega(\mathcal{G}) = 2(1 - V(\mathcal{G})). \tag{7.55}$$

As a result, ω is negative for $V > 1$. For $V = 1$, the degree vanishes, so that such a graph with one vertex diverges logarithmically. The two possible diagrams are pictured in Figure 7.3a and 7.3b. But by direct inspection, it can be shown that the graph of Figure 7.3b is finite, with divergent degree: $\omega = -2 + 1 - 1 = -2$. The *melopole*[2] of Figure 7.3a however has a vanishing divergent degree :$\omega = -2+3-1 = 0$, so that it diverges logarithmically. Hence, the only divergent graphs in our model are the melopole ones, the only ones that need to be renormalized[3].

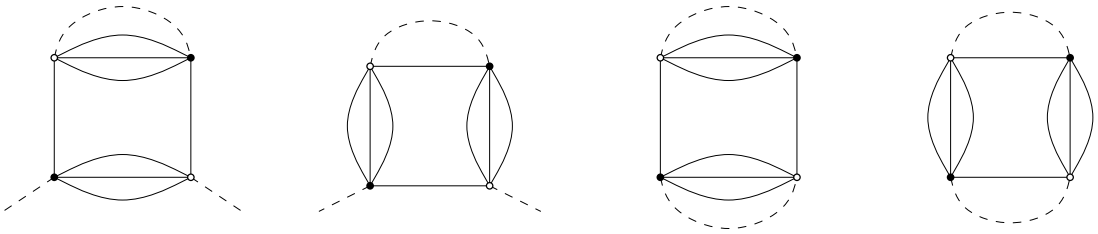

Figure 7.3: The two configurations for tadpole graphs and the two vacuum graphs with one vertex.

In the same way, for a vacuum amplitude, we can show that the melonic bound 7.55 is replaced by :

$$\omega(\mathcal{G}) = 3 - 2V(\mathcal{G}). \tag{7.56}$$

One more time, the degree is negative for $V > 1$, and the two possible configurations for $V = 1$ are pictured in Figure 7.3c and 7.3d. A direct calculation shows that the contribution 7.3d converges. Indeed, there are $2+3 = 5$ faces, 2 lines and $R = 2$, so that: $\omega = -2\times2+(5-2) = -1$. The melonic contribution 7.3c however, with $2\times3+1 = 7$ faces, is linearly divergent: $\omega = -2\times2+(7-2) = 1$, and have to be renormalized.

7.3.2 Counter-terms and renormalization

As seen previously, only the melopole needs to be renormalized. Let us start with the non-vacuum case. Let $\mathcal{A}_{\mathcal{M}_i}(p)$ the amplitude for a melopole $\mathcal{M}_i$, of color i. From Feynman rules, using sharp momentum regularization on discrete interval $[-N, N]$, we find:

$$\mathcal{A}_{\mathcal{M}_i}(p) = -2\lambda \sum_{\vec{q}\in[-N,N]^4} \frac{\delta\big(\sum_{j=1}^4 q_j\big)}{\vec{q}^2 + m^2}\delta_{pq_i} \sim \ln(N), \tag{7.57}$$

so that only the first term, $\mathcal{A}_{\mathcal{M}_i}(0)$ of its Taylor expansion around $p = 0$ diverges and must be subtracted. This subtraction can be systematically implemented with an appropriate ordering of the fields in the interaction S_{int}, called *melordering* [12], and consisting, for each melonic

[2]For our purpose, a melopole is a melonic tadpole

[3]The finiteness of the number of divergent graphs is a characteristic of super-renormalizable theories.

interaction bubble, in the subtraction of all the contractions over the *meloforest* of the corresponding vacuum melopole. These contractions appear as *mass counter-terms* in the *partially renormalized classical action* S_{int}^{PR}, defined as:

$$S_{int}^{PR}[\bar{T},T] = \lambda \sum_{i=1}^{4} \mathrm{Tr}_{b_i}[\bar{T},T] - 4\delta m^2 \int \bar{T}T, \tag{7.58}$$

with:

$$\delta m^2 := \mathcal{A}_{\mathcal{M}_i}(0) = -2\lambda \sum_{\vec{q}\in[-N,N]^4} \frac{\delta\big(\sum_{j=1}^{4} q_j\big)}{\vec{q}^2+m^2}\delta_{0q_i}, \tag{7.59}$$

so that all the non-vacuum amplitudes generated by the *non-vacuum renormalized generating functional*

$$\mathcal{Z}_{ren}[\bar{J},J] := \int d\mu_C[\bar{T},T] e^{-S_{int}^{R}[\bar{T},T]+\langle\bar{J},T\rangle+\langle\bar{T},J\rangle} \tag{7.60}$$

are finite. Taking into account the vacuum divergences requires additional counter-terms, subtracting divergent graphs. From the conclusions of the previous section, the vacuum melon graphs of the type of Figure 7.3c must be subtracted, requiring the counter-term (one for each bubble b_i):

$$CT_v^1 = \lambda \sum_{\vec{q}_1\in[-N,N]^4} \sum_{\vec{q}_2\in[-N,N]^4} \frac{\delta\big(\sum_j q_{1j}\big)}{\vec{q}_1^2+m^2} \frac{\delta\big(\sum_j q_{2j}\big)}{\vec{q}_2^2+m^2} \delta_{q_{11}q_{21}}. \tag{7.61}$$

The index 1 signals the fact that an additional counter-term is necessary to make the vacuum contributions finite. Indeed, the mass counter-term introduced previously generates a divergent vacuum graph, and must be renormalized, with corresponding counter-term :

$$CT_v^2 = -2\lambda \sum_{\vec{q}_1\in[-N,N]^4} \sum_{\vec{q}_2\in[-N,N]^4} \frac{\delta\big(\sum_j q_{1j}\big)}{\vec{q}_1^2+m^2} \frac{\delta\big(\sum_j q_{1j}\big)}{\vec{q}_2^2+m^2} \delta_{0q_{22}}. \tag{7.62}$$

Taking into account all these counter-terms, the *completely renormalized classical action*

$$S_{int}^{R}[\bar{T},T] = \lambda \sum_{i=1}^{4} \mathrm{Tr}_{b_i}[\bar{T},T] - 4\delta m^2 \int \bar{T}T - 4CT_v^1 - 4CT_v^2$$

subtracts all the divergences of the original model, and all the amplitudes generated by the *completely renormalized generating functional*

$$\mathcal{Z}_{ren}[\bar{J},J] := e^{4CT_v^1+4CT_v^2} \int d\mu_C[\bar{T},T] e^{-\lambda\sum_{i=1}^{4}\mathrm{Tr}_{b_i}[\bar{T},T]+4\delta m^2\int\bar{T}T+\langle\bar{J},T\rangle+\langle\bar{T},J\rangle} \tag{7.63}$$

are finite.

7.3.3 Hubbard-Stratonovic decomposition and subtraction

In this section, we shall recast the renormalized theory that we have just obtained in the intermediate field language. Explicitly, the partially renormalized action 7.58 with counter-terms writes as:

$$S_{int}^{PR} = \lambda \sum_{i=1}^{4} \sum_{\{\vec{p}_i\}} \mathcal{W}^{(i)}_{\vec{p}_1,\vec{p}_2,\vec{p}_3,\vec{p}_4} T_{\vec{p}_1}\bar{T}_{\vec{p}_2}T_{\vec{p}_3}\bar{T}_{\vec{p}_4} - 4\delta m^2 \sum_{\vec{p}} \bar{T}_{\vec{p}}T_{\vec{p}}. \tag{7.64}$$

Introducing the four Hermitian matrices $\mathbb{M}^i$ with elements

$$\mathbb{M}^i_{mn} := \sum_{\{\vec{p}_1,\vec{p}_2\}} \prod_{j\neq i} \delta_{p_{1j}p_{2j}}\delta_{p_{1i}n}\delta_{p_{2i}m}T_{\vec{p}_1}\bar{T}_{\vec{p}_2}, \tag{7.65}$$

the renormalized action 7.64 writes as:

$$S^{PR}_{int} = \lambda\sum_{i=1}^{4}\left[\mathrm{tr}(\mathbb{M}^i)^2 - \delta m^2\mathrm{tr}(\mathbb{M}^i)\right] \tag{7.66}$$

$$= \lambda\sum_{i=1}^{4}\mathrm{tr}\left[\mathbb{M}^i - \frac{\delta m^2}{\lambda}\right]^2 - 8N\frac{(\delta m^2)^2}{\lambda}, \tag{7.67}$$

where "tr" means the trace over indices of the matrices $\mathbb{M}^i$. The last term can be added to the vacuum counter-terms, so that the renormalized classical action becomes:

$$S^{R}_{int} = \lambda\sum_{i=1}^{4}\mathrm{tr}\left[\mathbb{M}^i - \frac{\delta m^2}{\lambda}\right]^2 - 4\left[2N\frac{(\delta m^2)^2}{\lambda} + CT^1_v + CT^2_v\right]. \tag{7.68}$$

The required mass counter-term can then be absorbed in a global translation of the quartic interaction. Then, denoting

$$X := 4\left[2N\frac{(\delta m^2)^2}{\lambda} + CT^1_v + CT^2_v\right],$$

the Hubbard-Stratanovic transformed partition function writes as:

$$\mathcal{Z}[J,\bar{J},\lambda] = e^X\int d\nu_{\mathbb{I}}(\sigma)e^{-\mathrm{Tr}\ln(1-i\sqrt{2\lambda}C\Sigma)-i\sum_{j=1}^{4}\sqrt{2\lambda}\bar{\delta}m^2\mathrm{tr}[\sigma_i]-\bar{J}RJ} \tag{7.69}$$

where the integration over $\bar{T}, T$ have been performed, and we recall that $R := (1-i\sqrt{2\lambda}C\Sigma)^{-1}C$ is the *resolvent matrix*, $d\nu_{\mathbb{I}}(\sigma)$ is the normalized Gaussian integration over the σ_i ($\mathbb{I}$ designates the covariance), $\bar{\delta}m^2 := \delta m^2/\lambda$, and:

$$\Sigma := \sum_{i=1}^{4}\otimes_{j=1}^{i-1}\mathbb{I}\otimes\sigma_i\otimes_{i+1}^{4}\mathbb{I}. \tag{7.70}$$

The additional term $i\sum_{j=1}^{4}\sqrt{2\lambda}\bar{\delta}m^2\mathrm{tr}[\sigma_i]$ in 7.69 exactly compensates the divergences of the term of order $\sqrt{\lambda}$ coming from the perturbative expansion of the logarithm. As a result, the partition function 7.69 can be rewritten as:

$$\mathcal{Z}[J,\bar{J},\lambda] = e^X\int d\nu_{\mathbb{I}}(\sigma)e^{-\mathrm{Tr}\,\ln_2(1-i\sqrt{2\lambda}C\Sigma)-i\sum_{j=1}^{4}\sqrt{2\lambda}\sum_{p_i}A(p_i)\sigma_{i,p_ip_i}-\bar{J}RJ} \tag{7.71}$$

with $\ln_2(1-x) := x + \ln(1-x) = O(x^2)$ and:

$$\sum_i\sum_{p_i}A(p_i)\sigma_{i,p_ip_i} := \mathrm{Tr}(C\Sigma) - \bar{\delta}m^2\sum_i\mathrm{tr}(\sigma_i). \tag{7.72}$$

Note that $-2\lambda A(p_i)$ is nothing but the renormalized amplitude $\mathcal{A}_{\mathcal{M}_i}(p_i)$ for the melopole $\mathcal{M}_i$. As a result:

$$\lambda\sum_{i=1}^{4}\sum_{p_i\in[-N,N]}A^2(p_i) = X. \tag{7.73}$$

As already explained in [4], due to the closure constraint, only the *diagonal part* $\tau_i(p_i) := (\sigma_i)_{p_i p_i}$ of the matrix σ_i contributes, so that 4.58 writes as

$$\mathcal{Z}[J,\bar{J},\lambda] = e^X \int d\nu_{\mathbb{I}}(\tau) e^{-\sum_{\vec{p}\in\mathcal{P}} \ln_2(1-i\sqrt{2\lambda}C_0(\vec{p})\Gamma(\vec{p}))-i\sqrt{2\lambda}\sum_{j=1}^4\sum_{p_j\in\mathcal{P}} A(p_j)\tau_j(p_j)} \tag{7.74}$$
$$\times\, e^{-\sum_{\vec{p}\in\mathcal{P}} \bar{J}(\vec{p})(1-i\sqrt{2\lambda}C_0(\vec{p}))\Gamma(\vec{p}))^{-1}C_0(\vec{p})J(\vec{p})},$$

where $C_0(\vec{p}) := (\vec{p}^2+m^2)^{-1}$, $\mathcal{P} := \{\vec{p}\in\mathbb{Z}^4 | \sum_i p_i = 0\}$, $\Gamma(\vec{p}) := \sum_i \tau_i$, and $d\nu_{\mathbb{I}}(\tau)$ is the Gaussian measure of the three vector fields, defined as:

$$\int d\nu_{\mathbb{I}}(\tau)\tau_i(p)\tau_j(p') := \delta_{ij}\delta_{pp'}. \tag{7.75}$$

Interestingly, the definition 7.74 can be further simplified. Indeed, because of equality 7.73,

$$\sum_{i=1}^4\sum_{p_i}\frac{1}{2}\tau_i^2(p_i) + i\sqrt{2\lambda}\sum_{j=1}^4\sum_{p_i\in\mathcal{P}} A(p_i)\tau_i(p_i) - X = \frac{1}{2}\sum_{i=1}^4\sum_{p_i}\big(\tau_i(p_i) - i\sqrt{2\lambda}A(p_i)\big)^2, \tag{7.76}$$

the Gaussian measure for the intermediate field involves a translation. Taking into account this translation, the partition function 7.74 becomes:

$$\mathcal{Z}[J,\bar{J},\lambda] = \int d\nu_{\mathbb{I}}(\tau) e^{-\sum_{\vec{p}\in\mathcal{P}} \ln_2(1-i\sqrt{2\lambda}C_0(\vec{p})\Gamma(\vec{p})+2\lambda D(\vec{p}))} \tag{7.77}$$
$$\times\, e^{-\sum_{\vec{p}\in\mathcal{P}} \bar{J}(\vec{p})(1-i\sqrt{2\lambda}C_0(\vec{p}))\Gamma(\vec{p})+2\lambda D(\vec{p}))^{-1}C_0(\vec{p})J(\vec{p})}, \tag{7.78}$$

with the definition:

$$D(\vec{p}) := C_0(\vec{p})\sum_i A(p_i). \tag{7.79}$$

7.3.4 Slicing the intermediate field decomposition

The regularization adopted in the previous part, in the cubic domain $[-N,N]^4$ is not the most natural with respect to the rotational invariance of the Laplacian. A more natural choice, taking into account this invariance, and closer to the Schwinger regularization used in Chapter 4 is the restriction: $0 \le \vec{p}^2 \le N^2$, and we shall adopt such a cutoff for the rest of this chapter. In addition, we shall proceed to a *slicing*, in order to make multi-scale analysis. To this end, we introduce an integer $M > 1$, the reason of a geometric progression M^j so that the upper $j = j_{max}$ verifies: $M^{j_{max}} = N$, and the notation $\chi_{\le x}(y) := \theta(x-y)$, with θ the Heaviside step function. Then, we define the following functions on $\ell^2(\mathbb{Z}^4)$, implementing closure constraint:

$$\chi_{\le 1} := \theta(M^2 - \vec{p}^2)\delta\Big(\sum_{i=1}^4 p_i\Big) \tag{7.80}$$

$$\chi_{\le j} := \theta(M^{2j} - \vec{p}^2)\delta\Big(\sum_{i=1}^4 p_i\Big) \quad j \ge 2 \tag{7.81}$$

$$\chi_j := \chi_{\le j} - \chi_{\le j-1} \quad j \ge 2, \tag{7.82}$$

where χ_i defines the i-th *slice*. With the definition

$$U(\vec{\tau}) := i\sqrt{2\lambda}C_0(\vec{p})\Gamma(\vec{p}) + 2\lambda D(\vec{p}) \tag{7.83}$$

where $\vec{\tau} = (\tau_1, \tau_2, \tau_3, \tau_4)$; the interaction with cutoff M^j writes

$$V_{\leq j} := \mathrm{Tr}\ln_2(1 - U_{\leq j}) = \mathrm{Tr}[\chi_{\leq j}\ln(1-U)] \tag{7.84}$$

$$U_{\leq j} := i\sqrt{2\lambda}C_0(\vec{p})\Gamma(\vec{p})\chi_{\leq j} + 2\lambda D(\vec{p})\chi_{\leq j}, \tag{7.85}$$

and the interaction *in the slice* j is defined as the difference:

$$V_j := V_{\leq j} - V_{\leq j-1} \tag{7.86}$$

so that the sum over scale is equal to the original interaction with cut-off N:

$$\sum_{j=0}^{j_{max}} V_j = V, \tag{7.87}$$

and the partition function 7.77 can be written as

$$\mathcal{Z}[J, \bar{J}, \lambda] = \int d\nu_{\mathbb{I}}(\tau) \prod_{j=0}^{j_{max}} e^{-V_j}. \tag{7.88}$$

From the definitions 7.84 and 7.86, we deduce the explicit expression for V_j:

$$V_j := \mathrm{Tr}[\chi_j \ln_2(1-U)] = \mathrm{Tr}\ln_2(1-U_j) \tag{7.89}$$

with the definition:

$$U_j := i\sqrt{2\lambda}C_0(\vec{p})\Gamma(\vec{p})\chi_j + 2\lambda D(\vec{p})\chi_j. \tag{7.90}$$

7.3.5 Two-levels jungle expansion

As explained briefly in the introduction, the two-levels jungle expansion of the MLVE, which we summarize in this section, follows closely [13]. It is an improved version of the standard Loop-Vertex Expansion, combining two successive forest-formulas.

We start with the definition

$$W_j(\vec{\tau}) := e^{-V_j(\vec{\tau})} - 1 \tag{7.91}$$

and rewrite the product over scales in 7.88 as a Grassmann integration:

$$\mathcal{Z}[J, \bar{J}, \lambda] = \int d\nu_{\mathbb{I}}(\tau) \prod_{j=0}^{j_{max}} d\mu(\bar{\eta}_j, \eta_j) e^{-\sum_j \bar{\eta}_j W_j(\vec{\tau})\eta_j}. \tag{7.92}$$

Let $\mathcal{S} := [0, j_{max}]$ the integer set of scales, and $\mathbb{I}_S$ the $|\mathcal{S}| \times |\mathcal{S}|$ identity matrix, which is the covariance of the Grassmann integration measure. Hence, the previous decomposition can be rewritten as:

$$\mathcal{Z}[J, \bar{J}, \lambda] = \int d\nu_{\mathbb{I}}(\tau) d\mu_{\mathbb{I}_S}(\bar{\eta}, \eta) e^{-W} = \sum_{n=0}^{\infty} \frac{1}{n!} \int d\nu_{\mathbb{I}}(\tau) d\mu_{\mathbb{I}_S}(\bar{\eta}, \eta)(-W)^n \tag{7.93}$$

where $W := \sum_j \bar{\eta}_j W_j(\vec{\tau})\eta_j$, and $\eta, \bar{\eta}$ denote all the Grassmann variables collectively. The first step is to introduce a *replica trick* for the Bosonic intermediate fields. We duplicate the intermediate field into copies, so that:

$$(-W(\tau))^n \to \prod_{m=1}^{n} (-W_m(\tau_m)) \tag{7.94}$$

and at the same time we replace the covariance $\mathbb{I}$ by $\mathbf{1}_n$, the $n \times n$ matrix with all entries equal to 1, so that our measure writes as $d\nu_{\mathbf{1}}(\tau_m)$. Exchanging sum and Gaussian integration, 7.93 becomes:

$$\mathcal{Z}[J,\bar{J},\lambda] = \sum_{n=0}^{\infty} \frac{1}{n!} \int d\nu_{\mathbf{1}_n}(\tau_m) d\mu_{\mathbb{I}_S}(\bar{\eta},\eta) \prod_{m=1}^{n} (-W_m(\tau_m)). \tag{7.95}$$

The obstacle to factorize this integral over vertices lies now in the Bosonic degenerate blocs $\mathbf{1}_n$ and the Fermionic fields, which couple the vertices W_m. Following the method exposed in [13], solving this difficulty requires two successive forest formulas. The first one concerns the Bosonic fields. Introducing the *coupling parameters* x_{mp}, so that $x_{mp} = x_{pm}$, $x_{pp} = 1$ between the vertex vector replicas, the equation 7.95 can be rewritten as:

$$\begin{aligned} \mathcal{Z}[J,\bar{J},\lambda] \;\; = \;\; & \sum_{n=0}^{\infty} \frac{1}{n!} \Bigg[e^{\frac{1}{2}\sum_{a,b=1}^{n} x_{ab} \sum_{i=1}^{4} \frac{\partial}{\partial \tau_i^a} \frac{\partial}{\partial \tau_i^b} + \sum_{j=0}^{j_{max}} \frac{\partial}{\partial \bar{\eta}_j} \frac{\partial}{\partial \eta_j}} \\ & \prod_{m=1}^{n} \Big(- \sum_j \bar{\eta}_j W_j(\vec{\tau}_m) \eta_j \Big) \Bigg]_{\substack{\vec{\tau},\bar{\eta},\eta=0 \\ x_{ab}=1}} \end{aligned} \tag{7.96}$$

where as in [13] we use the derivative formula equivalent to Gaussian integration. Applying the BKAR forest formula for the variables x_{ab}, it follows:

$$\begin{aligned} \mathcal{Z}[J,\bar{J},\lambda] = \sum_{n=0}^{\infty} \frac{1}{n!} \sum_{\mathcal{B}_n} \int_0^1 \Big(\prod_{l \in \mathcal{B}_n} dw_l \Big) \Bigg[& e^{\frac{1}{2}\sum_{a,b=1}^{n} X_{ab}(w_l) \sum_{i=1}^{4} \frac{\partial}{\partial \tau_i^a} \frac{\partial}{\partial \tau_i^b} + \sum_{j=0}^{j_{max}} \frac{\partial}{\partial \bar{\eta}_j} \frac{\partial}{\partial \eta_j}} \\ & \times \prod_{l \in \mathcal{B}_n} \Big(\frac{\partial^2}{\partial \tau_{is(l)} \partial \tau_{it(l)}} \Big) \prod_{m=1}^{n} \Big(- \sum_j \bar{\eta}_j W_j(\vec{\tau}_m) \eta_j \Big) \Bigg]_{\vec{\tau},\bar{\eta},\eta=0} \end{aligned} \tag{7.97}$$

where $\mathcal{B}_n$ denotes a *Bosonic forest* with n vertices, and where the positive symmetric matrices X_{ab} are defined in Theorem 8. The forest $\mathcal{B}_n$ partitions the set of vertices into blocs, corresponding to its connected components, which are trees, and that we denote by $\mathfrak{V}$. Obviously, each vertex belongs to a unique Bosonic block. Contracting every Bosonic block into an "effective vertex", we obtain a graph which we denote by $\{1,...,n\}/\mathcal{B}_n$. The last forest formula concerns Fermionic fields. We introduce replica Fermionic fields $\eta_j^{\mathfrak{V}}$ for the effective vertices of $\{1,...,n\}/\mathcal{B}_n$, and replica coupling parameters $y_{\mathfrak{V}\mathfrak{V}'}$. Applying the forest formula to these variables, and denoting by $\mathcal{F}$ the generic Fermionic forest connecting blocks, and $\mathfrak{V}(l_f), \mathfrak{V}(l_f)$ the end blocks of the Fermionic lines in $l_f \in \mathcal{F}$, we find:

$$\begin{aligned} \mathcal{Z}[J,\bar{J},\lambda] = & \sum_{n=0}^{\infty} \frac{1}{n!} \sum_{\mathcal{B}_n} \sum_{\mathcal{F}} \int_0^1 \prod_{l \in \mathcal{B}_n} dw_l \prod_{l_f \in \mathcal{F}} dw_{l_f} \\ & \times \Bigg[e^{\frac{1}{2}\sum_{a,b=1}^{n} X_{ab}(w_l) \sum_{i=1}^{4} \frac{\partial}{\partial \tau_i^a} \frac{\partial}{\partial \tau_i^b} + \sum_{\mathfrak{V},\mathfrak{V}'} Y_{\mathfrak{V}\mathfrak{V}'}(w_{l_f}) \sum_{j=0}^{j_{max}} \frac{\partial}{\partial \bar{\eta}_j^{\mathfrak{V}}} \frac{\partial}{\partial \eta_j^{\mathfrak{V}'}}} \\ & \times \prod_{l \in \mathcal{B}_n} \Big(\frac{\partial^2}{\partial \tau_{is(l)} \partial \tau_{it(l)}} \Big) \prod_{l_f \in \mathcal{F}} \Big(\sum_{j=0}^{j_{max}} \big(\frac{\partial}{\partial \bar{\eta}_j^{\mathfrak{V}(l_f)}} \frac{\partial}{\partial \eta_j^{\mathfrak{V}'(l_f)}} + \frac{\partial}{\partial \bar{\eta}_j^{\mathfrak{V}'(l_f)}} \frac{\partial}{\partial \eta_j^{\mathfrak{V}(l_f)}} \big) \Big) \\ & \times \prod_{\mathfrak{V}} \prod_{m \in \mathfrak{V}} \Big(- \sum_j \bar{\eta}_j^{\mathfrak{V}} W_j(\vec{\tau}_m) \eta_j^{\mathfrak{V}} \Big) \Bigg]_{\vec{\tau},\bar{\eta},\eta=0}. \end{aligned} \tag{7.98}$$

Note that the Fermionic lines are oriented. Expanding the sums over j, using the basic properties of the derivations for Bosonic and Fermionic fields, and expanding explicitly each sum over pairs

of internal vertices in blocks $\mathfrak{V}$ in order to reveal the *detailed Fermionic edges* ℓ_f between vertices in the end blocks of a given Fermionic line l_f joining together these two blocks (see Figure 7.4 below); we obtain, following [13] the *two-levels jungle formula*:

$$\mathcal{Z}[J,\bar{J},\lambda] = \sum_{n=0}^{\infty} \frac{1}{n!} \sum_{\mathcal{J}} \Big[\prod_{k=1}^{n} \sum_{j_k=0}^{j_{max}} \Big] \int dw_{\mathcal{J}} \int d\nu_{\mathcal{J}} \partial_{\mathcal{J}} \Big[\prod_{\mathfrak{V}} \prod_{m\in\mathfrak{V}} W_{j_m}(\vec{\tau}_m) \bar{\eta}^{\mathfrak{V}}_{j_m} \eta^{\mathfrak{V}}_{j_m} \Big]$$

where

• The sum over $\mathcal{J}$ runs over all two-levels jungles, hence over all oriented pairs $\mathcal{J} = (\mathcal{B}_n, \mathcal{F}_F)$ of two disjoint forests on the set $\{1,...,n\}$, such that $\bar{\mathcal{J}} = \mathcal{B}_n \cup \mathcal{F}_F$ is still a forest on $\{1,...,n\}$. The $\mathcal{B}_n$ and $\mathcal{F}_F$ are called the Bosonic and Fermionic components of $\mathcal{J}$. Note that the lines of $\mathcal{J}$ are partitioned into Bosonic and Fermionic lines.

• $\int dw_{\mathcal{J}}$ means integration from 0 to 1 over parameters $w_{\mathcal{J}}$, one for each line in $\bar{\mathcal{J}}$, coming from the forest formula.

•

$$\partial_{\mathcal{J}} = \prod_{l\in\mathcal{B}_n} \Big(\frac{\partial^2}{\partial\tau_{is(l)}\partial\tau_{it(l)}} \Big) \prod_{\ell_f\in\mathcal{F}_F} \delta_{j_{s(\ell_f)} j_{t(\ell_f)}} \Big(\frac{\partial}{\partial\bar{\eta}^{\mathfrak{V}(s(\ell_f))}_{j_{s(\ell_f)}}} \frac{\partial}{\partial\eta^{\mathfrak{V}(t(\ell_f))}_{j_{t(\ell_f)}}} + \frac{\partial}{\partial\bar{\eta}^{\mathfrak{V}(t(\ell_f))}_{j_{t(\ell_f)}}} \frac{\partial}{\partial\eta^{\mathfrak{V}(s(\ell_f))}_{j_{s(\ell_f)}}} \Big) \tag{7.99}$$

where $\mathfrak{V}(m)$ denotes the Bosonic blocks to which m belongs.

• The measure $d\nu_{\mathcal{J}}$, mixing Bosonic and Fermionic integrations is defined by

$$\int d\nu_{\mathcal{J}} F := e^{\frac{1}{2}\sum_{a,b=1}^{n} X_{ab}(w_l) \sum_{i=1}^{4} \frac{\partial}{\partial\tau_i^a}\frac{\partial}{\partial\tau_i^b} + \sum_{\mathfrak{V},\mathfrak{V}'} Y_{\mathfrak{V}\mathfrak{V}'}(w_{l_f}) \sum_{m\in\mathfrak{V},m'\in\mathfrak{V}'} \delta_{j_m j_{m'}} \frac{\partial}{\partial\bar{\eta}^{\mathfrak{V}}_{j_m}} \frac{\partial}{\partial\eta^{\mathfrak{V}'}_{j_{m'}}}} F \Big|_{\vec{\tau},\bar{\eta},\eta=0} \tag{7.100}$$

where F is the function to integrate.
Since the slice assignments, the fields, the measure and the integral are now factorized over the connected components of $\bar{\mathcal{J}}$, the logarithm of Z is easily computed as the restriction of the previous sum 7.99 to the two-levels spanning trees (the connected component of the two-levels forests):

$$\ln \mathcal{Z}[J,\bar{J},\lambda] = \sum_{n=1}^{\infty} \frac{1}{n!} \sum_{\mathcal{J}\, tree} \Big[\prod_{k=1}^{n} \sum_{j_k=0}^{j_{max}} \Big] \int dw_{\mathcal{J}} \int d\nu_{\mathcal{J}} \partial_{\mathcal{J}} \Big[\prod_{\mathfrak{V}} \prod_{m\in\mathfrak{V}} W_{j_m}(\vec{\tau}_m) \bar{\eta}^{\mathfrak{V}}_{j_m} \eta^{\mathfrak{V}}_{j_m} \Big]. \tag{7.101}$$

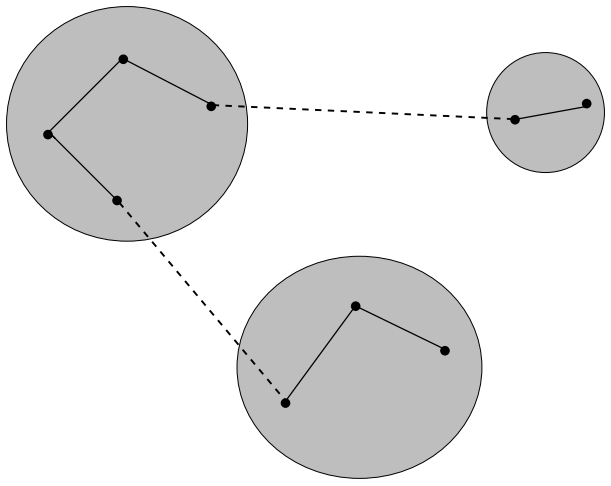

Figure 7.4: An example of two levels tree. Each grey blob represents a Bosonic bloc $\mathfrak{V}$ whose internal vertices are joined by Bosonic lines (the solid lines) to form a tree, and the blobs are joined together by Fermonic detailed lines (the dashed lines), linking black vertices of different blobs.

The rest of this section is devoted to the proof of the following Theorem

Theorem 11. *Let $\lambda = \rho e^{i\phi}$, $\phi \in [0, \pi/2]$. For ρ small enough, the series 7.101 is absolutely and uniformly convergent in j_{max}, for g in the small open cardioid domain defined by $|\lambda| \leq \rho \cos(\phi/2)$. The ultra-violet limit $\ln(Z) = \lim_{j_{max}\to\infty} \ln(Z[\lambda, j_{max}])$ is therefore well-defined and analytic in that cardioid domain, and is the Borel sum of its perturbative expansion in power of λ.*

7.3.6 Bound of the Grassmann integrals

The sum 7.101 splits into Grassmann and Bosonic integrals, and we start with the first. As explained in [13]], due to the standard properties of Grassmann integration, the Gaussian integration over these variables can be written as:

$$\prod_{\mathfrak{V}} \prod_{m\in\mathfrak{V}} \left(\frac{\partial}{\partial \bar{\eta}^{\mathfrak{V}}_{j_m}} \frac{\partial}{\partial \eta^{\mathfrak{V}}_{j_m}} \right) e^{\sum_{\mathfrak{V},\mathfrak{V}'} Y_{\mathfrak{V}\mathfrak{V}'}(w_{l_f}) \sum_{m\in\mathfrak{V}, m'\in\mathfrak{V}} \delta_{j_m j_{m'}} \bar{\eta}^{\mathfrak{V}}_{j_m} \eta^{\mathfrak{V}'}_{j_{m'}}}$$
$$\times \prod_{\ell_f \in \mathcal{F}_F} \delta_{j_{s(\ell_f)} j_{t(\ell_f)}} \left(\bar{\eta}^{\mathfrak{V}(s(\ell_f))}_{j_{s(\ell_f)}} \eta^{\mathfrak{V}(t(\ell_f))}_{j_{t(\ell_f)}} + \bar{\eta}^{\mathfrak{V}(t(\ell_f))}_{j_{t(\ell_f)}} \eta^{\mathfrak{V}(s(\ell_f))}_{j_{s(\ell_f)}} \right) \Big|_{\bar{\eta},\eta=0}. \tag{7.102}$$

Denoting $\mathbf{Y}_{mm'} := Y_{\mathfrak{V}(m)\mathfrak{V}(m')}\delta_{j_m j_{m'}}$, and taking into account that this matrix is symmetric, the previous Gaussian integral turns to the more familiar form:

$$\int \prod_{\mathfrak{V}} \prod_{m\in\mathfrak{V}} d\bar{\eta}^{\mathfrak{V}}_{j_m} d\eta^{\mathfrak{V}}_{j_m} \qquad e^{-\sum_{a,b}^{n} \bar{\eta}^{\mathfrak{V}(m)}_{j_m} \mathbf{Y}_{mm'} \eta^{\mathfrak{V}(m')}_{j_m}} \tag{7.103}$$
$$\prod_{\ell_f \in \mathcal{F}_F} \delta_{j_{s(\ell_f)} j_{t(\ell_f)}} \left(\bar{\eta}^{\mathfrak{V}(s(\ell_f))}_{j_{s(\ell_f)}} \eta^{\mathfrak{V}(t(\ell_f))}_{j_{t(\ell_f)}} + \bar{\eta}^{\mathfrak{V}(t(\ell_f))}_{j_{t(\ell_f)}} \eta^{\mathfrak{V}(s(\ell_f))}_{j_{s(\ell_f)}} \right).$$

Defining:

$$\mathbf{Y}^{p_1,\dots,p_k}_{m_1,\dots,m_k} := \int \prod_{\mathfrak{V}} \prod_{m\in\mathfrak{V}} d\bar{\eta}^{\mathfrak{V}}_{j_m} d\eta^{\mathfrak{V}}_{j_m} e^{-\sum_{a,b}^{n} \bar{\eta}^{\mathfrak{V}(m)}_{j_m} \mathbf{Y}_{mm'} \eta^{\mathfrak{V}(m')}_{j_m}} \prod_{r=1}^{k} \bar{\eta}^{\mathfrak{V}(r)}_{j_r} \eta^{\mathfrak{V}(r)}_{j_r}, \tag{7.104}$$

and taking into account what the authors of [13] have called the *hard core constraint inside each blocks*, meaning that the integral 7.103 vanishes if two vertices belong to the same Bosonic block $\mathfrak{V}$ with the same scale attribution,7.103 rewrites as:

$$\left(\prod_{\mathfrak{V}} \prod_{\substack{m,m'\in\mathfrak{V} \\ m\neq m'}} (1 - \delta_{j_m j_{m'}}) \right) \left(\prod_{\ell_f \in \mathcal{F}_F} \delta_{j_{s(\ell_f)} j_{t(\ell_f)}} \right) \left(\mathbf{Y}^{p_1,\dots,p_k}_{m_1,\dots,m_k} + \mathbf{Y}^{m_1,\dots,p_k}_{p_1,\dots,m_k} + \cdots + \mathbf{Y}^{m_1,\dots,m_k}_{p_1,\dots,p_k} \right) \tag{7.105}$$

where the sum runs over the 2^k ways to exchange the upper and lower indices, and $k := |\mathcal{F}_F|$ is the cardinal of the Fermionic forest, and the first product implements the hard core constraint. For our purpose, the following result, for which a proof can be found in [13], is important:

Lemma 6. *Due to the positivity of the covariance $\boldsymbol{Y}$, for any $\{m_i\}$ and $\{p_i\}$ the minor $\boldsymbol{Y}^{p_1,\dots,p_k}_{m_1,\dots,m_k}$ defined in 7.104 satisfies:*

$$|\, \boldsymbol{Y}^{p_1,\dots,p_k}_{m_1,\dots,m_k}| \leq 1. \tag{7.106}$$

7.3.7 Bosonic integrals

We now move on to the problem of the Bosonic integrals, whose bound is more subtle than the Fermionic one. From formula 7.101, Bosonic integration factorizes over each blocks $\mathfrak{V}$. As a result, we can only consider and bound one of these block contributions. Let us consider such a block $\mathfrak{V}$. It involves the Gaussian integration:

$$\int d\nu_{\mathfrak{V}} F_{\mathfrak{V}}(\vec{\tau}) = e^{\frac{1}{2}\sum_{a,b=1}^{n} X_{ab}(w_l)\sum_{i=1}^{4}\frac{\partial}{\partial\tau_i^a}\frac{\partial}{\partial\tau_i^b}} F_{\mathfrak{v}}(\vec{\tau})\big|_{\vec{\tau}=0} \tag{7.107}$$

with $F_{\mathfrak{v}}(\vec{\tau})$ defined as:

$$F_{\mathfrak{V}}(\vec{\tau}) = \prod_{l\in\mathfrak{V}}\left(\frac{\partial^2}{\partial\tau_{is(l)}\partial\tau_{it(l)}}\right)\prod_{m\in\mathfrak{V}} W_{j_m}(\vec{\tau}_m). \tag{7.108}$$

The derivatives $\partial/\partial\tau$ can be evaluated from the famous Faà di Bruno formula, extending the standard derivation rule for composed functions, and easily proved by induction:

$$\partial_x^q f(g(x)) = \sum_{\pi} f^{|\pi|}(g(x))\prod_{B\in\pi} g^{|B|}(x), \tag{7.109}$$

where π runs over the partitions of the set $\{1,...,q\}$ and B runs through the blocks of the partition π. With this helpful result, and from the definitions 7.89 and 7.91, we have, for $k>0$:

$$\partial_\tau^k(-V_j) = (i\sqrt{2\lambda})^k(k-1)!\sum_{\vec{p}\in\mathcal{P}_j} C_0^k(\vec{p})R_j^k \tag{7.110}$$

where $\mathcal{P}_j$ is the intersection of the gauge invariant subset $\mathcal{P}\in\mathbb{Z}^4$ with the support of the function χ_j on the slice j and:

$$R_j := \frac{1}{1-U_j}. \tag{7.111}$$

The k-th derivative of W_j can be deduced from the Faà di Bruno formula. For $k>0$:

$$\partial_\tau^k(-V_j) = e^{-V_j}\sum_{\substack{\{m_l\}\\ \sum_{l\geq1} l m_l = k}} \frac{k!}{\prod_{l\geq1} m_l!(l!)^{m_l}}\prod_{l\geq1}[\partial_\tau^l(-V_j)]^{m_l}. \tag{7.112}$$

In 7.108, we can rewrite the product as a product over the *arcs* of the vertices:

$$F_{\mathfrak{V}}(\vec{\tau}) = \prod_{m\in\mathfrak{V}}\left(\frac{\partial}{\partial\tau_{im}}\right)^{c(m)} W_{j_m}(\vec{\tau}_m), \tag{7.113}$$

where $c(m)$ is the *coordination number* of the vertex m, equal to the number of half lines of the intermediate-fields hooked to this vertex. Then, the Bosonic integral 7.107 becomes:

$$\int d\nu_{\mathfrak{V}}\Bigg[\prod_{m\in\mathfrak{V}}(i\sqrt{2\lambda})^{c(m)}\sum_{\substack{\{x_l^{(m)}\}\\ \sum_{l\geq1} l x_l^{(m)} = c(m)}} \frac{c(m)!}{\prod_{l\geq1} x_l^{(m)}! l^{x_l^{(m)}}} \tag{7.114}$$

$$\times\left(\sum_{\vec{p}_{\alpha_1}\in\mathcal{P}_{j_m}} C_0(\vec{p})U_{j_m}(\vec{p})R_{j_m}(\vec{p})\right)^{x_1^{(m)}}\left(\sum_{\vec{p}_{\alpha_l}\in\mathcal{P}_{j_m}} C_0^l(\vec{p})R_{j_m}^l(\vec{p})\right)^{x_l^{(m)}}\Bigg].$$

Lemma 7. *Because C_0 and Γ are real, and $D(\vec{p})$ is positive, R_{j_m} obeys the following bounds:*

$$|R_j| \leq \left| \frac{1}{\cos(\phi/2)} \right| \tag{7.115}$$

with $\phi := \arg(\lambda) \in]-\pi, \pi[$.

Then, using the constraint: $\sum_m c(m) = 2(|\mathfrak{V}| - 1)$, with $|\mathfrak{V}|$ the number of vertices of $\mathfrak{V}$, 7.114 admits the bound:

$$\begin{aligned} \Big| \int d\nu_{\mathfrak{V}} F_{\mathfrak{V}}(\vec{\tau}) \Big| \leq \left(\frac{2\lambda}{\cos^2(\phi/2)} \right)^{|\mathfrak{V}|-1} \int d\nu_{\mathfrak{V}} \Big[\prod_{m \in \mathfrak{V}} e^{-V_{j_m}(\vec{\tau}_m)} \sum_{\substack{\{x_l^{(m)}\} \\ \sum_{l\geq 1} l x_l^{(m)} = c(m)}} \frac{c(m)!}{\prod_{l\geq 1} x_l^{(m)}! l^{x_l^{(m)}}} \\ \times \Big(\sum_{\vec{p}_{\alpha_1} \in \mathcal{P}_{j_m}} C_0(\vec{p}) U_{j_m}(\vec{p}) \Big)^{x_1^{(m)}} \prod_{l>1} \Big(\sum_{\vec{p}_{\alpha_l} \in \mathcal{P}_{j_m}} C_0^l(\vec{p}) \Big)^{x_l^{(m)}} \Big]. \end{aligned} \tag{7.116}$$

Note that U_{j_m} involves intermediate fields. Defining:

$$\begin{aligned} G_{\mathfrak{V}} := \prod_{m \in \mathfrak{V}} \sum_{\substack{\{x_l^{(m)}\} \\ \sum_{l\geq 1} l x_l^{(m)} = c(m)}} \frac{c(m)!}{\prod_{l\geq 1} x_l^{(m)}! l^{x_l^{(m)}}} \Big(\sum_{\vec{p}_{\alpha_1} \in \mathcal{P}_{j_m}} C_0(\vec{p}) U_{j_m}(\vec{p}) \Big)^{x_1^{(m)}} \\ \prod_{l>1} \Big(\sum_{\vec{p}_{\alpha_l} \in \mathcal{P}_{j_m}} C_0^l(\vec{p}) \Big)^{x_l^{(m)}}, \end{aligned} \tag{7.117}$$

and since the Gaussian measure $d\nu_{\mathfrak{V}}$ is positive, we can use the Cauchy-Schwarz inequality to get:

$$\int d\nu_{\mathfrak{V}} \prod_{m \in \mathfrak{V}} e^{-V_{j_m}(\vec{\tau}_m)} G_{\mathfrak{V}} \leq \Big(\int d\nu_{\mathfrak{V}} \prod_{m \in \mathfrak{V}} \big| e^{-2V_{j_m}(\vec{\tau}_m)} \big| \Big)^{1/2} \Big(\int d\nu_{\mathfrak{V}} |G_{\mathfrak{V}}|^2 \Big)^{1/2}. \tag{7.118}$$

We shall treat separately each term, calling the first term the *non-perturbative factor*, and the second the *perturbative factor*, following the conventions of [13]. Note that in our derivation of the bound 7.118, we have not considered the special case for which the tree has one vertex only. This particular contribution involves melonic vacuum diagrams, discarded by construction with their corresponding counter-terms, and non-melonic vacuum diagrams. Because these diagrams are convergent, these contributions can be easily bounded, and they do not spoil the conclusion[4].

7.3.8 Bound of the Bosonic integral

We begin with the first term, the non perturbative contribution:

$$B_1 := \int d\nu_{\mathfrak{V}} \prod_{m \in \mathfrak{V}} \Big| e^{-2V_{j_m}(\vec{\tau}_m)} \Big|. \tag{7.119}$$

[4]This can be easily proved rigorously with integration by part with respect to the intermediate field, following a standard strategy exposed for instance in [13].

Firstly, note that: $\left|e^{-2V_{j_m}(\vec{\tau}_m)}\right| \leq e^{2|V_{j_m}(\vec{\tau}_m)|}$. Secondly, because of the identity:

$$\ln_2(1-x) = \int_0^1 dt \frac{tx^2}{1-tx}, \tag{7.120}$$

we have, from Lemma 7:

$$|V_j| \leq \left|\frac{1}{\cos(\phi/2)}\right| \left|\sum_{\vec{p}} U_j(\vec{p})\right|^2 \leq \left|\frac{1}{\cos(\phi/2)}\right| \sum_{\vec{p}} |U_j(\vec{p})|^2 \tag{7.121}$$

and we get:

$$B_1 \leq \int d\nu_{\mathfrak{V}} \prod_{m\in\mathfrak{V}} \exp\left(\left|\frac{2}{\cos(\phi/2)}\right| \sum_{\vec{p}} |U_j(\vec{p})|^2\right). \tag{7.122}$$

Using Definition 7.77,

$$\sum_{\vec{p}} |U_j(\vec{p})|^2 = 2|\lambda|\big[C_0^2(\vec{p})\Gamma^2(\vec{p}) + 2|\lambda|D^2(\vec{p}) + 2\sqrt{2|\lambda|}C_0(\vec{p})D(\vec{p})\Gamma(\vec{p})\big]. \tag{7.123}$$

From Definition 7.79 of $D(\vec{p})$, and because the renormalized function $A(p)$ behaves as $\ln(p^2+m^2)$, $D^2(\vec{p}) \leq \mathcal{O}(1)$. Similarly, $\sum_{\vec{p}} \delta_{p_1 p} C_0(\vec{p}) D(\vec{p}) \leq \mathcal{O}(1)$. For λ small enough, we deduce that:

$$\sum_{\vec{p}} |U_j(\vec{p})|^2 \leq 2\lambda\big[\mathcal{O}(1) + \sum_{\vec{p}\in\mathcal{P}_j} C_0^2(\vec{p})\Gamma^2(\vec{p})\big]. \tag{7.124}$$

Since one more time, $\sum_{\vec{p}} \delta_{p_1 p} C_0^2(\vec{p}) \leq \mathcal{O}(1)$, it leads to

$$\sum_{\vec{p}} |U_{j_m}(\vec{p})|^2 \leq 2\lambda \sup\big(\mathcal{O}(1)\big)\left[1 + \sum_{i,j}\sum_{p_i,p_j} \tau_{im}(p_i)\tau_{jm}(p_j)\right] \tag{7.125}$$

where the notation $\sup\big(\mathcal{O}(1)\big)$ stands for the highest of the numerical constants involved in the first bound. The term of degree 2 in τ gives an effective variance $\mathbb{I}_4 \otimes X_{\mathcal{B}}^{-1} - \left|\frac{8\lambda}{\cos(\phi/2)}\right| \mathbf{1}_4 \otimes \mathbb{I}_{\mathcal{B}}$, where $\mathbf{1}_4$ is the matrix in the color space of intermediate fields with all entries equal to 1, $\mathbb{I}_4$ the identity matrix in the same space, and $\mathbb{I}_{\mathcal{B}}$ is the identity matrix in replica space. The Gaussian integration is easy, and gives (taking into account the normalization of the original Gaussian measure):

$$B_1 \leq e^{\mathcal{O}(1)\left|\frac{4\lambda|\mathfrak{V}|}{\cos(\phi/2)}\right|} \times \det\left[\mathbb{I}_4 \otimes \mathbb{I}_{\mathcal{B}} - \left|\frac{8\lambda}{\cos(\phi/2)}\right| \mathbf{1}_4 \otimes X_{\mathcal{B}}\right]. \tag{7.126}$$

The determinant can be computed in terms of traces with the formula $\det(1-X) = e^{\mathrm{Tr}\ln(1-X)}$. Denoting:

$$X = \left|\frac{8\lambda}{\cos(\phi/2)}\right| \mathbf{1}_4 \otimes X_{\mathcal{B}}, \tag{7.127}$$

we have:

$$\mathrm{Tr}(X) = \left|\frac{32\lambda}{\cos(\phi/2)}\right| |\mathcal{B}|, \tag{7.128}$$

and, for the norm of X:

$$||X|| \leq \left|\frac{32\lambda}{\cos(\phi/2)}\right|. \tag{7.129}$$

where in both cases we used the fact that all diagonal entries of $X_{\mathcal{B}}$ are equal to 1. Using the Taylor expansion $-\ln(1-X) = \sum_{n\geq 1} X^n/n$, the two previous bounds imply:

$$-\operatorname{Tr}\ln(1-X) = \sum_{n\geq 1}\frac{\operatorname{Tr}(X^n)}{n} \leq \operatorname{Tr}(X)\sum_{n\geq 2}\frac{||X||^n}{n} \leq |\mathcal{B}| \times \sum_{n\geq 1}\left|\frac{32\lambda}{\cos(\phi/2)}\right|^n \tag{7.130}$$

and for λ small enough, we find:

$$B_1 \leq e^{\mathcal{O}(1)\left|\frac{\lambda}{\cos(\phi/2)}\right||\mathfrak{V}|}. \tag{7.131}$$

We now move on to the perturbative bound:

$$B_2 := \left(\int d\nu_{\mathfrak{V}}|G_{\mathfrak{V}}|^2\right)^{1/2}. \tag{7.132}$$

For $l > 1$ we have:

$$\sum_{\vec{p}\in\mathcal{P}_j} C_0^l(\vec{p}) \leq \sum_{\vec{p}\in\mathcal{P}_j} C_0^2(\vec{p}) \leq \frac{1}{M^{4(j-1)}}\sum_{\vec{p}\in\mathcal{P}_j} 1. \tag{7.133}$$

The last sum can be bounded by the integral over the volume of the intersection between the plane of $\mathbb{R}^4$ of equation $\sum_{i=1}^4 p_i = 0$ and the volume in between the hyper-spheres of equations $\vec{p}^2 = M^{2(j-1)}$ and $\vec{p}^2 = M^{2j}$. This volume corresponds to the volume between the two spheres of $\mathbb{R}^3$ of radius M^j and M^{j-1}, times a factor $1/2$ coming from the normalization of Kronecker delta:

$$\sum_{\vec{p}\in\mathcal{P}_j} 1 \leq \frac{1}{2}\times\left(\mathbb{V}_j - \mathbb{V}_{j-1}\right) \leq \frac{2}{3}\pi M^{3j} \tag{7.134}$$

and:

$$\sum_{\vec{p}\in\mathcal{P}_j} C_0^l(\vec{p}) \leq \frac{2}{3}\pi M^4 M^{-j}. \tag{7.135}$$

The Gaussian integrals can be computed more easily by reversing the field translation 7.76. Because, obviously: $|e^{-i\sqrt{2\lambda}\sum_{j=1}^4\sum_{p_j\in\mathcal{P}} A(p_j)\tau_j(p_j)}| \leq 1$, we can treat the integral for the back-translated intermediate fields with the simple replacement: $C_0(\vec{p})U_{j_m}(\vec{p}) \to i\sqrt{2\lambda}C_0(\vec{p})\chi_{j_m}\Gamma_m(\vec{p})$, and an additional factor $e^{-4\operatorname{Tr}(X_{\mathcal{B}})\sum_p A^2(p)\chi_j} \leq 1$. We then have a Gaussian integral of the form:

$$H_{\mathfrak{V}} := \int d\nu_{\mathfrak{V}} \prod_{m\in\mathfrak{V}}\left(\sum_{\vec{p}_{\alpha_1}\in\mathcal{P}_{j_m}} C_0^2(\vec{p})\Gamma_m(\vec{p})\right)^{k_m}. \tag{7.136}$$

Such an integral can be pictured as a graph with $|\mathfrak{V}|$ vertices, labeled by m, and with m half colored intermediate field lines hooked to them. By Wick theorem, the Gaussian integration joins together half lines between the vertices. In the worst case the graph has no loop, and because $||X_{\mathcal{B}}|| \leq 1$, it follows that the Gaussian integration 7.136 is bounded by:

$$|H_{\mathfrak{V}}| \leq 4^{\sum_m k_m}\prod_{m\in\mathfrak{V}}\left(\frac{2}{3}\pi M^4 M^{-j_m}\right)^{k_m} \times \left(\sum_{m\in\mathfrak{V}} k_m\right)!! \tag{7.137}$$

where we have taken into account the 4 choices for the colors of intermediate field lines through the factor $4^{\sum_m k_m}$. For 7.132, the double factorial is:

$$\left(2\sum_{m\in\mathfrak{V}} x_1^{(m)}\right)!! \leq (4|\mathfrak{V}|-4)!! \tag{7.138}$$

Moreover, taking into account that

$$\sum_{\substack{\{x_l^{(m)}\} \\ \sum_{l\geq 1} l x_l^{(m)} = c(m)}} \frac{1}{\prod_{l\geq 1} x_l^{(m)}! l^{x_l^{(m)}}} \tag{7.139}$$

is the coefficient of $x^{c(m)}$ in the Taylor expansion of $\prod_k e^{x^k/k} = 1/(1-x)$ allows to treat easily the square of the combinatorial factor in 7.132. We find the bound:

$$|B_2| \leq \sqrt{(4|\mathfrak{V}|-4)!!} \times \prod_{m\in\mathfrak{V}} \sum_{\substack{\{x_l^{(m)}\} \\ \sum_{l\geq 1} l x_l^{(m)} = c(m)}} \frac{c(m)!}{\prod_{l\geq 1} x_l^{(m)}! l^{x_l^{(m)}}} (2\lambda)^{x_1^{(m)}/2} \left(\frac{8\pi}{3}\right)^{c(m)} M^{-(j_m-4)} \tag{7.140}$$

where, following [13], we assume that the scales j have an inferior bound $j_{min} > 4$ (this is certainly not essential, since the first slices can be treated by a simple LVE). Choosing $|\lambda| \leq 1$, and with the remark following 7.139, we find finally the pessimistic bound

$$|B_2| \leq \sqrt{(4|\mathfrak{V}|-4)!!} \times \prod_{m\in\mathfrak{V}} \left(\frac{8\pi}{3}\right)^{c(m)} c(m)! M^{-j_m}. \tag{7.141}$$

Taking into account the bound 7.131, we find, using 7.118:

$$\Big| \int d\nu_{\mathfrak{V}} \prod_{m\in\mathfrak{V}} e^{-V_{j_m}(\vec{\tau}_m)} G_{\mathfrak{V}} \Big| \leq e^{\mathcal{O}(1)\left|\frac{\lambda}{\cos(\phi/2)}\right|^{|\mathfrak{V}|}} \sqrt{(4|\mathfrak{V}|-4)!!} \times \prod_{m\in\mathfrak{V}} c(m)! \left(\frac{8\pi}{3}\right)^{c(m)} M^{-j_m} \tag{7.142}$$

and:

$$\Big| \int d\nu_{\mathfrak{V}} F_{\mathfrak{V}}(\vec{\tau}) \Big| \leq \left(\frac{2\lambda}{\cos^2(\phi/2)}\right)^{|\mathfrak{V}|-1} \sqrt{(4|\mathfrak{V}|-4)!!} \times \prod_{m\in\mathfrak{V}} c(m)! \left(\frac{8\pi}{3}\right)^{c(m)} M^{-j_m}. \tag{7.143}$$

7.3.9 Final Bound

Collecting together the results of sections 7.3.6 and 7.3.8, we find the bound for the expansion 7.101 of the free energy $\ln(Z)$:

$$\begin{aligned} |\ln \mathcal{Z}[J,\bar{J},\lambda]| \leq \sum_{n=1}^{\infty} \frac{1}{n!} \sum_{\mathcal{J}\, tree} \left[\prod_{k=1}^{n} \sum_{j_k=0}^{j_{max}}\right] 2^{L(\mathcal{F}_F)} \left(\prod_{\ell_f\in\mathcal{F}_F} \delta_{j_{s(\ell_f)} j_{t(\ell_f)}}\right) \prod_{\mathfrak{V}} \prod_{\substack{m,m'\in\mathfrak{V} \\ m\neq m'}} (1-\delta_{j_m j_{m'}}) \\ \times \left(\frac{2|\lambda|}{\cos^2(\phi/2)}\right)^{|\mathfrak{V}|-1} \sqrt{(4|\mathfrak{V}|-4)!!} \times \prod_{m\in\mathfrak{V}} c(m)! \left(\frac{8\pi}{3}\right)^{c(m)} M^{-j_m}. \end{aligned} \tag{7.144}$$

At this stage, the reasoning follows exactly that of [13]. Thanks to *Cayley's Theorem*, the number of trees with n labeled vertices and coordination numbers c_i for each vertex $i = 1, ..., n$ is given by:

$$\frac{(n-2)!}{\prod_i (c_i - 1)!}. \tag{7.145}$$

This result shows that the sum involved in 7.144 obeys

$$\sum_{\substack{c(m)|\sum_m c(m)=2\\ \mathfrak{V}|-2}} \prod_{m\in\mathfrak{V}} c(m) = \frac{(3|\mathfrak{V}|-3)!}{(|\mathfrak{V}|-2)!(2|\mathfrak{V}|-1)!}\ . \tag{7.146}$$

Collecting all the factorials leads to:

$$\sqrt{(4|\mathfrak{V}|-4)!!}\frac{(3|\mathfrak{V}|-3)!}{(2|\mathfrak{V}|-1)!}. \tag{7.147}$$

Using Stirling's formula as in [13]

$$2\sqrt{(4|\mathfrak{V}|-4)!!}\frac{(3|\mathfrak{V}|-3)!}{(2|\mathfrak{V}|-1)!} \leq (|\mathfrak{V}|-1)!3^{|3\mathfrak{V}|}e^{-|\mathfrak{V}|}|\mathfrak{V}|^{|\mathfrak{V}|}. \tag{7.148}$$

We now move on to the sum over scale attributions, taking into account the hard core constraint. As explained in details in [13], the hard core constraint imposes that the scale assignments of vertices in a same block are all different, which implies:

$$\sum_{m\in\mathfrak{V}} j_m \geq j_{min} + (j_{min}+1) + \cdots + (j_{min}+|\mathfrak{V}|-1) = j_{min}|\mathfrak{V}| + \frac{|\mathfrak{V}|(|\mathfrak{V}|-1)}{4} \tag{7.149}$$

and:

$$\sum_{m\in\mathfrak{V}} (j_m-2) \geq \frac{1}{2}\sum_{m\in\mathfrak{V}} j_m + \frac{j_{min}-4}{2}|\mathfrak{V}| + \frac{|\mathfrak{V}|(|\mathfrak{V}|-1)}{4}, \tag{7.150}$$

where we have introduced explicitly the minimal scale $j_{min} > 4$. This result implies that,

$$\sum_{\{j_m\}} \prod_{\substack{m,m'\in\mathfrak{V}\\ m\neq m'}} (1-\delta_{j_m j_{m'}}) \prod_{m\in\mathfrak{V}} M^{-j_m} \leq \left(\sum_{j=j_{min}}^{j_{max}} M^{-j/2}\right)^{|\mathfrak{V}|} \frac{1}{M^{\frac{j_{min}-4}{2}|\mathfrak{V}|+\frac{|\mathfrak{V}|(|\mathfrak{V}|-1)}{4}}} \tag{7.151}$$

which, for $j_{min} > 4$ and $M > 4$, is uniformly bounded by $M^{-|\mathfrak{V}|^2/4}$. The upper bound j_{max} can now be sent to infinity without any divergence, allowing to define non-perturbatively the ultraviolet limit of the theory.

The final step is to sum over the Fermionic forest. Such a forest can be partitioned into components of cardinal b_k, associated to connected blocks of size k, hence with k sub-vertices. The number of Fermionic lines is then $\sum_k b_k - 1$. For each component with k sub-vertices, there are n^{b_k} ways to hook a Fermionic line. Moreover, Cayley's theorem (without constraint on the coordinate number) states that the number of trees with v labeled vertices is v^{v-2}, giving in our case a contribution $n^{\sum_k b_k - 2}$. Finally, with the constraint $\sum_k k b_k = n$, when the number of (sub) vertices is fixed to n, and the easy bound, coming from Stirling formula : $n^{(\sum_k b_k)-2} \leq (\sum_k b_k)! e^n$, we find

$$\begin{aligned} |\ln \mathcal{Z}[J,\bar{J},\lambda]| \leq \sum_n \frac{1}{n!} \sum_{\substack{\{b_k\}\\ \sum_k k b_k = n}} & \frac{n!}{\prod_k b_k!(k!)^{b_k}} 2^{\sum_k b_k - 1} k^{(\sum_k b_k)-2} \prod_k n^{b_k} \\ & \times \prod_k \left[\left(\frac{128\pi^2|\lambda|}{9\cos^2(\phi/2)}\right)^{k-1} \sqrt{(4k-4)!!}\frac{(3k-3)!}{(2k-1)!} M^{-k^2/4}\right]^{b_k}. \end{aligned} \tag{7.152}$$

Taking into account the bound 7.148, in addition to the easy bound, coming from Stirling formula : $n^{(\sum_k b_k)-2} \leq (\sum_k b_k)! e^n$, and performing the sum over the b_i, we find the final bound:

$$|\ln \mathcal{Z}[J, \bar{J}, \lambda]| \leq \sum_{b \geq 0} \left[\sum_{n \geq 1} \left(\frac{128\pi^2 |\lambda|}{9 \cos^2(\phi/2)} \right)^{n-1} 3^{3n} n^n M^{-n^2/4} \right]^b . \tag{7.153}$$

The power of M ensures that, for M sufficiently large, this factor compensates the bad divergence associated to n^n. The radius of convergence is then finite, and the factor $\cos^2(\phi/2)$ establishes the domain of uniform convergence as stated in Theorem 11.

Bibliography

[1] R. Gurau and T. Krajewski, "Analyticity results for the cumulants in a random matrix model", arXiv:1409.1705 [math-ph].

[2] V. Rivasseau, "Constructive Tensor Field Theory", arXiv : 1603.07312 [math-ph].

[3] R. Gurau, V. Rivasseau, A. Sfondrini, "Renormalization: an advanced overview", arXiv: 1401.5003. V. Rivasseau and A. Tanasa, "Generalized constructive tree weights", arXiv: 1310.2424.

[4] V. Lahoche, "Constructive Tensorial Group Field Theory I:The $U(1) - T_3^4$ Model," arXiv:1510.05050 [hep-th].

[5] V. Lahoche, "Constructive Tensorial Group Field Theory II: The $U(1) - T_4^4$ Model," arXiv:1510.05051 [hep-th].

[6] V. Rivasseau, "From perturbative to constructive renormalization", Princeton University Press (1991).

[7] V. Rivasseau, "Constructive Matrix Theory," JHEP **0709**, 008 (2007) [arXiv:0706.1224 [hep-th]].

J. Magnen and V. Rivasseau, "Constructive phi**4 field theory without tears," Annales Henri Poincare **9**, 403 (2008) [arXiv:0706.2457 [math-ph]].

V. Rivasseau and Z. Wang, "Loop Vertex Expansion for Phi**2K Theory in Zero Dimension," J. Math.Phys.51, 092304 (2010), arXiv:1003.1037 [math-ph].

V. Rivasseau and Z. Wang, "Corrected Loop Vertex Expansion for Phi42 Theory", arXiv:1406.7428[math-ph].

[8] R. Gurau, "The $1/N$ Expansion of Tensor Models Beyond Perturbation Theory", Comm. Math. Phys.330, 973-1019 (2014), arXiv:1304.2666.

T. Delepouve, R. Gurau and V. Rivasseau, "Universality and Borel Summability of Arbitrary Quartic Tensor Models", arXiv:1403.0170 [hep-th].

[9] T. Delepouve and V. Rivasseau, "Constructive Tensor Field Theory: The T_3^4 Model", arXiv:1412.5091 [math-ph].

[10] V. Rivasseau and Z. Wang, "How to Resum Feynman Graphs", Ann. Henri Poincare 15, 2069-2083(2014), arXiv:1304.5913 [math-ph].

[11] A. Abdesselam and V. Rivasseau, "Explicit fermionic tree expansions," Lett. Math. Phys. **44**, 77 (1998).

[12] S. Carrozza, D. Oriti and V. Rivasseau, "Renormalization of Tensorial Group Field Theories: Abelian U(1) Models in Four Dimensions," Commun. Math. Phys. **327**, 603 (2014) [arXiv:1207.6734 [hep-th]].

S. Carrozza, D. Oriti and V. Rivasseau, "Renormalization of a SU(2) Tensorial Group Field Theory in Three Dimensions," Commun. Math. Phys. **330**, 581 (2014) [arXiv:1303.6772 [hep-th]].

S. Carrozza, "Tensorial methods and renormalization in Group Field Theories," Springer Theses, 2014 (Springer, NY, 2014), arXiv:1310.3736 [hep-th].

[13] R. Gurau and V. Rivasseau, "The Multiscale Loop Vertex Expansion", arXiv:1312.7226 [math-ph].

[14] R. Gurau and J. P. Ryan, "Colored Tensor Models - a review," SIGMA **8**, 020 (2012) [arXiv:1109.4812 [hep-th]].

[15] D. Brydges and T. Kennedy, "Mayer expansions and the Hamilton-Jacobi equation?, Journal of Statistical Physics 48, 19 (1987).

A. Abdesselam and V. Rivasseau, "Trees, forests and jungles: A botanical garden for cluster expansions", arXiv:hep-th/9409094.

[16] A. Sokal, An improvement of Watson's theorem on Borel sulmmability, Journ. Math. Phys. **21**, 261, (1980).

Chapter 8

Conclusion, perspectives and further topics

This concluding chapter has two goals. The first one is to summarize the achievements of the last four chapters. The second one is to put these conclusions in a dynamic light, and to discuss the perspectives and current works in continuation with the matters previously considered.

8.1 The functional renormalization group

In Chapters 5 and 6 we have introduced the functional renormalization group for TGFTs with closure constraint. Chapter 5 has detailed the method, and provided a derivation of the so-called *Wetterich equation* in full generality, i.e. without restriction on the valence of the interaction bubbles. Secondly, we have discussed a current approximation, the truncation procedure, corresponding to a projection of the renormalization group flow provided by the complete Wetterich equation in a finite dimensional subspace of the theories' space. The procedure is well adapted to the case of TGFTs, and the one-loop structure of the resulting equation allows to obtain the flow equations for the selected set of couplings in an economic way. In that same chapter, following this path, we have derived the flow equation for an Abelian model both in the UV and IR limits for a truncation around marginal couplings with respect to the perturbative power counting. In both cases[1], we highlight the existence of a non-trivial fixed point in the area of the phase space connected to the Gaussian fixed point i.e. above the singularity line due to the vanishing of the denominator of η. This non-Gaussian fixed point, with one relevant and one irrelevant direction, is very reminiscent of the well-known Wilson-Fisher fixed point, the relevant direction drawing a critical line between a "symmetric phase", where the RG-trajectories reach the Gaussian fixed point, and a "broken phase", with negative mass parameter. This is an important conclusion, because a phase transition to a "condensate phase" has been suggested in relation with space-time emergence, and has a cosmological interpretation (see Chapter 2).

At this stage, the tensorial structure prevents two of the standard applications of the FRG: the vacuum translation and the dimensional regularization. Indeed, we have used the simplest approximation for the truncation, and both the qualitative dimensional argument presented in Chapter 5 and the results of Chapter 6 seem to indicate that a better control over the neglected terms in the action is required to make our conclusion solid. Usually, as for the Ising model

[1]Note that the "large sphere radius" argument advocated in Chapter 5 matches exactly with the results obtained for a TGFT on $\mathbb{R}^d$ in [1].

for instance, the field vacuum is translated into a non-zero value, depending on the cut-off k, as $V(\phi) = \lambda(\phi^2 - \rho_k)^2$, and we study the running of both the coupling and the minimum ρ_k. Such a parametrization is quite appropriate, because no singularities occur (at least for $\rho_k \geq 0$). However, because of the tensorial structure of the interaction, the minimization of the potential is non-trivial[2]. The same conclusions have been found in [2, 1], and the exact solution for the ground state of TGFTs remains an open problem in the FRG approach. Moreover, as mentioned at the end of Chapter 5, in standard field theory, dimensional regularization and ϵ-expansion allow to keep control over the distance between the Gaussian and non-Gaussian fixed points, providing an independent confirmation. The same kind of regularization for TGFT is the subject of a current research, in collaboration with Dario Benedetti [10], for a class of models without closure constraint. The strategy consists in a modification of the power of the Laplacian in the propagator, such that the λ coupling remains marginal in any dimension. More concretely, we consider the $U(1)^D - T_d^4$ without closure constraint, and with the propagator:

$$C(\vec{\mathbf{p}}) = \frac{1}{\sum_{i=1}^{d} |\mathbf{p}_i|^{2\kappa} + m^{2\eta}}\,, \tag{8.1}$$

where κ is chosen such that $[\lambda] = 0$, leading to $\kappa = D(d-1)/4$. The aim is to built a perturbative expansion for the beta function, which, because all the expressions are analytic functions of the dimension of the group manifold D, can be obtained by an ϵ-expansion around $D = 1$:

$$\beta(\lambda) = -\beta^{(2)}(d)\lambda^2 + \beta^{(3)}(d)\lambda^3 + \cdots\,. \tag{8.2}$$

Reproducing the success of the ϵ-expansion then requires that all the discarded terms $\beta^{(n)}$, $n > 3$ are of order $\mathcal{O}(\lambda_*^2)$ and higher, with $\lambda_* = \beta^{(2)}(d)/\beta^{(3)}(d)$ assumed to be a decreasing function of d. For the moment, the two-loops computations seem to match with this hypothesis. The remaining question concerns the behavior of the generic terms in the expansions.

Finally, we can return to the main conclusion of Chapter 6. In addition to the fixed points already found for the T_6^4 truncation, acting on the group dimension, we have built a continuous path between a quartic model defined on the group $U(1)^4$ and the ϕ^6 model defined on $U(1)^3$. The FRG allows to track between these two limits the non-trivial fixed points occurring in the ϵ-expansion, and finally, completed with a treatment of the limit case $U(1)^3$ with ϕ^6 truncation, provides at the same time a new solid argument in favor of the asymptotic safety of the ϕ^6 tensor model, and a confirmation of the validity of the ϵ-expansion method. For the moment, the result is too strongly dependent on the approximations to transform such results into a mathematically rigorous theorem. But the arguments accumulate around this conjecture, which seems to become stronger as time passes. Another interesting project [**?**] concerns an application to the FRG for a rank-4 TGFT beyond the world of melons, inspired by a purely tensor model studied in [7]. The basic idea is to add *necklace graphs* to the melonic $U(1) - T_4^4$, enhanced by a momentum dependent coupling. An elementary necklace corresponds to the graph pictured on equation 8.6, and the Ansatz action that we would like to consider, has the following form (we use a graphical representation for this informal discussion):

$$\mathcal{S}_{int} = \lambda_1 \sum_{\ell=1}^{4} \quad + \lambda_2 \sum_{\ell=1}^{3} \left(\quad \sum_{\ell'=1}^{4} (|p_{1\,\ell'}| + |p_{2\,\ell'}|) \right) \tag{8.3}$$

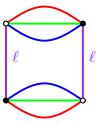

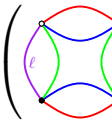

[2]Even if we limit our attention to the zero mode only, we recover an algebraic equation, like the familiar Ginsburg-Landau equation. Such an approximation, corresponding to a continuation to the zero dimensional case, seems to be bad, and remains a qualitative indication.

with the propagator 8.1 for $D = 1$, $d = 4$, and where $\vec{p}_i$, $i = 1, 2$ are the momenta associated to the two tensor field T involved in the necklace interaction. The power counting of this model has been established from a multi-scale expansion [6], providing the divergent degree:

$$\omega(\mathcal{G}) = -2\kappa L(\mathcal{G}) + (F(\mathcal{G}) + \sum_f \eta(\partial f)) \tag{8.4}$$

where $\eta(\partial f)$ corresponds to the number of derivative couplings along the boundary lines of the face f. We can tune κ such that both melonic and enhanced necklace interactions are marginal. This occurs at $\kappa = 3/4$. Computing the canonical dimension, we find that essential and marginal couplings have to be added. In particular, we find necklace graphs of valence six and eight, respectively with canonical dimensions $1/2$ and 0. Moreover, we have to introduce four valence necklaces, with coupling of dimension 1, and a 2-points interaction, with linear momentum dependent term, and coupling of dimension $1/2$. For the interested readers, we recall that a necklace graph of arbitrary valency is obtained as a sum of the *elementary necklaces* pictured on equation 8.6, where a sum between two graphs consists in the contraction of a single 0-dipole between two different vertex bubbles. Then, the crude truncation around marginal coupling takes the form:

$$\Gamma_{s,kin}[T, \bar{T}] = \sum_{\vec{p}\in\mathbb{Z}^4} \bar{T}_{\vec{p}}(Z_1(s)|\vec{p}|^{3/2} + Z_2(s)e^s|\vec{p}|^{1/2} + e^{2s}m^2)T_{\vec{p}} \tag{8.5}$$

$$\Gamma_{s,int}[T, \bar{T}] = \lambda_1 \sum_{\ell=1}^{4}$$
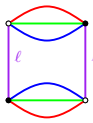

$$+ \lambda_2 \sum_{\ell=1}^{3} \left($$
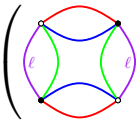

$$\sum_{\ell'=1}^{4} (|p_{1\,\ell'}| + |p_{2\,\ell'}|)\right)$$

$$+ \lambda_3 e^s \sum_{\ell=1}^{3}$$
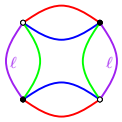

$$+ \lambda_4 e^{s/2} \sum_{\ell=1}^{3}$$
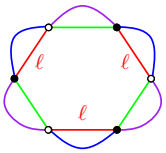

$$+ \cdots \tag{8.6}$$

The interest of this study comes from the result pointed out in [7], where the authors show that the leading sector of the $1/N$-expansion possesses both a branched polymer phase and a $2D$ quantum gravity planar phase, providing a new class of leading order graphs, mixing melons and planar maps. The enrichment of the theory with non-melonic interactions could improve the problem of the continuum transition from the branched polymer phase of the melonic sector, especially because it provides a positive entropy exponent. Indeed, when both the branching and the planar phases are critical, we find a proliferation of baby-universes with entropy exponent $1/3$. Even if our field theory is quite complicated because of the large number of couplings, preliminary results seem to provide a dynamical picture for these different regimes.

Finally, I would like to briefly return to the problem of the control over the approximations we used. Chapter 6 has pointed some limitations, or "orange-lights", of the truncation method, as truncation around the marginal interactions with respect to the perturbative power counting turns out to be wrong. Moreover, particular truncations seem to sometimes introduce pathological effects as lines of fixed points, which disappear by increasing the valence of the interactions in the truncation. These questions remain of primordial importance for the future.

8.2 Perturbative renormalization and closed melonic equations

The closed melonic equations are for the moment a frozen research project. But it is not the same for the perturbative renormalization. We started to investigate the case of a theory with geometrical degrees of freedom. The common strategy to tackle this problem in LQG consists in implementing a discrete version of the *symplicity constraint*, which, at the classical level, allows to pass from the topological BF theory to the $4d$-Palatini formulation of general relativity. A representation of this discrete constraint has been considered in [4], exploiting an extended GFT formalism. Considering a field $\Psi_k(\mathbf{g})$, with $\mathbf{g} \in SO(4)^4$ and $k \in SU(2)$, the authors introduce the improved gauge invariance:

$$\Psi_k(hg_1, hg_2, hg_3, hg_4) = \Psi_{h \triangleright k}(g_1, g_2, g_3, g_4)\,, \tag{8.7}$$

where $h \triangleright k := h^+ k (h^-)^{-1}$ is the vector k rotated by h. Implementing this constraint allows to recover the path integral amplitude for a constrained BF theory of the Plebanski type. The Immirzi parameter can be introduced to recover the Holst-Plebanski gravity. Following this path, the question of renormalization of an $SU(2)$ TGFT with both closure and geometrical constraints has been addressed in [12]. We have in particular shown that power counting makes sense, and we have studied the case of a rank-4 just-renormalizable field theory with quartic melonic interaction, for which we have proved the finiteness of the renormalized amplitude and the asymptotic freedom at one-loop. The next step is to extend these results to a more realistic model in dimension on the group manifold $SO(4)^4$. This is the subject of a current work [11]. A preliminary analysis seems to indicate that melonic graphs should be absent, and that a just-renormalizable theory may be built for necklace interactions of valence six. But the meaning of this construction remains an open question for the future.

8.3 Constructive field theory

In Chapter 7, we have established Borel-summability in the coupling constant for the two simplest TGFT models with closuer constraint, namely an UV divergence-free model and a super-renormalizable one with a (short) finite list of divergent graphs. We used for the first one the loop vertex expansion, and for the second one the enhanced technique called multi-scale loop-vertex expansion, which allows to treat the subtraction of the divergent graphs with a scale decomposition. We pointed out the simplification coming from the closure constraint, which reduces the effective degrees of freedom of the intermediate fields, from matrices to vectors.

The constructive program for TGFTs is still in its infancy, and should extend to more complicated models in the coming years. The next steps, in continuation with our program, is the proof of Borel summability for the super-renormalizable T^4_5 and the just-renormalizable T^4_6. Due to the gauge invariance, we recover the same simplifications as for the T^4_4. The list of the divergent graphs becomes much longer, but at least for the T^4_5 model a 2-jungle formula should again suffice, as shown recently in a similar work for the T^4_4 without gauge invariance [5].

The case of the just-renormalizable model T^4_6 remains however a much more difficult step. Just renormalizable models require infinitely many subtractions, and we thus need an improved multi-scale loop vertex expansion, which remains to be developed. However the T^4_6 model can take advantage of some key properties, in particular its UV asymptotic freedom. This leads to a reasonable amount of optimism in the final success of this program. Indeed we can take comfort in the full construction and Borel summability of the Gross-Neveu model [13], which is also

asymptotically free (when the number of Fermions is strictly higher than 1). Finally, note that the set of super and just-renormalizable models in TFGT is a big family [3], which reserves many unexpected challenges, in particular for the treatment of models with higher order interactions, such as the ϕ^6 model considered in Chapter 6.

Bibliography

[1] J. Ben-Geloun, R. Martini and D. Oriti, "Functional Renormalization Group analysis of Tensorial Group Field Theories on $\mathbb{R}^d$", arXiv:1601.08211 [hep-th];

[2] J. Ben-Geloun, T. A. Koslowski, "Nontrivial UV behavior of rank-4 tensor field models for quantum gravity", arXiv: 1606.04044 [gr-qc];

[3] J. Ben Geloun, "Renormalizable Models in Rank $d \geq 2$ Tensorial Group Field Theory," arXiv:1306:1201 [hep-th];

[4] A. Baratin and D. Oriti, "Group field theory and simplicial gravity path integrals: A model for Holst-Plebanski gravity", arXiv: 1111.5842, [hep-th];

[5] V. Rivasseau and F. Vignes-Tourneret, in preparation;

[6] T. Delepouve and V. Lahoche, "Non-perturbative renormalization group for a rank-4 Tensorial Group Field Theory with derivative couplings", in preparation;

[7] V. Bonzom, T. Delepouve and V. Rivasseau, "Enhancing non-melonic triangulations: A tensor model mixing melonic and planar maps", arXiv: 1502.01365;

[8] S. Carrozza and V. Lahoche, "Functional renormalization group for a rank-3 Tensorial Group Field Theory in the deep UV", in preparation;

[9] D. Samary-Ousmane, V. Lahoche, "Functional renormalization group for the T_5^6 TGFT with closure constraint", in preparation;

[10] D. Benedetti and V. Lahoche, "Modified propagator and regularization in TGFTs", in preparation;

[11] S. Carrozza, V. Lahoche and D. Oriti, "A just-renormalizable Group Field Theory with $Spin(4)$ Barrett-Crane constraints", in preparation;

[12] V. Lahoche and D. Oriti, "Renormalization of a tensorial field theory on the homogeneous space SU(2)/U(1)," arXiv:1506.08393 [hep-th].

[13] K. Gawedzki, A. Kupiainen, "Gross-Neveu model through convergent perturbation expansions". Comm. Math. Phys. 102, 1-30, 1985;

J. Feldman, J. Magnen, V. Rivasseau, R. Séléor, "Massive Gross-Neveu Model: A renormalizable field theory in two dimensions", Comm. Math. Phys. 103, 67-103, 1986;

V. Mastropietro, "Non-perturbative renormalization", World Scientific, 2008;

université PARIS-SACLAY

ÉCOLE DOCTORALE
Physique en île-de-France (EDPIF)

Titre : De la renormalisation perturbative à la renormalisation non-perturbative dans les théories de champ sur groupe à interactions tensorielles

Mots clefs : Gravité quantique, théories effectives, renormalisation, géométrie aléatoire

Résumé : Cette thèse présente quelques outils permettant d'approfondir notre compréhension de la physique sous-jacente de théories des champs appelées "Group Field Theories" (GFT) en anglais. Ces théories trouvent leur origine dans plusieurs voies de recherche en gravité quantique, en particulier les mousses de spins et les tenseurs aléatoires. Elles sont interprétés comme des modèles "prégéométriques" d'espace-temps quantiques, dont les amplitudes de Feynman sont indexées par des triangulations.
La compréhension de passage de cette vision discrétisée à notre espace-temps reste un des grands défi de cette voie de recherche, en vue de laquelle la renormalisation, les théories effectives, ainsi que la recherche de points fixes et de transitions de phases s'avère primordiale. C'est donc dans le but de comprendre les outils nécessaires à cette description que cette thèse a vue le jour.
Nous nous attacherons dans un premier temps à donner une description concise de la renormalisation perturbative, en montrant dans le même temps que l'ordre dominant de la théorie peut être entièrement capturé dans un système d'équations fermé. Dans un second temps, nous détaillerons la mise en application de méthodes non-perturbatives. Le formalism du groupe de renormalization fonctionnel en premier lieu, permettra de donner une description non-perturbative de ces théories, et de voir apparaêtre certain points fixes non-triviaux. Une approche constructive enfin, discutée sur deux modèles, ouvre la voie vers un programme visant à donner une définition rigoureuse des GFTs avec interactions

Title : From perturbative to non-perturbative renormalization in Tensorial Group Field Theories

Keywords : Quantum gravity, renormalization, effective physics, random geometry

Abstract : This thesis is presenting a few tools allowing to go deeper into our understanding of the physics underlying the field theories called Group Field Theories (GFTs). These theories are coming from different research areas in quantum gravity, in particular the spin foams and random tensors. They are an interpretation of "pre-geometric" quantum space-time models, with Feynman amplitudes indexed by triangulations.
Understanding the transition from this discrete version to our continuous space-time remains the greatest challenge for these theories. For this challenge, renormalization, the building of effective theories, the search of fixed points and phase transitions are essential: my aim in this thesis is to understand these necessary tools.
In a first time, we will give a tight description of perturbative renormalization and we will establish a system of closed equations describing the leading order of the theory. In a second time, we will detail the implementation of non-perturbative methods: firstly, the functional renormalization group will held us give a first non-perturbative description of these theories and reveal some non-trivial fixed-points. Then, a constructive approach, discussed in two models, will open the way to a program offering a rigorous definition of interacting GFTs.

Université Paris-Saclay
Espace Technologique / Immeuble Discovery
Route de l'Orme aux Merisiers RD 128 / 91190 Saint-Aubin, France